CORA Cork Open Research Archive
Cartlann Taighde Oscailte Chorcaí

Title	The microbiota and colon cancer risk: cause or consequence?
Authors	Keane, Jonathan
Publication date	2019
Original Citation	Keane, J. 2019. The microbiota and colon cancer risk: cause or consequence? PhD Thesis, University College Cork.
Type of publication	Doctoral thesis
Rights	© 2019, Jonathan Keane. - http://creativecommons.org/licenses/by-nc-nd/3.0/
Download date	2024-04-20 01:41:48
Item downloaded from	https://hdl.handle.net/10468/9625

UCC
University College Cork, Ireland
Coláiste na hOllscoile Corcaigh

The Microbiota and Colon Cancer Risk: Cause or Consequence?

Submitted to the National University of Ireland, Cork

in fulfilment of the

requirements for the degree of Doctorate of Philosophy

Thesis presented by

Jonathan Keane BSc, MRes

Departments of Medicine and Pharmacology & Therapeutics, and Schools of Microbiology and Biochemistry

Under the joint supervision of

Dr. Aileen Houston, Dr. Niall Hyland, Dr. Cormac Gahan and Dr. Susan Joyce

September 2019

Table of Contents

Declaration vi

List of publications vii

Awards and Grants ix

Abstract x

Acknowledgements xii

Abbreviations xiii

1. General Introduction **1**

1.0.1 Introduction 1

1.1 Cancer 1

1.1.1 Colon cancer 3

1.1.1.1 Risk factors in CRC 3

1.1.1.2 Types of CRC 3

1.1.1.3 Staging of CRC 5

1.1.1.4 Pathogenesis of CRC 5

1.1.1.5 Key genes and pathways in CRC 9

1.1.1.6 Genetic instability in CRC 11

1.1.1.7 The tumour microenvironment 12

1.1.1.7.1 Stroma 12

1.1.1.7.2 Angiogenesis 13

1.1.1.7.3 Cytokines and chemokines in the tumour microenvironment 14

1.1.1.7.4 Immune cells 15

1.1.1.8 Clinical treatment of CRC 20

1.2 Mouse models of CRC 22

1.2.1 APC^{MIN} mice, a model of familial CRC 22

1.2.1.1 Adenomatous polyposis coli, the β-catenin destruction complex and Wnt 22

1.2.1.2 APC^{MIN} mice 23

1.2.2 Inducible models of sporadic CRC 24

1.2.2.1 Azoxymethane-treated mice 24

1.2.2.2 Strain sensitivity to AOM 26

1.2.2.3 Pathways to CRC in AOM-treated mice 26

1.3 The gut microbiota 29

1.3.0.1 16S rRNA gene sequencing 29

1.3.1 The gut microbiota - bacteria 30
1.3.1.1 Colonisation and composition of the gut microbiota 30
1.3.2 The microbiota and colorectal cancer 31
1.3.2.1 Probiotics 34
1.3.3 Microbial metabolites 38
1.4 Bile salts 39
1.4.1 Bile salt structure and function 39
1.4.2 Bile acid regulation 43
1.4.3 Bile acid transport 44
1.4.3.1 Ileal transporters 44
1.4.3.2 Hepatic transport 46
1.4.4 FXR and CRC 46
1.4.5 Microbial bile salt metabolism 47
1.4.5.1 Deconjugation 47
1.4.5.2 Dehydroxylation 48
1.4.5.3 Other modifications 49
1.4.6 Other bile acid receptors 50
1.4.6.1 Sensing X receptor/pregnane X receptor (SXR/PXR) 50
1.4.6.2 Constitutive androstane receptor (CAR) 51
1.4.6.3 Vitamin D receptor (VDR) 51
1.4.6.4 *Takeda G protein-coupled receptor 5 (TGR5*) 52
1.4.6.5 Liver X receptor (LXR) 52
1.4.7 Bile acids and CRC 52
1.4.7.1 Mechanisms of bile acid-induced carcinogenesis 53
1.4.7.1.1 COX 53
1.4.7.1.2 Reactive oxygen species 54
1.4.7.1.3 Reactive nitrogen species 55
1.4.7.1.4 Apoptosis 55
1.4.7.1.5 Compromised repair and aneuploidy 56
1.5 Aims and objectives 58
1.5.1 Hypotheses 59
1.6 References 60
2. Materials and Methods 95
2.1 Reagents 95

2.2 Mice and experimental design 95
2.2.1 Azoxymethane-treated mice and experimental design (Chapter 3) 95
2.2.2 APC^{MIN} mice and experimental design (Chapter 4) 98
2.2.3 APC^{MIN} mice and experimental design (Chapter 5) 98
2.2.4 *Bsh* cloning 100
2.2.5 Tissue collection and processing 100
2.3 Immunohistochemistry 101
2.4 Quantitative real time PCR 102
2.5 Faecal 16S rRNA gene sequencing 103
2.6 Generating co-abundance groups 106
2.7 Ultra-performance liquid chromatography – mass spectrometry 107
2.8 Statistics 108
2.9 References 109
3. Concurrent temporal changes in host immune profile, microbiota and bile acids in a chemically-induced murine model of colonic tumorigenesis 110
3.0 Abstract 111
3.1 Introduction 113
3.2 Results 116
3.2.1 AOM-treated mice displayed faecal occult blood and aberrant crypt foci at 24 weeks and colonic adenomas at 48 weeks post-AOM injection 116
3.2.2 AOM-treated mice gained less epididymal fat 116
3.2.3 Proliferation and apoptosis are unchanged in AOM-treated mice 120
3.2.4 Cytokine profile in the large intestine and spleen weight 120
3.2.5 The faecal microbiota is altered in AOM-treated mice 123
3.2.6 Bile acids are altered in AOM-treated mice 129
3.2.7 Correlation analysis reveals relationship between gut bacteria and bile acids 132
3.2.8 Neither the metagenomic diversity nor the bile acid-metabolising capacity of the microbiota predicted by PICRUSt differs between treatments 143
3.3 Discussion 146
3.4 References 159
4. Time course analysis of the gastrointestinal microbiome of APC^{MIN} mice and association with bile acid signalling 172
4.0 Abstract 173
4.1 Introduction 175
4.2 Results 177

4.2.1 APC^{MIN} mice develop significantly more polyps in their small intestine 177
4.2.2 Faecal microbial diversity is significantly different in APC^{MIN} mice 177
4.2.3 Bile acid composition in APC^{MIN} mice 189
4.2.4 Cell proliferation is not increased in APC^{MIN} mice 189
4.2.5 Weight gain was not affected in APC^{MIN} mice 193
4.2.6 Cytokine and chemokine gene transcription in in APC^{MIN} mice 193
4.2.7 Transcription of FXR target genes is decreased in the ileum of APC^{MIN} mice 193
4.2.8 Correlation analysis reveals a relationship between polyps, FXR and Wnt 197
4.2.9 PICRUSt predicts a significant increase in bile acid-metabolising genes..... 199
4.3 Discussion 202
4.4 References 211
5. Polyposis in APC^{MIN} mice is suppressed by bacteria expressing bile salt hydrolase **216**
5.0 Abstract 217
5.1 Introduction 219
5.2 Results 221
5.2.1 Administration of E. coli expressing bsh decreased polyposis in APC^{MIN} mice .. 221
5.2.2 Levels of bacterial colonisation were similar in EC and EC-BSH mice 221
5.2.3 Epididymal fat is reduced in mice administered E. coli 221
5.2.4 Ki67 staining is not increased in APC^{MIN} mice 224
5.2.5 Bacterial gavage affects cytokine transcription in APC^{MIN} mice 224
5.2.6 The faecal microbiota is significantly different in APC^{MIN} mice 228
5.2.7 Tauro-ursodeoxycholic acid is enriched in EC-BSH mice 234
5.2.8 The transcription of *I-babp* is increased by bacterial gavage in APC^{MIN} mice ... 234
5.2.9 The transcription of Wnt target genes is increased by bacterial gavage 238
5.2.10 Correlation analysis reveals relationship between polyps, *I-babp* and T-UDCA 238
5.2.11 Diversity of the metagenome predicted by PICRUSt differs between groups 241
5.3 Discussion 243
5.4 References 252
6. Final Discussion **261**
6.1 Future perspectives 265
6.2 References 268
7. Appendix **270**

Declaration

I hereby declare that this thesis is the result of my own work and has not been submitted in whole or in part elsewhere for any award. Any assistance and contribution by others in this work is duly acknowledged within the text.

_____

Jonathan Keane

List of Publications

This work has been published in the following formats:

Oral Presentations

APC Microbiome Ireland Innovation Platform, Cork, Ireland

J. Keane, C. Gahan, S. Joyce, N. Hyland, A. Houston (2017)

Analysis of the Role of Host-Microbe Interactions in Colon Cancer

APC Microbiome Ireland Innovation Platform, Cork, Ireland

J. Keane, C. Gahan, S. Joyce, N. Hyland, A. Houston (2016)

Analysis of the Role of Host-Microbe Interactions in Colon Cancer

Thesis in 3, Dublin, Ireland

J. Keane, C. Gahan, S. Joyce, N. Hyland, A. Houston (2016)

The Gut Microbiota in Human Health

Science for All, Cork, Ireland

J. Keane, C. Gahan, S. Joyce, N. Hyland, A. Houston (2016)

The Modern Microbiome and Colon Cancer

Budding Biologists, Cork, Ireland

J. Keane, C. Gahan, S. Joyce, N. Hyland, A. Houston (2016)

The Modern Microbiome and Colon Cancer

APC Microbiome Ireland Innovation Platform, Cork, Ireland

J. Keane, C. Gahan, S. Joyce, N. Hyland, A. Houston (2016)

Mouse Models of Colorectal Cancer and Probiotic Amelioration of Tumorigenesis

APC Microbiome Ireland Innovation Platform, Cork, Ireland

J. Keane, C. Gahan, S. Joyce, N. Hyland, A. Houston (2015)

The Microbiota and Colon Cancer

Poster Presentations

Irish Association of Cancer Researchers Annual Meeting, Kilkenny, Ireland

J. Keane, S.L. Long, P. Casey, S. Melgar, C. Gahan, A. Houston, N. Hyland, S. Joyce (2017)

Analysis of the Role of Host-Microbe Interactions in Colon Cancer

Exploring the Microbe-Immune System Interface, Cork, Ireland

J. Keane, S.L. Long, P. Casey, S. Melgar, F. Shanahan, C. Gahan, A. Houston, N. Hyland, S. Joyce (2017)

Mouse Models for the Analysis of the Microbiome in Colorectal Cancer

Irish Association of Cancer Researchers Annual Meeting, Cork, Ireland

J. Keane, S.L. Long, P. Casey, S. Melgar, F. Shanahan, C. Gahan, A. Houston, N. Hyland, S. Joyce (2017)

Mouse Models for the Analysis of the Microbiome in Colorectal Cancer

New Horizons, Cork, Ireland

J. Keane, S.L. Long, P. Casey, S. Melgar, F. Shanahan, C. Gahan, A. Houston, N. Hyland, S. Joyce (2017)

Exploring the Microbe-Immune System Interface

APC Microbiome Ireland Symposium, Cork, Ireland

J. Keane, S.L. Long, P. Casey, S. Melgar, C. Gahan, A. Houston, N. Hyland, S. Joyce (2016)

Analysis of the Role of Host-Microbe Interactions in Colon Cancer

Mining Microbes for Mankind, Cork, Ireland

J. Keane, S.L. Long, P. Casey, S. Melgar, C. Gahan, A. Houston, N. Hyland, S. Joyce (2015)

Analysis of the Role of Host-Microbe Interactions in Colon Cancer

Newspaper article

Are Your Gut Bacteria Causing Cancer? It Could Depend On Your Diet.

Evening Echo, August 2016

Awards and Grants

This research was conducted with the financial support of Science Foundation Ireland (SFI) under Grant Number SFI/12/RC/2273.

College of Medicine and Health Doctoral Student Travel Bursary to attend the Metagenomics Bioinformatics course at the European Bioinformatics Institute (EMBL-EBI) at the Wellcome Genome Campus, Cambridge.

Free registration for the *Accelerating Cancer Immunotherapy* conference in London, UK, to attend as a correspondent for the European Association of Cancer Researchers.

Abstract

Background: Colorectal cancer (CRC) has a complex aetiology involving both genetic and environmental factors. Recently, attention has turned to the influence of the gut microbiota upon the development of CRC. The human gut microbiota is altered in CRC and certain microbial patterns are associated with increased cancer risk, but definitive identification of mechanisms and specific bacteria involved has proven elusive as species associated with human CRC are not consistent across studies. Moreover, research into the role of the microbiota in CRC has primarily focussed on changes that exist in and around tumour sites at a single point in time. This has made it difficult to differentiate between changes that promote cancer initiation in healthy tissue from changes that are a result of tumour development. We therefore tracked changes in the host and microbiota throughout the course of colon cancer development in mouse models of sporadic and familial CRC to elucidate their contribution to disease. Our aim was to identify changes in each of these criteria and establish their temporal relationships in order to generate a timeline of alterations and define causative and consequential events. One possible mechanism by which the gut microbiota may affect host processes leading to the development of CRC is the production of bacterial metabolites. We furthermore investigated the role of one of these metabolic pathways; in particular changes in free bile acids formed by the enzyme *bile salt hydrolase* (*bsh*), which is widespread in the microbiota.

Results: We observed pro-tumorigenic changes in the microbial composition of our model of sporadic CRC prior to detection of host neoplastic transformation. The microbiota present in the gut of our familial model also differs prior to the onset of disease with the potential to contribute to disease initiation. Our longitudinal studies also identified a distinct set of microbial alterations associated with disease progression. This included a reduction of taxa associated with suppression of inflammation prior to the onset of pro-inflammatory

signalling in our sporadic model, followed by enrichment for cancer-associated taxa later. In our intervention study, mice administered a research strain of *E. coli* overexpressing *bsh* displayed significantly fewer intestinal polyps compared to *E. coli* or PBS controls, possibly mediated by an enrichment of hydrophilic bile acid tauro-ursodeoxycholic acid and bile acid signalling.

Conclusion: These results suggest that the microbiota is dynamic over time and may act as an instigating factor in CRC development. Moreover, it highlights prophylactic treatment of the gut microbiota as a potential avenue to reduce cancer risk. This could be explored by administration of probiotics, for example *bsh*-expressing species, to human subjects in a prospective clinical trial of CRC risk.

Acknowledgements

I would like to thank my supervisors, Aileen, Niall, Susan and Cormac for their support and guidance over the course my research. Their hard work and dedication made this degree achievable.

I want to thank Aisling, whom I met when I started this PhD, and Bump, whom I am looking forward to meeting here at the end. I love you both. And thanks to Jessica, Laura and Nan for their support over the years.

Foremost, I would like to thank my parents, who have been working on this PhD for 30 years to give me the opportunity to finish it today. I dedicate this thesis to them.

Abbreviations

5-FU	5-fluorouracil
7-keto-LCA	7-keto-lithocholic acid
ABC	Avidin-biotin complex
Acetyl-CoA	Acetyl coenzyme A
ACF	Aberrant crypt foci
AKT	RAC-alpha serine/threonine-protein kinase
ALDH	Aldehyde dehydrogenase
ANOVA	Analysis of variance
AOM	Azoxymethane
AP-1	Activator protein 1
APC	Adenomatous polyposis coli *or* Antigen presenting cell
APC^{MIN}	Adenomatous polyposis coli, multiple intestinal neoplasia
APC^{mNLS}	Adenomatous polyposis coli, mutant nuclear localisation signal
ASBT	Apical sodium-dependant bile acid transporter
ATP	Adenosine triphosphate
BA	Bile acid
Bai	Bile acid inducible
BAR	Bile acid receptor (also known as FXR)
BAT	Bile acid-CoA:amino acid N-acyltransferase
BAX	B-cell lymphoma 2-associated X
Bcl-2	B-cell lymphoma 2
Bcl-xL	B-cell lymphoma-extra large
Beta (β)-Trcp1	E3 ubiquitin ligase transducin repeat containing protein 1

BLAST	Basic local alignment search tool
BRCA	Breast cancer gene
B_{REG}	Regulatory B cell
BSEP	Bile salt export pump
BSH	Bile salt hydrolase
CA	Cholic acid
CA-d4	Deuterated cholic acid
CAC	Colitis-associated cancer
CAF	Cancer-associated fibroblast
CAG	Co-abundance group
CAR	Constitutive androstane receptor
CCND1	Cyclin D1
CD	Crohn's disease
CD#	Cluster of differentiation #
CDCA	Chenodeoxycholic acid
CDCA-d4	Deuterated chenodeoxycholic acid
Cdk4	Cyclin-dependent kinase 4
cDNA	Complementary deoxyribonucleic acid
CFU	Colony forming unit
CIMP	CpG island methylator phenotype
CIN	Chromosomal instability
CKK	Cholecystokinin
c-myc	Cellular myelocytomatosis
COG	Clusters of orthologous groups
COX	Cyclooxygenase

CpG	5'-cysteine-phosphate-guanine-3'
CRC	Colorectal cancer
CTL	Cytotoxic T lymphocyte
CTLA	Cytotoxic T-lymphocyte-associated protein
Cxcl	C-X-C chemokine ligand
CYP	Cytochrome P450
DAB	3,3'-diaminobenzidine
DC	Dendritic cell
DCA	Deoxycholic acid
DCC	Deleted in colorectal carcinoma
DEPC	Diethyl pyrocarbonate
DHCA	Dehydrocholic acid
DMH	1,2-dimethylhydrazine
DNA	Deoxyribonucleic acid
dNTP	Deoxynucleotide triphosphate
DSS	Dextran sodium sulphate
ECM	Extracellular matrix
EDTA	Ethylenediaminetetraacetic acid
EGF	Epidermal growth factor
EGFR	Epidermal growth factor receptor
Elk-1	E26 transformation-specific-like-1
ELR	Glutamic acid-leucine-arginine
EMT	Epithelial–mesenchymal transition
EpCAM	Epithelial cell adhesion molecule
ERK	Extracellular signal-regulated kinases

FAP	Familial adenomatous polyposis
FDR	False discovery rate
FGF	Fibroblast growth factor
FGFR	Fibroblast growth factor receptor
FLASH	Fast length adjustment of short reads
FMT	Faecal microbial transfer
FOB	Faecal occult blood
FXR	Farnesoid X Receptor (also known as BAR)
g	Gravity
G-	Glycine-conjugated bile acid
G1-to-S	Gap 1 to synthesis phase
G2/M	Gap 2 to mitotic phase
GADD	Growth arrest and DNA damage-inducible
GB	Gnotobiotic
GF	Germ-free
GM-CSF	Granulocyte-macrophage colony-stimulating factor
GPBAR1	G protein-coupled bile acid receptor (also known as TGR5)
GSK3β	Glycogen synthase kinase 3β
GST	Glutathione-S-transferase
GTPase	Guanosine triphosphatase
HAT	Histone acetyltransferase
HCA	Hyocholic acid
HCC	Hepatocellular carcinoma
HDAC	Histone deacetylase
HDCA	Hyodeoxycholic acid

HNPCC	Hereditary non-polyposis colorectal cancer
HSD	Honest significant difference
HSDH	Hydroxysteroid dehydrogenase
HZ	Heterozygote
i.p.	Intraperitoneal
I-BABP	Ileal bile acid binding protein
IBD	Irritable bowel disease
IDO	Indoleamine 2,3-dioxygenase
IFN	Interferon
IHC	Immunohistochemistry
IL	Interleukin
iNOS	Inducible nitric oxide synthase
JAK	Janus kinase
KO	Knockout (superscript) *or* Kegg orthologue
KW	Kruskal-Wallis
LAB	Lactic acid bacteria
LAG-3	Lymphocyte-activation gene 3
LCA	Lithocholic acid
LEF	Lymphoid enhancer-binding factor
Lgr5	Leucine-rich repeat-containing G-protein coupled receptor 5
LOH	Loss of heterozygosity
LOX	Lipoxygenase
LPS	Lipopolysaccharide
LRH-1	Liver receptor homolog-1
LXR	Liver X receptor

MAM	Methylazoxymethanol
MAPK	Mitogen-activated protein kinase
MCA	Muricholic acid
MCP	Macrophage chemo-attractant protein
MDM2	Mouse double minute 2 homolog
MDSC	Myeloid-derived suppressor cell
MGMT	O_6-methylguanine-DNA-methyltransferase
MHC	Major histocompatibility complex
Min	Multiple intestinal neoplasia
miRNA	Micro ribonucleic acid
MLH1	MutL homolog 1
M-MDSC	Monocytic myeloid-derived suppressor cell
MMP	Matrix metalloproteinase
MNNG	Methylnitronitrosoguanidine
MNU	N-nitroso-N-methylurea
MoCA	Murocholic acid
mRNA	Messenger ribonucleic acid
MSI	Microsatellite instability
MWU-test	Mann-Whitney U-test
NADP	Nicotinamide adenine dinucleotide phosphate
NCRI	National cancer registry Ireland
NF-κB	Nuclear factor kappa-B
NK	Natural killer
NO	Nitric oxide
NOS	Nitric oxide synthase

NSAID	Non-steroidal anti-inflammatory drug
NTCP	Na^+-taurocholate co-transporting polypeptide
N-terminus	Amino terminus
OATP	Organic anion-transporting peptides
Olfm4	Olfactomedin 4
Ost	Organic solute transporter
OTU	Operational taxonomic unit
P16INK4a	Inhibitor of CDK4
PBS	Phosphate-buffered saline
PCoA	Principle coordinate analysis
PD	Phylogenetic diversity
PD-1	Programmed death-1
PERMANOVA	Permutational multivariate analysis of variance
PGE_2	Prostaglandin E_2
PICRUSt	Phylogenetic investigation of communities by reconstruction of unobserved states
PIK3CA	Phosphatidylinositol-4,5-bisphosphate 3-kinase catalytic subunit alpha
PKC	Protein kinase C
PMN-MDSC	Polymorphonuclear myeloid-derived suppressor cell
PXR	Pregnane X receptor (also known as SXR)
PyNAST	Python nearest alignment space termination
QIIME	Quantitative insights into microbial ecology
qPCR	Quantitative real time polymerase chain reaction
Raf	Rapidly accelerated fibrosarcoma
RAR	Retinoic acid receptor

RAS	Rat sarcoma
Rb	Retinoblastoma protein
RNS	Reactive nitrogen species
ROS	Reactive oxygen species
rRNA	Ribosomal ribonucleic acid
RTK	Receptor tyrosine kinase
RXR	Retinoid X receptor
SCFA	Short chain fatty acid
SHP	Small heterodimer protein
SMAD	Small mothers against decapentaplegic
Sox9	SRY-Box 9
SPSS	Statistical package for social sciences
STAT	Signal transducer and activator of transcription protein
SXR	Sensing X receptor (also known as PXR)
T-	Taurine-conjugated bile acid
TAM	Tumour associated macrophage
Tap1	Transporter associated with antigen processing 1
TCF	Transcription factor
TCR	T cell receptor
TGF	Transforming growth factor
TGR5	Takeda G Protein-Coupled Receptor 5 (also known as GPBAR1)
T_h	Helper T cell
TIIDM	Type II diabetes mellitus
TIM-3	T-cell immunoglobulin and mucin-domain containing-3
TIMP	Tissue inhibitor of metalloproteinase

TME	Tumour microenvironment
TNF	Tumour necrosis factor
TNM	Tumour-node-metastasis
T_{REG}	Regulatory T cell
TS	Thymidylate synthase
UC	Ulcerative colitis
UCA	Ursocholic acid
UCG	Uncultured group
UDCA	Ursodeoxycholic acid
UPL	Universal probe library
UPLC-MS	Ultra performance liquid chromatography – tandem mass spectrometry
URB	Uncultured rumen bacterium
VDR	Vitamin D receptor
VEGF	Vascular endothelial growth factor
Wnt	Wingless mouse mammary tumour virus integration site family
WT	Wild-type
WT1	Wilm's tumour 1

1.0.1 Introduction

The following research project will investigate the role of the microbiota in colorectal cancer (CRC) using two mouse models. This literature review will describe CRC and those models. It will then introduce the microbiota and delineate our understanding of its role in health and disease, as well as highlight the gaps in our knowledge relating to CRC. One mechanism by which the microbiota can contribute to disease is by the production of microbial metabolites. Our research focusses on one particular set of such processes, the microbial metabolism of endogenous bile acids, which we will define in the following section, before presenting our aims and objectives.

1.1 Cancer

Cancer is a complex family of diseases characterised by abnormal cell growth with the potential to spread to other parts of the body. It is a multi-step process that develops through epigenetic changes and mutations in multiple genes, including loss of function of tumour suppressor genes and gain of function of oncogenes. In 2000, Hanahan and Weinberg described a series of six “hallmarks” acquired by most types of cancers during their development. These hallmarks are sustained proliferative signalling, replicative immortality, activated invasion and metastasis, induced angiogenesis, cell death resistance and evasion of growth suppressors. In 2011, they added a further two hallmarks, deregulation of cellular energetics and avoidance of immune destruction, as well as two enabling characteristics, tumour-promoting inflammation and genome instability/mutation (Figure 1.1) (1, 2).

Cancer represents the second leading cause of death globally, responsible for approximately 9.6 million deaths per year (3). Cancer overtook circulatory diseases to become the number

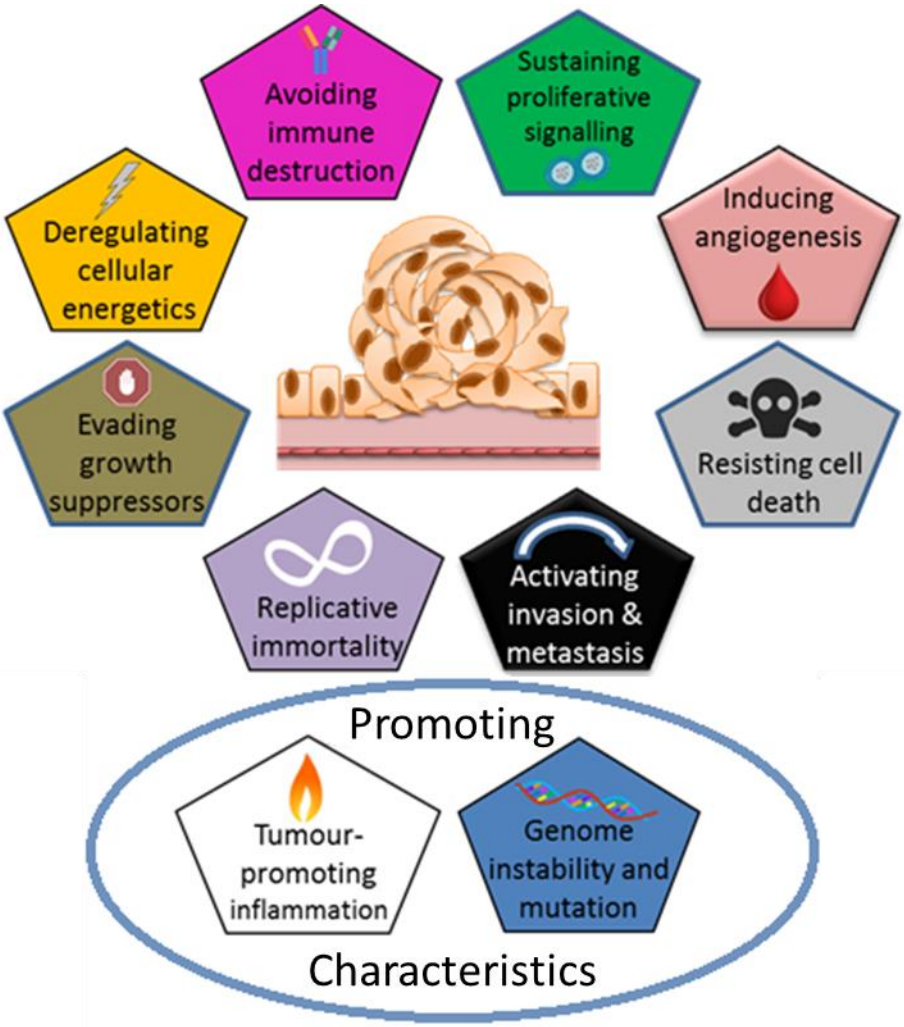

Figure 1.1: Hallmarks of cancer. Hanahan and Weinberg described eight "hallmarks" of cancer, as well as two enabling characteristics, genome instability/mutation and tumour-promoting inflammation, which are present in virtually all cancers (1, 2). These factors combine to create malignant disease.

one cause of death in Ireland in 2016, accounting for 30.7% of total fatalities at a rate of 2.0 per 1,000 population (4). Approximately 40,000 new cancer cases are diagnosed in Ireland every year with a total cost to the economy of €1.4bn in 2009, and this rate is expected to double by 2040 according to the National Cancer Registry Ireland (NCRI) (5-7).

1.1.1 Colon Cancer

Colorectal cancer (CRC) is a major cause of cancer-related death worldwide, with the NCRI predicting that the incidence of CRC will increase by ~130% by 2040 (7). Of the €1.4bn cost burden of cancer to Ireland, €158m was associated with CRC (6). CRC is the 3rd most common cancer both in Ireland (excluding non-melanoma skin cancer) and globally. It is also the 3rd highest cause of cancer-related death in Ireland and 2nd globally (3, 8).

1.1.1.1 Risk factors in CRC

Lifestyle choices play a large role in colon cancer risk, with up to 90% of cases believed to involve environmental factors (9). These factors include diet, obesity, smoking, alcohol consumption and a sedentary lifestyle (10, 11). Diet itself is believed to account for around 30% of the total cancers in the western world, second only to tobacco as a preventable cause of cancer, and for 80% of the increased CRC rates between developed and developing countries (12, 13). Indeed, the "Western diet" which is high in fat, protein and sugar and low in fibre, fruit and vegetables has been the focus of recent research investigating the high rates of CRC.

1.1.1.2 Types of Colon Cancer

CRC has a complex pathogenesis but cases fall into three broad categories, sporadic, inflammation-associated and genetic. The majority of cases (approximately 75%) are sporadic with no direct inherited or comorbid cause (14). Sporadic cancer generally occurs later in life and displays a progressive accumulation of mutations in genes such as *APC*, *RAS*, *SMAD4* and *TP53* and subsequent genomic instability (14).

Approximately 20% of CRC cases display a familial inheritance pattern (15). Hereditary Non-Polyposis colorectal cancer (HNPCC) accounts for ~5% of these cases, while Familial Adenomatous Polyposis (FAP) accounts for ~1%. HNPCC, also known as Lynch syndrome, is an autosomal-dominant condition caused by mutations in DNA mismatch repair proteins, leading to a 50-70% lifetime risk of CRC (15). FAP is also an autosomal-dominant condition caused by mutations in the *adenomatous polyposis coli (APC*) gene which causes hundreds to thousands of adenomatous polyps to develop in the large intestine, and has a CRC risk approaching 100% in middle age (16).

Thirdly, inflammatory bowel disease (IBD)-related CRC is responsible for approximately 2% of the annual mortality from CRC overall, but 10–15% of the annual deaths in IBD patients (17). Here, chronic inflammation and epithelial disruption in the large intestine provide the genotoxic background that promotes cancer initiation and progression. IBD-CRC patients, specifically those suffering from ulcerative colitis (UC) and Crohn's disease (CD), are also affected at a younger age than sporadic CRC patients and have a 5-year survival rate of 50%. Indeed, patients with IBD have a CRC relative risk of 0.8 – 23 and undergo close monitoring, treatment with immune-suppressor drugs and frequent colectomy to address both the IBD and CRC risk (18). Relative risk is approximately twice as high in UC patients compared to CD, possibly due to the involvement of a greater area of the colonic epithelium (19).

1.1.1.3 Staging of Colon Cancer

Colon cancers are divided into five stages, 0 to IV. These summarise the tumour-node-metastasis (TNM) characteristics of the disease. “Tumour” describes how deeply the tumour has penetrated the intestine epithelium and bowel lining. “Node” relates to whether or not tumour cells are detected in regional lymph nodes, while “metastasis” refers to whether the cancer has spread to other body parts. Each stage is described in Table 1.1.

1.1.1.4 Pathogenesis of CRC

Colon cancer development normally follows a gradient process, in which various genetic mutations gradually accumulate over time. Adenocarcinomas make up 95% of colon cancer cases. They are believed to arise from aberrant crypt foci (ACF); abnormal lesions in the colonic mucosa identifiable by their raised and thickened epithelium and enlarged luminal openings (20). Some ACF can eventually progress to benign adenomatous polyps, which then develop into an advanced adenoma with high grade dysplasia. This is followed by progression to carcinoma and ultimately to metastasis (Figure 1.2).

The progression from normal epithelium to ACF, adenoma, adenocarcinoma and metastasis is a stepwise process as initial mutations disable cellular maintenance systems, allowing the accumulation of further cytogenetic damage and assumption by the cell of additional tumorigenic characteristics. The approximate rate in which key mutations appear in the sequence is presented in Table 1.2.

Another tumorigenic pathway which bypasses the exophytic adenomatous stage and is believed to account for around one third of CRC cases is termed the *de novo* or flat adenomatous stage. These tumours also arise from ACF that are not elevated above the

Table 1.1: Stages of CRC (modified from Hardy *et al*. (21))

Stage	Characteristics	Survival (%)
Stage 0	Carcinoma in situ	90-100
Stage I	Tumour invades the submucosa or muscularis propria	90-100
Stage II	Tumour invades the subserosa or surface of the visceral peritoneum	75-85
Stage III	Tumour cells have spread to the regional lymph nodes	30-40
Stage IV	Cancer has distant metastases	<5

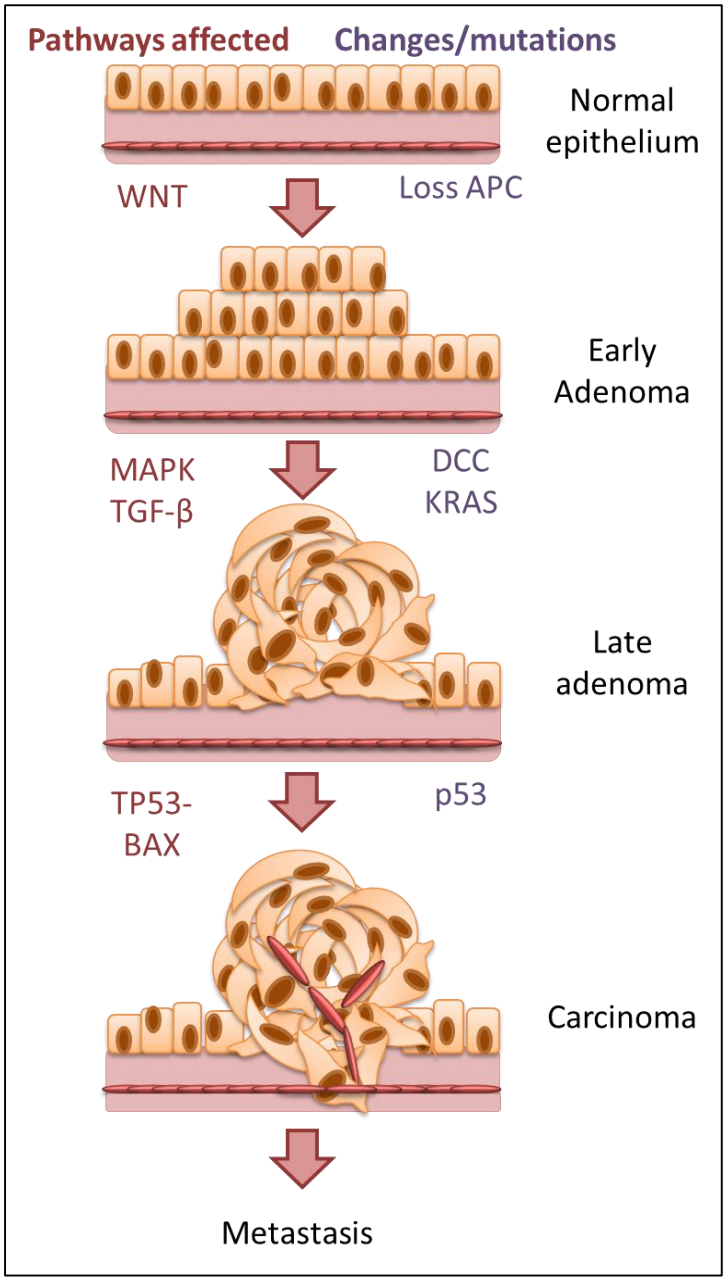

Figure 1.2: The adenoma-carcinoma sequence and associated pathways. Loss of APC is an initiating mutation in many colorectal cancers that leads to loss of cell cycle control and abnormal proliferation. Exposure to additional genetic insults such as chronic inflammation or repeated exposure to dietary carcinogens, e.g. heterocyclic amines and heme iron, can cause an accumulation of mutations in the colonic epithelium and the subsequent loss of proto-oncogenes such as KRAS, Deleted in Colorectal Cancer (DCC) and TP53. This can cause the sequential progression of normal epithelium through the early and late adenoma stages into invasive carcinoma and metastasis.

Table 1.2: Mutations in CRC progression (modified from Alrawi *et al*. (20))

Lesion	Mutation Frequency (%)				
	APC	B-Catenin	KRAS	DCC	TP53
ACF	<5	0	10-95	0	0
Adenoma	40-65	0	0-40	0	0
Adenocarcinoma	40-80	15	40-60	40-70	50-80

colonic mucosa making it harder to identify and hence are less well understood (22, 23). These ACF differ from classical ACF by early dysregulation of β-catenin, fast growing crypts and more consistent progression to tumours in mouse models (24).

1.1.1.5 Key Genes and Pathways in CRC

Mutations in the Wnt signalling pathway are regarded as the instigating factor in colorectal cancer development and mutations in *APC* are the most common mutation in these cancers, being found in 80% of colorectal adenomas and carcinomas (25, 26). APC forms part of the β-catenin destruction complex and loss of APC leads nuclear accumulation of β-catenin and expression of the TCF/LEF pathway. These transcription factors are involved in the activation of *cyclin D1*, *Cdk4* and *c-myc* which control G1-to-S phase cell cycle transition, and their constitutive activation leads to aberrant cell proliferation, differentiation and migration (27-29). Germ-line mutations of *APC* in humans lead to FAP and a similar phenotype occurs due to β-catenin stabilising mutations even in the presence of wild-type APC (30, 31).

Humans have three *RAS* genes; *KRAS*, *NRAS* and *HRAS*; with *KRAS* mutated in ~45% of colon cancers. It is part of the mitogen activated protein kinase (MAPK) signalling pathway and encodes a guanosine triphosphatase (GTPase) which regulates cell proliferation and survival. It is activated in response to a ligand binding a receptor tyrosine kinase (RTK) such as epidermal growth factor receptor (EGFR) (32). Aberrant activation of KRAS without concurrent *APC* mutation usually leads to self-limiting hyperplastic lesions but KRAS mutation occurring downstream of initiating mutations in *APC* can result in tumour progression (33). There is also evidence that activated KRAS is required for tumour maintenance, as withdrawal of inducible *Ras* from mouse models of CRC leads to tumour

regression (34-36). This could involve the role of KRAS in the Warburg effect, which is the utilisation of aerobic glycolysis by malignant tumour cells (37).

P53 is a tumour suppressor transcription factor described as the “guardian of the genome” (38). In normal conditions, p53 is subject to several layers of post-translational regulation, primarily binding and ubiquitylation by mouse double minute 2 homolog (MDM2) and degradation by the proteasome (39). It is activated by alteration of normal cell homeostasis such as DNA damage or oxidative stress, upon which it can halt cell cycle progression and trigger pathways involved in DNA repair or apoptosis to prevent damaged cells from proliferating (40). The mechanisms for deciding between these two pathways have not been determined. P53 can halt cell cycle progression at G1/S phase by up-regulating *CDKN1A* (p21) or at G2/M via GADD45 to allow DNA repair enzymes to act (41). If the damage is beyond repair, it can instigate programmed cell death which is believed to be its primary tumour-suppressor function (42). It can achieve this by up-regulating pro-apoptotic genes, down-regulating anti-apoptotic genes and via transcription-independent mechanisms (38). P53 is inactivated on over half of human cancers and this leads to loss of this tumour suppressive effect, tumour progression, metastasis, and worse prognosis (43).

Deleted in Colorectal Carcinoma (*DCC*) is another gene down-regulated in more than half of colorectal cancers. DCC is a transmembrane receptor which suppresses apoptosis when bound to its ligand netrin-1 but promotes apoptosis when netrin-1 is absent via a novel caspase-dependent pathway (44, 45). DCC can act as a tumour suppressor in the absence of netrin-1 via this pro-apoptotic function, but also as an oncogene in the presence of its ligand or activating mutation by suppressing apoptosis (44). Similar to *KRAS*, mutation in *DCC* is not an activating mutation in CRC but contributes to CRC progression downstream of *APC*.

1.1.1.6 Genetic Instability in CRC

CRCs can arise from one or a combination of three different mechanisms, namely chromosomal instability (CIN), CpG island methylator phenotype (CIMP), and microsatellite instability (MSI). Aneuploidy and loss of heterozygosity (LOH) are major factors in CIN tumours which constitute most sporadic tumours (~85%) and are most likely caused by dysfunctional chromosome duplication or segregation during mitosis (46). Other than *APC*, mutations in the CIN pathway include the activation of proto-oncogenes such as *KRAS*, *BRAF* and deactivation of tumour suppressors *p53*, *p15*, *p16*, *BRCA1*, retinoblastoma (*RB*), *SMAD4*, *DCC* and loss of heterozygosity in 17p and 18q chromosome arms (47-50).

Microsatellite instability (MSI) involves inactivating mutations in the DNA mismatch repair genes that are responsible for correcting DNA replication errors, due to genetic alterations in short repeated sequences called microsatellites. Microsatellites are repetitive sequences of DNA generally featuring 1-6 base pairs repeated 5-50 times. Errors in repair of this microsatellite DNA can cause frameshift mutations and MSI as seen in HNPCC and 12-15% of sporadic CRCs (51-54). There is an overlap of genes involved in the CIN and MSI pathways which contain microsatellites including genes for *TGFβ*, *CCND1* and *SMAD* (55). MSI abnormalities are observed in HNPCC ACF in 100% of cases, highlighting its importance as an early event in this form of familial CRC (20)

The CpG island methylator phenotype (CIMP) involves hypermethylation of CpG dinucleotides in the promotor regions of key genes leading to their epigenetic silencing (56). This promotor methylation is observed in ~25% of CRC. CRC-associated genes affected by CIMP silencing include *BRAF*, *p16INK4a*, *MGMT* and *PIK3CA* (55). Moreover, the DNA mismatch repair protein MLH1 is silenced in this manner in 80% of sporadic MSI colorectal

cancers, with the DNA methyltransferase inhibitors representing a new class of drugs targeting this aspect of carcinogenesis (57, 58)

Finally, microRNAs (miRNAs) are small, non-coding RNA molecules containing ~22 nucleotides involved in gene silencing and post-transcriptional regulation of gene expression by base-pairing with mRNA (55, 59). Recent research has highlighted the role of miRNA dysregulation in cancer. miRNAs are involved in aberrant proliferation and differentiation, evading apoptosis and growth suppression, promoting invasion, metastasis and angiogenesis. Attention is now turning to using miRNAs as biomarkers for tumorigenesis and as targets for cancer treatment (60-62).

1.1.1.7 The Tumour Microenvironment

Tumours are composed of both tumour cells and non-tumour cells, and the surrounding environment becomes significantly altered once neoplastic transformation has begun. This tumour microenvironment (TME) consists of blood vessels, immune cells, fibroblasts and the extracellular matrix (ECM) surrounding the tumour and plays a central role in tumour maintenance and progression.

1.1.1.7.1 Stroma: The stromal tissue of a tumour is the collection of supportive and connective tissue comprising different cell types, ECM and the vasculature. Immune cells in the stroma initially provide an anti-tumour response but this can be co-opted by the tumour to contribute to pathogenesis.

Remodelling of the ECM is a feature of the TME. This is largely achieved by the production of matrix metalloproteinases (MMPs) by cancer-associated fibroblasts (CAFs). Degradation of the ECM by MMPs allows infiltration by endothelial cells leading to angiogenesis (63). Growth factors are also released from the ECM, such as FGFR1 and TGFβ, which can promote angiogenesis, as well as some potential inhibitors, highlighting the complex role of MMPs in the TME (64-68).

Degradation of the ECM can lead to tumour cell growth as well as an endothelial cell migration, facilitating invasion and metastasis. Indeed, inhibitors of MMPs have been shown to reduce cancer cell invasiveness *in vitro* and *in vivo* (69-71).

1.1.1.7.2 Angiogenesis: Angiogenesis plays a critical role in tumorigenesis. Tumours may exist *in situ* for months or years limited to 2-3mm diameter until alterations in the TME lead to the growth of vasculature allowing further growth, either by the production of pro-angiogenic factors or down-regulation of angiogenic inhibitors (72, 73). These mediators of angiogenesis in cancer, especially vascular endothelial growth factor (VEGF), are a target for anti-cancer drugs but concerns exist about the ability of anti-angiogenic therapy to select for aggressive cancer cells and possibly drive invasion and metastasis (74-76), while clinical trials showed only modest survival benefits (77-79).

VEGF is up-regulated in around half of CRC cases (80). It acts on endothelial cells to stimulate proliferation and invasion by the vasculature (81-83). It also stimulates the expression of anti-apoptotic proteins and promotes the survival of these cells (84-86). Hypoxia and necrosis induce the expression of VEGF which is exploited by tumours proliferating beyond their available blood supply, as evidenced by the specific induction of VEGF in tumour cells immediately proximal to necrotic foci (87, 88). VEGF expression is also correlated with

activation of oncogenes during carcinogenesis and can be promoted by inflammatory mediators common in the tumour microenvironment such as interleukin (IL)1β and IL6, and can be induced by tumour necrosis factor (TNF)α in an nuclear factor (NF)-κB-dependent manner (87, 89-92).

1.1.1.7.3: Cytokines and Chemokines in the Tumour Microenvironment: A dysregulated immune response plays a key role in tumour initiation and promotion. This can be via pro-inflammatory signals which induce DNA damage, inhibit apoptosis and stimulate cell proliferation and angiogenesis, and anti-inflammatory mediators which can allow tumour cells to evade immune surveillance. The normal immune response to tissue injury is self-limiting while the response in cancer is chronic and uncontrolled, so tumours have been described as “wounds that do not heal”.

A dysregulated immune response and chronic inflammation is a significant risk factor for CRC, for example by the production of reactive oxygen species (ROS) by NADPH oxidase or reactive nitrogen species (RNS) by nitric oxide synthase, whose production can be promoted by cytokines such as TNFα, IL6 and TGFβ. ROS and RNS cause oxidative stress to the cell which can lead to tumorigenesis (93-96). As such, some cytokines and chemokines that are important in the immune response to cancer can also promote tumorigenesis in some contexts.

IL1β, IL6 and TNFα are pro-inflammatory cytokines which can act as tumour initiators by producing ROS and RNS, and as tumour promoters by mechanisms such as suppressing apoptosis and driving proliferation and angiogenesis (97-101). They also form part of the anti-tumour response, such as the activation and trafficking of T-cells of the adaptive immune system (100). These complex effects can depend on factors such as the location or

degree of expression (100, 101). For example, TNFα expression in macrophages and mast cells is associated with higher survival, while a poorer prognosis is associated with TNFα in the tumour stroma (93, 102, 103). In contrast, IL10 is also associated with anti-inflammatory responses. IL10 can reduce pro-tumorigenic inflammation by suppressing NF-κB signalling but can also allow tumours to evade immune surveillance and facilitate apoptosis resistance, with elevated levels of IL10 associated with poor prognosis in B cell lymphoma (93, 104-108).

Chemokines are a class of chemotactic cytokines (109). Generally, *glutamic acid-leucine-arginine* (ELR)-positive chemokines such as CXCL1, CXCL2 and CXCL5 are pro-angiogenic while ELR-negative chemokines are angiostatic (110). CXCL1 is the most abundant chemokine expressed by TAMs and has been implicated in cancer growth and metastasis via NF-κB activation (111). CXCL2 is also involved in tumorigenesis, with knockdown of CXCL2 in a metastatic human colon cancer cell line (LoVo cells) leading to a decrease in the expression of cancer stem cell markers (112). CXCL5 is also associated with cancer proliferation and metastasis and is over-expressed in late-stage human cancers, where it correlates with poor prognosis (113-116).

1.1.1.7.4 Immune Cells in the Tumour Microenvironment: The pro- and anti-tumorigenic roles of key immune cells are presented in Figure 1.3. Cancer-associated fibroblasts (CAFs) are the predominant cell in the stroma and can promote angiogenesis as well as primary tumour growth, invasion and metastasis (117-123). CAFs induce an inflammatory environment by overexpressing cyclooxygenase (COX)-2 as well as chemoattractants such as macrophage chemoattractant protein (MCP)-1, granulocyte-macrophage colony-stimulating factor (GM-CSF) and IL8 which promote infiltration of neutrophils and other pro-inflammatory leukocytes (124-128).

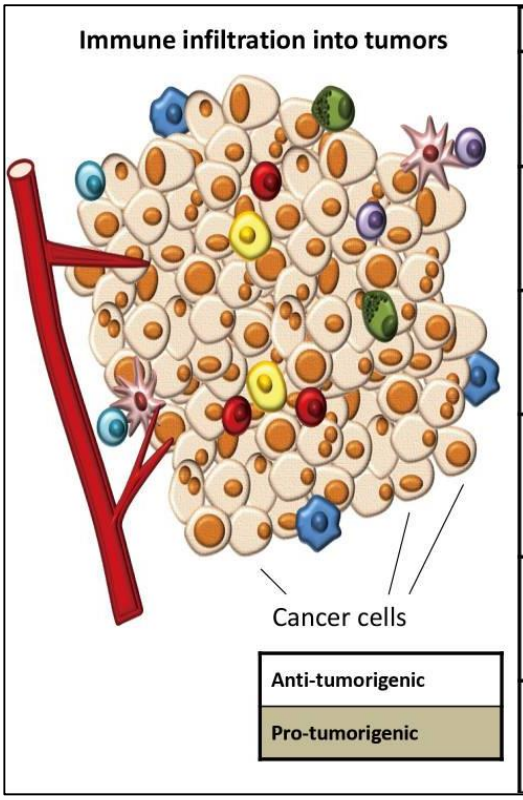

Immune Cell		Roles in cancer
	Dendritic cell (DC)	Release cytotoxic cytokines Antigen presentation to T cells
		Suppress T cell functions Promote tumor growth and progression
	T cell (CD8+, CD4+)	Directly lyse cancer cells Release cytotoxic cytokines
		Release tumor promoting cytokines
	Treg	Restore homeostasis to reduce chronic inflammation
		Suppress anticancer immune responses Stimulate inflammatory cytokine production
	Macrophage	Release cytotoxic cytokines Antigen presentation to T cells
		Promote angiogenesis, tumor proliferation, chemotaxis, invasiveness, and metastasis
	Myeloid derived suppressor cell (MDSC)	Limited
		Suppress T cell functions Recruit immunosuppressive immune cells
	NK cell	Release cytotoxic cytokines Directly cytotoxic to cancer cells
		Limited

Figure 1.3: Key cells in the tumour microenvironment. A range of immune cells can be found in different parts of the tumour microenvironment at different stages of cancer development. These can produce pro- and anti-inflammatory cytokines and chemokines that can have pro or anti-tumorigenic effects depending on a number of factors, including the level and duration of their expression, their location and the receptors expressed on the surrounding stromal, immune and tumour cells. Figure from Markman and Shiao, 2015 (129).

Myeloid-derived suppressor cells (MDSCs) are a family of immune cells similar to immature monocytes and neutrophils with potent immune-suppressive activity (130). They are divided into two classes; monocytic MDSCs (M-MDSC) and polymorphonuclear (also called granulocytic) MDSCs (PMN-MDSC), with PMN-MDSCs predominant in tumour-bearing mice (131). MDSCs suppress immune function by a number of mechanisms including the production of ROS and RNS which suppress $CD8^+$ T-cells (132-136), by depleting L-arginine and L-cysteine which leads to the down-regulation of the T cell receptor (TCR) complex, and by expansion of regulatory T (T_{REG}) cells (137-139). MDSCs also interfere with T-cell trafficking by reducing L-selectin in naïve T-cells, and nitration of chemokines such as CCL2 which inhibits T-cell infiltration (140, 141). As well as inhibiting the anti-tumour T-cell response, MDSCs suppress natural killer (NK) cells and dendritic cells (DCs), and cross-talk between MDSCs and macrophages increases production of immune-suppressive IL10 by MDSCs and reduces expression of anti-tumorigenic IL12 by macrophages (142-144). This suppression facilitates immune evasion by the tumour and contributes to cancer progression, with MDSCs associated with advanced disease and poor prognosis in human cancers, whilst elimination of MDSCs increases the CD4- and CD8-mediated anti-tumour response (145).

Natural killer (NK) cells are potent anti-cancer effectors of the innate immune system. They can generate a cytotoxic response to cancer cells which do not express Major Histocompatibility Complex (MHC)-I fragments, leading to necrosis or apoptosis of the targeted cell (146). NKs also mediate the downstream inflammatory response by production of cytokines and chemokines (147). These cells are often reduced in cancer and low NK activity is associated with poor prognosis (148-150). As a result, methods for improving the anti-tumorigenic activity of NK cells have been investigated including adoptive transfer of NK cells, enhancing NK cell activation and proliferation, and breaking NK cell anergy (146, 151).

Dendritic cells (DCs) are antigen-presenting cells (APCs) of the immune system with both pro- and anti-tumorigenic roles in cancer development (152). In their role as APCs, they present antigens to T-cells to activate the adaptive immune response. Despite the presence of DCs in the TME, immune surveillance fails which suggests impaired DC function. This may be due to hypoxia, increased levels of lactate and adenosine, decreased pH and expression of IL10 in the TME (152). As well as failing to prime an anti-tumour response, DCs can promote tumour progression by overexpressing pro-tumorigenic IL6 and galectin-1, and can induce the differentiation of naive $CD4^+$ T-cells into IL10-producing T_{REG} cells leading to immune suppression (153, 154). Reactivating or normalising DCs' anti-tumour response could be an effective cancer treatment, and vaccination using DCs activated and loaded with tumour antigen-associated peptides *ex vivo* induced a favourable immune response (155).

Macrophages are a class of immune cells with important functions in antigen-presentation and phagocytosis (156-158). They also have pro- and anti-inflammatory and pro- and anti-tumorigenic roles. In cancer, M1-type macrophages generate a chronic inflammatory environment via production of cytokines such as IL6 and TNFα which induce mutagenesis and apoptosis-resistance (159). Later, tumour-associated macrophages (TAMs) promote angiogenesis, migration, invasion and metastasis in the primary tumour via production or stimulation of factors such as VEGF, EGF and MMPs. At this stage, the predominant macrophage phenotype in the TME changes to the M2 immune-suppressive type, facilitating immune evasion by the tumour (160, 161). A meta-analysis of human studies shows strong evidence that macrophage density in the TME correlates with poor prognosis (162).

T-cells are classed according to their expression of T-Cell Receptor (TCR) as either γδ or αβ. The αβT-cells are further subdivided into $CD8^+$ cytotoxic T-cells (CTLs) and $CD4^+$ helper T-cells (T_h) cells. CTLs can have potent cytotoxic effects on cancer cells by releasing granules containing perforin and granzymes, and can also induce FasL-mediated apoptosis (163). Their

effectiveness is reduced in tumours by deficiency of APCs such as DCs and macrophages, and the maintenance of an immuno-suppressive environment by CAFs, TAMs and T_{REG} cells. A subset of pro-tumorigenic CTLs which are deficient in perforin but express pro-inflammatory cytokines have also been identified (164).

$CD4^+$ T_h cells include T_h1, T_h2, T_h17 and T_{REG} cells. T_h1 cells suppress tumorigenesis by producing IFNγ, TNFα, IL2 and IL12 by activating and regulating CTLs, and by inducing the secretion of IL1β and IL6 by macrophages (165, 166). This demonstrates that even pro-inflammatory cytokines associated with cancer risk can be effective against tumour cells when accurately managed.

T_h2 cells have been associated with increased cancer risk by inducing proliferation, angiogenesis, invasion and metastasis via a number of mechanisms including inducing VEGF expression, activation of EGF-producing TAMs, and tumour-promoting inflammation (167-171). However this is an oversimplification of their role and other facets of T_h2 immune response, such as production of IL4 and infiltration of eosinophils, can inhibit tumour growth (172). Moreover, T_h2 cells do not rely on presentation of Major Histocompatibility Complex (MHC)-I molecules as CTLs do, and so can respond to MHC-I-negative tumours (173). T_h2 cell transfection has also been shown to eliminate tumour cells in cancer models by inducing eosinophil chemotaxis, macrophage activation and tumour necrosis, in a T_h1- and CTL-dependent manner (173-175). A similar result was observed following T_h2 cell adoptive transfer into myeloma and B-cell lymphoma cancer models, which eradicated cancer cells by inducing inflammation and macrophage infiltration in a manner independent of B-cells, Natural Killer T cells, CTLs cells and IFNγ (176).

T_h17 cells are also associated with increased cancer risk by inducing inflammation, proliferation, angiogenesis and recruitment of pro-tumorigenic neutrophils, but are also involved in the anti-tumour response by activating CTLs (177-180).

In contrast, T_{REG} cells contribute to cancer progression by their immuno-suppressive properties. Tumours display preferential recruitment of T_{REG} cells which may constitute 20-30% of the $CD4^+$ cells in the TME, as opposed to 5-10% of the normal pool (181). T_{REG} cells correlate with poor prognosis in a number of cancers and these cells have been shown to enhance pro-tumorigenic actions of CAFs, tumour cells, macrophages, MDSCs and regulatory B cells (B_{REG}), while inhibiting tumour-suppressive NK cells and CTLs (182, 183). However, T_{REG} cells can also reduce cancer risk by down-regulating excess inflammation and are associated with improved prognosis in some cancers, including CRC (181, 184-186).

1.1.1.8 Clinical Treatment of CRC

Treatment for CRC depends on stage of the cancer. Surgery alone is used in Stage 0 and I, and has a high rate of success. Chemotherapy is used to treat Stage III and IV and occasionally Stage II. Radiotherapy is not routinely used due to the sensitivity of the bowel to radiation (187). The major chemotherapy agents used to target CRC include 5-fluorouracil (5-FU), principally a thymidylate synthase (TS) inhibitor; capecitabine, which is metabolised to 5-FU; irinotecan, an inhibitor of topoisomerase I; oxaliplatin, a non-targeted cytotoxin believed to inhibit DNA synthesis by forming crosslinks between DNA strands; and trifluridine/tipiracil, a compound drug comprising cytotoxin trifluridine and the thymidine phosphorylase inhibitor tipiracil (188-192). Targeted therapies are also available such as bevacizumab, which inhibits VEGF with limited success; cetuximab, which is an EGFR inhibitor; and regorafenib, a multi-kinase inhibitor approved for use against metastatic CRC (193-195).

More recently, immunotherapy has been successful in improving the prognoses of many cancers. Unfortunately, progress in using immunotherapy to treat CRC has been slower. Programmed Death-1 (PD-1) inhibitors have been shown to effectively treat only MSI CRC deficient for mismatch repair (MMR-d) which comprise ~15% of sporadic CRCs (196-199).

Tumours up-regulate PD-L1 to suppress the immune response by binding to PD-1 receptor on effector T cells, a defence that can be targeted by PD-1 inhibitors. Anti-CTLA-4 immunotherapy drugs have also so far proved ineffective in CRC, although studies using anti-CTLA-4 in combination therapy are ongoing, as well as trials on immunotherapy targets LAG-3, TIM-3 and IDO (198). Finally, recent studies have shown that cancer treatment can be affected by the composition of the host microbiota. For example, studies have suggested a role for the microbiota in PD-1 immunotherapy for melanoma, non–small cell lung cancer, and renal cell carcinoma, as well as in response to chemotherapy (200-203). Clinical response to PD-L1 correlated with the relative abundances of *Ruminococcaceae* and *Akkermansia muciniphila*, and oral supplementation of *A. muciniphila* increased the recruitment of $CCR9^{+}CXCR3^{+}CD4^{+}$ T-cells into mouse tumours (200, 201).

Microbial interventions have also been considered for the treatment for CRC and these are addressed in section *1.3.2.1.*

1.2 Mouse Models of CRC

In this thesis, I have used two common mouse models of colorectal cancer; APC^{MIN} mice, a model of familial CRC; and AOM-treated mice, a model of sporadic CRC.

1.2.1 APC^{MIN} Mice – A Model of Familial CRC

Research into familial CRC makes use of mouse models characterised by defects in the *Apc* gene. Several models encompassing different *Apc* mutations have been established, with the *multiple intestinal neoplasia* (APC^{MIN}) model predominant in the literature. Familial Adenomatous Polyposis (FAP), the hereditary human cancer, is also caused by mutations in the *APC* gene.

1.2.1.1 Adenomatous Polyposis Coli, the β-catenin Destruction Complex and Wnt

APC is a tumour suppressor gene that forms part of the intracellular β-catenin destruction complex where it facilitates the phosphorylation of β-catenin by glycogen synthase kinase 3β (GSK3β), leading to β-catenin being marked for degradation by E3 ubiquitin ligase TrCP1 (β-Trcp). Once marked with ubiquitin, β-catenin is degraded by the proteasome by the normal pathway. Disruption of the β-catenin destruction complex thus leads to the activation of the Wnt signalling pathway, as was described in section *1.1.1.5 Key Genes and Pathways in CRC.* Dysregulation of APC-mediated β-catenin degradation can therefore lead to loss of cell cycle control in a cell-autonomous manner (204).

1.2.1.2 APC^{MIN} Mice

Mice heterozygous for the *Apc* gene are well established as models for familial CRC. The first *Apc* mouse mutant generated, referred to as the *multiple intestinal neoplasia* (*Min)* model (205), developed around 30 tumours in C57BL/6J mice, mostly in the small intestine. The mutation was identified as fully penetrant and autosomal dominant, with mice demonstrating a shortened lifespan of ~119 days. This mutation was subsequently identified as a nonsense mutation at amino acid 850 of APC (206) on proximal mouse chromosome 18 (207).

Subsequent studies determined that the development of intestinal neoplasia was a result of Knudson's two-hit hypothesis, involving loss of the wild-type APC protein as a result of random mutation or mitotic recombination, thus causing a loss of heterozygosity (LOH) of *Apc* (208, 209).

APC localises to the nucleus as well as the cytoplasm and regulates the nuclear export and cytoplasmic degradation of β-catenin via two N-terminal nuclear export signals (210, 211). Zeineldin *et al*. investigated the nuclear role of APC by generating a mouse model with a compromised APC nuclear import signal (APC^{mNLS}*)* which displayed increased tumorigenesis when treated with genotoxic agent azoxymethane (AOM) and colitis-inducing dextran sulphate sodium (DSS) (212). The authors suggest that aberrant Wnt signalling is insufficient for tumorigenesis and that inflammation is also necessary, highlighting another study in which mice treated with a single dose of AOM fail to develop tumours without subsequent DSS-induced colitis (213). They propose *Apc*-mutant mice undergo tumorigenesis due to an additional anti-inflammatory role of APC and show how APC^{mNLS} mice display increased inflammation and a reduction in goblet cells and mucin production, possibly contributing to epithelial barrier permeability. Mutations in *K-ras* and *p53* have not been observed in APC^{MIN} tumours despite being common in human sporadic cancer, although their short lifespans

prevent the accumulation of mutations and transition from benign adenoma to invasive carcinoma (214-216).

1.2.2 Inducible Models of Sporadic CRC

As a model for sporadic cancer, mice can be treated by a number of genotoxic agents that cause widespread untargeted mutation in the murine colonic epithelium. This reflects the accumulation of genetic damage seen in the human intestine which can lead to CRC in later life. The first chemically-induced models of CRC involved mice fed dibenzanthracene and 20-methylcholanthrene (217). Later, hydrazine in cycad flour was identified as a possible colonic carcinogen in humans, which caused tumours in the liver, kidney, lung and intestine when fed chronically to rats (218). The carcinogen was subsequently identified as cycasin, which is hydrolysed to methylazoxymethanol (MAM) in the liver (219-221). Later studies used 1,2-dimethylhydrazine (DMH), which is metabolised to azomethane and azoxymethane (AOM). AOM is subsequently hydroxylated to form MAM in the liver (Figure 1.4) (220, 222-225). AOM has now become the preferred method as it is more stable in solution and requires fewer metabolic steps to become active, and hence can be used in lower doses (226, 227).

1.2.2.1 Azoxymethane-Treated Mice

Repeated administration of AOM to rodents results in the development of intestinal tumours, and is a well-studied model of sporadic CRC. The reactive metabolite(s) of AOM initiate cancer development by alkylating guanine residues in DNA, thereby facilitating base mispairing. The AOM-induced carcinogenic insult ultimately leads to tumours primarily in the distal large intestine which reflects the predominant localization of spontaneous CRC in humans. These tumours, however, rarely display invasion or metastasis (228).

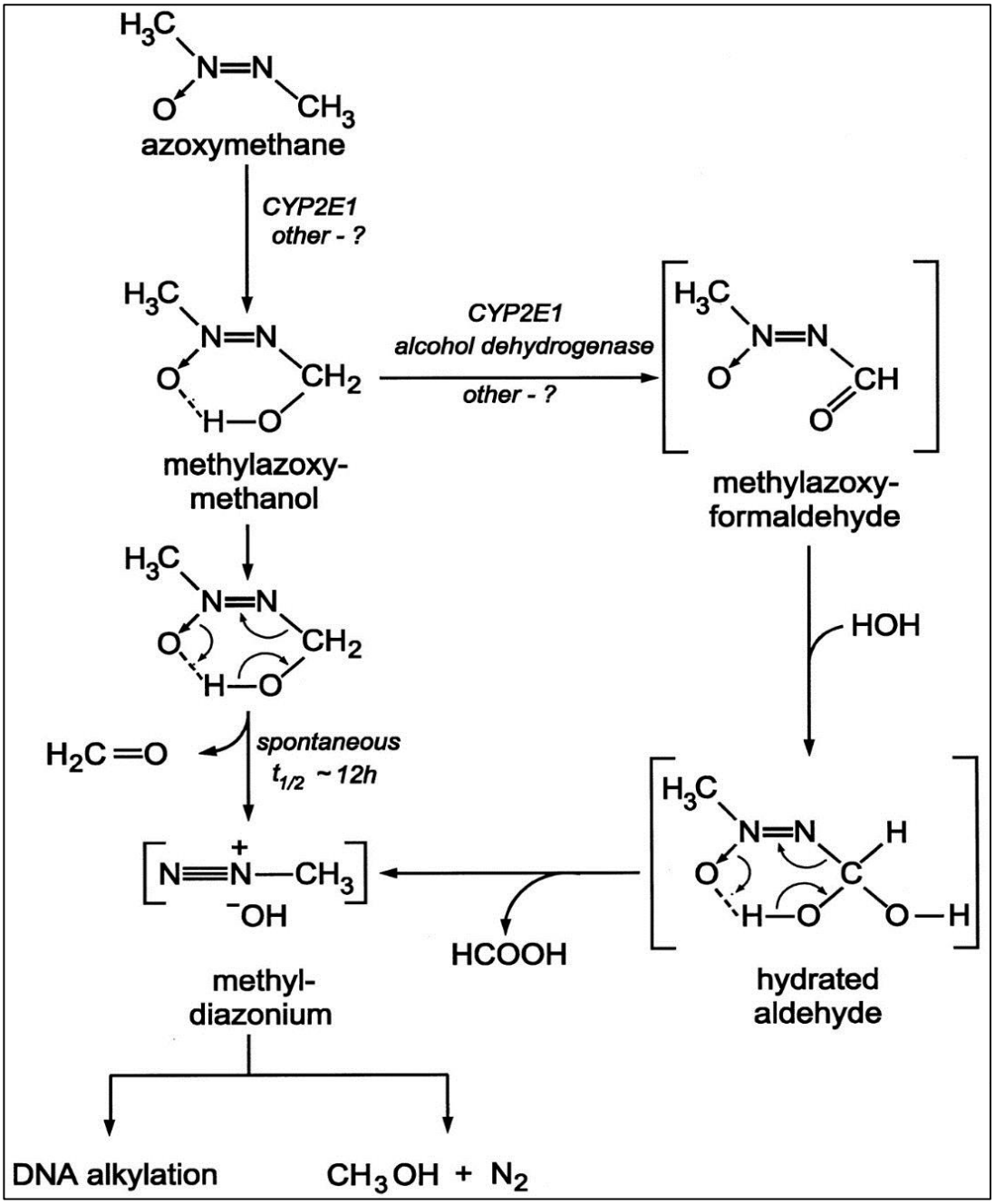

Figure 1.4: Two metabolic pathways of AOM and MAM activation. AOM is hydroxylated by P450 enzymes in the liver to form MAM, which is in turn oxidised to the methyldiazonium ion which has the capacity to alkylate DNA. Alternatively, MAM may decay spontaneously to the methyldiazonium ion. Figure from Sohn *et al*., 2001 (229).

1.2.2.2 Strain Sensitivity to AOM

Different mouse strains have been shown to exhibit differential sensitivity to tumorigenesis following AOM administration (Table 1.3) (230-233). Sensitive strains such as A/J mice can develop over 40 colonic adenomas after AOM treatment while resistant strains such as AKR/J develop <1. This can reflect the genetic background of the mouse but must also account for the environmental conditions in which the mice are housed, including the diet and the gut bacteria that the mice acquire, as well as procedural differences such as route of administration and dosage (234). This is further complicated by interaction between confounding factors, such as between diet and strain, and an apparent complex and polygenic interaction between backgrounds observed in crossed strains (234). Tumours produced were of similar morphology regardless of AOM sensitivity suggesting similar pathways lead to tumorigenesis in each strain (235). A study on the relative levels of DNA alkylation in susceptible and resistance mouse strains suggested that the difference is not a result of the number of DNA methyl adducts produced, nor were CYP2A1 levels found to correlate with tumour susceptibility, suggesting that the foundation for differential strain susceptibility is downstream of DNA alkylation (226, 236). Back-cross experiments showed that tumour susceptibility is not inherited as a dominant trait and suggested a "resistance factor" exists in resistant AKR/J mice. AOM-susceptible A/J mice did show an increase in apoptosis, proliferation and expression of c-myc mRNA in the top third of colonic crypts compared to resistant AKR/J mice, suggesting a role for cell turnover (232).

1.2.2.3 Pathways to CRC in AOM-Treated Mice

While the mutations induced by AOM administration are untargeted, studies in mice and rats have revealed that AOM-induced tumours resemble human CRC in many respects at the molecular level. In particular, AOM-induced tumours display aberrant protein expression for

Table 1.3: Strain sensitivity to carcinogens (modified from Rosenberg *et al*. (233))

Strain	Carcinogen	Tumours per Mouse	References
A/J	DMH, AOM	9.2–41.6	(234, 237-240)
SWR/J	DMH, AOM	9.5–16	(237, 239-241)
FVB/N	AOM	3.6	(235)
C57Bl/6b	DMH, AOM, MAM	0–5.5	(235, 237, 241-244)
BALB/cJ	AOM	1–2	(245-247)
AKR/J	DMH, AOM, MAM	<1.0	(234, 235, 237, 239, 240, 246, 248)

APC and altered cellular localization of β-catenin (249). Moreover, consistent with findings in human CRC, AOM-induced tumours have mutations of *K-ras*. Levels of enzymes involved in prostaglandin and nitric oxide synthesis, such as COX-2 and inducible nitric oxide synthase, have also been reported to be elevated (249). In contrast, *Apc* mutations are less common in ACF but are observed in adenomas and adenocarcinomas, while mutations in *Tp53* are uncommon in chemically-induced models of carcinogenesis in rodents (250-253). Moreover, in a study of genomic instability on AOM-induced models, 75% of mice showed no evidence of CIN but 81% showed low level MSI with high level MSI observed in an A/J colon tumour-derived cell line (254). Finally, similar to humans whereby CRC incidence rates are generally higher among males than females, the incidence of CRC in DMH-treated outbred male Wistar rats was higher than in female rats, although no differences were observed in AOM-treated inbred mice (234, 255).

1.3 The Gut Microbiota

The human microbiota is the community of bacteria, archaea, protists, fungi and viruses that live in and on the human body (256). The cells of our microbiota are estimated to outnumber our nucleated human cells by a ratio of about 13:1, about 70% of which occupy our gastrointestinal tract (203, 257), although this ratio drops to approximately 1.3:1 when enucleated hematopoietic cells are included (258). These gut microbiota, most importantly gut bacteria, play vital roles in immune modulation, metabolism, inhibition of pathogens and structural development (259-262). They have also been implicated in intestinal disease, including CRC and IBD (263, 264). The gut "microbiome" is sometimes used synonymously with the gut "microbiota" but can also refer to the full collection of genes present in the microbiota of a community. The "gut microbiota" will henceforth be used to describe the gut bacteria only.

1.3.0.1 16S rRNA Gene Sequencing

16S ribosomal RNA (rRNA) is a component of the prokaryotic ribosome used for phylogenic reconstruction. The DNA region coding bacterial 16S rRNA comprises nine hypervariable regions separated by conserved regions that can be targeted with universal primers. 16S rRNA gene sequencing provides high-throughput and affordable taxonomic analysis of communities such as the microbiota, but disadvantages include biases introduced by the universal primers, copy number variation or sequencing platform. Another limitation is the inability to consistently annotate to species level, with fewer than 20% of operational taxonomic units (OTUs) assigned to a species in an evaluation of 16S rRNA gene sequencing methodologies (265). OTUs are functional clusters, into which 16S rRNA sequences sharing an arbitrary level of similarity (usually >97%) are collapsed (266). More informative analysis

can be achieved through metagenomic shotgun sequencing but this is expensive and generates huge amounts of data that require advanced bioinformatics analysis (267, 268).

1.3.1 The Gut Microbiota - Bacteria

The bacterial gut microbiota comprises over 5000 bacterial species and 3 million genes, and possibly over 35,000 species in the collective human microbiome (269, 270). It is dominated by the phyla *Firmicutes* and *Bacteroidetes*, featuring smaller proportions of *Proteobacteria*, *Verrucomicrobia*, *Actinobacteria*, *Fusobacteria*, and *Cyanobacteria* (261, 271). This consistency of phyla, combined with significant inter-individual variation within the phyla, suggests a selective pressure to maintain the higher taxonomic structure with a functional redundancy at lower levels sufficient to maintain proper function (203, 271, 272).

3.1.1 Colonisation and Composition of the Gut Microbiota

The intestinal tract has been considered sterile at birth, with colonisation beginning immediately through contact with the mother and environmental bacteria, and although recent research has suggested colonisation of the placenta by *Streptococcus agalactiae* in approximately 5% of pregnancies, the possibility remains that this is as a result of sample contamination (273-277). The newborn microbiota is reflective of the delivery method, with babies delivered by Caesarean section having a microbiota characterised by fewer *Bifidobacterium* species compared to vaginal births (278). This colonisation period is crucial in development and lasts for approximately 1-2.5 years (279-281). The microbiota then remains largely stable until old age, in the absence of disruptions such as long-term dietary changes or migration (282, 283). Further changes to the microbiota are observed later in life, such as reduced diversity and symbiotic species and increased enteric bacteria. The

association between these changes and old age, age-related chronic inflammation, changes to diet and shared living spaces is being investigated (284-287).

The upper GI tract contains relatively few microbial inhabitants. The stomach and duodenum contain approximately 10^2 organisms per gram of contents. This rises to 10^4-10^7 in the jejunum, finally reaching ~10^9 colony forming units (CFUs)/mL in the terminal ileum and ~10^{12} CFU/mL of primarily anaerobic bacteria in the colon (261, 288). The composition also changes along the length of the GI tract, with *Bacilli* and *Actinobacteria* enriched in the small intestine, while *Bacteroidetes* and *Lachnospiraceae* are enriched in the large intestine (270).

In general, the healthy microbiota is dominated by the phyla *Firmicutes* and *Bacteroidetes*. The ratio between these phyla is affected by dietary habits and geographic location, both of which correlate closely (289). Different studies have reported both *Bacteroidetes* and *Firmicutes* increased in obesity, possibly due to differences in environmental variables, when in reality the effects probably manifest on a lower taxonomic level (290-293). High diversity is also reported as a characteristic of a healthy microbiota. Indeed, diversity is reduced in diseases such as inflammatory disease, obesity and diabetes, while pathobionts such as *Enterobacteria* and *Fusobacterium* are increased (294-298). Diversity in CRC is more variable however, with some studies reporting decreased diversity in the disease state while others report increased diversity due to outgrowth of pathogenic species such as *Fusobacterium, Clostridia* and *Peptostreptococcus* suited to the tumour microenvironment (299-305).

1.3.2 The Microbiota and Colorectal Cancer

Research has focussed on the role in the microbiota in colon cancer, given the close apposition between the gut microbiome and colonic epithelium (Table 1.4) (306). The proposed mechanisms by which the microbiota may impact CRC include its effects on proto-

Table 1.4: Bacteria associated with human CRC (modified from Jahani-Sherafat *et al*. (263))

Sample	Bacteria	Reference
Faecal	*F. nucleatum*	(307-309)
Tumour	*F. nucleatum*	(310-312)
Faecal	*F. nucleatum, C. difficile*	(313)
Tumour	*F. nucleatum, B. fragilis*	(314)
Faecal, mucosal	*F. nucleatum, Enterobacteriaceae*	(315)
CRC	*F. nucleatum, Pan-fusobacterium*	(316)
Tumour	*Fusobacterium*	(317, 318)
Tumour	*Fusobacterium, Providencia*	(319)
Tumour	*Fusobacteria, Firmicutes*	(320)
Faeces	*Fusobacterium, Atopobium/Porphyromonas*	(321)
Faeces	*Fusobacterium, Porphyromonas*	(322)
CRC	*Fusobacterium, ETBF*	(323)
Tumour	*Fusobacterium, Roseburia*	(324)
Tumour	*Fusobacterium, E.faecalis, ETBF*	(325)
CRC	*Fusobacterium, Leptotrichia, Campylobacter*	(326)
Faecal	*Bacteroides/Prevotella*	(327)
Faeces	*Enterococcus faecalis*	(328)
Faecal, mucosal	*Bacteroidetes, Prevotella*	(329)
Tumour, mucosal	*E. coli*	(330)
Meta-analysis	*H. pylori*	(331)
Bloodstream	*S. gallolyticus, , C. perfringens, C. septicum, Peptostreptococcus*	(332)
Bloodstream	*S. bovis*	(333)

oncogenic pathways such as immune regulation/inflammation, metabolism, proliferation and apoptosis, and the production of microbial metabolites which also have pro- and anti-tumorigenic associations (334). There is precedence for the involvement of bacteria in GI cancer. *Helicobacter pylori* is a constituent of the stomach microbiota which is present in half the global population (335). Nonetheless, it is the strongest known risk factor for gastric cancer and its links to this disease are well established (336).

However, only associative evidence for the role of the microbiota in human CRC exists. The microbiota is altered in the colon of CRC patients and in the tumour tissue compared to healthy controls, with adenomatous polyps representing an intermediate step between the two states (301). Studies investigating these alterations showed that the colonic mucosa of carcinoma patients, but not controls, was colonised by adherent and invasive *E. coli* (330, 337). Moreover, a high-risk CRC group had increased carcinogenic microbial metabolites, including hydrogen sulphide and cresol, in their faeces compared to a low-risk group despite having similar diets, with the difference ascribed to their different levels of enzymatically-active anaerobic bacteria (338). The gut bacteria can also modulate the production of mucus in the intestinal lumen, which in itself can play an important role in CRC by regulating the interaction of the gut bacteria and luminal contents with the colonic epithelium (339-342). Similar to the aforementioned rodent studies, *Lactobacillus* have been shown to reduce faecal and urinary mutagenicity induced by fried meat consumption and to reduce faecal β-glucuronidase, β-glucosidase, nitroreductase and glycocholic acid hydrolase activity (343-348). The microbiota has also been investigated as a potential predictive biomarker for human CRC. Two meta-analyses of human faecal shotgun sequencing studies identified microbial taxonomic signatures with sensitivity to and specificity for CRC which was comparible to common non-invasive clinical screening tests (349, 350). Models based on the functional gene content of the faecal microbiome were also generated, and enrichment of

the *bai* operon, which is involved in microbial bile acid metabolism, was demonstrated at both the genomic and transcriptomic levels (349, 350).

In contrast, evidence for the role of the gut bacteria in promoting CRC in animal models is more widespread. Germ-free (GF) animals completely lack microbial colonisation and tumour formation is reduced in these animals (351-354). Results from the APC^{MIN} mouse model of familial CRC in GF conditions are more ambiguous (355, 356). Faecal microbial transfer (FMT) from CRC patients or animal models of CRC to GF or conventional mice, either APC^{MIN} or administered AOM with or without DSS, increases tumorigenesis in these animals (357-361). Antibiotic treatment also affected tumorigenesis; reducing it in inflammatory models of CRC, but had neutral to harmful effects in APC^{MIN} mice (362-366). It was protective, however, in APC^{MIN} mice with compound mutations in DNA repair or interleukin receptor genes (367-369). Moreover, administration of bacteria associated with cancer risk, for example *Streptococcus bovis* or *Fusobacterium nucleatum*, to susceptible animals was shown to increase proliferation, inflammation and tumorigenesis (370, 371). Furthermore, Onoue *et al*. observed decreased numbers of ACF in DMH-treated GF rats compared to conventional rats. Tumour multiplicity was also increased in gnotobiotic (GB) rats colonised by enterococci compared to GB rats without enterococci, with the tumour numbers in the former group significantly decreased by inclusion of probiotic strain *Bifidobacterium breve* (372). A similar result was achieved by Horie *et al*. concerning adenomas, with the lowest incidence observed in rats mono-associated with probiotic *Lactobacillus acidophilus* (373).

1.3.2.1 Probiotics: Bacteria can also be used to suppress CRC. One such approach involves exploiting prebiotics or probiotic bacteria. Probiotic bacteria are characterised as “live microorganisms that, when administered in adequate amounts, confer a health benefit on

the host", while prebiotics are food compounds which promote the growth and survival of beneficial microorganisms (374-378).

Clinical trials have provided evidence for the beneficial role of prebiotics and probiotics in CRC (Table 1.5). One trial administering a probiotic-prebiotic mixture of inulin, *Lactobacillus* and *Bifidobacterium* to CRC and polypectomised patients showed that the treatment lead to a decrease in colonic epithelial proliferation, decreased abundance of *C. perfringens* and reduced ability of faecal water to induce necrosis in colon cells *in vitro* (379). It also improved epithelial barrier function, reduced patients' exposure to genotoxins and increased production of IFNγ. Similar studies replicated this effect (380-383). Moreover, administration of a mixture of *Lactobacillus* and *Propionibacterium* to healthy subjects reduced faecal levels of bacterial enzyme β-glucuronidase, which is implicated in the activation of AOM and other carcinogens in the colon, as well as β-glucosidase and urease, while *Bifidobacterium*-fermented milk maintained remission in UC patients (384). A prebiotic mixture also decreased irinotecan-induced diarrhoea and enterocolitis in chemotherapy patients (385). However, a study on the effect of prebiotics in post-operative cancer patients showed no improvement in serum levels of IL6, CRP, fibrinogen, white cell count, differential blood count or any reductions in subsequent complications (386).

In animal studies, *Bifidobacterium longum* has been shown to ameliorate AOM/DMH-induced colon carcinogenesis, an effect that is enhanced by co-administration with the prebiotics inulin and lactulose (387, 388). A similar effect was seen with *Lactobacillus* species, although this effect was absent when probiotic administration was delayed until 9 weeks into DMH-administration, suggesting *Lactobacillus* was only protective in the early stages of tumorigenesis (389, 390). Moreover, a reduction in the numbers of tumours that developed was observed after 20 weeks, and not 36 weeks, suggesting *Lactobacillus* increased the latency or induction period of CRC (390).

Table 1.5: Microbial suppression of CRC (modified from Wollowski *et al*. (391))

Probiotic/Prebiotic	Protective Mechanism	References
L. casei, omniflora, or yogurt	Mutations in the Ames test decreased	(392, 393)
Strains of *Lactobacillus* and *Bifidobacterium*, cellular components and metabolites of LAB	DNA damage in colon cells decreased (antigenotoxicity)	(394, 395)
Fermented milk with *L. acidophilus*, *B. bifidum*, *Streptococcus lactis*, and *Streptococcus cremoris*; lactulose	Procarcinogenic enzyme activity decreased: β-glucuronidase, nitroreductase, azoreductase, and detoxifying enzyme activity increased; Glutathione-S-transferase (GST)	(396-399)
L. acidophilus, *S. cremoris*, cell wall of LAB	Binding of mutagens	(400-402)
Milk fermented with *L. acidophilus*	Excretion of mutagens decreased	(403)
Milk fermented with *L. acidophilus* and *Bifidobacterium*	Immune stimulation increased	(404)
Fermentation of prebiotics	SCFA increased, pH decreased, probiotics increased	(405, 406)
Butyrate	Proliferation of transformed cells decreased, apoptosis of transformed cells increased	(407-409)

The ability of probiotics to effect early stage cancer development could be due to their function as anti-mutagenic agents. For instance, *Lactobacillus casei* gavage attenuated DNA damage induced by MNNG in rat colonic and gastric mucosa, while in another study, a selection of lactic acid bacteria (LAB) inhibited the genotoxic effects of MNNG and DMH in the rat colon (394, 395). In both studies, heat treatment eliminated the protective effect of the bacteria suggesting that viable bacteria are required for this effect, although the peptidoglycan fraction and whole freeze-dried *L. acidophilus* were anti-genotoxic. Arimochi *et al*. also demonstrated a reduction in ACF in AOM-treated rats after administration of *L. acidophilus* and *Clostridium perfringens* (410). In particular, *L. acidophilus* reduced the half-life of O_6-methylguanine adducts, suggesting a role in repair by DNA methyltransferase. Other potential mechanisms include the ability of LAB to bind dietary mutagens which limits their ability to interact with the colonic epithelium (400, 411). For example, toxic compounds are detoxified by glucuronidation in the liver, but bacterial β-glucuronidase activity may hydrolyse these molecules and liberate carcinogens. The activity of this enzyme was shown to be reduced in AOM- and DMH-treated rats following gavage with the probiotic *B. longum*; an effect that was enhanced by co-administration with prebiotic inulin, possibly as a result of acidification of the intestinal environment and displacement of bacteria expressing β-glucuronidase (412-414).

Probiotic and commensal bacteria can also provide health benefits by competing with more harmful organisms and preventing them from becoming established in the GI tract (415). LAB have been shown to inhibit the growth of coliforms in the GIT and return *E.coli*-infected rats to a normal microbiota composition while reducing β-glucuronidase activity (416). Probiotics can also produce antimicrobial compounds that inhibit enteric pathogens (417, 418).

LAB have also been demonstrated to modulate the immune response. *L. reuteri,* for example, suppressed inflammatory TNFα and CCL-2 production by lipopolysaccharide (LPS)-

activated monocytes and macrophages in children with Crohn's Disease by inhibiting c-Jun and AP-1 (419-423). A similar anti-inflammatory effect was also observed in rat pups (424). As well as inhibiting pro-inflammatory responses, bacteria may also mediate inflammation to suppress tumorigenesis. *L. casei* strain Shirota administered into the intrapleural cavity of tumour-bearing mice induced the production of pro-inflammatory IFNγ, IL1β and TNFα, which in turn inhibited tumour growth and increased survival (425).

The microbiota may also play a role in the reponse to cancer chemotherapy and immunotherapy, and these have been discussed in section *1.1.1.8*.

The microbiota can also mediate CRC risk by the production of short chain fatty acids (SCFAs). SCFAs, particularly butyrate, have been associated with positive health effects and protection against colon carcinogenesis (426). The majority of butyrate is produced by bacteria in *Clostridium* clusters XIVa and IV, particularly *Roseburia*/*Eubacterium rectale*-related bacteria in cluster XIVa and *Faecalibacterium prausnitzii* relatives in cluster IV (427-430).

1.3.3 Microbial Metabolites

Another key interaction between the host and the microbiota is through the production of microbial-derived metabolites (431). The next section will address microbial metabolism of bile acids.

1.4 Bile Salts

Bile salts are endogenous steroid molecules stored in the gallbladder for post-prandial release into the duodenum to aid lipid digestion. They are derived from cholesterol and are the major route of cholesterol elimination from the body. Food entering the duodenum triggers the production and secretion of cholecystokinin (CCK) from epithelial enteroendocrine cells. CCK then stimulates contraction of the gallbladder and the relaxation of the sphincter of Oddi, allowing bile and pancreatic juices to flow from the ampulla of Vater into the duodenum to aid digestion. Bile in the gallbladder is composed of about 92% water, 6% bile salts, 0.3% bilirubin, 2% fats, and 200mEq/L inorganic salts (432, 433). The major unconjugated bile acids are presented in Table 1.6.

1.4.1 Bile Salt Structure and Function

Bile salts consist of a bile acid conjugated to a taurine or glycine residue. Bile acids are synthesised in hepatocytes via cytochrome P450-mediated oxidation of cholesterol in a multi-step process, with the rate limiting step catalysed by the addition of a hydroxyl group to the carbon-7 position of the steroid nucleus by CYP7A1 or CYP7B1 (434-436). Bile acids are composed of a sterane core comprising three 6-carbon rings and one 5-carbon ring, with the 5-carbon ring featuring a 5- or 8-carbon side chain emanating from 17-carbon position (Figure 1.5). They can display a number of hydroxyl groups at various positions and the number and orientation of these hydroxyl groups define the different bile acids. The primary human bile acids are cholic acid (CA) and chenodeoxycholic acid (CDCA). CA has hydroxyl groups in the 3-, 7- and 12-carbon position of the steroid ring, each in the α-orientation. CDCA is identical except for missing the 12-carbon hydroxyl group. Bile acids are conjugated to a taurine or glycine residue by Bile acid-CoA:amino acid N-acyltransferase (BAT) to form bile salts (437).

Table 1.6: Major unconjugated bile acids.

	Bile Acid	Abbreviation
Individual Bile Acids	Dehydrocholic Acid	DHCA
	Lithocholic Acid	LCA
	Ursodeoxycholic Acid	UDCA
	Chenodeoxycholic Acid	CDCA
	Hyodeoxycholic Acid	HDCA
	Deoxycholic Acid	DCA
	Cholic Acid	CA
	Hyocholic Acid	HCA
	Muricholic Acids (α, β, ω)	α/β/ω-MCA

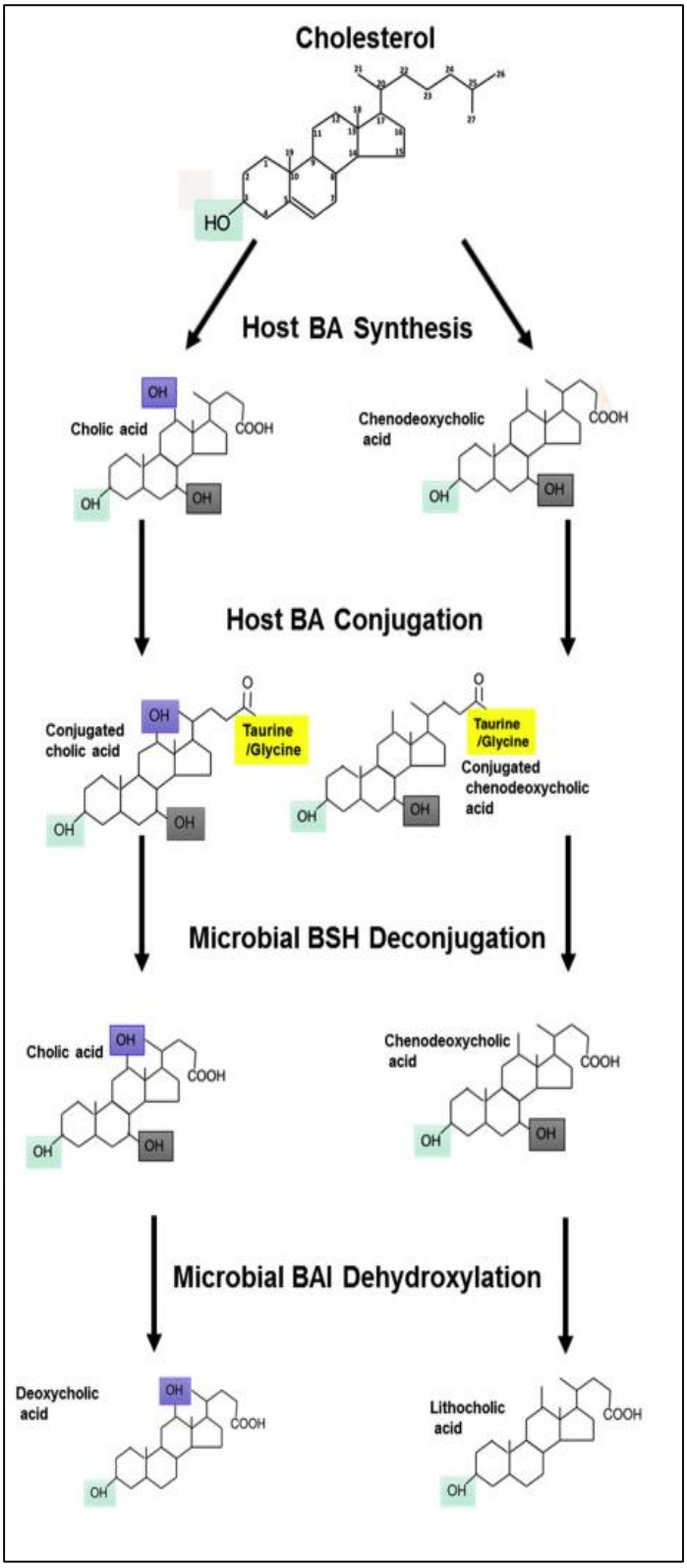

Figure 1.5: Cholesterol, primary and secondary bile acids. Cholic acid (CA) and chenodeoxycholic acid (CDCA) are the primary human bile acids which are formed from cholesterol in the liver by a multi-step pathway. After conjugation and release into the duodenum, 95% are reabsorbed at the terminal ileum but 5% escape to the large intestine to be modified by the microbiota. This includes deconjugation and 7α-dehydroxylation to form deoxycholic acid and lithocholic acid from CA and CDCA respectively. Figure modified from Long *et al*., 2017 (438).

Once released into the duodenum, the amphipathic bile salts emulsify lipids forming micelles. This increases the efficiency of pancreatic lipase-mediated hydrolysis of triglycerides into two fatty acids and a monoglyceride which can then be absorbed from the jejunum. This absorption process is believed to be protein-dependent, but passive diffusion or a combination of both is possible (440, 441). Bile salts themselves are not taken up by the enterocyte in this process but are complexed to plasma proteins and reabsorbed from the distal ileum into the bloodstream by active transport. They are then returned via the portal vein to the liver by the process of enterohepatic circulation (442). Upon reaching the liver, they are efficiently absorbed by active transporters on the sinusoidal surface of hepatocytes and secreted into bile canaliculi for return to the gallbladder.

The relative hydrophobicities of bile acids are relevant to their biological effects. Bile acids with greater hydrophobicity are more cytotoxic and more closely associated with disease (443-445). Bile acids show a gradient of increasing hydrophobicity proceeding UDCA < CA < CDCA < DCA < LCA (446, 447). The biplanar sterane core of bile acids has a hydrophobic face (convex, β face) and a less hydrophobic face (concave, α face) (448). Hydroxyl groups which project from the core in the β-orientation therefore do more to reduce the hydrophobicity of the bile acid by obscuring its hydrophobic β face, for example UDCA and MCA which have β-orientated hydroxyl groups in the 7- and 6-carbon positions respectively. Conjugation also decreases the hydrophobicity of bile salts as the amino acid moiety terminates in a ionic polar residue which contributes a strong hydrophilic effect (448). This relative hydrophobicity also contributes to bile acid transport since conjugated bile acids require active transport to cross cellular membranes while free bile acids can be taken up by passive diffusion.

1.4.2 Bile Acid Regulation

Bile acid homeostasis is regulated by Farnesoid X Receptor (FXR; also known as Bile Acid Receptor (BAR)) which is a nuclear receptor expressed by liver hepatocytes and small intestine enterocytes (449-451). Upon activation, FXR forms a dimer with retinoid X receptor (RXR), translocates to the nucleus and directly binds DNA to moderate gene expression. It is activated by all four major human bile acids, with reducing affinity for CDCA>DCA=LCA>CA (452). Activation of FXR was enhanced in conjugated bile acids in cells expressing bile acid transporters required to transport these molecules across the cellular membrane (452-456). Hydrophilic bile acid α-MCA does not activate FXR (449), while β-MCA did not activate FXR in human HepG2 hepatocellular carcinoma cell line which express FXR and organic anion–transporting polypeptides (OATPs) required for hepatic uptake of hydrophobic bile acids (450, 457). However, conjugates of MCAs act as FXR antagonists with IC_{50} values of 28mM and 40mM for T-αMCA and T-βMCA respectively (458-461). UDCA may also act as a weak FXR antagonist (462). CA does not appear to activate FXR in humans but does in mice which lack CDCA, the most potent endogenous human FXR agonist (463, 464).

Bile acid synthesis is the primary route of cholesterol elimination in the body. It progresses through two major pathways. The classic pathway produces CA and the alternative pathway produced CDCA. Sterol 12α-hydroxylase (CYP8B1) mediates the production of CA and the alternative pathway produces CDCA when CYP8B1 is deficient (465). Cytochrome P450 7A (CYP7A1) catalyses the rate-limiting step in classical pathways for bile acid biosynthesis. Regulation of these enzymes allows maintenance of bile acid homeostasis.

Ileal FXR inhibits *CYP7A1* by up-regulating FGF19 in the intestine, from where it is circulated to the liver to activate its receptor FGFR4 which complexes with β-Klotho on the surface of hepatocytes (466, 467). CYP7A1 can also be inhibited by FXR expressed in hepatocytes by a

mechanism dependent on small heterodimer protein (SHP) (468), and can be suppressed by cytokines which are produced as a result of rising concentration of bile acids (469).

1.4.3 Bile Acid Transport

1.4.3.1 Ileal Transporters

Apical sodium-dependant bile acid transporter (ASBT) is found on the apical brush border of ileal enterocytes and transports bile acids from the lumen across the membrane into the cell (Figure 1.6) (470). FXR down-regulates ASBT in mouse enterocytes via the FXR target gene small heterodimer protein (SHP) which interacts with liver receptor-1 (LRH-1) to prevent it binding ASBT response elements and promoting transcription (471). In contrast, if rats lack an LRH-1 responsive element within the ASBT promoter, this gene is not inhibited by FXR. Human ASBT is also down-regulated by SHP interfering with retinoic acid receptor (RAR)/RXR activation in a similar fashion to mice (472), with ASBT deficiency causing bile acid malabsorption, resulting in steatorrhea and reduced plasma cholesterol (473, 474).

Ileal bile acid binding protein (I-BABP), on the other hand, is localised to the enterocyte cytoplasm and is believed to shuttle bile acids from ASBT at the apical membrane to organic solute transporter (Ost)α/β at the basolateral membrane. It is also expressed in the terminal ileum (475). Bile acids up-regulate the expression of I-BABP *in vitro* and *in vivo* by forming a FXR/RXR heterodimer (476, 477).

To complete transport across the cell, Ostα and Ostβ form a heterodimer at the basolateral membrane to shuttle bile acids across into portal circulation (478). Their expression is up-regulated by FXR signalling (479, 480). Ostα and Ostβ are expressed in the intestine and kidney in mice, as well as the liver in humans (481).

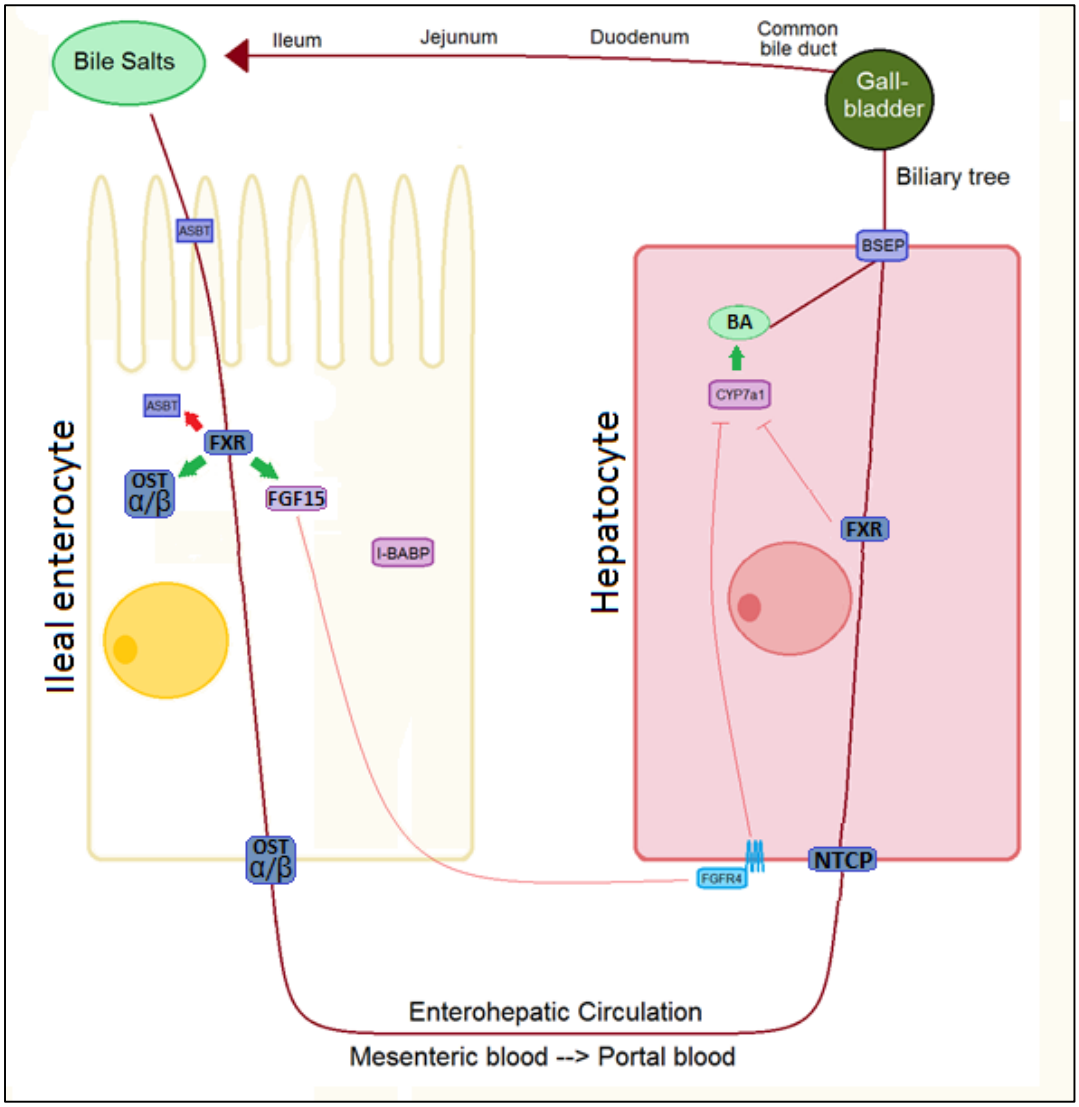

Figure 1.6: Enterohepatic circulation. Bile salts are produced in the hepatocyte and stored in the gallbladder in bile. Fat entering the duodenum triggers the secretion of cholecystokinin (CCK) from epithelial enteroendocrine cells. CCK then stimulates contraction of the gallbladder and release of bile into the duodenum via the common bile duct. Bile salts then aid the digestion and absorption of dietary fats in the small intestine before being transported across the apical membrane of terminal ileal enterocytes by Apical Sodium-dependent Bile acid Transporter (ASBT), possible aided by Ileal Bile Acid Binding Protein (I-BABP). Here, bile salts interact with Farnesoid X Receptor (FXR), which translocates to the nucleus to up-regulate Organic Solute Transporters α and β (Ostα/β) and Fibroblast Growth Factor 15 (FGF15), and down-regulate ASBT. Bile salts are then transported across the basolateral enterocyte membrane by the Ostα/β heterodimer into the mesenteric and portal blood which transport it back to the hepatocyte. It is transported across the basolateral hepatocyte membrane by Na^+-Taurocholate Co-transporting Polypeptide (NTCP) where is can interact with hepatic FXR to down-regulate bile acid (BA) synthesis by inhibiting CYP7A1. Bile salts are then transported from the hepatocyte back into the biliary system by Bile Salt Export Pump (BSEP). Bile acid synthesis can also be suppressed by ileal FGF15 which translocates to the hepatocyte to bind FGFR4 and inhibit CYP7A1 (466).

1.4.3.2 Hepatic Transport

Na^+-taurocholate co-transporting polypeptide (NTCP) and organic anion-transporting peptides (OATPs) are responsible for the uptake of conjugated and unconjugated bile acids, respectively, from the portal blood at the hepatocyte basolateral membrane (482, 483). FXR inhibits the expression of NTCP via the induction of SHP (484). The bile salt export pump (BSEP) transports recycled or newly synthesised bile acids across the apical membrane into the bile canaliculi for transport and storage in the gallbladder (485, 486). BSEP is also a target gene of FXR (487).

1.4.4 FXR and CRC

Bile acids have also been associated with cancer via FXR signalling (488). *FXR* expression is down-regulated in human colorectal tumours and colon cancer cell lines (489). Moreover, *Fxr*$^{-/-}$ mice are predisposed to cancer, displaying increased IL1β, IL6, β-catenin, cyclin D1, and c-myc at three months of age, and hepatocellular adenoma, carcinoma and hepatocholangiocellular carcinoma after 12 months (490, 491). These phenotypes are not simply the result of elevated bile acids as a result of FXR deficiency as they were not ameliorated by co-administration of bile acid-sequestrant cholestyramine (492). Furthermore, administration of the bile acid T-βMCA, which is an FXR antagonist bile acid, increases stem cell proliferation by activating Wnt, impairs intestinal integrity, accelerates tumour growth, induces dysplastic morphology and chromosome instability, and increases levels of serum IFNγ, IL6 and IL17 in APC^{MIN} mice, *in vitro* and *ex vivo* in an FXR-dependent manner (493). In addition, FXR agonists promoted apoptosis, down-regulated the intestinal stem cell genes *Lgr5*, *Olfm4* and the Wnt-dependent cancer stem cell gene *Ascl2*, and also inhibited Wnt signalling (492). FXR agonists also delayed tumour progression, reduced tumour multiplicity, proliferation and serum cytokines, and improved intestinal morphology,

differentiation, barrier function and bile acid homeostasis (493). The APC^{MIN} phenotype can also contribute to bile acid dysregulation via FXR, as these mice display increased CpG methylation in the *Fxr* promoter which silences *Fxr* expression (494). *Fxr* has also been demonstrated to modulate the microbiota. FXR antagonism increased the proportion of *Bacteroidetes* compared to *Firmicutes*, a ratio which may contribute to the pathogenicity of obesity in mice fed a high fat diet (458, 495). FXR can also suppress expression of pro-inflammatory cytokines (496) to the extent that a synthetic FXR ligand protected mice from DSS-induced colitis (497). Impaired FXR function has also been implicated in hepatocellular carcinoma due to dysregulation of bile acid homeostasis and pro-inflammatory signalling (498).

1.4.5 Microbial Bile Salt Metabolism

Although most bile salts are reabsorbed in the distal ileum, around 5% escape to the large intestine where they can be modified by intestinal bacteria (499). This loss is balanced by *de novo* bile acid synthesis from cholesterol in the liver. These bile acids undergo deconjugation and 7α-dehydroxylation by the gut bacteria, as well as a number of other minor modifications (500).

1.4.5.1 Deconjugation

Deconjugation of bile salts involves hydrolysis of their amino acid moiety to form free bile acids. This is performed by bacteria expressing bile salt hydrolase (*bsh*), a family of enzymes that are widespread in the colonic microbiota. *Bsh* enzymes have been cloned for a number of bacteria (501-503). Their function may be detoxifying bile salts since Bsh activity appears to be proportional to the toxicity of conjugated bile acids to the bacteria, at least in

Lactobacilli (504). This is complicated by the fact that deconjugated bile acids are more toxic than their conjugates (505). However, unconjugated bile acids which undergo subsequent 7α-dehydroxylation can precipitate and bind to fibre to be excreted, or may be passively reabsorbed across the colonic membrane, reducing their concentrations in the lumen (506). Liberated taurine can also act as a source of sulphur which is utilised by a number of bacteria including *Bacteroides* (507, 508). Dehydroxylation to DCA was also promoted when the initial substrate was T-CA rather than CA, and glycine may provide a similar function to some bacteria (509). *Bsh* from *B. longum* is also co-transcribed with a component of the nitrogen regulation cascade, suggesting nitrogen scavenging from the liberated amino group could be an incentive for deconjugation (510). A Bsh enzyme from *Listeria monocytogenes* was identified as a virulence factor, ostensibly by facilitating colonisation in the presence of bile salts (511, 512). Several *bsh* genes have been identified and can differ in their substrate specificity (513), and bacterial strains can express several different *bsh* alleles (514).

1.4.5.2 Dehydroxylation

Deconjugated bile acids are susceptible to hydrolysis of the hydroxyl group at their 7-carbon position by the 7α/β-dehydroxylase pathway by other microbes. From CA, this forms deoxycholic acid (DCA) with hydroxyl groups at the 3- and 12-carbon position. From CDCA, it forms lithocholic acid (LCA) with a hydroxyl group at the 3-carbon position only. DCA then accumulates in the bile acid pool via passive absorption by the colonic epithelium as the human liver is unable to hydroxylate DCA, as has been observed rodents (515). While some LCA is also reabsorbed, it is sulphated in the liver and secreted into the intestine where it is poorly soluble and subsequently excreted in the faeces (516). As a result, the composition of the human bile salt pool secreted from the gallbladder is ~35% CA and CDCA, ~25% DCA and <5% LCA, while in mice the majority of CDCA is converted into muricholic acid (MCA) (517).

However, DCA and LCA each make up about a third of faecal bile acid, with their precursors CA and CDCA only making up around 2% each, demonstrating the efficiency of this dehydroxylation by the gut bacteria despite only a small portion of *Clostridia* having this capability. The benefit of this pathway to the bacteria involved is the utilisation of bile acids as electron acceptors, with the 7α/β-dehydroxylation pathway producing a two-electron reduction (506).

Bacteria which dehydroxylate bile acids do so with genes expressed on the *bile acid inducible* (*bai*) operon which has been characterised in a number of *Clostridium* species (518-520).

1.4.5.3 Other Modifications

The colonic microbiota can also reversibly epimerise the hydroxyl groups of bile acids between the α- and β-position by the enzyme hydroxysteroid dehydrogenase (HSDH) through an oxo-intermediate (521). This can produce bile acids such as hydrophilic ursodeoxycholic acid, an epimer of CDCA with the hydroxyl group at the 7-carbon position in the β-orientation (522). Specific HSDH enzymes also exist for hydroxyl groups at other positions on the bile acid sterane core (523). Bacteria may benefit from this reaction by generating adenosine triphosphate (ATP) or by reducing the toxicity of bile acids, for example CDCA to UDCA (524-526). UDCA also inhibits HSDH in *Clostridium absonum*, suggesting this is the intended product. This reaction can be performed on conjugated and unconjugated bile acids (527). Sulphatase activity has also been detected in a subset of gut bacteria, including *Clostridium*, *Peptococcus*, *Fusobacterium* and *Pseudomonas* (528), which can remove a sulpho-group in the 3α- or 3β-position on bile acids. Toxic bile acid LCA and other xenobiotics are sulphated in order to aid their excretion in the faeces, mediated by bile acid receptor Pregnane X Receptor (PXR) (529, 530). A reduction in desulphation activity was also observed in IBD patients and may be contribute to a pro-inflammatory character of the bile

acid pool in these patients (531). Esters of bile acids are also found in the faeces and are believed to be the product of esterification by *Bacteroides*, *Eubacterium* and *Lactobacillus* species in the gut bacteria (528, 532).

1.4.6 Other Bile Acid Receptors

The family of bile acid receptors includes cell membrane and nuclear receptors with a variety of functions and ligand specificities.

1.4.6.1 Sensing X Receptor/Pregnane X Receptor (SXR/PXR)

Human SXR and its rodent homolog PXR are receptors activated by the bile acid LCA and its 3-keto metabolite. These receptors are involved in the detoxification of various toxic xenobiotics such as LCA which are risk factors for cancer (533). The role of PXR in cancer is unclear. In one study, activation of PXR increased cell growth, invasion and metastasis in a human colon cancer cell line (HT29) and a xenograft model, an effect which was eliminated by PXR knockdown (534). It also promoted the expression of apoptosis inhibitors Bcl-2 and Bcl-xL in human and rat hepatocytes, possibly related to its protecting role in detoxification, and suppressed p53 (535, 536). However, PXR is also lost on many colon tumours. Moreover, ectopic expression of PXR inhibited cell growth in HT29 cells and in a xenograft model by regulating p21 (WAF1/CIP1) and E2F/Rb pathways, in exact contrast to the finding in Wang *et al*. (537). This suggests PXR has pro- and anti-tumorigenic roles depending on the context of its activation and expression (538).

1.4.6.2 Constitutive Androstane Receptor (CAR)

CAR has a similar role as PXR in the hydroxylation, conjugation, and excretion of toxic compounds including LCA, which acts as its ligand (539). It also affects bile acid composition, shifting synthesis toward the formation of less toxic trihydroxy bile acids, decreasing hepatic bile acid concentrations and increasing faecal elimination, by which it may protect against LCA-induced liver injury (540, 541). As well as its cancer-protective role in eliminating possible carcinogens, CAR enhances the expression of tumour suppressor genes WT1 and MGMT. However, CAR-mediated suppression of apoptosis in the presence of chronic xenobiotic stress can increase the risk of hepatic carcinogenesis (542, 543).

1.4.6.3 Vitamin D Receptor (VDR)

VDR is a receptor for LCA and is significantly more sensitive to this secondary bile acid than other nuclear receptors (544). It is also activated by the metabolites of LCA; 3-keto-LCA, G-LCA, and 6-keto-LCA (544).

Vitamin D, also a VDR agonist, has been shown to inhibit tumorigenesis in *N*-nitroso-*N*-methylurea (MNU)-treated rats, up-regulate CYP3A in CRC cells *in vitro*, and has been associated with a reduced risk of CRC in humans in observational studies (545, 546). Vitamin D reduces proliferation in colonocytes, induces differentiation in a calcium-dependent manner, induces apoptosis, inhibits invasion and metastasis and maintains genomic integrity in cooperation with p53 (547-551). It also has a role in immune modulation via T-cell and B-cell suppression, stimulation of monocytes to macrophages and inhibition of dendritic cells (552-556).

1.4.6.4 Takeda G Protein-Coupled Receptor 5 (TGR5)

GPBAR1/TGR5 is a cell surface G protein-coupled receptor sensitive to bile acids. Upon activation, it internalises and activates ERK/MAPK signalling (557). It is highly expressed in human spleen and resting monocytes, with very low expression in rat and mouse (557). TGR5 shows greater affinity for conjugated bile acids, with a decreasing potency for LCA>DCA>CDCA>CA (453, 454, 557). While TGR5 has been associated with gastric carcinoma, no direct link has yet been made with CRC (558).

1.4.6.5 Liver X Receptor (LXR)

LXRs are a family of nuclear receptors. LXRα is primarily expressed in liver, intestine, adipose tissue, and macrophages while LXRβ is expressed ubiquitously (559, 560). Their primary ligands are oxysterols but are also activated by hyodeoxycholic acid (HDCA) (559, 561, 562). LXRs are involved in the conversion of cholesterol to bile acids in the presence of high cholesterol concentrations by promoting expression of CYP7A1 (559, 561). LXRs suppress apoptosis in macrophages and are involved in apoptotic cell clearance and the maintenance of immune tolerance. LXR-deficient macrophages displayed defective phagocytosis and pro-inflammatory response to apoptotic cells, towards which they develop auto-antibodies (563).

1.4.7 Bile Acids and CRC

Secondary bile acids are hydrophobic, cytotoxic molecules and evidence suggests they play a role in colon cancer. For example, numerous epidemiological studies have highlighted higher faecal bile acid content in populations with increased CRC rates (564-570). Moreover, DCA has been shown to be higher in patients with colorectal adenomas and was first

proposed as a carcinogen in 1940 based on its induction of tumours in mice (571, 572). Bile acids were initially classified as tumour promoters rather than tumour initiators, as studies primarily demonstrated their action when co-administered with chemical carcinogens such as MAM or MNNG (573-576). However, the role of bile acids as aetiologic agents of cancer in their own right is now emerging (577).

A diet high in fat and low in fibre is a known risk factor for colon cancer and this diet was also associated with increased secondary bile acids, as well as increased glucuronidase deconjugation (578).

Interestingly, GF rats are generally resistant to chemical carcinogen-induced colorectal cancer (579). However, rats treated with MNNG and DCA displayed colonic adenocarcinomas, suggesting microbial production of DCA could play a role in tumorigenesis and may explain the resistance to CRC observed in GF animals (580).

1.4.7.1 Mechanisms of Bile Acid-induced Carcinogenesis

Bile acids can increase cancer risk by a number of mechanisms. These include the induction of DNA damage via the production of reactive oxygen and nitrogen species, the compromising of DNA repair, the selection for apoptosis-resistant cells and the promotion of inflammation.

1.4.7.1.1 COX: COX-1 is constitutively expressed in many mammalian tissues whilst COX-2 is expressed during inflammation. COX-2 has been shown to play a role on tumour growth and progression, with COX inhibitors such as non-steroidal anti-inflammatory drugs (NSAIDs) and COX-2-specific drugs shown to reduce the risk of colon cancer (581-585). Interestingly, the dihydroxy bile acids DCA and CDCA were shown to up-regulate COX-2 and its downstream

inflammatory product PGE_2 in a protein kinase C (PKC)-dependent manner, whilst activating c-Jun and AP-1 (586, 587). In contrast, neither CA nor conjugated bile acids had any effect. DCA-induced expression of COX-2 is also reliant on intact NF-κB in HCT116 cells (586).

1.4.7.1.2 Reactive Oxygen Species: Bile acids generate ROS via a detergent effect on membrane enzymes which produces arachidonic acid (588). These in turn act as a substrate for COX and lipoxygenase (LOX) which produce ROS during the formation of prostaglandins and leukotrienes (588-590). Activation of this pathway also stimulates the proliferation of the colonic epithelium (588).

ROS have been shown to induce DNA damage, promote neoplastic growth, induce nucleotide substitutions and encourage microsatellite instability (439, 591-593). Oxidative damage has been described as the primary cause of spontaneous mutation in mammalian cells and although over 20 resultant DNA lesions have been described, only a small number have been characterised (594, 595).

Studies have shown that the hydrophobic bile acids, DCA and CDCA, indirectly activate protein PKC, enhance proliferation and produce ROS (596). PKC activation and subsequent ROS generation was inhibited by retinoic acid. Both DCA and LCA were shown to induce DNA damage in a dose-dependent manner *in vitro* and this was inhibited by both α-tocopherol and retinol, which may involve an antioxidant effect in the case of the former and reduced PKC activation or membrane stabilisation in the latter (597). Intra-colonic administration of DCA also induced proliferation and ornithine decarboxylase (ODC) activity, an effect that was abolished by superoxide dismutase, suggesting a role for reactive oxygen in the stimulation of colonic proliferation by bile salts (589). *In vitro*, DCA and LCA induced DNA damage that was inhibited by endonuclease III treatment, suggesting oxidative DNA damage, at concentrations associated with pathological conditions such as CRC (598).

1.4.7.1.3 Reactive Nitrogen Species: DCA has been shown to activate inducible nitric oxide synthase (iNOS) in a PKC-dependent manner *in vitro* (439, 599). Overexpression of iNOS leads to increased levels of nitric oxide (NO) and other RNS which promote pro-tumorigenic states such as apoptosis resistance and DNA damage (600). Consistent with this, DCA-induced colitis is attenuated in *Nos2*-knockout mice, and exposure of a human colon cancer cell (HCT116 cells) to DCA resulted in S-nitrosylated proteins, which are a biomarker for nitrosative stress that can result in apoptosis resistance (601, 602).

1.4.7.1.4 Apoptosis: Bile acids appear to induce apoptosis in the short term but select for apoptosis-resistant cells in the longer term (603). Oxidative damage caused by ROS induces apoptosis (604). DCA induced apoptosis in HCT116 cells by releasing cytochrome c from mitochondria, an effect that was inhibited by UDCA downstream of cytochrome c release (605). A study on another human colon cancer cell line (SW480 cells) suggested apoptosis was triggered by DCA via the induction of mitochondria-mediated apoptosis, and was independent of the death receptor CD95-mediated apoptotic pathway which is often down-regulated in CRC (606). Moreover, Payne *et al*. showed DCA-induced apoptosis could be prevented in HCT116 cells by inhibition of mitochondrial complexes I-V, implicating mitochondrial crosstalk with apoptotic signalling pathways and mitochondrial-nucleolar crosstalk in the development of apoptosis resistance (607). The ability of bile acids to induce apoptosis appears to be related to their hydrophobicity, with the most powerful effect displayed by the most hydrophobic bile acids, DCA and CDCA (608).

These findings are counter-intuitive to the common understanding of tumorigenic cells as displaying apoptosis resistance. In fact, colon cancer patients' normal tumour-adjacent tissue displays resistance to bile salt- and bile acid-induced apoptosis, and this is mediated by an up-regulation of the anti-apoptotic protein Bcl-xL (603, 609-613). This appears to occur

particularly in the top third of colonic crypts, suggesting adenomas may arise in fields of apoptosis-resistant cells. Indeed, rats chronically fed CA displayed apoptosis resistance and a similar result was observed with HCT116 cells *in vivo* (614, 615). A study in the HT29 human colon cancer cell line implicates NO in apoptosis resistance (616). A proteomic study of HCT116 cells stimulated with DCA identified 18 over-expressed anti-apoptotic proteins and 11 under-expressed pro-apoptotic proteins, again highlighting the role of this bile acid in apoptosis resistance (617).

One mechanism by which bile acids may induce resistance to apoptosis is via inhibition of p53. Tumour-suppressor p53 plays an important role in the context of DNA damage by stimulating the repair of damaged DNA and by inducing apoptosis in irreparable cells. DCA inhibits the p53 response to DNA damage in a dose-dependent manner *in vitro*, likely by proteasomal degradation of p53 via a pathway involving extracellular signal-regulated kinase (ERK) signalling (618). This effect was not observed for CA or UDCA. *In vitro*, HCT116 cells are more susceptible to DCA-induced apoptosis than HT29s, which is consistent with p53-mediated apoptosis resistance mediated by bile acids, as HCT116 cells contain an intact p53 gene while HT29s do not (586, 619). Additionally, a variant of cytosolic bile acid shuttle protein I-BABP, whose expression is controlled by NF-κB instead of nuclear bile acid receptor FXR, has also been shown to mediate the survival of HCT116 cells at physiological DCA concentrations (620).

1.4.7.1.5 Compromised Repair and Aneuploidy: Bile acids can also induce chromosomal abnormality such as aneuploidy and micronucleus formation (621, 622). DCA, LCA, CDCA and CA each induced mitotic chromosome aneuploidy in yeast, while T-DCA and G-DCA did not (623). Oxidative stress is a well-established source chromosomal instability and this is a plausible route of bile-acid induced DNA damage and increased CRC risk (624, 625).

LCA was demonstrated to inhibit the repair activity of DNA polymerase β which could exacerbate the consequences of bile acid-induced DNA damage (626). A proteomic study of CRC cell lines induced with DCA identified ten alterations in ten proteins involved in DNA repair and cell cycle checkpoints (617).

1.5 Aims and Objectives

The role of the microbiota in human health and disease is complex. It is possible that changes in the gut microbiota in the pre-neoplastic colon could drive or inhibit tumorigenesis and evidence for this has been provided by animal studies. However, it is also possible that tumorigenesis occurs entirely as a result of host processes independent of the microbiota, and so far human studies have failed to provide hard evidence to the contrary. This question of "cause or consequence" is an important unanswered problem in the study of the role of the microbiota in disease. Similarly, after cancer initiation, components of the microbiota may suppress or promote growth, invasion and metastasis but human evidence for this is lacking.

CRC pathogenesis is a process that takes place over decades. This makes it difficult to track the microbiota of a sufficiently large cohort and impossible to combine those data with the invasive colonoscopies and biopsies necessary to provide samples before, during and after tumorigenesis. As such, we rely on animal studies to investigate these effects.

We begin this investigation in **Chapter 3** with a time-course study using the AOM mouse model of sporadic colon cancer. Our objective was to identify the changes that occur in a tumorigenic colon in the host and the microbiota and set them to a timeline. This should provide clarity on which changes are potential causal events occurring earlier in the process from those which occur later. This novel understanding of the nature of host-microbe interaction during tumorigenesis could reveal further research potential, including the possibility of reducing cancer risk via early intervention in the microbiota, which we will address in **Chapter 5**.

We perform a second time-course study in **Chapter 4**, this time with the APC^{MIN} mouse model of familial CRC. Here, we sample the faecal microbiota of our mouse model and wild-type controls before, during and after the onset of tumorigenesis to reveal the temporal order of

host and microbial changes during this process. This has important implications for our understanding of the role of the microbiota and the interaction between host and microbial factors in colon cancer, similar to our AOM time-course study.

We return to the APC^{MIN} mouse for an intervention study in **Chapter 5**. These mice are administered a commensal gut bacteria engineered to overexpress *bsh*, an enzyme common in probiotic bacteria and associated with beneficial health effects. Although this enzyme is widespread in probiotic bacteria, its role in liberating bile salts for modification into secondary bile acids has elicited caution. Our objective is to determine the role of this enzyme in cancer risk and attempt to elucidate its potential mechanisms of action, as well as provide further data on the role of the microbiota in CRC and the feasibility of probiotic gavage as a prophylactic intervention against cancer risk.

1.5.1 Hypotheses

Therefore our hypotheses were:

- That the microbiota is involved in the initiation and progression of CRC, and that changes in the microbiota occur upstream of hyperplastic and neoplastic changes in the host epithelium (overarching hypothesis)
- This hypothesis also applies to **Chapters 3**
- Disease onset has a predominantly genetic basis in APC^{MIN} mice in **Chapter 4**, but we hypothesise that the gut microbiota may nonetheless modulate this process
- We hypothesise that bacteria expressing *bsh* are protective against CRC risk (**Chapter 5**)

1.6 References

1. Hanahan D, Weinberg RA. The hallmarks of cancer. Cell. 2000;100(1):57-70.
2. Hanahan D, Weinberg Robert A. Hallmarks of Cancer: The Next Generation. Cell. 2011;144(5):646-74.
3. World Health Organisation. Latest global cancer data: Cancer burden rises to 18.1 million new cases and 9.6 million cancer deaths in 2018 2018 [Available from: https://www.who.int/cancer/PRGlobocanFinal.pdf.
4. Central Statistics Office. Vital Statistics Annual Report 2016 2019 [Available from: https://www.cso.ie/en/releasesandpublications/ep/p-vsar/vitalstatisticsannualreport2016/deaths2016/.
5. Irish Cancer Society. Cancer statistics 2018 [Available from: https://www.cancer.ie/about-us/media-centre/cancer-statistics#sthash.ss6m9Qwy.ieCDpQaK.dpbs.
6. Luengo-Fernandez R, Leal J, Gray A, Sullivan R. Economic burden of cancer across the European Union: a population-based cost analysis. The Lancet Oncology. 2013;14(12):1165-74.
7. National Cancer Registry Ireland. Cancer projections for Ireland 2015 – 2040 2014 [Available from: https://www.ncri.ie/publications/cancer-trends-and-projections/cancer-projections-ireland-2015-%E2%80%93-2040.
8. Health Service Executive. Cancer Incidence, Survival and Mortality Data 2013 [Available from: https://www.hse.ie/eng/services/list/5/cancer/pubs/intelligence/registrydata.html.
9. Doll R, Peto R. The causes of cancer: quantitative estimates of avoidable risks of cancer in the United States today. Journal of the National Cancer Institute. 1981;66(6):1191-308.
10. Penrose HM, Heller S, Cable C, Nakhoul H, Baddoo M, Flemington E, et al. High-fat diet induced leptin and Wnt expression: RNA-sequencing and pathway analysis of mouse colonic tissue and tumors. Carcinogenesis. 2017;38(3):302-11.
11. Basen-Engquist K, Chang M. Obesity and cancer risk: recent review and evidence. Curr Oncol Rep. 2011;13(1):71-6.
12. Key TJ, Schatzkin A, Willett WC, Allen NE, Spencer EA, Travis RC. Diet, nutrition and the prevention of cancer. Public health nutrition. 2004;7(1a):187-200.
13. Key TJ, Allen NE, Spencer EA, Travis RC. The effect of diet on risk of cancer. The Lancet. 2002;360(9336):861-8.
14. Yamagishi H, Kuroda H, Imai Y, Hiraishi H. Molecular pathogenesis of sporadic colorectal cancers. Chin J Cancer. 2016;35:4-.
15. Gryfe R. Inherited colorectal cancer syndromes. Clin Colon Rectal Surg. 2009;22(4):198-208.
16. Powell SM, Petersen GM, Krush AJ, Booker S, Jen J, Giardiello FM, et al. Molecular diagnosis of familial adenomatous polyposis. The New England journal of medicine. 1993;329(27):1982-7.
17. Keller DS, Windsor A, Cohen R, Chand M. Colorectal cancer in inflammatory bowel disease: review of the evidence. Techniques in coloproctology. 2019;23(1):3-13.
18. Triantafillidis JK, NASIOULAS G, KOSMIDIS PA. Colorectal Cancer and Inflammatory Bowel Disease: Epidemiology, Risk Factors, Mechanisms of Carcinogenesis and Prevention Strategies. Anticancer Research. 2009;29(7):2727-37.
19. Dyson JK, Rutter MD. Colorectal cancer in inflammatory bowel disease: what is the real magnitude of the risk? World J Gastroenterol. 2012;18(29):3839-48.
20. Alrawi SJ, Schiff M, Carroll RE, Dayton M, Gibbs JF, Kulavlat M, et al. Aberrant crypt foci. Anticancer Res. 2006;26(1a):107-19.

21. Hardy RG, Meltzer SJ, Jankowski JA. ABC of colorectal cancer. Molecular basis for risk factors. BMJ. 2000;321(7265):886-9.
22. Bird RP. Role of aberrant crypt foci in understanding the pathogenesis of colon cancer. Cancer letters. 1995;93(1):55-71.
23. Mori H, Yamada Y, Kuno T, Hirose Y. Aberrant crypt foci and beta-catenin accumulated crypts; significance and roles for colorectal carcinogenesis. Mutation research. 2004;566(3):191-208.
24. Paulsen JE, Steffensen I-L, Løberg EM, Husøy T, Namork E, Alexander J. Qualitative and Quantitative Relationship between Dysplastic Aberrant Crypt Foci and Tumorigenesis in the Min/+ Mouse Colon. Cancer research. 2001;61(13):5010-5.
25. Markowitz SD, Bertagnolli MM. Molecular origins of cancer: Molecular basis of colorectal cancer. The New England journal of medicine. 2009;361(25):2449-60.
26. Goss KH, Groden J. Biology of the adenomatous polyposis coli tumor suppressor. Journal of clinical oncology : official journal of the American Society of Clinical Oncology. 2000;18(9):1967-79.
27. Behrens J, von Kries JP, Kuhl M, Bruhn L, Wedlich D, Grosschedl R, et al. Functional interaction of [beta]-catenin with the transcription factor LEF-1. Nature. 1996;382(6592):638-42.
28. Molenaar M, van de Wetering M, Oosterwegel M, Peterson-Maduro J, Godsave S, Korinek V, et al. XTcf-3 transcription factor mediates beta-catenin-induced axis formation in Xenopus embryos. Cell. 1996;86(3):391-9.
29. Morin PJ, Sparks AB, Korinek V, Barker N, Clevers H, Vogelstein B, et al. Activation of beta-catenin-Tcf signaling in colon cancer by mutations in beta-catenin or APC. Science (New York, NY). 1997;275(5307):1787-90.
30. Sparks AB, Morin PJ, Vogelstein B, Kinzler KW. Mutational analysis of the APC/beta-catenin/Tcf pathway in colorectal cancer. Cancer research. 1998;58(6):1130-4.
31. Harada N, Tamai Y, Ishikawa T, Sauer B, Takaku K, Oshima M, et al. Intestinal polyposis in mice with a dominant stable mutation of the beta-catenin gene. The EMBO journal. 1999;18(21):5931-42.
32. Porru M, Pompili L, Caruso C, Biroccio A, Leonetti C. Targeting KRAS in metastatic colorectal cancer: current strategies and emerging opportunities. Journal of Experimental & Clinical Cancer Research. 2018;37(1):57.
33. Vogelstein B, Kinzler KW. Cancer genes and the pathways they control. Nature medicine. 2004;10(8):789-99.
34. Cox AD, Fesik SW, Kimmelman AC, Luo J, Der CJ. Drugging the undruggable RAS: Mission possible? Nat Rev Drug Discov. 2014;13(11):828-51.
35. Chin L, Tam A, Pomerantz J, Wong M, Holash J, Bardeesy N, et al. Essential role for oncogenic Ras in tumour maintenance. Nature. 1999;400(6743):468-72.
36. Fisher GH, Wellen SL, Klimstra D, Lenczowski JM, Tichelaar JW, Lizak MJ, et al. Induction and apoptotic regression of lung adenocarcinomas by regulation of a K-Ras transgene in the presence and absence of tumor suppressor genes. Genes & development. 2001;15(24):3249-62.
37. Kawada K, Toda K, Sakai Y. Targeting metabolic reprogramming in KRAS-driven cancers. International Journal of Clinical Oncology. 2017;22(4):651-9.
38. Surget S, Khoury MP, Bourdon J-C. Uncovering the role of p53 splice variants in human malignancy: a clinical perspective. Onco Targets Ther. 2013;7:57-68.
39. Meek DW, Anderson CW. Posttranslational modification of p53: cooperative integrators of function. Cold Spring Harbor perspectives in biology. 2009;1(6):a000950.
40. Han ES, Muller FL, Perez VI, Qi W, Liang H, Xi L, et al. The in vivo gene expression signature of oxidative stress. Physiological genomics. 2008;34(1):112-26.

41. Taylor WR, Stark GR. Regulation of the G2/M transition by p53. Oncogene. 2001;20(15):1803-15.
42. Kuribayashi K, El-Deiry WS. Regulation of programmed cell death by the p53 pathway. Advances in experimental medicine and biology. 2008;615:201-21.
43. Levine AJ, Momand J, Finlay CA. The p53 tumour suppressor gene. Nature. 1991;351(6326):453-6.
44. Arakawa H. Netrin-1 and its receptors in tumorigenesis. Nature Reviews Cancer. 2004;4(12):978-87.
45. Forcet C, Ye X, Granger L, Corset V, Shin H, Bredesen DE, et al. The dependence receptor DCC (deleted in colorectal cancer) defines an alternative mechanism for caspase activation. Proceedings of the National Academy of Sciences of the United States of America. 2001;98(6):3416-21.
46. Vargas-Rondón N, Villegas VE, Rondón-Lagos M. The Role of Chromosomal Instability in Cancer and Therapeutic Responses. Cancers (Basel). 2017;10(1):4.
47. Hsieh JS, Lin SR, Chang MY, Chen FM, Lu CY, Huang TJ, et al. APC, K-ras, and p53 gene mutations in colorectal cancer patients: correlation to clinicopathologic features and postoperative surveillance. The American surgeon. 2005;71(4):336-43.
48. Conlin A, Smith G, Carey FA, Wolf CR, Steele RJ. The prognostic significance of K-ras, p53, and APC mutations in colorectal carcinoma. Gut. 2005;54(9):1283-6.
49. Esteller M, Gonzalez S, Risques RA, Marcuello E, Mangues R, Germa JR, et al. K-ras and p16 aberrations confer poor prognosis in human colorectal cancer. Journal of clinical oncology : official journal of the American Society of Clinical Oncology. 2001;19(2):299-304.
50. Remvikos Y, Vogt N, Muleris M, Salmon RJ, Malfoy B, Dutrillaux B. DNA-repeat instability is associated with colorectal cancers presenting minimal chromosome rearrangements. Genes, chromosomes & cancer. 1995;12(4):272-6.
51. Fishel R. Mismatch repair, molecular switches, and signal transduction. Genes & development. 1998;12(14):2096-101.
52. Sameer AS. Colorectal cancer: molecular mutations and polymorphisms. Front Oncol. 2013;3:114-.
53. Boland CR, Thibodeau SN, Hamilton SR, Sidransky D, Eshleman JR, Burt RW, et al. A National Cancer Institute Workshop on Microsatellite Instability for cancer detection and familial predisposition: development of international criteria for the determination of microsatellite instability in colorectal cancer. Cancer research. 1998;58(22):5248-57.
54. Vasen HF, Moslein G, Alonso A, Bernstein I, Bertario L, Blanco I, et al. Guidelines for the clinical management of Lynch syndrome (hereditary non-polyposis cancer). Journal of medical genetics. 2007;44(6):353-62.
55. Colussi D, Brandi G, Bazzoli F, Ricciardiello L. Molecular pathways involved in colorectal cancer: implications for disease behavior and prevention. Int J Mol Sci. 2013;14(8):16365-85.
56. Ogino S, Odze RD, Kawasaki T, Brahmandam M, Kirkner GJ, Laird PW, et al. Correlation of pathologic features with CpG island methylator phenotype (CIMP) by quantitative DNA methylation analysis in colorectal carcinoma. The American journal of surgical pathology. 2006;30(9):1175-83.
57. Armaghany T, Wilson JD, Chu Q, Mills G. Genetic alterations in colorectal cancer. Gastrointest Cancer Res. 2012;5(1):19-27.
58. Popovic R, Licht JD. Emerging epigenetic targets and therapies in cancer medicine. Cancer Discov. 2012;2(5):405-13.
59. Peng Y, Croce CM. The role of MicroRNAs in human cancer. Signal Transduction And Targeted Therapy. 2016;1:15004.

60. Wen SY, Lin Y, Yu YQ, Cao SJ, Zhang R, Yang XM, et al. miR-506 acts as a tumor suppressor by directly targeting the hedgehog pathway transcription factor Gli3 in human cervical cancer. Oncogene. 2014;34:717.
61. Liu G, Sun Y, Ji P, Li X, Cogdell D, Yang D, et al. MiR-506 suppresses proliferation and induces senescence by directly targeting the CDK4/6–FOXM1 axis in ovarian cancer. The Journal of Pathology. 2014;233(3):308-18.
62. Hosseinahli N, Aghapour M, Duijf PHG, Baradaran B. Treating cancer with microRNA replacement therapy: A literature review. Journal of Cellular Physiology. 2018;233(8):5574-88.
63. Stetler-Stevenson WG. Matrix metalloproteinases in angiogenesis: a moving target for therapeutic intervention. J Clin Invest. 1999;103(9):1237-41.
64. Yu Q, Stamenkovic I. Cell surface-localized matrix metalloproteinase-9 proteolytically activates TGF-β and promotes tumor invasion and angiogenesis. Genes & development. 2000;14(2):163-76.
65. John A, Tuszynski G. The role of matrix metalloproteinases in tumor angiogenesis and tumor metastasis. Pathology Oncology Research. 2001;7(1):14.
66. Levi E, Fridman R, Miao HQ, Ma YS, Yayon A, Vlodavsky I. Matrix metalloproteinase 2 releases active soluble ectodomain of fibroblast growth factor receptor 1. Proceedings of the National Academy of Sciences. 1996;93(14):7069-74.
67. Kamphaus GD, Colorado PC, Panka DJ, Hopfer H, Ramchandran R, Torre A, et al. Canstatin, a Novel Matrix-derived Inhibitor of Angiogenesis and Tumor Growth. Journal of Biological Chemistry. 2000;275(2):1209-15.
68. Colorado PC, Torre A, Kamphaus G, Maeshima Y, Hopfer H, Takahashi K, et al. Anti-angiogenic cues from vascular basement membrane collagen. Cancer research. 2000;60(9):2520-6.
69. Bernhard EJ, Gruber SB, Muschel RJ. Direct evidence linking expression of matrix metalloproteinase 9 (92-kDa gelatinase/collagenase) to the metastatic phenotype in transformed rat embryo cells. Proceedings of the National Academy of Sciences. 1994;91(10):4293-7.
70. Khokha R, Zimmer MJ, Graham CH, Lala PK, Waterhouse P. Suppression of Invasion by Inducible Expression of Tissue Inhibitor of Metalloproteinase-1 (TIMP-1) in B 16-F10 Melanoma Cells. JNCI: Journal of the National Cancer Institute. 1992;84(13):1017-22.
71. Polette M, Birembaut P. Membrane-type metalloproteinases in tumor invasion. The International Journal of Biochemistry & Cell Biology. 1998;30(11):1195-202.
72. Folkman J, Mendelsohn J, Howley P, Israel M, Liotta L. The molecular basis of cancer. J Mendelson, PM Howley, MA Israle, and LA Liotta (eds). 1995:206-32.
73. Yadav L, Puri N, Rastogi V, Satpute P, Sharma V. Tumour Angiogenesis and Angiogenic Inhibitors: A Review. J Clin Diagn Res. 2015;9(6):XE01-XE5.
74. Blagosklonny MV. Antiangiogenic therapy and tumor progression. Cancer Cell. 2004;5(1):13-7.
75. Wang D, Tan C, Xiao F, Zou L, Wang L, Wei Yg, et al. The “inherent vice” in the anti-angiogenic theory may cause the highly metastatic cancer to spread more aggressively. Scientific Reports. 2017;7(1):2365.
76. Carmeliet P. VEGF as a key mediator of angiogenesis in cancer. Oncology. 2005;69 Suppl 3:4-10.
77. D'Agostino RB. Changing End Points in Breast-Cancer Drug Approval — The Avastin Story. New England Journal of Medicine. 2011;365(2):e2.
78. Gilbert MR, Dignam JJ, Armstrong TS, Wefel JS, Blumenthal DT, Vogelbaum MA, et al. A Randomized Trial of Bevacizumab for Newly Diagnosed Glioblastoma. New England Journal of Medicine. 2014;370(8):699-708.

79. Perren TJ, Swart AM, Pfisterer J, Ledermann JA, Pujade-Lauraine E, Kristensen G, et al. A Phase 3 Trial of Bevacizumab in Ovarian Cancer. New England Journal of Medicine. 2011;365(26):2484-96.
80. Lee JC, Chow NH, Wang ST, Huang SM. Prognostic value of vascular endothelial growth factor expression in colorectal cancer patients. European Journal of Cancer. 2000;36(6):748-53.
81. Unemori EN, Ferrara N, Bauer EA, Amento EP. Vascular endothelial growth factor induces interstitial collagenase expression in human endothelial cells. J Cell Physiol. 1992;153(3):557-62.
82. Pepper MS, Ferrara N, Orci L, Montesano R. Potent synergism between vascular endothelial growth factor and basic fibroblast growth factor in the induction of angiogenesis in vitro. Biochemical and biophysical research communications. 1992;189(2):824-31.
83. Carmeliet P. VEGF as a Key Mediator of Angiogenesis in Cancer. Oncology. 2005;69(suppl 3)(Suppl. 3):4-10.
84. Tran J, Rak J, Sheehan C, Saibil SD, LaCasse E, Korneluk RG, et al. Marked induction of the IAP family antiapoptotic proteins survivin and XIAP by VEGF in vascular endothelial cells. Biochemical and biophysical research communications. 1999;264(3):781-8.
85. Gerber HP, McMurtrey A, Kowalski J, Yan M, Keyt BA, Dixit V, et al. Vascular endothelial growth factor regulates endothelial cell survival through the phosphatidylinositol 3'-kinase/Akt signal transduction pathway. Requirement for Flk-1/KDR activation. The Journal of biological chemistry. 1998;273(46):30336-43.
86. Gerber HP, Dixit V, Ferrara N. Vascular endothelial growth factor induces expression of the antiapoptotic proteins Bcl-2 and A1 in vascular endothelial cells. The Journal of biological chemistry. 1998;273(21):13313-6.
87. Ferrara N, Davis-Smyth T. The Biology of Vascular Endothelial Growth Factor. Endocrine Reviews. 1997;18(1):4-25.
88. Shweiki D, Itin A, Soffer D, Keshet E. Vascular endothelial growth factor induced by hypoxia may mediate hypoxia-initiated angiogenesis. Nature. 1992;359(6398):843-5.
89. van Uden P, Kenneth NS, Rocha S. Regulation of hypoxia-inducible factor-1alpha by NF-kappaB. Biochem J. 2008;412(3):477-84.
90. Cohen T, Nahari D, Cerem LW, Neufeld G, Levi BZ. Interleukin 6 induces the expression of vascular endothelial growth factor. The Journal of biological chemistry. 1996;271(2):736-41.
91. Li J, Perrella MA, Tsai JC, Yet SF, Hsieh CM, Yoshizumi M, et al. Induction of vascular endothelial growth factor gene expression by interleukin-1 beta in rat aortic smooth muscle cells. The Journal of biological chemistry. 1995;270(1):308-12.
92. Rak J, Yu JL, Klement G, Kerbel RS. Oncogenes and angiogenesis: signaling three-dimensional tumor growth. The journal of investigative dermatology Symposium proceedings. 2000;5(1):24-33.
93. Landskron G, De la Fuente M, Thuwajit P, Thuwajit C, Hermoso MA. Chronic inflammation and cytokines in the tumor microenvironment. J Immunol Res. 2014;2014:149185-.
94. da Silva Krause M, Bittencourt A, Homem de Bittencourt PI, Jr., McClenaghan NH, Flatt PR, Murphy C, et al. Physiological concentrations of interleukin-6 directly promote insulin secretion, signal transduction, nitric oxide release, and redox status in a clonal pancreatic beta-cell line and mouse islets. The Journal of endocrinology. 2012;214(3):301-11.
95. Sturrock A, Cahill B, Norman K, Huecksteadt TP, Hill K, Sanders K, et al. Transforming growth factor-beta1 induces Nox4 NAD(P)H oxidase and reactive oxygen species-dependent proliferation in human pulmonary artery smooth muscle cells. American journal of physiology Lung cellular and molecular physiology. 2006;290(4):L661-l73.

96. Yang D, Elner SG, Bian Z-M, Till GO, Petty HR, Elner VM. Pro-inflammatory cytokines increase reactive oxygen species through mitochondria and NADPH oxidase in cultured RPE cells. Exp Eye Res. 2007;85(4):462-72.
97. Balkwill F. TNF-alpha in promotion and progression of cancer. Cancer metastasis reviews. 2006;25(3):409-16.
98. Havell EA, Fiers W, North RJ. The antitumor function of tumor necrosis factor (TNF), I. Therapeutic action of TNF against an established murine sarcoma is indirect, immunologically dependent, and limited by severe toxicity. The Journal of experimental medicine. 1988;167(3):1067-85.
99. Hodge DR, Hurt EM, Farrar WL. The role of IL-6 and STAT3 in inflammation and cancer. European journal of cancer (Oxford, England : 1990). 2005;41(16):2502-12.
100. Fisher DT, Appenheimer MM, Evans SS. The two faces of IL-6 in the tumor microenvironment. Semin Immunol. 2014;26(1):38-47.
101. Song X, Voronov E, Dvorkin T, Fima E, Cagnano E, Benharroch D, et al. Differential effects of IL-1 alpha and IL-1 beta on tumorigenicity patterns and invasiveness. Journal of immunology (Baltimore, Md : 1950). 2003;171(12):6448-56.
102. Szlosarek P, Charles KA, Balkwill FR. Tumour necrosis factor-alpha as a tumour promoter. European journal of cancer (Oxford, England : 1990). 2006;42(6):745-50.
103. Moore RJ, Owens DM, Stamp G, Arnott C, Burke F, East N, et al. Mice deficient in tumor necrosis factor-alpha are resistant to skin carcinogenesis. Nature medicine. 1999;5(7):828-31.
104. Schottelius AJ, Mayo MW, Sartor RB, Baldwin AS, Jr. Interleukin-10 signaling blocks inhibitor of kappaB kinase activity and nuclear factor kappaB DNA binding. The Journal of biological chemistry. 1999;274(45):31868-74.
105. Hamidullah, Changkija B, Konwar R. Role of interleukin-10 in breast cancer. Breast cancer research and treatment. 2012;133(1):11-21.
106. Alas S, Emmanouilides C, Bonavida B. Inhibition of interleukin 10 by rituximab results in down-regulation of bcl-2 and sensitization of B-cell non-Hodgkin's lymphoma to apoptosis. Clinical cancer research : an official journal of the American Association for Cancer Research. 2001;7(3):709-23.
107. Zeng L, O'Connor C, Zhang J, Kaplan AM, Cohen DA. IL-10 promotes resistance to apoptosis and metastatic potential in lung tumor cell lines. Cytokine. 2010;49(3):294-302.
108. Lech-Maranda E, Bienvenu J, Michallet AS, Houot R, Robak T, Coiffier B, et al. Elevated IL-10 plasma levels correlate with poor prognosis in diffuse large B-cell lymphoma. European cytokine network. 2006;17(1):60-6.
109. Chow MT, Luster AD. Chemokines in cancer. Cancer Immunol Res. 2014;2(12):1125-31.
110. Strieter RM, Burdick MD, Gomperts BN, Belperio JA, Keane MP. CXC chemokines in angiogenesis. Cytokine Growth Factor Rev. 2005;16(6):593-609.
111. Wang N, Liu W, Zheng Y, Wang S, Yang B, Li M, et al. CXCL1 derived from tumor-associated macrophages promotes breast cancer metastasis via activating NF-κB/SOX4 signaling. Cell Death & Disease. 2018;9(9):880.
112. Chen M-C, Baskaran R, Lee N-H, Hsu H-H, Ho T-J, Tu C-C, et al. CXCL2/CXCR2 axis induces cancer stem cell characteristics in CPT-11-resistant LoVo colon cancer cells via Gαi-2 and Gαq/11. Journal of Cellular Physiology. 2019;234(7):11822-34.
113. Zhou SL, Dai Z, Zhou ZJ, Wang XY, Yang GH, Wang Z, et al. Overexpression of CXCL5 mediates neutrophil infiltration and indicates poor prognosis for hepatocellular carcinoma. Hepatology (Baltimore, Md). 2012;56(6):2242-54.
114. Park JY, Park KH, Bang S, Kim MH, Lee JE, Gang J, et al. CXCL5 overexpression is associated with late stage gastric cancer. Journal of cancer research and clinical oncology. 2007;133(11):835-40.

115. Dai Z, Wu J, Chen F, Cheng Q, Zhang M, Wang Y, et al. CXCL5 promotes the proliferation and migration of glioma cells in autocrine- and paracrine-dependent manners. Oncology reports. 2016;36(6):3303-10.
116. Li A, King J, Moro A, Sugi MD, Dawson DW, Kaplan J, et al. Overexpression of CXCL5 is associated with poor survival in patients with pancreatic cancer. The American journal of pathology. 2011;178(3):1340-9.
117. Sewell-Loftin MK, Bayer SVH, Crist E, Hughes T, Joison SM, Longmore GD, et al. Cancer-associated fibroblasts support vascular growth through mechanical force. Scientific Reports. 2017;7(1):12574.
118. De Francesco EM, Lappano R, Santolla MF, Marsico S, Caruso A, Maggiolini M. HIF-1alpha/GPER signaling mediates the expression of VEGF induced by hypoxia in breast cancer associated fibroblasts (CAFs). Breast cancer research : BCR. 2013;15(4):R64.
119. Xing F, Saidou J, Watabe K. Cancer associated fibroblasts (CAFs) in tumor microenvironment. Front Biosci (Landmark Ed). 2010;15:166-79.
120. Dimanche-Boitrel MT, Vakaet L, Jr., Pujuguet P, Chauffert B, Martin MS, Hammann A, et al. In vivo and in vitro invasiveness of a rat colon-cancer cell line maintaining E-cadherin expression: an enhancing role of tumor-associated myofibroblasts. International journal of cancer. 1994;56(4):512-21.
121. Yu Y, Xiao CH, Tan LD, Wang QS, Li XQ, Feng YM. Cancer-associated fibroblasts induce epithelial-mesenchymal transition of breast cancer cells through paracrine TGF-β signalling. Br J Cancer. 2014;110(3):724-32.
122. Jobe NP, Rosel D, Dvorankova B, Kodet O, Lacina L, Mateu R, et al. Simultaneous blocking of IL-6 and IL-8 is sufficient to fully inhibit CAF-induced human melanoma cell invasiveness. Histochemistry and cell biology. 2016;146(2):205-17.
123. Guan J, Zhang H, Wen Z, Gu Y, Cheng Y, Sun Y, et al. Retinoic acid inhibits pancreatic cancer cell migration and EMT through the downregulation of IL-6 in cancer associated fibroblast cells. Cancer letters. 2014;345(1):132-9.
124. Nakagawa H, Liyanarachchi S, Davuluri RV, Auer H, Martin EW, Jr., de la Chapelle A, et al. Role of cancer-associated stromal fibroblasts in metastatic colon cancer to the liver and their expression profiles. Oncogene. 2004;23(44):7366-77.
125. Min A, Zhu C, Wang J, Peng S, Shuai C, Gao S, et al. Focal adhesion kinase knockdown in carcinoma-associated fibroblasts inhibits oral squamous cell carcinoma metastasis via downregulating MCP-1/CCL2 expression. Journal of biochemical and molecular toxicology. 2015;29(2):70-6.
126. Wu MH, Hong HC, Hong TM, Chiang WF, Jin YT, Chen YL. Targeting galectin-1 in carcinoma-associated fibroblasts inhibits oral squamous cell carcinoma metastasis by downregulating MCP-1/CCL2 expression. Clinical cancer research : an official journal of the American Association for Cancer Research. 2011;17(6):1306-16.
127. Mueller L, Goumas FA, Affeldt M, Sandtner S, Gehling UM, Brilloff S, et al. Stromal fibroblasts in colorectal liver metastases originate from resident fibroblasts and generate an inflammatory microenvironment. The American journal of pathology. 2007;171(5):1608-18.
128. Harada A, Sekido N, Akahoshi T, Wada T, Mukaida N, Matsushima K. Essential involvement of interleukin-8 (IL-8) in acute inflammation. Journal of leukocyte biology. 1994;56(5):559-64.
129. Markman JL, Shiao SL. Impact of the immune system and immunotherapy in colorectal cancer. J Gastrointest Oncol. 2015;6(2):208-23.
130. Veglia F, Perego M, Gabrilovich D. Myeloid-derived suppressor cells coming of age. Nature Immunology. 2018;19(2):108-19.
131. Gabrilovich DI, Ostrand-Rosenberg S, Bronte V. Coordinated regulation of myeloid cells by tumours. Nat Rev Immunol. 2012;12(4):253-68.

132. Dolcetti L, Peranzoni E, Ugel S, Marigo I, Fernandez Gomez A, Mesa C, et al. Hierarchy of immunosuppressive strength among myeloid-derived suppressor cell subsets is determined by GM-CSF. European journal of immunology. 2010;40(1):22-35.
133. Mazzoni A, Bronte V, Visintin A, Spitzer JH, Apolloni E, Serafini P, et al. Myeloid suppressor lines inhibit T cell responses by an NO-dependent mechanism. Journal of immunology (Baltimore, Md : 1950). 2002;168(2):689-95.
134. Movahedi K, Guilliams M, Van den Bossche J, Van den Bergh R, Gysemans C, Beschin A, et al. Identification of discrete tumor-induced myeloid-derived suppressor cell subpopulations with distinct T cell-suppressive activity. Blood. 2008;111(8):4233-44.
135. Schmielau J, Finn OJ. Activated granulocytes and granulocyte-derived hydrogen peroxide are the underlying mechanism of suppression of t-cell function in advanced cancer patients. Cancer research. 2001;61(12):4756-60.
136. Youn JI, Nagaraj S, Collazo M, Gabrilovich DI. Subsets of myeloid-derived suppressor cells in tumor-bearing mice. Journal of immunology (Baltimore, Md : 1950). 2008;181(8):5791-802.
137. Pan PY, Ma G, Weber KJ, Ozao-Choy J, Wang G, Yin B, et al. Immune stimulatory receptor CD40 is required for T-cell suppression and T regulatory cell activation mediated by myeloid-derived suppressor cells in cancer. Cancer research. 2010;70(1):99-108.
138. Rodriguez PC, Quiceno DG, Zabaleta J, Ortiz B, Zea AH, Piazuelo MB, et al. Arginase I production in the tumor microenvironment by mature myeloid cells inhibits T-cell receptor expression and antigen-specific T-cell responses. Cancer research. 2004;64(16):5839-49.
139. Srivastava MK, Sinha P, Clements VK, Rodriguez P, Ostrand-Rosenberg S. Myeloid-derived suppressor cells inhibit T-cell activation by depleting cystine and cysteine. Cancer research. 2010;70(1):68-77.
140. Hanson EM, Clements VK, Sinha P, Ilkovitch D, Ostrand-Rosenberg S. Myeloid-derived suppressor cells down-regulate L-selectin expression on CD4+ and CD8+ T cells. Journal of immunology (Baltimore, Md : 1950). 2009;183(2):937-44.
141. Molon B, Ugel S, Del Pozzo F, Soldani C, Zilio S, Avella D, et al. Chemokine nitration prevents intratumoral infiltration of antigen-specific T cells. The Journal of experimental medicine. 2011;208(10):1949-62.
142. Hoechst B, Voigtlaender T, Ormandy L, Gamrekelashvili J, Zhao F, Wedemeyer H, et al. Myeloid derived suppressor cells inhibit natural killer cells in patients with hepatocellular carcinoma via the NKp30 receptor. Hepatology (Baltimore, Md). 2009;50(3):799-807.
143. Li H, Han Y, Guo Q, Zhang M, Cao X. Cancer-expanded myeloid-derived suppressor cells induce anergy of NK cells through membrane-bound TGF-beta 1. Journal of immunology (Baltimore, Md : 1950). 2009;182(1):240-9.
144. Sinha P, Clements VK, Bunt SK, Albelda SM, Ostrand-Rosenberg S. Cross-talk between myeloid-derived suppressor cells and macrophages subverts tumor immunity toward a type 2 response. Journal of immunology (Baltimore, Md : 1950). 2007;179(2):977-83.
145. Kusmartsev S, Cheng F, Yu B, Nefedova Y, Sotomayor E, Lush R, et al. All-Trans-Retinoic Acid Eliminates Immature Myeloid Cells from Tumor-bearing Mice and Improves the Effect of Vaccination. Cancer research. 2003;63(15):4441-9.
146. Zamai L, Ponti C, Mirandola P, Gobbi G, Papa S, Galeotti L, et al. NK Cells and Cancer. The Journal of Immunology. 2007;178(7):4011-6.
147. Wu J, Lanier LL. Natural killer cells and cancer. Advances in cancer research. 2003;90:127-56.
148. Aktas ON, Ozturk AB, Erman B, Erus S, Tanju S, Dilege S. Role of natural killer cells in lung cancer. Journal of cancer research and clinical oncology. 2018;144(6):997-1003.
149. Pross HF, Lotzova E. Role of natural killer cells in cancer. Natural immunity. 1993;12(4-5):279-92.

150. Halama N, Braun M, Kahlert C, Spille A, Quack C, Rahbari N, et al. Natural killer cells are scarce in colorectal carcinoma tissue despite high levels of chemokines and cytokines. Clinical cancer research : an official journal of the American Association for Cancer Research. 2011;17(4):678-89.
151. Höglund P, Ljunggren H-G. Natural killer cells in cancer2010. 55-64 p.
152. Veglia F, Gabrilovich DI. Dendritic cells in cancer: the role revisited. Curr Opin Immunol. 2017;45:43-51.
153. Ito T, Yang M, Wang YH, Lande R, Gregorio J, Perng OA, et al. Plasmacytoid dendritic cells prime IL-10-producing T regulatory cells by inducible costimulator ligand. The Journal of experimental medicine. 2007;204(1):105-15.
154. Tesone AJ, Rutkowski MR, Brencicova E, Svoronos N, Perales-Puchalt A, Stephen TL, et al. Satb1 Overexpression Drives Tumor-Promoting Activities in Cancer-Associated Dendritic Cells. Cell reports. 2016;14(7):1774-86.
155. Tel J, Aarntzen EH, Baba T, Schreibelt G, Schulte BM, Benitez-Ribas D, et al. Natural human plasmacytoid dendritic cells induce antigen-specific T-cell responses in melanoma patients. Cancer research. 2013;73(3):1063-75.
156. Qian B-Z, Pollard JW. Macrophage diversity enhances tumor progression and metastasis. Cell. 2010;141(1):39-51.
157. Grivennikov SI, Greten FR, Karin M. Immunity, inflammation, and cancer. Cell. 2010;140(6):883-99.
158. Ostuni R, Kratochvill F, Murray PJ, Natoli G. Macrophages and cancer: from mechanisms to therapeutic implications. Trends in immunology. 2015;36(4):229-39.
159. Mantovani A, Sozzani S, Locati M, Allavena P, Sica A. Macrophage polarization: tumor-associated macrophages as a paradigm for polarized M2 mononuclear phagocytes. Trends in immunology. 2002;23(11):549-55.
160. Biswas SK, Gangi L, Paul S, Schioppa T, Saccani A, Sironi M, et al. A distinct and unique transcriptional program expressed by tumor-associated macrophages (defective NF-kappaB and enhanced IRF-3/STAT1 activation). Blood. 2006;107(5):2112-22.
161. Mills CD. M1 and M2 Macrophages: Oracles of Health and Disease. Critical reviews in immunology. 2012;32(6):463-88.
162. Bingle L, Brown NJ, Lewis CE. The role of tumour-associated macrophages in tumour progression: implications for new anticancer therapies. J Pathol. 2002;196(3):254-65.
163. Farhood B, Najafi M, Mortezaee K. CD8+ cytotoxic T lymphocytes in cancer immunotherapy: A review. Journal of Cellular Physiology. 2019;234(6):8509-21.
164. Roberts SJ, Ng BY, Filler RB, Lewis J, Glusac EJ, Hayday AC, et al. Characterizing tumor-promoting T cells in chemically induced cutaneous carcinogenesis. Proceedings of the National Academy of Sciences of the United States of America. 2007;104(16):6770-5.
165. Haabeth OA, Lorvik KB, Hammarstrom C, Donaldson IM, Haraldsen G, Bogen B, et al. Inflammation driven by tumour-specific Th1 cells protects against B-cell cancer. Nature communications. 2011;2:240.
166. Knutson KL, Disis ML. Tumor antigen-specific T helper cells in cancer immunity and immunotherapy. Cancer Immunol Immunother. 2005;54(8):721-8.
167. Hong S, Qian J, Yang J, Li H, Kwak LW, Yi Q. Roles of Idiotype-Specific T Cells in Myeloma Cell Growth and Survival: Th1 and CTL Cells Are Tumoricidal while Th2 Cells Promote Tumor Growth. Cancer research. 2008;68(20):8456-64.
168. Powrie F, Menon S, Coffman RL. Interleukin-4 and interleukin-10 synergize to inhibit cell-mediated immunity in vivo. European journal of immunology. 1993;23(11):3043-9.
169. DeNardo DG, Barreto JB, Andreu P, Vasquez L, Tawfik D, Kolhatkar N, et al. CD4(+) T cells regulate pulmonary metastasis of mammary carcinomas by enhancing protumor properties of macrophages. Cancer Cell. 2009;16(2):91-102.

170. Aspord C, Pedroza-Gonzalez A, Gallegos M, Tindle S, Burton EC, Su D, et al. Breast cancer instructs dendritic cells to prime interleukin 13-secreting CD4+ T cells that facilitate tumor development. The Journal of experimental medicine. 2007;204(5):1037-47.
171. Protti MP, De Monte L. Cross-talk within the tumor microenvironment mediates Th2-type inflammation in pancreatic cancer. Oncoimmunology. 2012;1(1):89-91.
172. Ellyard JI, Simson L, Parish CR. Th2-mediated anti-tumour immunity: friend or foe? Tissue Antigens. 2007;70(1):1-11.
173. Mattes J, Hulett M, Xie W, Hogan S, Rothenberg ME, Foster P, et al. Immunotherapy of cytotoxic T cell-resistant tumors by T helper 2 cells: an eotaxin and STAT6-dependent process. The Journal of experimental medicine. 2003;197(3):387-93.
174. Nishimura T, Iwakabe K, Sekimoto M, Ohmi Y, Yahata T, Nakui M, et al. Distinct role of antigen-specific T helper type 1 (Th1) and Th2 cells in tumor eradication in vivo. The Journal of experimental medicine. 1999;190(5):617-27.
175. Hung K, Hayashi R, Lafond-Walker A, Lowenstein C, Pardoll D, Levitsky H. The central role of CD4(+) T cells in the antitumor immune response. The Journal of experimental medicine. 1998;188(12):2357-68.
176. Lorvik KB, Hammarström C, Fauskanger M, Haabeth OAW, Zangani M, Haraldsen G, et al. Adoptive Transfer of Tumor-Specific Th2 Cells Eradicates Tumors by Triggering an In Situ Inflammatory Immune Response. Cancer research. 2016;76(23):6864-76.
177. Murugaiyan G, Saha B. Protumor vs antitumor functions of IL-17. Journal of immunology (Baltimore, Md : 1950). 2009;183(7):4169-75.
178. Benevides L, da Fonseca DM, Donate PB, Tiezzi DG, De Carvalho DD, de Andrade JM, et al. IL17 Promotes Mammary Tumor Progression by Changing the Behavior of Tumor Cells and Eliciting Tumorigenic Neutrophils Recruitment. Cancer research. 2015;75(18):3788-99.
179. Knochelmann HM, Dwyer CJ, Bailey SR, Amaya SM, Elston DM, Mazza-McCrann JM, et al. When worlds collide: Th17 and Treg cells in cancer and autoimmunity. Cellular & Molecular Immunology. 2018;15(5):458-69.
180. Takahashi H, Numasaki M, Lotze MT, Sasaki H. Interleukin-17 enhances bFGF-, HGF- and VEGF-induced growth of vascular endothelial cells. Immunology letters. 2005;98(2):189-93.
181. Oleinika K, Nibbs RJ, Graham GJ, Fraser AR. Suppression, subversion and escape: the role of regulatory T cells in cancer progression. Clin Exp Immunol. 2013;171(1):36-45.
182. Mougiakakos D, Johansson CC, Trocme E, All-Ericsson C, Economou MA, Larsson O, et al. Intratumoral forkhead box P3-positive regulatory T cells predict poor survival in cyclooxygenase-2-positive uveal melanoma. Cancer. 2010;116(9):2224-33.
183. Najafi M, Farhood B, Mortezaee K. Contribution of regulatory T cells to cancer: A review. Journal of Cellular Physiology. 2019;234(6):7983-93.
184. Salama P, Phillips M, Grieu F, Morris M, Zeps N, Joseph D, et al. Tumor-infiltrating FOXP3+ T regulatory cells show strong prognostic significance in colorectal cancer. Journal of clinical oncology : official journal of the American Society of Clinical Oncology. 2009;27(2):186-92.
185. Nosho K, Baba Y, Tanaka N, Shima K, Hayashi M, Meyerhardt JA, et al. Tumour-infiltrating T-cell subsets, molecular changes in colorectal cancer, and prognosis: cohort study and literature review. J Pathol. 2010;222(4):350-66.
186. Erdman SE, Sohn JJ, Rao VP, Nambiar PR, Ge Z, Fox JG, et al. CD4+CD25+ regulatory lymphocytes induce regression of intestinal tumors in ApcMin/+ mice. Cancer research. 2005;65(10):3998-4004.
187. National Institute of Health. Colon Cancer Treatment (PDQ®)–Patient Version 2019 [Available from: https://www.cancer.gov/types/colorectal/patient/colon-treatment-pdq#section/all?redirect=true.

188. Longley DB, Harkin DP, Johnston PG. 5-fluorouracil: mechanisms of action and clinical strategies. Nature reviews Cancer. 2003;3(5):330-8.
189. Walko CM, Lindley C. Capecitabine: a review. Clinical therapeutics. 2005;27(1):23-44.
190. Fujita K-i, Kubota Y, Ishida H, Sasaki Y. Irinotecan, a key chemotherapeutic drug for metastatic colorectal cancer. World J Gastroenterol. 2015;21(43):12234-48.
191. Alcindor T, Beauger N. Oxaliplatin: a review in the era of molecularly targeted therapy. Curr Oncol. 2011;18(1):18-25.
192. Temmink OH, Emura T, de Bruin M, Fukushima M, Peters GJ. Therapeutic potential of the dual-targeted TAS-102 formulation in the treatment of gastrointestinal malignancies. Cancer science. 2007;98(6):779-89.
193. Yoshino T, Komatsu Y, Yamada Y, Yamazaki K, Tsuji A, Ura T, et al. Randomized phase III trial of regorafenib in metastatic colorectal cancer: analysis of the CORRECT Japanese and non-Japanese subpopulations. Invest New Drugs. 2015;33(3):740-50.
194. Keating GM. Bevacizumab: a review of its use in advanced cancer. Drugs. 2014;74(16):1891-925.
195. Merlano M, Occelli M. Review of cetuximab in the treatment of squamous cell carcinoma of the head and neck. Ther Clin Risk Manag. 2007;3(5):871-6.
196. Le DT, Uram JN, Wang H, Bartlett BR, Kemberling H, Eyring AD, et al. PD-1 Blockade in Tumors with Mismatch-Repair Deficiency. The New England journal of medicine. 2015;372(26):2509-20.
197. Dudley JC, Lin MT, Le DT, Eshleman JR. Microsatellite Instability as a Biomarker for PD-1 Blockade. Clinical cancer research : an official journal of the American Association for Cancer Research. 2016;22(4):813-20.
198. Arora SP, Mahalingam D. Immunotherapy in colorectal cancer: for the select few or all? J Gastrointest Oncol. 2018;9(1):170-9.
199. Sinicrope FA. DNA mismatch repair and adjuvant chemotherapy in sporadic colon cancer. Nat Rev Clin Oncol. 2010;7(3):174-7.
200. Routy B, Le Chatelier E, Derosa L, Duong CPM, Alou MT, Daillere R, et al. Gut microbiome influences efficacy of PD-1-based immunotherapy against epithelial tumors. Science (New York, NY). 2018;359(6371):91-7.
201. Gopalakrishnan V, Spencer CN, Nezi L, Reuben A, Andrews MC, Karpinets TV, et al. Gut microbiome modulates response to anti-PD-1 immunotherapy in melanoma patients. Science (New York, NY). 2018;359(6371):97-103.
202. Pouncey AL, Scott AJ, Alexander JL, Marchesi J, Kinross J. Gut microbiota, chemotherapy and the host: the influence of the gut microbiota on cancer treatment. Ecancermedicalscience. 2018;12:868-.
203. Sekirov I, Russell SL, Antunes LCM, Finlay BB. Gut Microbiota in Health and Disease. Physiological Reviews. 2010;90(3):859-904.
204. Gould KA, Dove WF. Localized gene action controlling intestinal neoplasia in mice. Proc Natl Acad Sci U S A. 1997;94(11):5848-53.
205. Moser AR, Pitot HC, Dove WF. A dominant mutation that predisposes to multiple intestinal neoplasia in the mouse. Science (New York, NY). 1990;247(4940):322-4.
206. Su LK, Kinzler KW, Vogelstein B, Preisinger AC, Moser AR, Luongo C, et al. Multiple intestinal neoplasia caused by a mutation in the murine homolog of the APC gene. Science (New York, NY). 1992;256(5057):668-70.
207. Luongo C, Gould KA, Su LK, Kinzler KW, Vogelstein B, Dietrich W, et al. Mapping of multiple intestinal neoplasia (Min) to proximal chromosome 18 of the mouse. Genomics. 1993;15(1):3-8.

208. Oshima M, Oshima H, Kitagawa K, Kobayashi M, Itakura C, Taketo M. Loss of Apc heterozygosity and abnormal tissue building in nascent intestinal polyps in mice carrying a truncated Apc gene. Proc Natl Acad Sci U S A. 1995;92(10):4482-6.
209. Knudson AG. Mutation and Cancer: Statistical Study of Retinoblastoma. Proceedings of the National Academy of Sciences of the United States of America. 1971;68(4):820-3.
210. Neufeld KL, White RL. Nuclear and cytoplasmic localizations of the adenomatous polyposis coli protein. Proceedings of the National Academy of Sciences of the United States of America. 1997;94(7):3034-9.
211. Henderson BR. Nuclear-cytoplasmic shuttling of APC regulates beta-catenin subcellular localization and turnover. Nature cell biology. 2000;2(9):653-60.
212. Zeineldin M, Miller MA, Sullivan R, Neufeld KL. Nuclear adenomatous polyposis coli suppresses colitis-associated tumorigenesis in mice. Carcinogenesis. 2014;35(8):1881-90.
213. Clapper ML, Cooper HS, Chang WC. Dextran sulfate sodium-induced colitis-associated neoplasia: a promising model for the development of chemopreventive interventions. Acta pharmacologica Sinica. 2007;28(9):1450-9.
214. Shoemaker AR, Luongo C, Moser AR, Marton LJ, Dove WF. Somatic Mutational Mechanisms Involved in Intestinal Tumor Formation in Min Mice. Cancer research. 1997;57(10):1999-2006.
215. Fodde R, Smits R. Disease model: familial adenomatous polyposis. Trends in molecular medicine. 2001;7(8):369-73.
216. Halberg RB, Waggoner J, Rasmussen K, White A, Clipson L, Prunuske AJ, et al. Long-lived Min mice develop advanced intestinal cancers through a genetically conservative pathway. Cancer research. 2009;69(14):5768-75.
217. Lorenz E, Stewart HL. Intestinal Carcinoma and Other Lesions in Mice Following Oral Administration of 1,2,5,6-Dibenzanthracene and 20-Methylcholanthrene1. JNCI: Journal of the National Cancer Institute. 1940;1(1):17-40.
218. Laqueur GL, Mickelsen O, Whiting MG, Kurland LT. Carcinogenic Properties of Nuts From Cycas Circinalis L. Indigenous to Guam2. JNCI: Journal of the National Cancer Institute. 1963;31(4):919-51.
219. Laqueur GL, Spatz M. Toxicology of cycasin. Cancer research. 1968;28(11):2262-7.
220. Fiala ES. Investigations into the metabolism and mode of action of the colon carcinogens 1,2-dimethylhydrazine and azoxymethane. Cancer. 1977;40(5 Suppl):2436-45.
221. Laqueur GL. CARCINOGENIC EFFECTS OF CYCAD MEAL AND CYCASIN, METHYLAZOXYMETHANOL GLYCOSIDE, IN RATS AND EFFECTS OF CYCASIN IN GERMFREE RATS. Federation proceedings. 1964;23:1386-8.
222. Druckrey H, Preussmann R, Matzkies F, Ivankovic S. [Selective production of intestinal cancer in rats by 1,2-dimethylhydrazine]. Die Naturwissenschaften. 1967;54(11):285-6.
223. Cruse JP, Lewin MR, Ferulano GP, Clark CG. Co-carcinogenic effects of dietary cholesterol in experimental colon cancer. Nature. 1978;276(5690):822-5.
224. Deschner EE, Long FC. Colonic neoplasms in mice produced with six injections of 1,2-dimethylhydrazine. Oncology. 1977;34(6):255-7.
225. Thurnherr N, Deschner EE, Stonehill EH, Lipkin M. Induction of adenocarcinomas of the colon in mice by weekly injections of 1,2-dimethylhydrazine. Cancer research. 1973;33(5):940-5.
226. Papanikolaou A, Shank RC, Delker DA, Povey A, Cooper DP, Rosenberg DW. Initial levels of azoxymethane-induced DNA methyl adducts are not predictive of tumor susceptibility in inbred mice. Toxicology and applied pharmacology. 1998;150(1):196-203.
227. Neufert C, Becker C, Neurath MF. An inducible mouse model of colon carcinogenesis for the analysis of sporadic and inflammation-driven tumor progression. Nature protocols. 2007;2(8):1998-2004.

228. Kobaek-Larsen M, Thorup I, Diederichsen A, Fenger C, Hoitinga MR. Review of colorectal cancer and its metastases in rodent models: comparative aspects with those in humans. Comparative medicine. 2000;50(1):16-26.
229. Sohn OS, Fiala ES, Requeijo SP, Weisburger JH, Gonzalez FJ. Differential Effects of CYP2E1 Status on the Metabolic Activation of the Colon Carcinogens Azoxymethane and Methylazoxymethanol. Cancer research. 2001;61(23):8435-40.
230. Delker DA, Wang QS, Papanikolaou A, Whiteley HE, Rosenberg DW. Quantitative assessment of azoxymethane-induced aberrant crypt foci in inbred mice. Experimental and molecular pathology. 1999;65(3):141-9.
231. Papanikolaou A, Wang QS, Mulherkar R, Bolt A, Rosenberg DW. Expression analysis of the group IIA secretory phospholipase A(2) in mice with differential susceptibility to azoxymethane-induced colon tumorigenesis. Carcinogenesis. 2000;21(2):133-8.
232. Guda K, Marino JN, Jung Y, Crary K, Dong M, Rosenberg DW. Strain-specific homeostatic responses during early stages of Azoxymethane-induced colon tumorigenesis in mice. International journal of oncology. 2007;31(4):837-42.
233. Rosenberg DW, Giardina C, Tanaka T. Mouse models for the study of colon carcinogenesis. Carcinogenesis. 2009;30(2):183-96.
234. Bissahoyo A, Pearsall RS, Hanlon K, Amann V, Hicks D, Godfrey VL, et al. Azoxymethane is a genetic background-dependent colorectal tumor initiator and promoter in mice: effects of dose, route, and diet. Toxicological sciences : an official journal of the Society of Toxicology. 2005;88(2):340-5.
235. Nambiar PR, Girnun G, Lillo NA, Guda K, Whiteley HE, Rosenberg DW. Preliminary analysis of azoxymethane induced colon tumors in inbred mice commonly used as transgenic/knockout progenitors. International journal of oncology. 2003;22(1):145-50.
236. Delker DA, Bammler TK, Rosenberg DW. A comparative study of hepatic and colonic metabolic enzymes in inbred mouse lines before and after treatment with the colon carcinogen, 1,2-dimethylhydrazine. Drug metabolism and disposition: the biological fate of chemicals. 1996;24(4):408-13.
237. Diwan BA, Meier H, Blackman KE. Genetic Differences in the Induction of Colorectal Tumors by 1,2-Dimethylhydrazine in Inbred Mice2. JNCI: Journal of the National Cancer Institute. 1977;59(2):455-8.
238. Ilsley JN, Belinsky GS, Guda K, Zhang Q, Huang X, Blumberg JB, et al. Dietary iron promotes azoxymethane-induced colon tumors in mice. Nutrition and cancer. 2004;49(2):162-9.
239. Papanikolaou A, Wang QS, Papanikolaou D, Whiteley HE, Rosenberg DW. Sequential and morphological analyses of aberrant crypt foci formation in mice of differing susceptibility to azoxymethane-induced colon carcinogenesis. Carcinogenesis. 2000;21(8):1567-72.
240. Papanikolaou A, Wang QS, Delker DA, Rosenberg DW. Azoxymethane-induced colon tumors and aberrant crypt foci in mice of different genetic susceptibility. Cancer letters. 1998;130(1-2):29-34.
241. Evans JT, Shows TB, Sproul EE, Paolini NS, Mittelman A, Hauschka TS. Genetics of colon carcinogenesis in mice treated with 1,2-dimethylhydrazine. Cancer research. 1977;37(1):134-6.
242. Diwan BA, Blackman KE. Differential susceptibility of 3 sublines of C57BL/6 mice to the induction of colorectal tumors by 1,2-dimethylhydrazine. Cancer letters. 1980;9(2):111-5.
243. Diwan BA, Blackman KE. Carcinogenic effects of combined treatment of inbred mice with 3-methylcholanthrene and 1,2-dimethylhydrazine. Journal of the National Cancer Institute. 1980;64(6):1491-3.

244. Evans JT, Hauschka TS, Mittelman A. Differential susceptibility of four mouse strains to induction of multiple large-bowel neoplasms by 1,2-dimethylhydrazine. Journal of the National Cancer Institute. 1974;52(3):999-1000.
245. Izumi K, Otsuka H, Furuya K, Akagi A. Carcinogenicity of 1,2-dimethylhydrazine dihydrochloride in BALB/c mice. Influence of the route of administration and dosage. Virchows Archiv A, Pathological anatomy and histology. 1979;384(3):263-7.
246. Turusov VS, Lanko NS, Krutovskikh VA, Parfenov YD. Strain differences in susceptibility of female mice to 1,2-dimethylhydrazine. Carcinogenesis. 1982;3(6):603-8.
247. Ilsley JN, Nakanishi M, Flynn C, Belinsky GS, De Guise S, Adib JN, et al. Cytoplasmic phospholipase A2 deletion enhances colon tumorigenesis. Cancer research. 2005;65(7):2636-43.
248. Boffa LC, Diwan BA, Gruss R, Allfrey VG. Differences in colonic nuclear proteins of two mouse strains with different susceptibilities to 1, 2-dimethylhydrazine-induced carcinogenesis. Cancer research. 1980;40(6):1774-80.
249. Chen J, Huang XF. The signal pathways in azoxymethane-induced colon cancer and preventive implications. Cancer biology & therapy. 2009;8(14):1313-7.
250. Maltzman T, Whittington J, Driggers L, Stephens J, Ahnen D. AOM-induced mouse colon tumors do not express full-length APC protein. Carcinogenesis. 1997;18(12):2435-9.
251. Bolt AB, Papanikolaou A, Delker DA, Wang QS, Rosenberg DW. Azoxymethane induces KI-ras activation in the tumor resistant AKR/J mouse colon. Molecular carcinogenesis. 2000;27(3):210-8.
252. Erdman SH, Wu HD, Hixson LJ, Ahnen DJ, Gerner EW. Assessment of mutations in Ki-ras and p53 in colon cancers from azoxymethane- and dimethylhydrazine-treated rats. Molecular carcinogenesis. 1997;19(2):137-44.
253. De Filippo C, Caderni G, Bazzicalupo M, Briani C, Giannini A, Fazi M, et al. Mutations of the Apc gene in experimental colorectal carcinogenesis induced by azoxymethane in F344 rats. Br J Cancer. 1998;77(12):2148-51.
254. Guda K, Upender MB, Belinsky G, Flynn C, Nakanishi M, Marino JN, et al. Carcinogen-induced colon tumors in mice are chromosomally stable and are characterized by low-level microsatellite instability. Oncogene. 2004;23(21):3813-21.
255. Breskvar L, Cerar A. A role of gender in the occurrence of dimethylhydrazine induced colorectal tumors in Wistar rats = Vpliv spola na indukcijo debelocrevesnega karcinoma z 1,2-dimetilhidrazinom (DMH) pri podganah Wistar. Radiology and oncology. 1997(31):374-9.
256. Group NHW, Peterson J, Garges S, Giovanni M, McInnes P, Wang L, et al. The NIH Human Microbiome Project. Genome Res. 2009;19(12):2317-23.
257. Sender R, Fuchs S, Milo R. Are We Really Vastly Outnumbered? Revisiting the Ratio of Bacterial to Host Cells in Humans. Cell. 2016;164(3):337-40.
258. Sender R, Fuchs S, Milo R. Revised estimates for the number of human and bacteria cells in the body. bioRxiv. 2016:036103.
259. Mazmanian SK, Liu CH, Tzianabos AO, Kasper DL. An immunomodulatory molecule of symbiotic bacteria directs maturation of the host immune system. Cell. 2005;122(1):107-18.
260. Konieczna P, Groeger D, Ziegler M, Frei R, Ferstl R, Shanahan F, et al. Bifidobacterium infantis 35624 administration induces Foxp3 T regulatory cells in human peripheral blood: potential role for myeloid and plasmacytoid dendritic cells. Gut. 2012;61(3):354-66.
261. Quigley EMM. Gut bacteria in health and disease. Gastroenterol Hepatol (N Y). 2013;9(9):560-9.
262. Patel RM, Lin PW. Developmental biology of gut-probiotic interaction. Gut microbes. 2010;1(3):186-95.

263. Jahani-Sherafat S, Alebouyeh M, Moghim S, Ahmadi Amoli H, Ghasemian-Safaei H. Role of gut microbiota in the pathogenesis of colorectal cancer; a review article. Gastroenterol Hepatol Bed Bench. 2018;11(2):101-9.
264. Nishida A, Inoue R, Inatomi O, Bamba S, Naito Y, Andoh A. Gut microbiota in the pathogenesis of inflammatory bowel disease. Clinical journal of gastroenterology. 2018;11(1):1-10.
265. Panek M, Čipčić Paljetak H, Barešić A, Perić M, Matijašić M, Lojkić I, et al. Methodology challenges in studying human gut microbiota – effects of collection, storage, DNA extraction and next generation sequencing technologies. Scientific Reports. 2018;8(1):5143.
266. Blaxter M, Mann J, Chapman T, Thomas F, Whitton C, Floyd R, et al. Defining operational taxonomic units using DNA barcode data. Philos Trans R Soc Lond B Biol Sci. 2005;360(1462):1935-43.
267. Venter JC, Remington K, Heidelberg JF, Halpern AL, Rusch D, Eisen JA, et al. Environmental genome shotgun sequencing of the Sargasso Sea. Science (New York, NY). 2004;304(5667):66-74.
268. Tyson GW, Chapman J, Hugenholtz P, Allen EE, Ram RJ, Richardson PM, et al. Community structure and metabolism through reconstruction of microbial genomes from the environment. Nature. 2004;428(6978):37-43.
269. Pasolli E, Asnicar F, Manara S, Zolfo M, Karcher N, Armanini F, et al. Extensive Unexplored Human Microbiome Diversity Revealed by Over 150,000 Genomes from Metagenomes Spanning Age, Geography, and Lifestyle. Cell. 2019;176(3):649-62.e20.
270. Frank DN, St Amand AL, Feldman RA, Boedeker EC, Harpaz N, Pace NR. Molecular-phylogenetic characterization of microbial community imbalances in human inflammatory bowel diseases. Proceedings of the National Academy of Sciences of the United States of America. 2007;104(34):13780-5.
271. Eckburg PB, Bik EM, Bernstein CN, Purdom E, Dethlefsen L, Sargent M, et al. Diversity of the human intestinal microbial flora. Science (New York, NY). 2005;308(5728):1635-8.
272. Gill SR, Pop M, Deboy RT, Eckburg PB, Turnbaugh PJ, Samuel BS, et al. Metagenomic analysis of the human distal gut microbiome. Science (New York, NY). 2006;312(5778):1355-9.
273. DiGiulio DB. Diversity of microbes in amniotic fluid. Seminars in fetal & neonatal medicine. 2012;17(1):2-11.
274. Dunn AB, Jordan S, Baker BJ, Carlson NS. The Maternal Infant Microbiome: Considerations for Labor and Birth. MCN Am J Matern Child Nurs. 2017;42(6):318-25.
275. Mandar R, Mikelsaar M. Transmission of mother's microflora to the newborn at birth. Biology of the neonate. 1996;69(1):30-5.
276. Redondo-Lopez V, Cook RL, Sobel JD. Emerging role of lactobacilli in the control and maintenance of the vaginal bacterial microflora. Reviews of infectious diseases. 1990;12(5):856-72.
277. de Goffau MC, Lager S, Sovio U, Gaccioli F, Cook E, Peacock SJ, et al. Human placenta has no microbiome but can contain potential pathogens. Nature. 2019;572(7769):329-34.
278. Huurre A, Kalliomaki M, Rautava S, Rinne M, Salminen S, Isolauri E. Mode of delivery - effects on gut microbiota and humoral immunity. Neonatology. 2008;93(4):236-40.
279. Marques TM, Wall R, Ross RP, Fitzgerald GF, Ryan CA, Stanton C. Programming infant gut microbiota: influence of dietary and environmental factors. Current opinion in biotechnology. 2010;21(2):149-56.
280. Fouhy F, Ross RP, Fitzgerald GF, Stanton C, Cotter PD. Composition of the early intestinal microbiota: knowledge, knowledge gaps and the use of high-throughput sequencing to address these gaps. Gut microbes. 2012;3(3):203-20.

281. Mackie RI, Sghir A, Gaskins HR. Developmental microbial ecology of the neonatal gastrointestinal tract. The American journal of clinical nutrition. 1999;69(5):1035s-45s.
282. Maskarinec G, Noh JJ. The effect of migration on cancer incidence among Japanese in Hawaii. Ethnicity & disease. 2004;14(3):431-9.
283. Turnbaugh PJ, Backhed F, Fulton L, Gordon JI. Diet-induced obesity is linked to marked but reversible alterations in the mouse distal gut microbiome. Cell host & microbe. 2008;3(4):213-23.
284. O'Toole PW, Claesson MJ. Gut microbiota: Changes throughout the lifespan from infancy to elderly. International Dairy Journal. 2010;20(4):281-91.
285. Hopkins MJ, Sharp R, Macfarlane GT. Age and disease related changes in intestinal bacterial populations assessed by cell culture, 16S rRNA abundance, and community cellular fatty acid profiles. Gut. 2001;48(2):198-205.
286. Nagpal R, Mainali R, Ahmadi S, Wang S, Singh R, Kavanagh K, et al. Gut microbiome and aging: Physiological and mechanistic insights. Nutr Healthy Aging. 2018;4(4):267-85.
287. Claesson MJ, Jeffery IB, Conde S, Power SE, O'Connor EM, Cusack S, et al. Gut microbiota composition correlates with diet and health in the elderly. Nature. 2012;488:178.
288. O'Hara AM, Shanahan F. The gut flora as a forgotten organ. EMBO reports. 2006;7(7):688-93.
289. Mariat D, Firmesse O, Levenez F, Guimarăes V, Sokol H, Doré J, et al. The Firmicutes/Bacteroidetes ratio of the human microbiota changes with age. BMC Microbiol. 2009;9:123-.
290. Castaner O, Goday A, Park Y-M, Lee S-H, Magkos F, Shiow S-ATE, et al. The Gut Microbiome Profile in Obesity: A Systematic Review. Int J Endocrinol. 2018;2018:4095789-.
291. Schwiertz A, Taras D, Schafer K, Beijer S, Bos NA, Donus C, et al. Microbiota and SCFA in lean and overweight healthy subjects. Obesity (Silver Spring, Md). 2010;18(1):190-5.
292. Ley RE, Turnbaugh PJ, Klein S, Gordon JI. Human gut microbes associated with obesity. Nature. 2006;444(7122):1022-3.
293. Koliada A, Syzenko G, Moseiko V, Budovska L, Puchkov K, Perederiy V, et al. Association between body mass index and Firmicutes/Bacteroidetes ratio in an adult Ukrainian population. BMC Microbiol. 2017;17(1):120-.
294. Valdes AM, Walter J, Segal E, Spector TD. Role of the gut microbiota in nutrition and health. BMJ. 2018;361:k2179.
295. Darfeuille-Michaud A, Boudeau J, Bulois P, Neut C, Glasser AL, Barnich N, et al. High prevalence of adherent-invasive Escherichia coli associated with ileal mucosa in Crohn's disease. Gastroenterology. 2004;127(2):412-21.
296. Lupp C, Robertson ML, Wickham ME, Sekirov I, Champion OL, Gaynor EC, et al. Host-mediated inflammation disrupts the intestinal microbiota and promotes the overgrowth of Enterobacteriaceae. Cell host & microbe. 2007;2(2):119-29.
297. Ohkusa T, Sato N, Ogihara T, Morita K, Ogawa M, Okayasu I. Fusobacterium varium localized in the colonic mucosa of patients with ulcerative colitis stimulates species-specific antibody. Journal of gastroenterology and hepatology. 2002;17(8):849-53.
298. Fite A, Macfarlane S, Furrie E, Bahrami B, Cummings JH, Steinke DT, et al. Longitudinal analyses of gut mucosal microbiotas in ulcerative colitis in relation to patient age and disease severity and duration. J Clin Microbiol. 2013;51(3):849-56.
299. Ai D, Pan H, Li X, Gao Y, Liu G, Xia LC. Identifying Gut Microbiota Associated With Colorectal Cancer Using a Zero-Inflated Lognormal Model. Front Microbiol. 2019;10(826).
300. Hibberd AA, Lyra A, Ouwehand AC, Rolny P, Lindegren H, Cedgård L, et al. Intestinal microbiota is altered in patients with colon cancer and modified by probiotic intervention. BMJ Open Gastroenterol. 2017;4(1):e000145-e.

301. Scanlan PD, Shanahan F, Clune Y, Collins JK, O'Sullivan GC, O'Riordan M, et al. Culture-independent analysis of the gut microbiota in colorectal cancer and polyposis. Environmental microbiology. 2008;10(3):789-98.
302. Wong SH, Zhao L, Zhang X, Nakatsu G, Han J, Xu W, et al. Gavage of Fecal Samples From Patients With Colorectal Cancer Promotes Intestinal Carcinogenesis in Germ-Free and Conventional Mice. Gastroenterology. 2017;153(6):1621-33.e6.
303. Sanapareddy N, Legge RM, Jovov B, McCoy A, Burcal L, Araujo-Perez F, et al. Increased rectal microbial richness is associated with the presence of colorectal adenomas in humans. The ISME journal. 2012;6(10):1858-68.
304. Feng Q, Liang S, Jia H, Stadlmayr A, Tang L, Lan Z, et al. Gut microbiome development along the colorectal adenoma–carcinoma sequence. Nature communications. 2015;6:6528.
305. Raskov H, Burcharth J, Pommergaard H-C. Linking Gut Microbiota to Colorectal Cancer. J Cancer. 2017;8(17):3378-95.
306. Hope ME, Hold GL, Kain R, El-Omar EM. Sporadic colorectal cancer – role of the commensal microbiota. FEMS Microbiology Letters. 2005;244(1):1-7.
307. Suehiro Y, Sakai K, Nishioka M, Hashimoto S, Takami T, Higaki S, et al. Highly sensitive stool DNA testing of Fusobacterium nucleatum as a marker for detection of colorectal tumours in a Japanese population. Annals of clinical biochemistry. 2017;54(1):86-91.
308. Wong SH, Kwong TNY, Chow T-C, Luk AKC, Dai RZW, Nakatsu G, et al. Quantitation of faecal Fusobacterium improves faecal immunochemical test in detecting advanced colorectal neoplasia. Gut. 2017;66(8):1441-8.
309. Liang Q, Chiu J, Chen Y, Huang Y, Higashimori A, Fang J, et al. Fecal Bacteria Act as Novel Biomarkers for Noninvasive Diagnosis of Colorectal Cancer. Clinical cancer research : an official journal of the American Association for Cancer Research. 2017;23(8):2061-70.
310. Castellarin M, Warren RL, Freeman JD, Dreolini L, Krzywinski M, Strauss J, et al. Fusobacterium nucleatum infection is prevalent in human colorectal carcinoma. Genome Res. 2012;22(2):299-306.
311. Li Y-Y, Ge Q-X, Cao J, Zhou Y-J, Du Y-L, Shen B, et al. Association of Fusobacterium nucleatum infection with colorectal cancer in Chinese patients. World J Gastroenterol. 2016;22(11):3227-33.
312. Mima K, Cao Y, Chan AT, Qian ZR, Nowak JA, Masugi Y, et al. Fusobacterium nucleatum in Colorectal Carcinoma Tissue According to Tumor Location. Clin Transl Gastroenterol. 2016;7(11):e200-e.
313. Fukugaiti MH, Ignacio A, Fernandes MR, Ribeiro Júnior U, Nakano V, Avila-Campos MJ. High occurrence of Fusobacterium nucleatum and Clostridium difficile in the intestinal microbiota of colorectal carcinoma patients. Braz J Microbiol. 2015;46(4):1135-40.
314. Wei Z, Cao S, Liu S, Yao Z, Sun T, Li Y, et al. Could gut microbiota serve as prognostic biomarker associated with colorectal cancer patients' survival? A pilot study on relevant mechanism. Oncotarget. 2016;7(29):46158-72.
315. Mira-Pascual L, Cabrera-Rubio R, Ocon S, Costales P, Parra A, Suarez A, et al. Microbial mucosal colonic shifts associated with the development of colorectal cancer reveal the presence of different bacterial and archaeal biomarkers. Journal of gastroenterology. 2015;50(2):167-79.
316. Tahara T, Yamamoto E, Suzuki H, Maruyama R, Chung W, Garriga J, et al. Fusobacterium in colonic flora and molecular features of colorectal carcinoma. Cancer research. 2014;74(5):1311-8.
317. Marchesi JR, Dutilh BE, Hall N, Peters WHM, Roelofs R, Boleij A, et al. Towards the human colorectal cancer microbiome. PloS one. 2011;6(5):e20447-e.
318. Kostic AD, Gevers D, Pedamallu CS, Michaud M, Duke F, Earl AM, et al. Genomic analysis identifies association of Fusobacterium with colorectal carcinoma. Genome Res. 2012;22(2):292-8.

319. Burns MB, Lynch J, Starr TK, Knights D, Blekhman R. Virulence genes are a signature of the microbiome in the colorectal tumor microenvironment. Genome medicine. 2015;7(1):55.
320. Gao Z, Guo B, Gao R, Zhu Q, Qin H. Microbiota disbiosis is associated with colorectal cancer. Front Microbiol. 2015;6:20-.
321. Ahn J, Sinha R, Pei Z, Dominianni C, Wu J, Shi J, et al. Human gut microbiome and risk for colorectal cancer. Journal of the National Cancer Institute. 2013;105(24):1907-11.
322. Sinha R, Ahn J, Sampson JN, Shi J, Yu G, Xiong X, et al. Fecal Microbiota, Fecal Metabolome, and Colorectal Cancer Interrelations. PloS one. 2016;11(3):e0152126-e.
323. Viljoen KS, Dakshinamurthy A, Goldberg P, Blackburn JM. Quantitative profiling of colorectal cancer-associated bacteria reveals associations between fusobacterium spp., enterotoxigenic Bacteroides fragilis (ETBF) and clinicopathological features of colorectal cancer. PloS one. 2015;10(3):e0119462.
324. Geng J, Fan H, Tang X, Zhai H, Zhang Z. Diversified pattern of the human colorectal cancer microbiome. Gut pathogens. 2013;5(1):2-.
325. Zhou Y, He H, Xu H, Li Y, Li Z, Du Y, et al. Association of oncogenic bacteria with colorectal cancer in South China. Oncotarget. 2016;7(49):80794-802.
326. Warren RL, Freeman DJ, Pleasance S, Watson P, Moore RA, Cochrane K, et al. Co-occurrence of anaerobic bacteria in colorectal carcinomas. Microbiome. 2013;1(1):16-.
327. Sobhani I, Tap J, Roudot-Thoraval F, Roperch JP, Letulle S, Langella P, et al. Microbial dysbiosis in colorectal cancer (CRC) patients. PloS one. 2011;6(1):e16393-e.
328. Balamurugan R, Rajendiran E, George S, Samuel GV, Ramakrishna BS. Real-time polymerase chain reaction quantification of specific butyrate-producing bacteria, Desulfovibrio and Enterococcus faecalis in the feces of patients with colorectal cancer. Journal of gastroenterology and hepatology. 2008;23(8 Pt 1):1298-303.
329. Flemer B, Lynch DB, Brown JMR, Jeffery IB, Ryan FJ, Claesson MJ, et al. Tumour-associated and non-tumour-associated microbiota in colorectal cancer. Gut. 2017;66(4):633-43.
330. Swidsinski A, Khilkin M, Kerjaschki D, Schreiber S, Ortner M, Weber J, et al. Association between intraepithelial Escherichia coli and colorectal cancer. Gastroenterology. 1998;115(2):281-6.
331. Zumkeller N, Brenner H, Zwahlen M, Rothenbacher D. Helicobacter pylori infection and colorectal cancer risk: a meta-analysis. Helicobacter. 2006;11(2):75-80.
332. Kwong TNY, Wang X, Nakatsu G, Chow TC, Tipoe T, Dai RZW, et al. Association Between Bacteremia From Specific Microbes and Subsequent Diagnosis of Colorectal Cancer. Gastroenterology. 2018;155(2):383-90.e8.
333. Gold JS, Bayar S, Salem RR. Association of Streptococcus bovis bacteremia with colonic neoplasia and extracolonic malignancy. Archives of surgery (Chicago, Ill : 1960). 2004;139(7):760-5.
334. Macarthur M, Hold GL, El-Omar EM. Inflammation and Cancer II. Role of chronic inflammation and cytokine gene polymorphisms in the pathogenesis of gastrointestinal malignancy. American journal of physiology Gastrointestinal and liver physiology. 2004;286(4):G515-20.
335. Correa P, Houghton J. Carcinogenesis of Helicobacter pylori. Gastroenterology. 2007;133(2):659-72.
336. Wroblewski LE, Peek RM, Jr., Wilson KT. Helicobacter pylori and gastric cancer: factors that modulate disease risk. Clin Microbiol Rev. 2010;23(4):713-39.
337. Martin HM, Campbell BJ, Hart CA, Mpofu C, Nayar M, Singh R, et al. Enhanced Escherichia coli adherence and invasion in Crohn's disease and colon cancer. Gastroenterology. 2004;127(1):80-93.

338. Kanazawa K, Konishi F, Mitsuoka T, Terada A, Itoh K, Narushima S, et al. Factors influencing the development of sigmoid colon cancer. Bacteriologic and biochemical studies. Cancer. 1996;77(8 Suppl):1701-6.
339. Velcich A, Yang W, Heyer J, Fragale A, Nicholas C, Viani S, et al. Colorectal cancer in mice genetically deficient in the mucin Muc2. Science (New York, NY). 2002;295(5560):1726-9.
340. Szentkuti L, Riedesel H, Enss ML, Gaertner K, Von Engelhardt W. Pre-epithelial mucus layer in the colon of conventional and germ-free rats. The Histochemical journal. 1990;22(9):491-7.
341. Freitas M, Axelsson LG, Cayuela C, Midtvedt T, Trugnan G. Microbial-host interactions specifically control the glycosylation pattern in intestinal mouse mucosa. Histochemistry and cell biology. 2002;118(2):149-61.
342. Campbell BJ, Yu LG, Rhodes JM. Altered glycosylation in inflammatory bowel disease: A possible role in cancer development. Glycoconjugate J. 2001;18(11-12):851-8.
343. Hayatsu H, Hayatsu T. Suppressing effect of Lactobacillus casei administration on the urinary mutagenicity arising from ingestion of fried ground beef in the human. Cancer letters. 1993;73(2):173-9.
344. Goldin BR, Swenson L, Dwyer J, Sexton M, Gorbach SL. Effect of Diet and Lactobacillus acidophilus Supplements on Human Fecal Bacterial Enzymes23. JNCI: Journal of the National Cancer Institute. 1980;64(2):255-61.
345. Ling WH, Korpela R, Mykkänen H, Salminen S, Hänninen O. Lactobacillus Strain GG Supplementation Decreases Colonic Hydrolytic and Reductive Enzyme Activities in Healthy Female Adults. The Journal of Nutrition. 1994;124(1):18-23.
346. Spanhaak S, Havenaar R, Schaafsma G. The effect of consumption of milk fermented by Lactobacillus casei strain Shirota on the intestinal microflora and immune parameters in humans. European Journal of Clinical Nutrition. 1998;52(12):899-907.
347. Lidbeck A, Övervik E, Rafter J, E. Nord C, Gustafsson JÅ. Effect of Lactobacillus acidophilus Supplements on Mutagen Excretion in Faeces and Urine in Humans2009. 59-67 p.
348. Ayebo AD, Angelo IA, Shahani KM. Effect of ingesting Lactobacillus acidophilus milk upon fecal flora and enzyme activity in humans. Milchwissenschaft. 1980;35(12):730-3.
349. Wirbel J, Pyl PT, Kartal E, Zych K, Kashani A, Milanese A, et al. Meta-analysis of fecal metagenomes reveals global microbial signatures that are specific for colorectal cancer. Nature medicine. 2019;25(4):679-89.
350. Thomas AM, Manghi P, Asnicar F, Pasolli E, Armanini F, Zolfo M, et al. Metagenomic analysis of colorectal cancer datasets identifies cross-cohort microbial diagnostic signatures and a link with choline degradation. Nature medicine. 2019;25(4):667-78.
351. Kado S, Uchida K, Funabashi H, Iwata S, Nagata Y, Ando M, et al. Intestinal microflora are necessary for development of spontaneous adenocarcinoma of the large intestine in T-cell receptor beta chain and p53 double-knockout mice. Cancer research. 2001;61(6):2395-8.
352. Engle SJ, Ormsby I, Pawlowski S, Boivin GP, Croft J, Balish E, et al. Elimination of colon cancer in germ-free transforming growth factor beta 1-deficient mice. Cancer research. 2002;62(22):6362-6.
353. Vannucci L, Stepankova R, Kozakova H, Fiserova A, Rossmann P, Tlaskalova-Hogenova H. Colorectal carcinogenesis in germ-free and conventionally reared rats: different intestinal environments affect the systemic immunity. International journal of oncology. 2008;32(3):609-17.
354. Reddy BS, Narisawa T, Maronpot R, Weisburger JH, Wynder EL. Animal models for the study of dietary factors and cancer of the large bowel. Cancer research. 1975;35(11 Pt. 2):3421-6.

355. Dove WF, Clipson L, Gould KA, Luongo C, Marshall DJ, Moser AR, et al. Intestinal neoplasia in the ApcMin mouse: independence from the microbial and natural killer (beige locus) status. Cancer research. 1997;57(5):812-4.
356. Li Y, Kundu P, Seow SW, de Matos CT, Aronsson L, Chin KC, et al. Gut microbiota accelerate tumor growth via c-jun and STAT3 phosphorylation in APCMin/+ mice. Carcinogenesis. 2012;33(6):1231-8.
357. Wong SH, Zhao L, Zhang X, Nakatsu G, Han J, Xu W, et al. Gavage of Fecal Samples From Patients With Colorectal Cancer Promotes Intestinal Carcinogenesis in Germ-Free and Conventional Mice. Gastroenterology. 2017;153(6):1621-33.e6.
358. Cao H, Xu M, Dong W, Deng B, Wang S, Zhang Y, et al. Secondary bile acid-induced dysbiosis promotes intestinal carcinogenesis. International journal of cancer. 2017;140(11):2545-56.
359. Zhang Y, Wang X-L, Zhou M, Kang C, Lang H-D, Chen M-T, et al. Crosstalk between gut microbiota and Sirtuin-3 in colonic inflammation and tumorigenesis. Exp Mol Med. 2018;50(4):21-.
360. Zackular JP, Baxter NT, Iverson KD, Sadler WD, Petrosino JF, Chen GY, et al. The gut microbiome modulates colon tumorigenesis. MBio. 2013;4(6):e00692.
361. Baxter NT, Zackular JP, Chen GY, Schloss PD. Structure of the gut microbiome following colonization with human feces determines colonic tumor burden. Microbiome. 2014;2:20-.
362. Zackular JP, Baxter NT, Iverson KD, Sadler WD, Petrosino JF, Chen GY, et al. The Gut Microbiome Modulates Colon Tumorigenesis. MBio. 2013;4(6):e00692-13.
363. Hattori N, Niwa T, Ishida T, Kobayashi K, Imai T, Mori A, et al. Antibiotics suppress colon tumorigenesis through inhibition of aberrant DNA methylation in an azoxymethane and dextran sulfate sodium colitis model. Cancer science. 2019;110(1):147-56.
364. Tanaka Y, Ito S, Isobe K-i. Vancomycin-sensitive bacteria trigger development of colitis-associated colon cancer by attracting neutrophils. Scientific Reports. 2016;6:23920.
365. Ijssennagger N, Belzer C, Hooiveld GJ, Dekker J, van Mil SWC, Müller M, et al. Gut microbiota facilitates dietary heme-induced epithelial hyperproliferation by opening the mucus barrier in colon. Proceedings of the National Academy of Sciences of the United States of America. 2015;112(32):10038-43.
366. Martin OC, Lin C, Naud N, Tache S, Raymond-Letron I, Corpet DE, et al. Antibiotic suppression of intestinal microbiota reduces heme-induced lipoperoxidation associated with colon carcinogenesis in rats. Nutrition and cancer. 2015;67(1):119-25.
367. Xiao H, Yin W, Khan MA, Gulen MF, Zhou H, Sham HP, et al. Loss of single immunoglobulin interlukin-1 receptor-related molecule leads to enhanced colonic polyposis in Apc(min) mice. Gastroenterology. 2010;139(2):574-85.
368. Kaur K, Saxena A, Debnath I, O'Brien JL, Ajami NJ, Auchtung TA, et al. Antibiotic-mediated bacteriome depletion in Apc(Min/+) mice is associated with reduction in mucus-producing goblet cells and increased colorectal cancer progression. Cancer medicine. 2018;7(5):2003-12.
369. Belcheva A, Irrazabal T, Robertson Susan J, Streutker C, Maughan H, Rubino S, et al. Gut Microbial Metabolism Drives Transformation of Msh2-Deficient Colon Epithelial Cells. Cell. 2014;158(2):288-99.
370. Yang Y, Weng W, Peng J, Hong L, Yang L, Toiyama Y, et al. Fusobacterium nucleatum Increases Proliferation of Colorectal Cancer Cells and Tumor Development in Mice by Activating Toll-Like Receptor 4 Signaling to Nuclear Factor-κB, and Up-regulating Expression of MicroRNA-21. Gastroenterology. 2017;152(4):851-66.e24.
371. Ellmerich S, Scholler M, Duranton B, Gosse F, Galluser M, Klein JP, et al. Promotion of intestinal carcinogenesis by Streptococcus bovis. Carcinogenesis. 2000;21(4):753-6.

372. Onoue M, Kado S, Sakaitani Y, Uchida K, Morotomi M. Specific species of intestinal bacteria influence the induction of aberrant crypt foci by 1,2-dimethylhydrazine in rats. Cancer letters. 1997;113(1-2):179-86.
373. Horie H, Kanazawa K, Okada M, Narushima S, Itoh K, Terada A. Effects of intestinal bacteria on the development of colonic neoplasm: an experimental study. European journal of cancer prevention : the official journal of the European Cancer Prevention Organisation (ECP). 1999;8(3):237-45.
374. Marteau PR, Vrese Md, Cellier CJ, Schrezenmeir J. Protection from gastrointestinal diseases with the use of probiotics. The American journal of clinical nutrition. 2001;73(2):430s-6s.
375. Ballongue J, Schumann C, Quignon P. Effects of lactulose and lactitol on colonic microflora and enzymatic activity. Scandinavian journal of gastroenterology Supplement. 1997;222:41-4.
376. Bouhnik Y, Flourie B, D'Agay-Abensour L, Pochart P, Gramet G, Durand M, et al. Administration of transgalacto-oligosaccharides increases fecal bifidobacteria and modifies colonic fermentation metabolism in healthy humans. J Nutr. 1997;127(3):444-8.
377. Campbell JM, Fahey GC, Jr., Wolf BW. Selected indigestible oligosaccharides affect large bowel mass, cecal and fecal short-chain fatty acids, pH and microflora in rats. J Nutr. 1997;127(1):130-6.
378. Food and Agriculture Organization of the United Nations, World Health Organization. Guidelines for the Evaluation of Probiotics in Food. 2002.
379. Rafter J, Bennett M, Caderni G, Clune Y, Hughes R, Karlsson PC, et al. Dietary synbiotics reduce cancer risk factors in polypectomized and colon cancer patients. The American journal of clinical nutrition. 2007;85(2):488-96.
380. Roessler A, Forssten SD, Glei M, Ouwehand AC, Jahreis G. The effect of probiotics on faecal microbiota and genotoxic activity of faecal water in patients with atopic dermatitis: a randomized, placebo-controlled study. Clinical nutrition (Edinburgh, Scotland). 2012;31(1):22-9.
381. Gianotti L, Morelli L, Galbiati F, Rocchetti S, Coppola S, Beneduce A, et al. A randomized double-blind trial on perioperative administration of probiotics in colorectal cancer patients. World J Gastroenterol. 2010;16(2):167-75.
382. Xia Y, Yang Z, Chen HQ, Qin HL. [Effect of bowel preparation with probiotics on intestinal barrier after surgery for colorectal cancer]. Zhonghua wei chang wai ke za zhi = Chinese journal of gastrointestinal surgery. 2010;13(7):528-31.
383. Roller M, Clune Y, Collins K, Rechkemmer G, Watzl B. Consumption of prebiotic inulin enriched with oligofructose in combination with the probiotics Lactobacillus rhamnosus and Bifidobacterium lactis has minor effects on selected immune parameters in polypectomised and colon cancer patients. The British journal of nutrition. 2007;97(4):676-84.
384. Ishikawa H, Akedo I, Umesaki Y, Tanaka R, Imaoka A, Otani T. Randomized controlled trial of the effect of bifidobacteria-fermented milk on ulcerative colitis. Journal of the American College of Nutrition. 2003;22(1):56-63.
385. Mego M, Chovanec J, Vochyanova-Andrezalova I, Konkolovsky P, Mikulova M, Reckova M, et al. Prevention of irinotecan induced diarrhea by probiotics: A randomized double blind, placebo controlled pilot study. Complementary therapies in medicine. 2015;23(3):356-62.
386. Krebs B. Prebiotic and Synbiotic Treatment before Colorectal Surgery--Randomised Double Blind Trial. Collegium antropologicum. 2016;40(1):35-40.
387. Challa A, Rao DR, Chawan CB, Shackelford L. Bifidobacterium longum and lactulose suppress azoxymethane-induced colonic aberrant crypt foci in rats. Carcinogenesis. 1997;18(3):517-21.

388. Rowland IR, Rumney CJ, Coutts JT, Lievense LC. Effect of Bifidobacterium longum and inulin on gut bacterial metabolism and carcinogen-induced aberrant crypt foci in rats. Carcinogenesis. 1998;19(2):281-5.
389. Goldin BR, Gualtieri LJ, Moore RP. The effect of Lactobacillus GG on the initiation and promotion of DMH-induced intestinal tumors in the rat. Nutrition and cancer. 1996;25(2):197-204.
390. Goldin BR, Gorbach SL. Effect of Lactobacillus acidophilus dietary supplements on 1,2-dimethylhydrazine dihydrochloride-induced intestinal cancer in rats. Journal of the National Cancer Institute. 1980;64(2):263-5.
391. Wollowski I, Rechkemmer G, Pool-Zobel BL. Protective role of probiotics and prebiotics in colon cancer. The American journal of clinical nutrition. 2001;73(2 Suppl):451s-5s.
392. Pool-Zobel BL, Munzner R, Holzapfel WH. Antigenotoxic properties of lactic acid bacteria in the S. typhimurium mutagenicity assay. Nutrition and cancer. 1993;20(3):261-70.
393. Bodana AR, Rao DR. Antimutagenic activity of milk fermented by Streptococcus thermophilus and Lactobacillus bulgaricus. Journal of dairy science. 1990;73(12):3379-84.
394. Pool-Zobel BL, Bertram B, Knoll M, Lambertz R, Neudecker C, Schillinger U, et al. Antigenotoxic properties of lactic acid bacteria in vivo in the gastrointestinal tract of rats. Nutrition and cancer. 1993;20(3):271-81.
395. Pool-Zobel BL, Neudecker C, Domizlaff I, Ji S, Schillinger U, Rumney C, et al. Lactobacillus- and bifidobacterium-mediated antigenotoxicity in the colon of rats. Nutrition and cancer. 1996;26(3):365-80.
396. Goldin BR, Gorbach SL. The effect of milk and lactobacillus feeding on human intestinal bacterial enzyme activity. The American journal of clinical nutrition. 1984;39(5):756-61.
397. Goldin BR, Gorbach SL, Saxelin M, Barakat S, Gualtieri L, Salminen S. Survival of Lactobacillus species (strain GG) in human gastrointestinal tract. Dig Dis Sci. 1992;37(1):121-8.
398. Benno Y, Mitsuoka T. Impact of Bifidobacterium longum on human fecal microflora. Microbiol Immunol. 1992;36(7):683-94.
399. Bouhnik Y, Flourie B, Andrieux C, Bisetti N, Briet F, Rambaud JC. Effects of Bifidobacterium sp fermented milk ingested with or without inulin on colonic bifidobacteria and enzymatic activities in healthy humans. Eur J Clin Nutr. 1996;50(4):269-73.
400. Orrhage K, Sillerstrom E, Gustafsson JA, Nord CE, Rafter J. Binding of mutagenic heterocyclic amines by intestinal and lactic acid bacteria. Mutation research. 1994;311(2):239-48.
401. Zhang XB, Ohta Y. In vitro binding of mutagenic pyrolyzates to lactic acid bacterial cells in human gastric juice. Journal of dairy science. 1991;74(3):752-7.
402. Morotomi M, Mutai M. In vitro binding of potent mutagenic pyrolysates to intestinal bacteria. Journal of the National Cancer Institute. 1986;77(1):195-201.
403. Lidbeck A, Övervik E, Rafter J, Nord CE, Gustafsson JÅ. Effect of Lactobacillus acidophilus Supplements on Mutagen Excretion in Faeces and Urine in Humans. Microbial Ecology in Health and Disease. 1992;5(1):59-67.
404. Link-Amster H, Rochat F, Saudan KY, Mignot O, Aeschlimann JM. Modulation of a specific humoral immune response and changes in intestinal flora mediated through fermented milk intake. FEMS immunology and medical microbiology. 1994;10(1):55-63.
405. Segal I, Hassan H, Walker AR, Becker P, Braganza J. Fecal short chain fatty acids in South African urban Africans and whites. Diseases of the colon and rectum. 1995;38(7):732-4.
406. Baghurst PA, Baghurst KI, Record SJ. Dietary fibre, non-starch polysaccharides and resistant starch: a review. Food Australia. 1996.

407. Hass R, Busche R, Luciano L, Reale E, Engelhardt WV. Lack of butyrate is associated with induction of Bax and subsequent apoptosis in the proximal colon of guinea pig. Gastroenterology. 1997;112(3):875-81.
408. Marchetti C, Migliorati G, Moraca R, Riccardi C, Nicoletti I, Fabiani R, et al. Deoxycholic acid and SCFA-induced apoptosis in the human tumor cell-line HT-29 and possible mechanisms. Cancer letters. 1997;114(1-2):97-9.
409. Hague A, Elder DJ, Hicks DJ, Paraskeva C. Apoptosis in colorectal tumour cells: induction by the short chain fatty acids butyrate, propionate and acetate and by the bile salt deoxycholate. International journal of cancer. 1995;60(3):400-6.
410. Arimochi H, Kinouchi T, Kataoka K, Kuwahara T, Ohnishi Y. Effect of intestinal bacteria on formation of azoxymethane-induced aberrant crypt foci in the rat colon. Biochemical and biophysical research communications. 1997;238(3):753-7.
411. Morotomi M, Mutal M. In Vitro Binding of Potent Mutagenic Pyrolyzates to Intestinal Bacteria. JNCI: Journal of the National Cancer Institute. 1986;77(1):195-201.
412. Kulkarni N, Reddy BS. Inhibitory Effect of Bifidobacterium longum Cultures on the Azoxymethane-Induced Aberrant Crypt Foci Formation and Fecal Bacterial β-Glucuronidase. Proceedings of the Society for Experimental Biology and Medicine. 1994;207(3):278-83.
413. Abdelali H, Cassand P, Soussotte V, Daubeze M, Bouley C, Narbonne JF. Effect of dairy products on initiation of precursor lesions of colon cancer in rats. Nutrition and cancer. 1995;24(2):121-32.
414. Rowland IR, Rumney CJ, Coutts JT, Lievense LC. Effect of Bifidobacterium longum and inulin on gut bacterial metabolism and carcinogen-induced aberrant crypt foci in rats. Carcinogenesis. 1998;19(2):281-5.
415. Collado MC, Meriluoto J, Salminen S. Role of commercial probiotic strains against human pathogen adhesion to intestinal mucus. Letters in applied microbiology. 2007;45(4):454-60.
416. Sreekumar O, Hosono A. Immediate effect of Lactobacillus acidophilus on the intestinal flora and fecal enzymes of rats and the in vitro inhibition of Escherichia coli in coculture. Journal of dairy science. 2000;83(5):931-9.
417. Spinler JK, Taweechotipatr M, Rognerud CL, Ou CN, Tumwasorn S, Versalovic J. Human-derived probiotic Lactobacillus reuteri demonstrate antimicrobial activities targeting diverse enteric bacterial pathogens. Anaerobe. 2008;14(3):166-71.
418. O'Shea EF, Cotter PD, Stanton C, Ross RP, Hill C. Production of bioactive substances by intestinal bacteria as a basis for explaining probiotic mechanisms: bacteriocins and conjugated linoleic acid. International journal of food microbiology. 2012;152(3):189-205.
419. Schiffrin EJ, Rochat F, Link-Amster H, Aeschlimann JM, Donnet-Hughes A. Immunomodulation of Human Blood Cells Following the Ingestion of Lactic Acid Bacteria. Journal of dairy science. 1995;78(3):491-7.
420. Kato I, Yokokura T, Mutai M. Macrophage Activation by Lactobacillus casei in Mice. Microbiology and Immunology. 1983;27(7):611-8.
421. Kato I, Endo K, Yokokura T. Effects of oral administration of Lactobacillus casei on antitumor responses induced by tumor resection in mice. International Journal of Immunopharmacology. 1994;16(1):29-36.
422. Sekine K, Toida T, Saito M, Kuboyama M, Kawashima T, Hashimoto Y. A New Morphologically Characterized Cell Wall Preparation (Whole Peptidoglycan) from Bifidobacterium infantis with a Higher Efficacy on the Regression of an Established Tumor in Mice. Cancer research. 1985;45(3):1300-7.
423. Lin YP, Thibodeaux CH, Pena JA, Ferry GD, Versalovic J. Probiotic Lactobacillus reuteri suppress proinflammatory cytokines via c-Jun. Inflammatory bowel diseases. 2008;14(8):1068-83.

424. Liu Y, Fatheree NY, Mangalat N, Rhoads JM. Human-derived probiotic Lactobacillus reuteri strains differentially reduce intestinal inflammation. American journal of physiology Gastrointestinal and liver physiology. 2010;299(5):G1087-96.
425. Matsuzaki T. Immunomodulation by treatment with Lactobacillus casei strain Shirota. International journal of food microbiology. 1998;41(2):133-40.
426. Wu X, Wu Y, He L, Wu L, Wang X, Liu Z. Effects of the intestinal microbial metabolite butyrate on the development of colorectal cancer. J Cancer. 2018;9(14):2510-7.
427. Barcenilla A, Pryde SE, Martin JC, Duncan SH, Stewart CS, Henderson C, et al. Phylogenetic relationships of butyrate-producing bacteria from the human gut. Appl Environ Microbiol. 2000;66(4):1654-61.
428. Louis P, Young P, Holtrop G, Flint HJ. Diversity of human colonic butyrate-producing bacteria revealed by analysis of the butyryl-CoA:acetate CoA-transferase gene. Environmental microbiology. 2010;12(2):304-14.
429. Louis P, Duncan SH, McCrae SI, Millar J, Jackson MS, Flint HJ. Restricted distribution of the butyrate kinase pathway among butyrate-producing bacteria from the human colon. Journal of bacteriology. 2004;186(7):2099-106.
430. Duncan SH, Louis P, Flint HJ. Cultivable bacterial diversity from the human colon. Letters in applied microbiology. 2007;44(4):343-50.
431. Louis P, Hold GL, Flint HJ. The gut microbiota, bacterial metabolites and colorectal cancer. Nature Reviews Microbiology. 2014;12:661.
432. Khonsary SA. Guyton and Hall: Textbook of Medical Physiology. Surg Neurol Int. 2017;8:275.
433. Boyer JL. Bile formation and secretion. Compr Physiol. 2013;3(3):1035-78.
434. Norlin M, Wikvall K. Enzymes in the conversion of cholesterol into bile acids. Current molecular medicine. 2007;7(2):199-218.
435. Russell DW. The enzymes, regulation, and genetics of bile acid synthesis. Annual review of biochemistry. 2003;72:137-74.
436. Bjorkhem I, Eggertsen G. Genes involved in initial steps of bile acid synthesis. Current opinion in lipidology. 2001;12(2):97-103.
437. He D, Barnes S, Falany CN. Rat liver bile acid CoA:amino acid N-acyltransferase: expression, characterization, and peroxisomal localization. Journal of lipid research. 2003;44(12):2242-9.
438. Long SL, Gahan CGM, Joyce SA. Interactions between gut bacteria and bile in health and disease. Molecular Aspects of Medicine. 2017;56:54-65.
439. Bernstein H, Bernstein C, Payne CM, Dvorakova K, Garewal H. Bile acids as carcinogens in human gastrointestinal cancers. Mutation Research/Reviews in Mutation Research. 2005;589(1):47-65.
440. Iqbal J, Hussain MM. Intestinal lipid absorption. Am J Physiol Endocrinol Metab. 2009;296(6):E1183-E94.
441. Wang TY, Liu M, Portincasa P, Wang DQH. New insights into the molecular mechanism of intestinal fatty acid absorption. Eur J Clin Invest. 2013;43(11):1203-23.
442. Vlahcevic Z. 13. Physiology and pathophysiology of enterohepatic circulation of bile acids. Hepatology: a textbook of liver desease. 1990.
443. Song P, Zhang Y, Klaassen CD. Dose-response of five bile acids on serum and liver bile Acid concentrations and hepatotoxicty in mice. Toxicological sciences : an official journal of the Society of Toxicology. 2011;123(2):359-67.
444. Palmer RH. Bile acids, liver injury, and liver disease. Archives of internal medicine. 1972;130(4):606-17.
445. Billington D, Evans CE, Godfrey PP, Coleman R. Effects of bile salts on the plasma membranes of isolated rat hepatocytes. Biochem J. 1980;188(2):321-7.

446. Heuman DM. Quantitative estimation of the hydrophilic-hydrophobic balance of mixed bile salt solutions. Journal of lipid research. 1989;30(5):719-30.
447. Thomas C, Pellicciari R, Pruzanski M, Auwerx J, Schoonjans K. Targeting bile-acid signalling for metabolic diseases. Nat Rev Drug Discov. 2008;7(8):678-93.
448. Armstrong MJ, Carey MC. The hydrophobic-hydrophilic balance of bile salts. Inverse correlation between reverse-phase high performance liquid chromatographic mobilities and micellar cholesterol-solubilizing capacities. Journal of lipid research. 1982;23(1):70-80.
449. Wang H, Chen J, Hollister K, Sowers LC, Forman BM. Endogenous bile acids are ligands for the nuclear receptor FXR/BAR. Molecular cell. 1999;3(5):543-53.
450. Makishima M, Okamoto AY, Repa JJ, Tu H, Learned RM, Luk A, et al. Identification of a nuclear receptor for bile acids. Science (New York, NY). 1999;284(5418):1362-5.
451. Parks DJ, Blanchard SG, Bledsoe RK, Chandra G, Consler TG, Kliewer SA, et al. Bile acids: natural ligands for an orphan nuclear receptor. Science (New York, NY). 1999;284(5418):1365-8.
452. Ding L, Yang L, Wang Z, Huang W. Bile acid nuclear receptor FXR and digestive system diseases. Acta Pharm Sin B. 2015;5(2):135-44.
453. Fiorucci S, Biagioli M, Zampella A, Distrutti E. Bile Acids Activated Receptors Regulate Innate Immunity. Frontiers in Immunology. 2018;9(1853).
454. Sepe V, Festa C, Renga B, Carino A, Cipriani S, Finamore C, et al. Insights on FXR selective modulation. Speculation on bile acid chemical space in the discovery of potent and selective agonists. Scientific Reports. 2016;6:19008.
455. Parks DJ, Blanchard SG, Bledsoe RK, Chandra G, Consler TG, Kliewer SA, et al. Bile Acids: Natural Ligands for an Orphan Nuclear Receptor. Science (New York, NY). 1999;284(5418):1365-8.
456. Chiang JYL, Kimmel R, Weinberger C, Stroup D. Farnesoid X Receptor Responds to Bile Acids and Represses Cholesterol 7α-Hydroxylase Gene (CYP7A1) Transcription. Journal of Biological Chemistry. 2000;275(15):10918-24.
457. Csanaky IL, Lu H, Zhang Y, Ogura K, Choudhuri S, Klaassen CD. Organic anion-transporting polypeptide 1b2 (Oatp1b2) is important for the hepatic uptake of unconjugated bile acids: Studies in Oatp1b2-null mice. Hepatology (Baltimore, Md). 2011;53(1):272-81.
458. Jiang C, Xie C, Lv Y, Li J, Krausz KW, Shi J, et al. Intestine-selective farnesoid X receptor inhibition improves obesity-related metabolic dysfunction. Nature communications. 2015;6:10166.
459. Zhang L, Xie C, Nichols RG, Chan SHJ, Jiang C, Hao R, et al. Farnesoid X Receptor Signaling Shapes the Gut Microbiota and Controls Hepatic Lipid Metabolism. mSystems. 2016;1(5):e00070-16.
460. Hu X, Bonde Y, Eggertsen G, Rudling M. Muricholic bile acids are potent regulators of bile acid synthesis via a positive feedback mechanism. Journal of internal medicine. 2014;275(1):27-38.
461. Sayin SI, Wahlstrom A, Felin J, Jantti S, Marschall HU, Bamberg K, et al. Gut microbiota regulates bile acid metabolism by reducing the levels of tauro-beta-muricholic acid, a naturally occurring FXR antagonist. Cell metabolism. 2013;17(2):225-35.
462. Campana G, Pasini P, Roda A, Spampinato S. Regulation of ileal bile acid-binding protein expression in Caco-2 cells by ursodeoxycholic acid: role of the farnesoid X receptor. Biochemical pharmacology. 2005;69(12):1755-63.
463. Modica S, Gadaleta RM, Moschetta A. Deciphering the nuclear bile acid receptor FXR paradigm. Nucl Recept Signal. 2010;8:e005-e.
464. Cui J, Heard TS, Yu J, Lo JL, Huang L, Li Y, et al. The amino acid residues asparagine 354 and isoleucine 372 of human farnesoid X receptor confer the receptor with high sensitivity to chenodeoxycholate. The Journal of biological chemistry. 2002;277(29):25963-9.

465. Kong B, Wang L, Chiang JYL, Zhang Y, Klaassen CD, Guo GL. Mechanism of tissue-specific farnesoid X receptor in suppressing the expression of genes in bile-acid synthesis in mice. Hepatology (Baltimore, Md). 2012;56(3):1034-43.
466. Matsubara T, Li F, Gonzalez FJ. FXR signaling in the enterohepatic system. Mol Cell Endocrinol. 2013;368(1-2):17-29.
467. Song KH, Li T, Owsley E, Strom S, Chiang JY. Bile acids activate fibroblast growth factor 19 signaling in human hepatocytes to inhibit cholesterol 7alpha-hydroxylase gene expression. Hepatology (Baltimore, Md). 2009;49(1):297-305.
468. Zhu Y, Li F, Guo GL. Tissue-specific function of farnesoid X receptor in liver and intestine. Pharmacol Res. 2011;63(4):259-65.
469. Miyake JH, Wang SL, Davis RA. Bile acid induction of cytokine expression by macrophages correlates with repression of hepatic cholesterol 7alpha-hydroxylase. The Journal of biological chemistry. 2000;275(29):21805-8.
470. Shneider BL. Intestinal bile acid transport: biology, physiology, and pathophysiology. Journal of pediatric gastroenterology and nutrition. 2001;32(4):407-17.
471. Chen F, Ma L, Dawson PA, Sinal CJ, Sehayek E, Gonzalez FJ, et al. Liver Receptor Homologue-1 Mediates Species- and Cell Line-specific Bile Acid-dependent Negative Feedback Regulation of the Apical Sodium-dependent Bile Acid Transporter. Journal of Biological Chemistry. 2003;278(22):19909-16.
472. Neimark E, Chen F, Li X, Shneider BL. Bile acid-induced negative feedback regulation of the human ileal bile acid transporter. Hepatology (Baltimore, Md). 2004;40(1):149-56.
473. Heubi JE, Balistreri WF, Fondacaro JD, Partin JC, Schubert WK. Primary bile acid malabsorption: defective in vitro ileal active bile acid transport. Gastroenterology. 1982;83(4):804-11.
474. Oelkers P, Kirby LC, Heubi JE, Dawson PA. Primary bile acid malabsorption caused by mutations in the ileal sodium-dependent bile acid transporter gene (SLC10A2). J Clin Invest. 1997;99(8):1880-7.
475. Coppola CP, Gosche JR, Arrese M, Ancowitz B, Madsen J, Vanderhoof J, et al. Molecular analysis of the adaptive response of intestinal bile acid transport after ileal resection in the rat. Gastroenterology. 1998;115(5):1172-8.
476. Grober J, Zaghini I, Fujii H, Jones SA, Kliewer SA, Willson TM, et al. Identification of a bile acid-responsive element in the human ileal bile acid-binding protein gene. Involvement of the farnesoid X receptor/9-cis-retinoic acid receptor heterodimer. The Journal of biological chemistry. 1999;274(42):29749-54.
477. Sinal CJ, Tohkin M, Miyata M, Ward JM, Lambert G, Gonzalez FJ. Targeted disruption of the nuclear receptor FXR/BAR impairs bile acid and lipid homeostasis. Cell. 2000;102(6):731-44.
478. Dawson PA, Hubbert M, Haywood J, Craddock AL, Zerangue N, Christian WV, et al. The heteromeric organic solute transporter alpha-beta, Ostalpha-Ostbeta, is an ileal basolateral bile acid transporter. The Journal of biological chemistry. 2005;280(8):6960-8.
479. Zollner G, Wagner M, Moustafa T, Fickert P, Silbert D, Gumhold J, et al. Coordinated induction of bile acid detoxification and alternative elimination in mice: role of FXR-regulated organic solute transporter-alpha/beta in the adaptive response to bile acids. American journal of physiology Gastrointestinal and liver physiology. 2006;290(5):G923-32.
480. Lee H, Zhang Y, Lee FY, Nelson SF, Gonzalez FJ, Edwards PA. FXR regulates organic solute transporters alpha and beta in the adrenal gland, kidney, and intestine. Journal of lipid research. 2006;47(1):201-14.
481. Dawson PA, Hubbert M, Haywood J, Craddock AL, Zerangue N, Christian WV, et al. The heteromeric organic solute transporter alpha-beta, Ostalpha-Ostbeta, is an ileal basolateral bile acid transporter. The Journal of biological chemistry. 2005;280(8):6960-8.

482. Stieger B, Hagenbuch B, Landmann L, Hochli M, Schroeder A, Meier PJ. In situ localization of the hepatocytic Na+/Taurocholate cotransporting polypeptide in rat liver. Gastroenterology. 1994;107(6):1781-7.
483. Hagenbuch B, Meier PJ. Molecular cloning, chromosomal localization, and functional characterization of a human liver Na+/bile acid cotransporter. J Clin Invest. 1994;93(3):1326-31.
484. Denson LA, Sturm E, Echevarria W, Zimmerman TL, Makishima M, Mangelsdorf DJ, et al. The orphan nuclear receptor, shp, mediates bile acid-induced inhibition of the rat bile acid transporter, ntcp. Gastroenterology. 2001;121(1):140-7.
485. Childs S, Yeh RL, Georges E, Ling V. Identification of a sister gene to P-glycoprotein. Cancer research. 1995;55(10):2029-34.
486. Li T, Chiang JYL. Bile acid signaling in metabolic disease and drug therapy. Pharmacol Rev. 2014;66(4):948-83.
487. Ananthanarayanan M, Balasubramanian N, Makishima M, Mangelsdorf DJ, Suchy FJ. Human bile salt export pump promoter is transactivated by the farnesoid X receptor/bile acid receptor. The Journal of biological chemistry. 2001;276(31):28857-65.
488. Degirolamo C, Modica S, Palasciano G, Moschetta A. Bile acids and colon cancer: Solving the puzzle with nuclear receptors. Trends in molecular medicine. 2011;17(10):564-72.
489. De Gottardi A, Touri F, Maurer CA, Perez A, Maurhofer O, Ventre G, et al. The Bile Acid Nuclear Receptor FXR and the Bile Acid Binding Protein IBABP Are Differently Expressed in Colon Cancer. Digestive Diseases and Sciences. 2004;49(6):982-9.
490. Maran RRM, Thomas A, Roth M, Sheng Z, Esterly N, Pinson D, et al. Farnesoid X Receptor Deficiency in Mice Leads to Increased Intestinal Epithelial Cell Proliferation and Tumor Development. Journal of Pharmacology and Experimental Therapeutics. 2009;328(2):469-77.
491. Kim I, Morimura K, Shah Y, Yang Q, Ward JM, Gonzalez FJ. Spontaneous hepatocarcinogenesis in farnesoid X receptor-null mice. Carcinogenesis. 2007;28(5):940-6.
492. Modica S, Murzilli S, Salvatore L, Schmidt DR, Moschetta A. Nuclear Bile Acid Receptor FXR Protects against Intestinal Tumorigenesis. Cancer research. 2008;68(23):9589-94.
493. Fu T, Coulter S, Yoshihara E, Oh TG, Fang S, Cayabyab F, et al. FXR Regulates Intestinal Cancer Stem Cell Proliferation. Cell. 2019;176(5):1098-112.e18.
494. Selmin OI, Fang C, Lyon AM, Doetschman TC, Thompson PA, Martinez JD, et al. Inactivation of Adenomatous Polyposis Coli Reduces Bile Acid/Farnesoid X Receptor Expression through Fxr gene CpG Methylation in Mouse Colon Tumors and Human Colon Cancer Cells. The Journal of Nutrition. 2015;146(2):236-42.
495. Bervoets L, Van Hoorenbeeck K, Kortleven I, Van Noten C, Hens N, Vael C, et al. Differences in gut microbiota composition between obese and lean children: a cross-sectional study. Gut pathogens. 2013;5(1):10.
496. Stojancevic M, Stankov K, Mikov M. The impact of farnesoid X receptor activation on intestinal permeability in inflammatory bowel disease. Can J Gastroenterol. 2012;26(9):631-7.
497. Vavassori P, Mencarelli A, Renga B, Distrutti E, Fiorucci S. The bile acid receptor FXR is a modulator of intestinal innate immunity. Journal of immunology (Baltimore, Md : 1950). 2009;183(10):6251-61.
498. Gadaleta RM, Cariello M, Sabbà C, Moschetta A. Tissue-specific actions of FXR in metabolism and cancer. Biochimica et Biophysica Acta (BBA) - Molecular and Cell Biology of Lipids. 2015;1851(1):30-9.

499. Dawson PA, Haywood J, Craddock AL, Wilson M, Tietjen M, Kluckman K, et al. Targeted Deletion of the Ileal Bile Acid Transporter Eliminates Enterohepatic Cycling of Bile Acids in Mice. Journal of Biological Chemistry. 2003;278(36):33920-7.
500. Hill MJ. Bile flow and colon cancer. Mutation Research/Reviews in Genetic Toxicology. 1990;238(3):313-20.
501. Coleman JP, Hudson LL. Cloning and characterization of a conjugated bile acid hydrolase gene from Clostridium perfringens. Applied and Environmental Microbiology. 1995;61(7):2514-20.
502. Christiaens H, Leer RJ, Pouwels PH, Verstraete W. Cloning and expression of a conjugated bile acid hydrolase gene from Lactobacillus plantarum by using a direct plate assay. Applied and Environmental Microbiology. 1992;58(12):3792-8.
503. Elkins CA, Moser SA, Savage DC. Genes encoding bile salt hydrolases and conjugated bile salt transporters in Lactobacillus johnsonii 100-100 and other Lactobacillus species. Microbiology. 2001;147(12):3403-12.
504. De Smet I, Van Hoorde L, Vande Woestyne M, Christiaens H, Verstraete W. Significance of bile salt hydrolytic activities of lactobacilli. The Journal of applied bacteriology. 1995;79(3):292-301.
505. Tannock GW, Dashkevicz MP, Feighner SD. Lactobacilli and bile salt hydrolase in the murine intestinal tract. Applied and Environmental Microbiology. 1989;55(7):1848-51.
506. Ridlon JM, Kang D-J, Hylemon PB. Bile salt biotransformations by human intestinal bacteria. Journal of lipid research. 2006;47(2):241-59.
507. Cook AM, Denger K. Dissimilation of the C2 sulfonates. Archives of Microbiology. 2002;179(1):1-6.
508. Van Eldere J, Celis P, De Pauw G, Lesaffre E, Eyssen H. Tauroconjugation of cholic acid stimulates 7 alpha-dehydroxylation by fecal bacteria. Applied and environmental microbiology. 1996;62(2):656-61.
509. Lengeler J, Drews G, Schlegel G. Biology of the Prokaryotes1998.
510. Tanaka H, Hashiba H, Kok J, Mierau I. Bile Salt Hydrolase of Bifidobacterium longum—Biochemical and Genetic Characterization. Applied and Environmental Microbiology. 2000;66(6):2502-12.
511. Dussurget O, Cabanes D, Dehoux P, Lecuit M, the European Listeria Genome C, Buchrieser C, et al. Listeria monocytogenes bile salt hydrolase is a PrfA-regulated virulence factor involved in the intestinal and hepatic phases of listeriosis. Molecular Microbiology. 2002;45(4):1095-106.
512. Jones BV, Begley M, Hill C, Gahan CGM, Marchesi JR. Functional and comparative metagenomic analysis of bile salt hydrolase activity in the human gut microbiome. Proceedings of the National Academy of Sciences. 2008;105(36):13580-5.
513. Allain T, Chaouch S, Thomas M, Vallée I, Buret AG, Langella P, et al. Bile-Salt-Hydrolases from the Probiotic Strain Lactobacillus johnsonii La1 Mediate Anti-giardial Activity in Vitro and in Vivo. Front Microbiol. 2018;8:2707-.
514. Lambert JM, Bongers RS, de Vos WM, Kleerebezem M. Functional Analysis of Four Bile Salt Hydrolase and Penicillin Acylase Family Members in Lactobacillus plantarum WCFS1. Applied and Environmental Microbiology. 2008;74(15):4719-26.
515. Jensen RT, Davis RA, Kern F, Jr. Increased Sulfation and Decreased 7α-Hydroxylation of Deoxycholic Acid in Ethinyl Estradiol-Induced Cholestasis in Rats. Gastroenterology. 1977;73(2):314-20.
516. Cowen AE, Korman MG, Hofmann AF, Cass OW, Coffin SB. Metabolism of lithocholate in healthy man. II. Enterohepatic circulation. Gastroenterology. 1975;69(1):67-76.
517. Li T, Chiang JYL. Bile Acid Signaling in Liver Metabolism and Diseases. Journal of Lipids. 2012;2012:9.

518. Wells JE, Hylemon PB. Identification and characterization of a bile acid 7alpha-dehydroxylation operon in Clostridium sp. strain TO-931, a highly active 7alpha-dehydroxylating strain isolated from human feces. Applied and environmental microbiology. 2000;66(3):1107-13.
519. Kang D-J, Ridlon JM, Moore DR, 2nd, Barnes S, Hylemon PB. Clostridium scindens baiCD and baiH genes encode stereo-specific 7alpha/7beta-hydroxy-3-oxo-delta4-cholenoic acid oxidoreductases. Biochimica et biophysica acta. 2008;1781(1-2):16-25.
520. Ridlon JM, Kang D-J, Hylemon PB. Isolation and characterization of a bile acid inducible 7alpha-dehydroxylating operon in Clostridium hylemonae TN271. Anaerobe. 2010;16(2):137-46.
521. Hirano S, Masuda N. Epimerization of the 7-hydroxy group of bile acids by the combination of two kinds of microorganisms with 7 alpha- and 7 beta-hydroxysteroid dehydrogenase activity, respectively. Journal of lipid research. 1981;22(7):1060-8.
522. MacDonald IA, Rochon YP, Hutchison DM, Holdeman LV. Formation of ursodeoxycholic acid from chenodeoxycholic acid by a 7 beta-hydroxysteroid dehydrogenase-elaborating Eubacterium aerofaciens strain cocultured with 7 alpha-hydroxysteroid dehydrogenase-elaborating organisms. Applied and Environmental Microbiology. 1982;44(5):1187-95.
523. A. Macdonald I, C. Meier E, E. Mahony D, A. Costain G. 3α-, 7α- And 12α-hydroxysteroid dehydrogenase activities from Clostridium perfringens1976. 142-53 p.
524. Macdonald IA, White BA, Hylemon PB. Separation of 7 alpha- and 7 beta-hydroxysteroid dehydrogenase activities from clostridium absonum ATCC# 27555 and cellular response of this organism to bile acid inducers. Journal of lipid research. 1983;24(9):1119-26.
525. Heuman DM, Pandak WM, Hylemon PB, Vlahcevic ZR. Conjugates of ursodeoxycholate protect against cytotoxicity of more hydrophobic bile salts: In vitro studies in rat hepatocytes and human erythrocytes. Hepatology (Baltimore, Md). 1991;14(5):920-6.
526. Sherrod JA, Hylemon PB. Partial purification and characterization of NAD-dependent 7α-hydroxysteroid dehydrogenase from Bacteroides thetaiotaomicron. Biochimica et Biophysica Acta (BBA) - Lipids and Lipid Metabolism. 1977;486(2):351-8.
527. A. Macdonald I, Roach P. Bile salt induction of 7α- and 7β-hydroxysteroid dehydrogenases in Clostridium absonum1981. 262–9 p.
528. Gérard P. Metabolism of cholesterol and bile acids by the gut microbiota. Pathogens. 2013;3(1):14-24.
529. Sonoda J, Xie W, Rosenfeld JM, Barwick JL, Guzelian PS, Evans RM. Regulation of a xenobiotic sulfonation cascade by nuclear pregnane X receptor (PXR). Proceedings of the National Academy of Sciences of the United States of America. 2002;99(21):13801-6.
530. Hofmann AF. Detoxification of lithocholic acid, a toxic bile acid: relevance to drug hepatotoxicity. Drug metabolism reviews. 2004;36(3-4):703-22.
531. Duboc H, Rajca S, Rainteau D, Benarous D, Maubert M-A, Quervain E, et al. Connecting dysbiosis, bile-acid dysmetabolism and gut inflammation in inflammatory bowel diseases. Gut. 2013;62(4):531-9.
532. Macdonald IA, Bokkenheuser VD, Winter J, McLernon AM, Mosbach EH. Degradation of steroids in the human gut. Journal of lipid research. 1983;24(6):675-700.
533. Staudinger JL, Goodwin B, Jones SA, Hawkins-Brown D, MacKenzie KI, LaTour A, et al. The nuclear receptor PXR is a lithocholic acid sensor that protects against liver toxicity. Proceedings of the National Academy of Sciences. 2001;98(6):3369-74.
534. Wang H, Venkatesh M, Li H, Goetz R, Mukherjee S, Biswas A, et al. Pregnane X receptor activation induces FGF19-dependent tumor aggressiveness in humans and mice. J Clin Invest. 2011;121(8):3220-32.

535. Zucchini N, de Sousa G, Bailly-Maitre B, Gugenheim J, Bars R, Lemaire G, et al. Regulation of Bcl-2 and Bcl-xL anti-apoptotic protein expression by nuclear receptor PXR in primary cultures of human and rat hepatocytes. Biochimica et biophysica acta. 2005;1745(1):48-58.
536. Robbins D, Bakke J, Cherian MT, Wu J, Chen T. PXR interaction with p53: a meeting of two masters. Cell death & disease. 2016;7(5):e2218-e.
537. Ouyang N, Ke S, Eagleton N, Xie Y, Chen G, Laffins B, et al. Pregnane X receptor suppresses proliferation and tumourigenicity of colon cancer cells. Br J Cancer. 2010;102(12):1753-61.
538. Pondugula SR, Pavek P, Mani S. Pregnane X Receptor and Cancer: Context-Specificity is Key. Nucl Receptor Res. 2016;3:101198.
539. Zhang J, Huang W, Qatanani M, Evans RM, Moore DD. The Constitutive Androstane Receptor and Pregnane X Receptor Function Coordinately to Prevent Bile Acid-induced Hepatotoxicity. Journal of Biological Chemistry. 2004;279(47):49517-22.
540. Beilke LD, Aleksunes LM, Holland RD, Besselsen DG, Beger RD, Klaassen CD, et al. Constitutive androstane receptor-mediated changes in bile acid composition contributes to hepatoprotection from lithocholic acid-induced liver injury in mice. Drug metabolism and disposition: the biological fate of chemicals. 2009;37(5):1035-45.
541. Sberna AL, Assem M, Gautier T, Grober J, Guiu B, Jeannin A, et al. Constitutive androstane receptor activation stimulates faecal bile acid excretion and reverse cholesterol transport in mice. Journal of hepatology. 2011;55(1):154-61.
542. Fukumasu H, Rochetti AL, Pires PR, Silva ER, Mesquita LG, Strefezzi RF, et al. Constitutive androstane receptor ligands modulate the anti-tumor efficacy of paclitaxel in non-small cell lung cancer cells. PloS one. 2014;9(6):e99484.
543. Huang W, Zhang J, Washington M, Liu J, Parant JM, Lozano G, et al. Xenobiotic Stress Induces Hepatomegaly and Liver Tumors via the Nuclear Receptor Constitutive Androstane Receptor. Molecular Endocrinology. 2005;19(6):1646-53.
544. Makishima M, Lu TT, Xie W, Whitfield GK, Domoto H, Evans RM, et al. Vitamin D Receptor As an Intestinal Bile Acid Sensor. Science (New York, NY). 2002;296(5571):1313-6.
545. Garland CF, Garland FC, Gorham ED. Calcium and vitamin D. Their potential roles in colon and breast cancer prevention. Annals of the New York Academy of Sciences. 1999;889:107-19.
546. Schmiedlin-Ren P, Thummel KE, Fisher JM, Paine MF, Lown KS, Watkins PB. Expression of Enzymatically Active CYP3A4 by Caco-2 Cells Grown on Extracellular Matrix-Coated Permeable Supports in the Presence of 1α,25-Dihydroxyvitamin D₃. Molecular Pharmacology. 1997;51(5):741-54.
547. Thorne J, Campbell MJ. The vitamin D receptor in cancer: Symposium on 'Diet and cancer'. Proceedings of the Nutrition Society. 2008;67(2):115-27.
548. Campbell MJ, Trump DL. Vitamin D Receptor Signaling and Cancer. Endocrinology and Metabolism Clinics of North America. 2017;46(4):1009-38.
549. Colston KW, Hansen CMr. Mechanisms implicated in the growth regulatory effects of vitamin D in breast cancer. Endocrine-related cancer Endocr Relat Cancer Endocr Relat Cancer. 2002;9(1):45-59.
550. Cross HS, Huber C, Peterlik M. Antiproliferative effect of 1,25-dihydroxyvitamin D3 and its analogs on human colon adenocarcinoma cells (CaCo-2): Influence of extracellular calcium. Biochemical and biophysical research communications. 1991;179(1):57-62.
551. Holt PR, Arber N, Halmos B, Forde K, Kissileff H, McGlynn KA, et al. Colonic Epithelial Cell Proliferation Decreases with Increasing Levels of Serum 25-Hydroxy Vitamin D. Cancer Epidemiology Biomarkers & Prevention. 2002;11(1):113-9.

552. Bhalla AK, Amento EP, Serog B, Glimcher LH. 1,25-Dihydroxyvitamin D3 inhibits antigen-induced T cell activation. Journal of immunology (Baltimore, Md : 1950). 1984;133(4):1748-54.
553. Shiozawa K, Shiozawa S, Shimizu S, Fujita T. 1 alpha,25-dihydroxyvitamin D3 inhibits pokeweed mitogen-stimulated human B-cell activation: an analysis using serum-free culture conditions. Immunology. 1985;56(1):161-7.
554. Griffin MD, Lutz WH, Phan VA, Bachman LA, McKean DJ, Kumar R. Potent inhibition of dendritic cell differentiation and maturation by vitamin D analogs. Biochemical and biophysical research communications. 2000;270(3):701-8.
555. Penna G, Adorini L. 1 Alpha,25-dihydroxyvitamin D3 inhibits differentiation, maturation, activation, and survival of dendritic cells leading to impaired alloreactive T cell activation. Journal of immunology (Baltimore, Md : 1950). 2000;164(5):2405-11.
556. Hewison M. Vitamin D and the immune system: new perspectives on an old theme. Endocrinology and metabolism clinics of North America. 2010;39(2):365-79.
557. Kawamata Y, Fujii R, Hosoya M, Harada M, Yoshida H, Miwa M, et al. A G Protein-coupled Receptor Responsive to Bile Acids. Journal of Biological Chemistry. 2003;278(11):9435-40.
558. Yasuda H, Hirata S, Inoue K, Mashima H, Ohnishi H, Yoshiba M. Involvement of membrane-type bile acid receptor M-BAR/TGR5 in bile acid-induced activation of epidermal growth factor receptor and mitogen-activated protein kinases in gastric carcinoma cells. Biochemical and biophysical research communications. 2007;354(1):154-9.
559. De Marino S, Carino A, Masullo D, Finamore C, Marchianò S, Cipriani S, et al. Hyodeoxycholic acid derivatives as liver X receptor α and G-protein-coupled bile acid receptor agonists. Scientific Reports. 2017;7:43290.
560. Baranowski M. Biological role of liver X receptors. Journal of physiology and pharmacology : an official journal of the Polish Physiological Society. 2008;59 Suppl 7:31-55.
561. Song C, Hiipakka RA, Liao S. Selective activation of liver X receptor alpha by 6α-hydroxy bile acids and analogs. Steroids. 2000;65(8):423-7.
562. Janowski BA, Willy PJ, Devi TR, Falck JR, Mangelsdorf DJ. An oxysterol signalling pathway mediated by the nuclear receptor LXR alpha. Nature. 1996;383(6602):728-31.
563. A-Gonzalez N, Bensinger SJ, Hong C, Beceiro S, Bradley MN, Zelcer N, et al. Apoptotic cells promote their own clearance and immune tolerance through activation of the nuclear receptor LXR. Immunity. 2009;31(2):245-58.
564. Jensen OM, MacLennan R, Wahrendorf J. Diet, bowel function, fecal characteristics, and large bowel cancer in Denmark and Finland. Nutrition and cancer. 1982;4(1):5-19.
565. Domellof L, Darby L, Hanson D, Mathews L, Simi B, Reddy BS. Fecal sterols and bacterial β-glucuronidase activity: A preliminary metabolic epidemiology study of healthy volunteers from Umea, Sweden, and metropolitan New York. Nutrition and cancer. 1982;4(2):120-7.
566. Cheah PY. Hypotheses for the etiology of colorectal cancer — an overview. Nutrition and cancer. 1990;14(1):5-13.
567. Crowther JS, Drasar BS, Hill MJ, Maclennan R, Magnin D, Peach S, et al. Faecal steroids and bacteria and large bowel cancer in Hong Kong by socio-economic groups. Br J Cancer. 1976;34(2):191-8.
568. Reddy BS, Wynder EL. Large-Bowel Carcinogenesis: Fecal Constituents of Populations With Diverse Incidence Rates of Colon Cancer2. JNCI: Journal of the National Cancer Institute. 1973;50(6):1437-42.
569. Reddy BS, Hedges AR, Laakso K, Wynder EL. Metabolic epidemiology of large bowel cancer. Fecal bulk and constituents of high-risk North American and low-risk finnish population. Cancer. 1978;42(6):2832-8.

570. Hill MJ, Taylor AJ, Thompson MH, Wait R. Fecal steroids and urinary volatile phenols in four Scandinavian populations. Nutrition and cancer. 1982;4(1):67-73.
571. Bayerdörffer E, Mannes GA, Ochsenkühn T, Dirschedl P, Wiebecke B, Paumgartner G. Unconjugated secondary bile acids in the serum of patients with colorectal adenomas. Gut. 1995;36(2):268-73.
572. Cook JW, Kennaway EL, Kennaway NM. Production of Tumours in Mice by Deoxycholic Acid. Nature. 1940;145(3677):627-.
573. Magnuson BA, Carr I, Bird RP. Ability of Aberrant Crypt Foci Characteristics to Predict Colonic T\imor Incidence in Rats Fed Cholic Acid. Cancer research. 1993;53(19):4499-504.
574. Reddy BS, Narasawa T, Weisburger JH, Wynder EL. Promoting Effect of Sodium Deoxycholate on Colon Adenocarcinomas in Germfree Rats2. JNCI: Journal of the National Cancer Institute. 1976;56(2):441-2.
575. Weidema WF, Deschner EE, Cohen BI, DeCosse JJ. Acute effects of dietary cholic acid and methylazoxymethanol acetate on colon epithelial cell proliferation; Metabolism of bile salts and neutral sterols in conventional and germfree SD rats. Journal of the National Cancer Institute. 1985;74(3):665-70.
576. Narisawa T, Magadia NE, Weisburger JH, Wynder EL. Promoting Effect of Bile Acids on Colon Carcinogenesis After Intrarectal Instillation of N-Methyl-N' nitro-N-nitrosoguanidine in Rats2. JNCI: Journal of the National Cancer Institute. 1974;53(4):1093-7.
577. Bernstein H, Bernstein C, Payne CM, Dvorakova K, Garewal H. Bile acids as carcinogens in human gastrointestinal cancers. Mutation research. 2005;589(1):47-65.
578. Reddy BS, Weisburger JH, Wynder EL. Effects of high risk and low risk diets for colon carcinogenesis on fecal microflora and steroids in man. J Nutr. 1975;105(7):878-84.
579. Sumi Y, Miyakawa M. Gastrointestinal carcinogenesis in germ-free rats given N-methyl-N'-nitro-N-nitrosoguanidine in drinking water. Cancer research. 1979;39(7 Pt 1):2733-6.
580. Reddy BS, Narasawa T, Weisburger JH, Wynder EL. Promoting effect of sodium deoxycholate on colon adenocarcinomas in germfree rats. Journal of the National Cancer Institute. 1976;56(2):441-2.
581. Liu B, Qu L, Yan S. Cyclooxygenase-2 promotes tumor growth and suppresses tumor immunity. Cancer Cell International. 2015;15(1):106.
582. Wakabayashi K. NSAIDs as Cancer Preventive Agents. Asian Pacific journal of cancer prevention : APJCP. 2000;1(2):97-113.
583. Ferrandez A, Prescott S, Burt RW. COX-2 and colorectal cancer. Current pharmaceutical design. 2003;9(27):2229-51.
584. Jacoby RF, Seibert K, Cole CE, Kelloff G, Lubet RA. The Cyclooxygenase-2 Inhibitor Celecoxib Is a Potent Preventive and Therapeutic Agent in the Min Mouse Model of Adenomatous Polyposis. Cancer research. 2000;60(18):5040-4.
585. Oshima M, Dinchuk JE, Kargman SL, Oshima H, Hancock B, Kwong E, et al. Suppression of Intestinal Polyposis in ApcΔ716 Knockout Mice by Inhibition of Cyclooxygenase 2 (COX-2). Cell. 1996;87(5):803-9.
586. Glinghammar B, Inoue H, Rafter JJ. Deoxycholic acid causes DNA damage in colonic cells with subsequent induction of caspases, COX-2 promoter activity and the transcription factors NF-kB and AP-1. Carcinogenesis. 2002;23(5):839-45.
587. Zhang F, Subbaramaiah K, Altorki N, Dannenberg AJ. Dihydroxy Bile Acids Activate the Transcription of Cyclooxygenase-2. Journal of Biological Chemistry. 1998;273(4):2424-8.
588. DeRubertis FR, Craven PA, Saito R. Bile salt stimulation of colonic epithelial proliferation. Evidence for involvement of lipoxygenase products. J Clin Invest. 1984;74(5):1614-24.
589. Craven PA, Pfanstiel J, DeRubertis FR. Role of reactive oxygen in bile salt stimulation of colonic epithelial proliferation. J Clin Invest. 1986;77(3):850-9.

590. Booth LA, Gilmore IT, Bilton RF. Secondary Bile Acid Induced DNA Damage in HT29 Cells: are Free Radicals Involved? Free Radical Research. 1997;26(2):135-44.
591. Jackson AL, Chen R, Loeb LA. Induction of microsatellite instability by oxidative DNA damage. Proceedings of the National Academy of Sciences. 1998;95(21):12468-73.
592. Feig DI, Reid TM, Loeb LA. Reactive Oxygen Species in Tumorigenesis. Cancer research. 1994;54(7 Supplement):1890s-4s.
593. Beckman KB, Ames BN. Oxidative Decay of DNA. Journal of Biological Chemistry. 1997;272(32):19633-6.
594. Rossman TG, Goncharova EI. Spontaneous mutagenesis in mammalian cells is caused mainly by oxidative events and can be blocked by antioxidants and metallothionein. Mutation Research/Fundamental and Molecular Mechanisms of Mutagenesis. 1998;402(1):103-10.
595. Cooke MS, Evans MD, Dizdaroglu M, Lunec J. Oxidative DNA damage: mechanisms, mutation, and disease. The FASEB Journal. 2003;17(10):1195-214.
596. Craven PA, Pfanstiel J, DeRubertis FR. Role of activation of protein kinase C in the stimulation of colonic epithelial proliferation and reactive oxygen formation by bile acids. J Clin Invest. 1987;79(2):532-41.
597. Booth LA, Gilmore IT, Bilton RF. Secondary bile acid induced DNA damage in HT29 cells: are free radicals involved? Free Radic Res. 1997;26(2):135-44.
598. Venturi M, Hambly RJ, Glinghammar B, Rafter JJ, Rowland IR. Genotoxic activity in human faecal water and the role of bile acids: a study using the alkaline comet assay. Carcinogenesis. 1997;18(12):2353-9.
599. Hirose Y, Rao CV, Reddy BS. Modulation of inducible nitric oxide synthase expression in rat intestinal cells by colon tumor promoters. International journal of oncology. 2001;18(1):141-6.
600. Payne CM, Bernstein C, Bernstein H, Gerner EW, Garewal H. Reactive Nitrogen Species in Colon Carcinogenesis. Antioxidants & Redox Signaling. 1999;1(4):449-67.
601. Dall'Agnol M, Bernstein C, Bernstein H, Garewal H, Payne CM. Identification of S-nitrosylated proteins after chronic exposure of colon epithelial cells to deoxycholate. Proteomics. 2006;6(5):1654-62.
602. Bernstein H, Holubec H, Bernstein C, Ignatenko NA, Gerner E, Dvorak K, et al. Deoxycholate-induced colitis is markedly attenuated in Nos2 knockout mice in association with modulation of gene expression profiles. Dig Dis Sci. 2007;52(3):628-42.
603. Bernstein H, Bernstein C, Payne CM, Dvorak K. Bile acids as endogenous etiologic agents in gastrointestinal cancer. World J Gastroenterol. 2009;15(27):3329-40.
604. Payne CM, Bernstein C, Bernstein H. Apoptosis Overview Emphasizing the Role of Oxidative Stress, DNA Damage and Signal- Transduction Pathways. Leukemia & Lymphoma. 1995;19(1-2):43-93.
605. Yui S, Saeki T, Kanamoto R, Iwami K. Characteristics of apoptosis in HCT116 colon cancer cells induced by deoxycholic acid. Journal of biochemistry. 2005;138(2):151-7.
606. Wachs FP, Krieg RC, Rodrigues CM, Messmann H, Kullmann F, Knuchel-Clarke R, et al. Bile salt-induced apoptosis in human colon cancer cell lines involves the mitochondrial transmembrane potential but not the CD95 (Fas/Apo-1) receptor. International journal of colorectal disease. 2005;20(2):103-13.
607. Payne CM, Crowley-Weber CL, Dvorak K, Bernstein C, Bernstein H, Holubec H, et al. Mitochondrial perturbation attenuates bile acid-induced cytotoxicity. Cell biology and toxicology. 2005;21(5-6):215-31.
608. Powell AA, LaRue JM, Batta AK, Martinez JD. Bile acid hydrophobicity is correlated with induction of apoptosis and/or growth arrest in HCT116 cells. Biochem J. 2001;356(Pt 2):481-6.

609. Garewal H, Bernstein H, Bernstein C, Sampliner R, Payne C. Reduced bile acid-induced apoptosis in "normal" colorectal mucosa: a potential biological marker for cancer risk. Cancer research. 1996;56(7):1480-3.
610. Payne CM, Bernstein H, Bernstein C, Garewal H. Role of apoptosis in biology and pathology: resistance to apoptosis in colon carcinogenesis. Ultrastructural pathology. 1995;19(4):221-48.
611. Badvie S, Hanna-Morris A, Andreyev HJ, Cohen P, Saini S, Allen-Mersh TG. A "field change" of inhibited apoptosis occurs in colorectal mucosa adjacent to colorectal adenocarcinoma. Journal of clinical pathology. 2006;59(9):942-6.
612. Bernstein H, Holubec H, Warneke JA, Garewal H, Earnest DL, Payne CM, et al. Patchy field defects of apoptosis resistance and dedifferentiation in flat mucosa of colon resections from colon cancer patients. Annals of surgical oncology. 2002;9(5):505-17.
613. Bernstein C, Bernstein H, Garewal H, Dinning P, Jabi R, Sampliner RE, et al. A bile acid-induced apoptosis assay for colon cancer risk and associated quality control studies. Cancer research. 1999;59(10):2353-7.
614. Magnuson BA, Shirtliff N, Bird RP. Resistance of aberrant crypt foci to apoptosis induced by azoxymethane in rats chronically fed cholic acid. Carcinogenesis. 1994;15(7):1459-62.
615. Crowley-Weber CL, Payne CM, Gleason-Guzman M, Watts GS, Futscher B, Waltmire CN, et al. Development and molecular characterization of HCT-116 cell lines resistant to the tumor promoter and multiple stress-inducer, deoxycholate. Carcinogenesis. 2002;23(12):2063-80.
616. Washo-Stultz D, Hoglen N, Bernstein H, Bernstein C, Payne CM. Role of Nitric Oxide and Peroxynitrite in Bile Salt-Induced Apoptosis: Relevance to Colon Carcinogenesis. Nutrition and cancer. 1999;35(2):180-8.
617. Bernstein H, Payne CM, Kunke K, Crowley-Weber CL, Waltmire CN, Dvorakova K, et al. A proteomic study of resistance to deoxycholate-induced apoptosis. Carcinogenesis. 2004;25(5):681-92.
618. Qiao D, Gaitonde SV, Qi W, Martinez JD. Deoxycholic acid suppresses p53 by stimulating proteasome-mediated p53 protein degradation. Carcinogenesis. 2001;22(6):957-64.
619. Chendil D, Oakes R, Alcock RA, Patel N, Mayhew C, Mohiuddin M, et al. Low dose fractionated radiation enhances the radiosensitization effect of paclitaxel in colorectal tumor cells with mutant p53. Cancer. 2000;89(9):1893-900.
620. Fang C, Dean J, Smith JW. A novel variant of ileal bile acid binding protein is up-regulated through nuclear factor-kappaB activation in colorectal adenocarcinoma. Cancer research. 2007;67(19):9039-46.
621. Jenkins GJ, D'Souza FR, Suzen SH, Eltahir ZS, James SA, Parry JM, et al. Deoxycholic acid at neutral and acid pH, is genotoxic to oesophageal cells through the induction of ROS: The potential role of anti-oxidants in Barrett's oesophagus. Carcinogenesis. 2007;28(1):136-42.
622. Assinder SJ, Upshall A. Mitotic aneuploidy induced by sodium deoxycholate in Aspergillus nidulans. Mutation research. 1982;93(1):101-8.
623. Ferguson LR, Parry JM. Mitotic aneuploidy as a possible mechanism for tumour promoting activity in bile acids. Carcinogenesis. 1984;5(4):447-51.
624. Limoli CL, Giedzinski E. Induction of chromosomal instability by chronic oxidative stress. Neoplasia (New York, NY). 2003;5(4):339-46.
625. Hunt CR, Sim JE, Sullivan SJ, Featherstone T, Golden W, Von Kapp-Herr C, et al. Genomic instability and catalase gene amplification induced by chronic exposure to oxidative stress. Cancer research. 1998;58(17):3986-92.

626. Ogawa A, Murate T, Suzuki M, Nimura Y, Yoshida S. Lithocholic Acid, a Putative Tumor Promoter, Inhibits Mammalian DNA Polymerase β. Japanese Journal of Cancer Research. 1998;89(11):1154-9.

2.0 Materials and Methods

2.1 Reagents

Reagents, their suppliers and catalogue numbers are presented for reference in Table 2.1.

2.2 Mice and Experimental Design

Animal experiments were conducted in accordance with the regulations and guidelines of the Irish Department of Health following approval by the University College Cork Animal Experimentation Ethics Committee (2011/023), licensed under the Cruelty to Animals Act 1876 and the European Union (Protection of Animals Used for Scientific Purposes) Regulation 2012, under licence number B100/4108.

2.2.1 Azoxymethane-Treated Mice and Experimental Design (Chapter 3)

25mg of azoxymethane was reconstituted as a 25mg/mL stock solution in sterile PBS, aliquoted and stored at -20^{o}C until required. Before use, it was diluted in sterile PBS for a 1mg/mL working solution.

C57BL/6J female mice between three and five weeks old were allowed to acclimatise for four weeks on a 12-hour light/dark cycle with access to water and chow *ad libitum*. After acclimatisation, mice were administered an intraperitoneal (i.p.) injection of 10mg/kg azoxymethane each week for five consecutive weeks. Control mice were given matching injections of PBS. Faeces were collected weekly and timed culls were performed at 8, 12, 24 and 48 weeks from the instigation of AOM treatment (Figure 2.1). Mice were culled and tissue was processed as per section 2.2.5.

Table 2.1: Reagents and their suppliers

Reagent	Supplier	Catalogue #
APCmin female mice	Charles River	002020
C57BL/6J female mice	Charles River	000664
Azoxymethane	Sigma Aldrich	A5486
Sucrose	Sigma Aldrich	S-9378
PBS	Sigma Aldrich	D8537
Streptomycin sulphate salt	Sigma Aldrich	S9137
Teklad 18% protein chow	Envigo	2018S
Vacutainer tubes - EDTA (K2)	BD	367525
Formalin	VWR Chemicals	9713-5000
Ki67 antibody	Thermo Scientific	RM-9106
Cleaved caspase-3	Cell Signaling Tech.	9661
GenElute mammalian total RNA	Sigma Aldrich	RTN70
Tetro cDNA synthesis kit	Bioline	BIO-65043
QIAamp Fast DNA Stool Kit	Qiagen	51604
3.5mm glass beads	Thistle Scientific	11079135
RNAlater	Sigma Aldrich	R0901
Ethanol	Sigma Aldrich	51976
β-Mercaptoethanol	Sigma Aldrich	M3148
SensiFAST No-ROX kit	Bioline	BIO-86020
Roche probe library	Roche	4683633001
Custom oligo qPCR primers	Eurofins Genomics	NA
Sodium citrate dihydrate	Sigma Aldrich	W302600
Hydrogen peroxide	Sigma Aldrich	H-1009
Saponin	Sigma Aldrich	S7900
Sodium chloride	Sigma Aldrich	S7653
Potassium chloride	VWR Chemicals	10198
Hydrochloric acid	Sigma Aldrich	84435
Acetic acid	Sigma Aldrich	A6283
Trizma hydrochloride	Sigma Aldrich	T5941
Trizma base	Sigma Aldrich	T1503
Serum	Sigma Aldrich	NA
Secondary antibodies	Dako	NA
Avidin/biotin blocking kit	Vector	SP-2001
Vectastatin ABC kit	Vector	PK-6100
DAB peroxidase substrate kit	Vector	SK-4100
Xylene	VWR Chemicals	28975.360
DPX moutant	VWR Chemicals	360294H
Histo-Clear II	National diagnostics	HS-202
Mayer's haematoxylin	Sigma Aldrich	MHS16
Eosin	Sakura Finetek USA	8702
LB Agar	Sigma Aldrich	L3022

Figure 2.1: Timeline of AOM study. Red lines denote 5 weekly intraperitoneal injections of 10mg/kg azoxymethane in treatment mice and equivalent volume of PBS in controls. Orange lines denote timed culls. Weeks are measured from the date of the first injection. *N*=8 per group, except for AOM Week 12 and PBS Week 24 (*N*=7).

2.2.2 APC^{MIN} Mice and Experimental Design (Chapter 4)

Ten C57BL/6J mice and ten APC^{MIN} mice on a C57BL/6J background were acquired from Charles River. Mice were female, age-matched and housed five per cage on a 12-hour light/dark cycle with access to water and chow *ad libitum*. Mice were individually removed from the cage at ~12pm each day and fresh faeces were collected at 4, 7, 11 and 14 weeks of age. At 14 weeks of age, mice were culled and tissue was processed as per section 2.2.5.

2.2.3 APC^{MIN} Mice and Experimental Design (Chapter 5)

25 APC^{MIN} mice on a C57BL/6J background were acquired from Charles River at four weeks of age. Mice were female, age-matched and housed five per cage on a 12-hour light/dark cycle with access to chow *ad libitum*, and to sterile-filtered drinking water containing 10g/L sterile-filtered streptomycin.

Mice were treated with 100µL by gavage of 15% sucrose/PBS (PBS group, *n*=5), $5x10^9$ CFUs K12 *E. coli* (EC group, *n*=10) or $5x10^9$ CFUs K12 *E. coli* modified to express bile salt hydrolase (*bsh*) (EC-BSH group, *n*=10). Treatment began at 4 weeks of age with gavage on two consecutive days with top-up doses at 8 and 12 weeks of age (Figure 2.2).

Successful colonisation was confirmed by analysis of faecal colony forming units (CFUs) of *E. coli* and *E. coli* engineered to overexpress *bsh.* Faecal pellets were suspended in PBS (25mg/mL) for 30 minutes before a serial dilution was prepared. 10µL dilute was inoculated in triplicate onto plates of LB agar with streptomycin and incubated at 37^{o}C overnight. Colonies were counted the following day and colony forming units (CFUs) per millilitre were determined.

At 14 weeks of age, mice were culled and tissue was processed as per section 2.2.5.

Figure 2.2: Chapter 5 timeline. Streptomycin antibiotic was provided in drinking water throughout the experiment. Mice were gavaged with PBS, *E. coli K12* or an isogenic *E. coli* strain engineered to overexpress *bile salt hydrolase* (*bsh*) on two consecutive days at 4, 8 and 12 weeks of age. Mice were culled at 14 weeks of age.

2.2.4 Bsh cloning

Bsh from a *Lactobacillus salivarius* strain had previously been cloned into *E.coli MG1655* using splicing by overlap extension PCR (1). Expression was under the control of the P44 promoter. Transposon integration was carried out as described by McGrath et al. (2).

Successful construction was confirmed by PCR downstream from the glmS region, and by sequence analysis (GATC Biotech).

2.2.5 Tissue Collection and Processing

Mice were culled by decapitation and blood was collected. Spleens were removed, weighed and flash frozen in liquid nitrogen. Gallbladders were sealed with surgical suture and stored on ice. Livers were weighed and divided into three equal proportions for storage in formalin, RNAlater and flash freezing in liquid nitrogen. Small intestine length was measured and two ~1cm portions were taken from the proximal and distal ends for storage in RNAlater or flash freezing in liquid nitrogen. The cecum was weighed and stored on ice. Mesenteric and epididymal fat was removed, weighed and stored on ice.

In AOM mice, the remaining length of small intestine was formalin-fixed and divided into three equal portions which were Swiss-rolled and wax-embedded. The colon was processed similarly to the small intestine but was opened longitudinally, washed with PBS, examined for hyperplasia or neoplasia and mounted on microscope slides before immersion in formalin. Formalin-fixed colon tissue was stained with methylene-blue and examined for ACF (3), before being Swiss-rolled and wax embedded.

In APC^{MIN} mice, the remaining small intestine tissue was divided into three equal lengths, opened longitudinally, rinsed with PBS, and polyps were enumerated under a dissecting microscope. Each portion of small intestine was then Swiss-rolled, formalin-fixed and wax-

embedded. The colon was processed similarly to the small intestine without division into different sections.

Subsequently, all tissue which was stored on ice or flash frozen was moved to -80^{o}C. Blood was centrifuged at 2,000xg for 10 minutes and plasma was stored at -80^{o}C. Samples immersed in RNAlater or formalin were stored at 4^{o}C for 24 hours. RNA samples were then decanted and moved to -80^{o}C. Formalin-fixed liver samples were also wax-embedded. Wax-embedded tissue was cut into 4µm sections for mounting onto microscope slides.

2.3 Immunohistochemistry

Immunohistochemistry was performed using the standard procedure on 4µm-sectioned, formalin-fixed, paraffin-embedded slides (4). Sections were deparaffinised in xylene and re-hydrated using an ethanol gradient. Antigen retrieval was performed by microwave-heating in 0.01M sodium citrate pH 6.0. Endogenous peroxidase activity and non-specific binding were blocked with 3% H_2O_2 and 5% normal serum, respectively, prior to blocking with avidin/biotin before overnight incubation with primary antibody. Tissue was exposed to a biotinylated secondary antibody the following day, amplified with an avidin-biotin peroxidase and visualised with 3,3'-diaminobenzidine (DAB). Slides were counterstained with haematoxylin. Negative controls were prepared without primary antibody.

Ki67 primary antibody was used at 1/1000 dilution. The percentage of Ki67-positive cells per crypt was determined by counting the total number of cells and the number of Ki67-positive cells in 10 morphologically-normal crypts in the large intestine.

Activated caspase-3 primary antibody was used at 1/200 dilution. Images were captured at 40x magnification and the number of positive-stained cells per image was determined for

three randomly selected fields in each of three representative mice from each group at Weeks 8 and 24.

2.4 Quantitative Real-Time PCR

Gene transcription was analysed in tissue taken from the distal 1cm of the large intestine in mice treated with AOM (Chapter 3), and from the distal 1cm of the small intestine in APC^{MIN} mice (Chapters 4 and 5). RNA extraction was performed using the GenElute Mammalian Total RNA kit. Frozen tissue was immersed in 500µL lysis buffer containing 1% β-mercaptoethanol and subjected to bead-beating (45 seconds x2 with a 20 second interval using 3.5mm glass beads). Lysate was filtered, bound to a collection column, washed and eluted. Successful extraction was confirmed by determining the RNA concentration of the elute in a NanoDrop 2000 at wavelength 260nm and a 260/280 ratio of between 1.8 and 2.2.

RNA was converted to cDNA using the Tetro cDNA Synthesis Kit. 1-8µL of RNA elute containing ~3µg RNA per sample was incubated for 10 minutes at 70^{o}C with 1µL deoxynucleotide triphosphates (dNTPs, 10mM) and 1µL random hexamer primer (50ng), with diethyl pyrocarbonate (DEPC)-treated sterile water added as necessary to make a total volume of 10µL. A mix of 0.5µL reverse transcriptase (100 units), 2µL reverse transcriptase buffer (5x), 0.5µL RNase inhibitor (5 units) and 7µL DEPC-treated sterile water was subsequently added to the RNA elute mix. This was incubated at room temperature for 10 minutes (initialisation), 37^{o}C for 50 minutes (elongation) and 90^{o}C for 5 minutes (termination).

Primers for qPCR were designed using the Roche Assay Design Centre and ordered as custom oligonucleotides from Eurofins Genomics. qPCR was performed using 1µL cDNA, 5µL SensiFAST No-ROX mix (2x), 0.5µL forward and reverse primers (5pmol), 3µL DEPC-treated

sterile water and 0.1µL Universal Probe Library (UPL, 10µM) hydrolysis probe from the Roche probe library as per Table 2.2, in a LightCycler 480 for 45 PCR cycles. Relative transcription was calculated using the $2^{-\Delta\Delta CT}$ method standardised to the average of the control group ΔCT (5).

2.5 Faecal 16S rRNA Gene Sequencing

Total DNA Extraction: Faecal samples were collected as described in section 2.2 and stored at -80^{o}C. Subsequently, DNA was extracted from one faecal pellet using the QIAamp Fast DNA Stool Kit as per manufacturer's instructions with the addition of a bead-beating step (45 seconds x2 with a 20 second delay using 3.5mm glass beads). Sequencing was performed by Teagasc Moorepark, Ireland.

Amplicon Sequencing: The V3-V4 variable region of the 16s rRNA gene was amplified from each extracted DNA sample according to the 16S metagenomic sequencing library protocol (Illumina, Sweden). Initially, the template DNA was amplified using primers specific to the V3-V4 region of the 16s rRNA gene which also incorporates the Illumina overhang adaptor (Table 2.2). Each PCR reaction contained 2.5µl DNA template, 5µl forward primer (1µM), 5µl reverse primer (1µM) (Sigma, Ireland) and 12.5µl Kapa HiFi HotStart ReadyMix (2X) (Kapa Biosystems, London, United Kingdom). The template DNA was amplified under the following PCR conditions: 95˚C for 3 min (initialisation); followed by 25 cycles of 95˚C for 30 sec (denaturation), 55˚C for 30 sec (annealing), 72˚C for 30 sec (elongation); followed by a final elongation period of 5 minutes. A negative control reaction whereby the DNA template was replaced with PCR grade water was employed to confirm lack of contamination and PCR products were visualised using gel electrophoresis (1X TAE buffer, 1.5% agarose gel, 100V) post PCR reaction. Successful amplicons were then cleaned using the AMPure XP purification system (Labplan, Dublin, Ireland). A second PCR reaction was then performed using the

Table 2.2: qPCR Primer Sequences and matching Universal Probe Library (UPL) probes

Gene	Forward Primer (5'-3')	Reverse Primer (5'-3')	UPL #
IL1β	agttgacggaccccaaaag	agctggatgctctcatcagg	#38
IL6	gctaccaaactggatataatcagga	ccaggtagctatggtactccagaa	#6
CXCL1	gactccagccacactccaac	tgacagcgcagctcattg	#83
CXCL2	aaaatcatccaaaagatactgaacaa	ctttggttcttccgttgagg	#26
CXCL5	tagagccccaatctccacac	gagctggaggctcattgtg	#67
IL10	cagagccacatgctcctaga	tgtccagctggtcctttgtt	#41
IL12	aaggaacagtgggtgtccag	gttagcttctgaggacacatcttg	#27
TNFα	ctgtagcccacgtcgtagc	ttgagatccatgccgttg	#25
TGFβ	tggagcaacatgtggaactc	gtcagcagccggttacca	#72
I-babp	ggcaaagaatgtgaaatgcag	ccgaagtctggtgatagttgg	#53
Fgf15	ggcaagatatacgggctgat	tccatttcctccctgaaggt	#69
Ostα	gctgcccacctctcatactt	ttgaagaaggcgtactggaaa	#3
Ostβ	atcctggcaaacagaaatcg	tgcaggtcttctggtgtttct	#5
Jun	ccagaagatggtgtggtgttt	ctgaccctctccccttgc	#11
Sox9	gtacccgcatctgcacaac	ctcctccacgaagggtctct	#66
Myc	cctagtgctgcatgaggaga	tccacagacaccacatcaattt	#77
Axin2	gagagtgagcggcagagc	cggctgactcgttctcct	#96
β-actin	ctaaggccaaccgtgaaaag	accagaggcatacagggaca	#64
16S Ribosomal RNA gene V3-V4 region, forward primer (5'-3'): tcgtcggcagcgtcagatgtgtataagagacagcctacgggnggcwgcag			
16S Ribosomal RNA gene V3-V4 region, reverse primer (5'-3'): gtctcgtgggctcggagatgtgtataagagacaggactachvgggtatctaatcc			

previously amplified and purified DNA as the template. Two indexing primers (Illumina Nextera XT indexing primers, Illumina) were used per sample to allow all samples to be pooled, sequenced and subsequently identified. Each reaction contained 25µl Kapa HiFi HotStart ReadyMix (2X), 5µl template DNA, 5µl index 1 primer (N7xx), 5µl index 2 primer (S5xx) and 10µl PCR grade water. PCR conditions were the same as previously described with the samples undergoing just eight cycles instead of 25. PCR products then underwent the same electrophoresis and cleaning protocols as described above. Samples were then quantified using the Qubit 2.0 Fluorometer (Invitrogen, Carlsbad, CA, USA) in conjunction with the broad range DNA quantification assay kit (Biosciences, Dublin, Ireland). All samples were then pooled to an equimolar concentration and the pool underwent a final cleaning step. The quality of the pool was determined using the Agilent Bioanalyser prior to sequencing. The sample pool was then denatured with 0.2 M NaOH, diluted to 4pM and combined with 10% (v/v) denatured 4pM PhiX. Samples were then sequenced on the MiSeq sequencing platform using a 2.300 cycle V3 Kit following protocols outlined by Illumina.

Bioinformatic and Statistical Analysis: Two-hundred and fifty base pair paired-end reads were assembled using FLASH (6). Reads were further processed with the inclusion of quality filtering, based on a quality score of >25, followed by subsequent removal of mismatched barcodes and sequences below length threshold using QIIME. USEARCH v7 (64-bit) was used for noise removal and chimera detection as well as clustering into operational taxonomic units (OTUs). PyNAST was used to align OTUs and taxonomy was assigned using BLAST against the SILVA SSURef database release 119.

Composition Analysis: The R package *compareGroups* (v. 3.1) was employed to detect statistically significant differences in abundances of individual taxa between groups using the Mann-Whitney U-test (MWU-test) with multiple corrections. Statistical significance was accepted as $P \leq 0.05$ after false discovery rate (FDR) multiple correction. Compositional alpha

diversity was calculated in QIIME (v. 1.9.1) and statistical differences between groups were detected using the MWU-test. The remaining statistical analyses were all performed in R (v. 3.2.3). The *phyloseq* package (v. 1.10) was used to calculate compositional β-diversity using genus-level relative abundance data. This was visualised by principal coordinate analysis (PCoA) using *ggplot2* (v. 2.1.0). Permutational multivariate analysis of variance (PERMANOVA) was used to test for differences in overall microbiome composition between groups using the *vegan* package's 'adonis' function.

Functional Analysis: PICRUSt was used to investigate the abundances of gene families based on the 16S rRNA gene data and, from this data, infer functional alterations in the microbiome. For this, the *pick OTUs* module was performed at 97% identity in a closed reference way using the Greengenes database (13_8) in QIIME. Data were normalised for 16S rRNA gene copy numbers and the metagenomes were predicted. KEGG Orthologs (KO) were identified from the inferred metagenomes and the R package *compareGroups* was used to identify differentially expressed functions between groups. Functional alpha diversity was calculated using the *vegan* package (v. 1.10) and statistical differences between groups were detected using the MWU-test. The *vegan* package was used to calculate functional β-diversity and this was visualised by principal coordinate analysis (PCoA) using *ggplot2*. Permutational multivariate analysis of variance (PERMANOVA) was used to test for differences in overall microbiome function between groups using the *vegan* package's 'adonis' function.

2.6 Generation of Co-abundance Groups

In order to identify patterns in the variation of the microbiota and investigate associations between these variations and disease states, a set of co-abundance groups (CAGs) were determined by clustering OTUs which tended to co-occur. Initially, OTUs were trimmed to

remove taxa present in less than 20% of samples (Chapter 3) or 50% of samples (Chapters 4 and 5), and all unclassified and non-prokaryotic taxa. A matrix of Kendall's Tau values was then generated for each pair of OTUs and these values were clustered by Ward-linkage according to their Pearson's correlation coefficient and visualised using the *Made4* package in R. Each cluster of taxa was then assigned to a CAG.

2.7 Ultra-Performance Liquid Chromatography – Mass Spectrometry

Faecal and plasma samples were used for analysis of bile acids. UPLC-MS was performed as described by Joyce *et al.* (1). Five microliters of extracted bile acids were injected onto a 50-mm T3 Acquity column (Waters Corp.) and were eluted using a 20-min gradient of 100% A to 100% B (A, water, 0.1% formic acid; B, methanol, 0.1% formic acid) at a flow rate of 400µL/min and column temperature of 50 °C. Samples were analysed using an Acquity UPLC system (Waters Ltd.) coupled online to an LCT Premier mass spectrometer (Waters MS Technologies, Ltd.) in negative electrospray mode with a scan range of 50–1,000 m/z. Bile acids ionize strongly in negative mode, producing a prominent [M-H] negative ion. Capillary voltage was 2.4Kv, sample cone was 35V, desolvation temperature was 350 °C, source temperature was 120 °C, and desolvation gas flow was 900 L/h. Principal components analysis (PCA) was performed in Markerlynx (Waters) by limiting the number of elements (N, H, S, C) to be detected in individual analytes. Furthermore, a template of defined known masses was applied to allow the detection of bile acid only. Each analyte was identified according to its mass and retention time. Standard curves were performed using known bile acids, and each analyte was quantified according to the standard curve and normalized according to the deuterated internal standards.

2.8 Statistics

Statistics were performed in SPSS Version 24 and R Version 3.5.0 using the *Made4*, *vegan, pairwiseAdonis, compareGroups, phyloseq* and *ggplot* packages. GraphPad Prism (Version 5) was used for the generation of some graphs. Statistical significance was set to $p<0.05$. Benjamini-Hochberg FDR adjustment for multiple comparisons was applied where noted, with a false discovery rate set to 5% (7). Normality was determined by a Shapiro-Wilk test (8). Groups were compared by student's T-test or MWU-test. Comparisons across time were made using ANOVA followed by pairwise comparison using Tukey's HSD, or Kruskal-Wallis Rank Sum Test followed by pairwise comparisons using the MWU-test. Permutational ANOVA (PERMANOVA) was used to compare β-diversity and CAGs, using unweighted Unifrac and Euclidean-squared distance matrices respectively. Correlations were examined using Pearson's R and Spearman's R^2 correlation coefficients. In figures, asterisks denote significance such that * is $p<0.05$, ** is $p<0.01$, and *** is $p<0.001$.

2.9 References

1. Joyce SA, MacSharry J, Casey PG, Kinsella M, Murphy EF, Shanahan F, et al. Regulation of host weight gain and lipid metabolism by bacterial bile acid modification in the gut. Proceedings of the National Academy of Sciences. 2014;111(20):7421-6.
2. McGrath S, Fitzgerald GF, van Sinderen D. Improvement and optimization of two engineered phage resistance mechanisms in Lactococcus lactis. Appl Environ Microbiol. 2001;67(2):608-16.
3. McGinley JN, Thompson MD, Thompson HJ. A method for serial tissue processing and parallel analysis of aberrant crypt morphology, mucin depletion, and Beta-catenin staining in an experimental model of colon carcinogenesis. Biol Proced Online. 2010;12(1):9032-.
4. Fernandes P, MacSharry J, Darby T, Fanning A, Shanahan F, Houston A, et al. Differential expression of key regulators of Toll-like receptors in ulcerative colitis and Crohn's disease: a role for Tollip and peroxisome proliferator-activated receptor gamma? Clin Exp Immunol. 2016;183(3):358-68.
5. Livak KJ, Schmittgen TD. Analysis of relative gene expression data using real-time quantitative PCR and the 2(-Delta Delta C(T)) Method. Methods (San Diego, Calif). 2001;25(4):402-8.
6. Magoc T, Salzberg SL. FLASH: fast length adjustment of short reads to improve genome assemblies. Bioinformatics (Oxford, England). 2011;27(21):2957-63.
7. Benjamini Y, Hochberg Y. Controlling the False Discovery Rate: A Practical and Powerful Approach to Multiple Testing. Journal of the Royal Statistical Society Series B (Methodological). 1995;57(1):289-300.
8. Shapiro SS, Wilk MB. An Analysis of Variance Test for Normality (Complete Samples). Biometrika. 1965;52(3/4):591-611.

Chapter 3

Concurrent temporal changes in host immune profile, microbiota and bile acids in a chemically-induced murine model of colonic tumorigenesis

3.0 Abstract

Background: The gut microbiota has been shown to be involved in the initiation and development of colorectal cancer (CRC) in animal models. Research into the role of the microbiota in CRC has primarily focussed on changes that exist in and around tumour sites at a single point in time. This has made it difficult to differentiate between changes that promote cancer initiation in healthy tissue from changes that are a result of tumour development. In this study, we tracked changes in the host and microbiota throughout the course of azoxymethane (AOM)-induced colon cancer development to elucidate their contribution to disease. Our aim was to identify changes in each of these criteria and establish their temporal relationships in order to generate a timeline of alterations and define causative and consequential events.

Methods: Mice received five weekly doses of 10mg/kg AOM or PBS control. Timed culls were performed at 8, 12, 24 and 48 weeks afterwards. Faecal microbial composition was determined by 16S rRNA gene sequencing, and faecal and plasma bile acids were measured by UPLC-MS at each time-point. Host response was measured by qPCR in the distal large intestine. Correlation analysis was performed to establish whether any relationships exist between microbial composition and diversity, transcription of inflammatory cytokines and bile acids.

Results: The initial changes were detected in gut microbiota which acquired a pro-tumorigenic profile, defined as an enrichment of bacterial species predominantly associated with increased cancer risk. These changes are suppressed concurrent with the onset of host inflammatory response but are re-established later, possibly due to selection for resistant species. The size and composition of the bile acid pool are also affected and correlation analysis implicates the microbiota in this effect and in cytokine transcription.

Conclusion: Disruption in the large intestine of mice administered AOM allows opportunistic pathogens to impart a pro-tumorigenic profile to the gut microbiota with the potential to contribute to cancer initiation and progression by a mechanism which may involve inflammation and suppression of bile acid signalling.

Acknowledgements: 16S rRNA gene sequencing of the faecal microbiota was performed by Calum Walsh in Teagasc Moorepark (*Materials and Methods* section 2.5, *Amplicon Sequencing* to end of *Functional Analysis*), who also produced the plots in Figure 3.5 and 3.16. UPLC-MS and extraction from faecal and plasma samples for the detection of bile acids was performed by Peter Cronin (*Materials and Methods* section 2.7, *Ultra-Performance Liquid Chromatography – Mass Spectrometry)*. Some of this work is presented in his submitted MRes thesis (April 2019). The materials and methods sections for these processes are provided by their respective executors. AOM administration and mouse culling was performed by Pat Casey.

3.1 Introduction

Colorectal cancer (CRC) has a complex aetiology involving the interaction of genetic and environmental factors. Attention has turned to the role of the gut microbiota in this process as it has been shown to be involved in tumorigenesis in animal models (1). The human gut microbiota is altered in CRC. Furthermore, certain microbial patterns are associated with increased cancer risk, but firm identification of mechanisms and specific pathogens involved has proven elusive as species associated with human CRC are not consistent across studies (2, 3).

Investigations to decipher the role of the human gut microbiota in CRC to date have largely examined patients already presenting with CRC (4). Moreover, observational studies have lacked the detailed investigation of the progression from the pre-tumorigenic state through to the adenoma-carcinoma sequence (2). These studies have allowed identification of patterns in the host and microbiota associated with active disease. However, they cannot distinguish between changes that are a result of tumorigenesis from characteristics that existed prior to and during tumour development. Animal models, in contrast, allow deep interrogation of the tumorigenic process over time by allowing timed sampling of large cohorts in controlled conditions.

Previous studies have examined the gut microbiota of mice treated with the carcinogenic compound azoxymethane (AOM) to elucidate changes associated with CRC. These have identified a number of bacterial taxa which have also been observed in human CRC (5, 6). These include increases in pathogenic bacteria that are enriched in human CRC, such as *Fusobacterium nucleatum*, and suppression of species associated with a reduction in cancer risk such as *Lactobacillus* and butyrate-producing *Faecalibacterium prausnitzii* (7-12). *F. prausnitzii* and *Lactobacillus* are also major reservoirs of bile acid-deconjugating enzyme *bile*

salt hydrolase (*bsh*) in the microbiota, along *Bifidobacterium* and some species of *Enterococcus* and *Bacteroides* (13, 14).

Modulation of the intestinal immune response and inflammation is one mechanism by which the microbiota may affect carcinogenesis (15). Cytokines and chemokines are soluble immune factors produced by tumour cells, stromal cells and tumour-infiltrating immune cells which can promote or suppress cancer initiation and progression by mediating inflammation and the immune response (16-20). This can occur by production of genotoxic compounds such as reactive oxygen species, induction of DNA damage and suppression of apoptosis, and is compounded by the chronic dysregulation of immune response associated with CRC (21). Inflammation in the gut can also affect the composition of the gut microbiota, especially in irritable bowel disease (IBD), resulting in complex reciprocal interactions (22). Moreover, research has suggested a role for the microbiota in the regulation of cytokines and chemokines in mouse models of CRC, especially by their production of short chain fatty acids such as butyrate (23-29).

Another possible mechanism by which the gut microbiota may affect host processes leading to the development of CRC is the production of pro- or anti-tumorigenic bacterial metabolites. Bile salts are endogenous, amphipathic molecules released into the duodenum after feeding to facilitate uptake of dietary fats. Bile salt dysregulation is associated with cancer risk, especially microbial metabolites of bile salts; primary bile acids and secondary bile acids (30). For example, rats administered AOM and fed cholic acid, a primary bile acid, had increased colonic tumours compared to rats treated with AOM alone, and this increase could be ameliorated by co-administration with ursodeoxycholic acid, a less hydrophobic bile acid (31-33). Moreover, a high fat diet is a known risk factor for colon cancer which also increases bile acid excretion and faecal concentration of deoxycholic acid and lithocholic acid

(34, 35). This suggests bile acids and their modifying organisms may represent a potential aetiologic agent of high fat diet-induced colon cancer risk.

Here, we perform a time-course study in a mouse model with a prolonged period of disease onset after AOM administration in the C57BL/6J mouse, in order to increase the temporal resolution of disease progression and allow examination of host and microbial changes during that period. We explore markers of host inflammation, the composition of the gut microbiota and the production of microbial metabolites in the murine colonic epithelium. Our aim was to investigate if there was a relationship between transcription of inflammatory cytokines, microbial composition and bile acids, and set these changes to a timeline. This should allow us to establish a set of causal and consequential events in the process of AOM-induced tumorigenesis as a model for sporadic human CRC.

3.2 Results

3.2.1 AOM-treated mice displayed faecal occult blood and aberrant crypt foci at 24 weeks and colonic adenomas at 48 weeks post-AOM injection

C57BL/6J mice were injected with AOM and changes in the host and microbiota were tracked through four timed culls performed 8, 12, 24 and 48 weeks after instigation of AOM treatment. The appearance of faecal occult blood (FOB) was detected, and the development of aberrant crypt foci (ACF) and adenomas was determined using methylene blue staining. Findings are presented in Table 3.1.

FOB was first detected in one AOM-treated mouse 22 weeks after AOM administration, with ACF detected in the large intestinal epithelium of this mouse at Week 24 (Figure 3.1A). FOB was also apparent in the faeces in three out of eight AOM-treated mice prior to Week 48 and two of these mice harboured at least one colonic adenoma (Figure 3.1B). No signs of neoplastic transformation were observed in mice at Week 8 (0/8) or Week 12 (0/7). As inflammation can lead to shortening of the large intestine, particularly in models of colitis-associated cancer, we measured the length of the large intestine at each dissection. However, no difference between AOM- and PBS-treated mice was detected at any time-point examined (Figure 3.1C; T-test and MWU-test, $p>0.05$).

3.2.2 AOM-treated mice gained less epididymal fat

At Week 8, AOM-treated mice had significantly less epididymal fat than PBS controls (Figure 3.2B; T-test, $p<0.001$). There was a trend towards a reduction in both epididymal and mesenteric fat in AOM-treated mice for the duration of the study, and AOM-treated mice gained less weight than the PBS-treated mice, but this was not statistically significant (Figure 3.2; T-tests and ANOVA, $p>0.05$).

Table 3.1: Incidence of faecal occult blood (FOB), aberrant crypt foci (ACF) and adenomas

		Week 8	Week 12	Week 24	Week 48
PBS	FOB	0/8	0/8	0/7	0/8
	ACF	0/8	0/8	0/7	0/8
	Adenoma	0/8	0/8	0/7	0/8
AOM	FOB	0/8	0/7	**1/8**	**3/8**
	ACF	0/8	0/7	**1/8**	0/8
	Adenoma	0/8	0/7	0/8	**2/8**

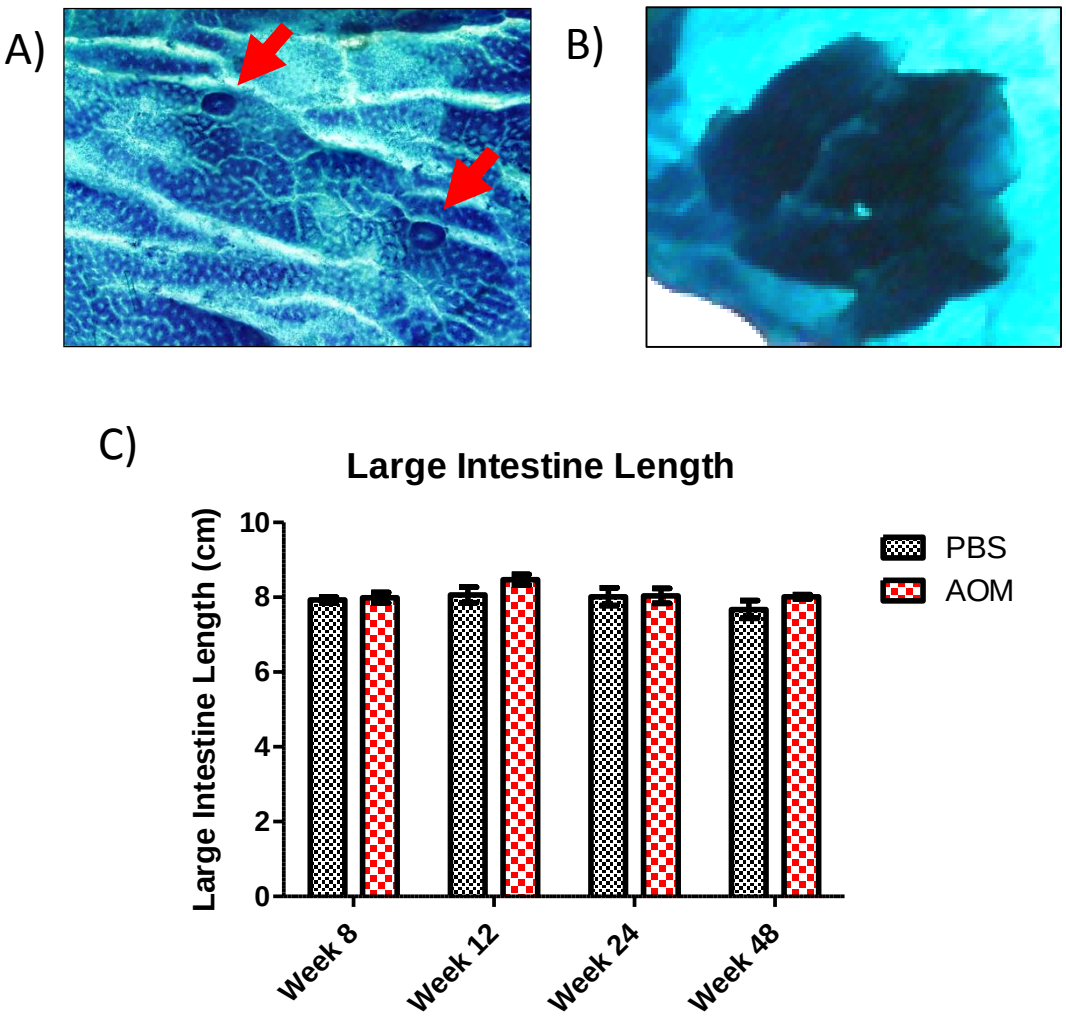

Figure 3.1: Detection of aberrant crypt foci and adenomas by methylene blue staining. Mice were culled by decapitation and colons excised, opened longitudinally and washed with PBS before fixation in 10% formalin overnight. Colons were then immersed in methylene blue for 3 minutes, rinsed in deionised water and photographed. **A)** Representative image of the colonic lumen epithelium stained with methylene blue from the dissection at Week 24 (10x magnification). ACF are highlighted with red arrows. They were identified by their protrusion from the epithelial surface and thickened crypt openings. **B)** Macroscopic image of a mouse colon stained with methylene blue displaying a large adenoma from the dissection at Week 48. Adenomas were detected in two mice at this time-point. **C)** The length of the large intestine was measured at each time-point. Graph represents the mean and SEM. *N*=8 per group, except for AOM Week 12 and PBS Week 24 (*N*=7).

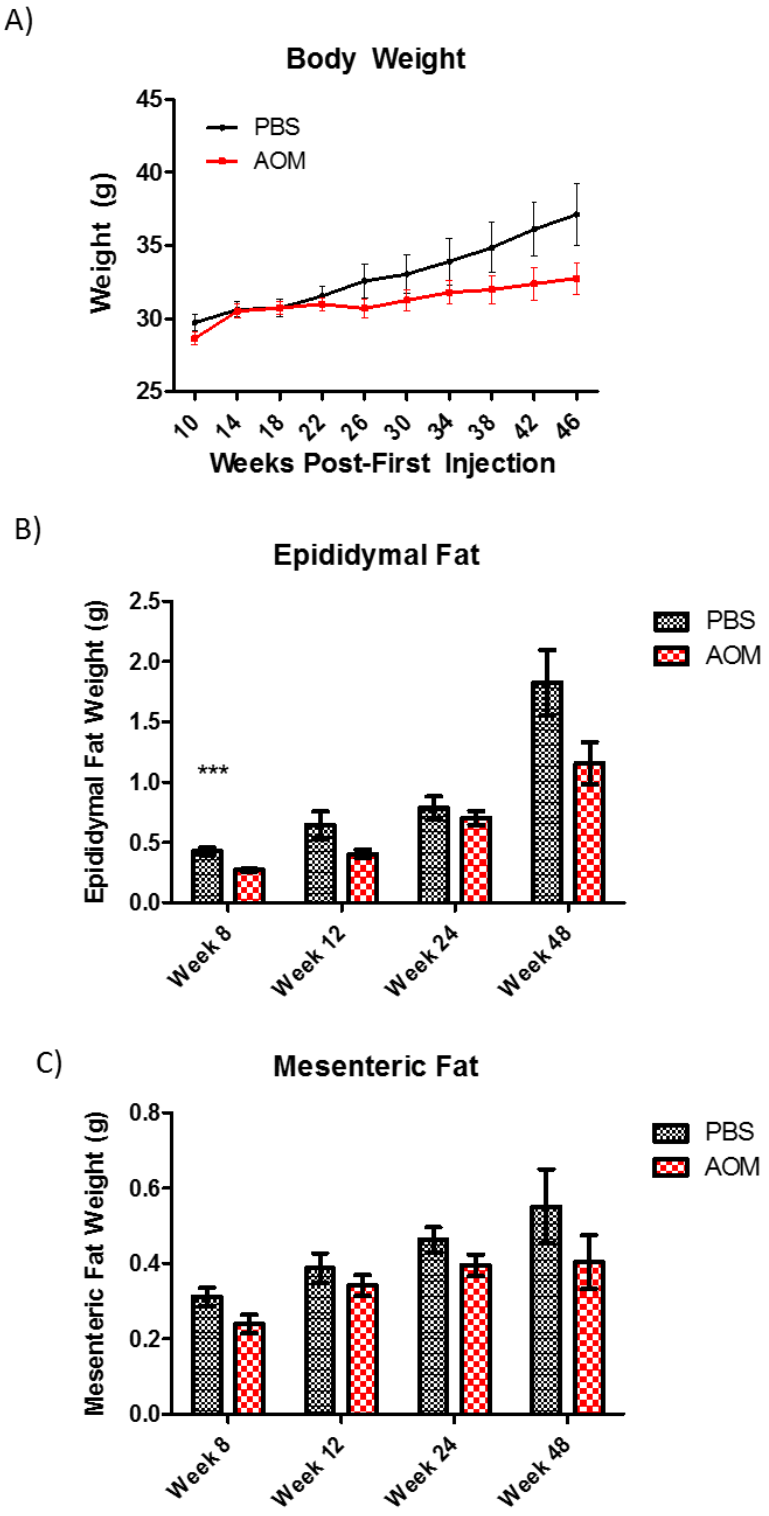

Figure 3.2: Fat gain was affected in mice treated with AOM at Week 8. Mice were weighed weekly over the course of the experiment. At each dissection, tissue samples were taken and weighed. **A)** The difference in body weight between the groups grew as the experiment progressed but this did not reach significance. **B)** The mass of epididymal fat was lower in mice exposed to AOM over the course of the experiment but this was only significant at Week 8. **C)** A similar trend was observed in the mass of mesenteric fat but this was not significant. Graphs present the mean and SEM. *N*=8 per group, except for AOM Week 12 and PBS Week 24 (*N*=7).

3.2.3 Proliferation and apoptosis are unchanged in AOM-treated mice at Week 8 or Week 24

In order to investigate if increased proliferation occurs prior to the development of ACF, intestinal tissue was immunohistochemically stained for Ki67 which detects proliferating cells, and the number of Ki67 positive cells per crypt was examined in PBS- and AOM-treated mice at 8 and 24 weeks post-first injection. These time-points were chosen as disruption to the microbiota began at Week 8 (see Figure 3.5 and 3.6), while the cytokine response peaked at Week 24 (see Figure 3.4). There were no significant differences in the expression of Ki67 or activation of caspase-3 at these time-points, suggesting that AOM does not contribute to tumorigenesis by inducing widespread proliferation of normal epithelial cells, or by suppression of apoptosis at these time-points (Figure 3.3; T-test, $p>0.05$).

3.2.4 Cytokine profile in the large intestine and spleen weight is altered in AOM-treated mice

Inflammation is a risk factor for colon cancer and the tumour microenvironment can modulate inflammatory conditions to promote tumour growth. As such, we measured the transcription of a number of cytokines in the distal large intestine by qPCR. *Cxcl5* was the only inflammatory factor found to be significantly changed at Week 8, where it was decreased in AOM-treated mice compared to PBS controls (Figure 3.4; T-test, $p=0.039$). Spleen weight was also increased in mice administered AOM at Week 8, suggesting an expansion of monocyte cells (Figure 3.4; MWU-test, $p=0.007$). In contrast, numerous cytokines/chemokines were significantly altered at Weeks 12 and 24, with *Il1β*, *Il6*, *Cxcl1*, *Cxcl2*, *Cxcl5*, *Il10*, *Il12* and *Tnfα* all found to be increased in AOM-treated mice during this timeframe (Figure 3.4; T-test and MWU-test, $p<0.05$). However, these alterations in cytokine/chemokine transcription was largely absent by Week 48 with only *Il12* significantly increased in AOM-treated mice (Figure 3.4; MWU-test, $p=0.04$).

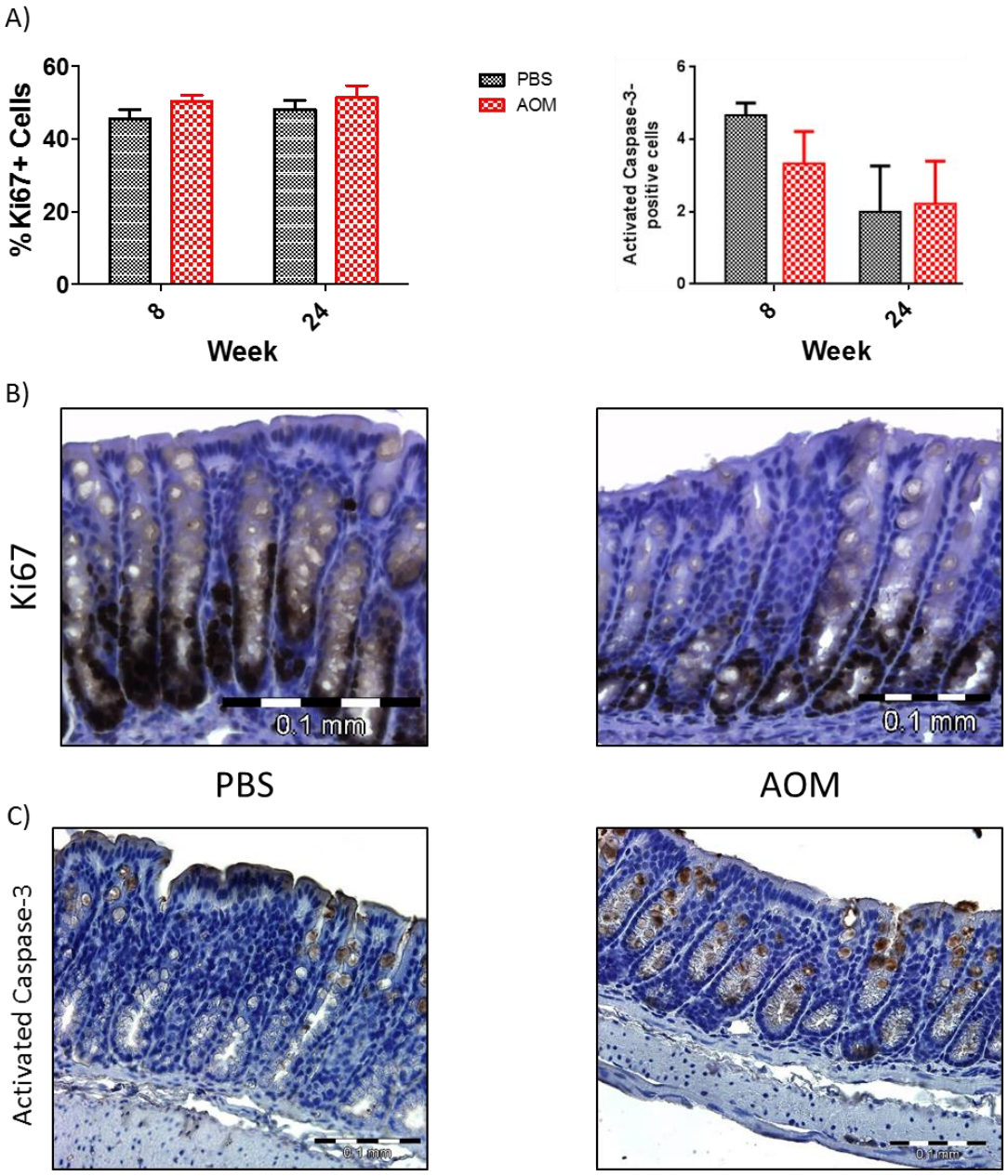

Figure 3.3: Proliferation and apoptosis were unchanged in the colonic crypts of mice administered AOM. Immunohistochemistry was performed with an antibody for proliferation marker Ki67 and an apoptosis marker, activated caspase-3, in the distal colons of PBS- and AOM-treated mice. For Ki67, the total number of epithelial cells were counted for ten crypts as well as the number of cells staining positive for Ki67 at Week 8 and Week 24. For activated caspase-3, three randomly selected microscope fields from three mice in each group were selected and the number of positively staining cells were counted. **A)** The percentage of Ki67-positive cells per crypt and the number of activated caspase-3-positive cells per field were determined in the normal mucosa of mice treated with PBS and AOM at Week 8 and Week 24. The differences were not significant. Graphs present the mean and SEM. N-numbers for Ki67 in PBS- and AOM-treated mice are 6 and 5 at Week 8, and 6 and 7 at Week 24. **B)** Ki67 staining of colon tissue of each group at Week 24 on a background stain of haematoxylin. **C)** Activated caspase-3 staining of colon tissue of each group at Week 24 on a background stain of haematoxylin. Images were taken at 400x magnification. *N*=8 per group, except for AOM Week 12 and PBS Week 24 (*N*=7).

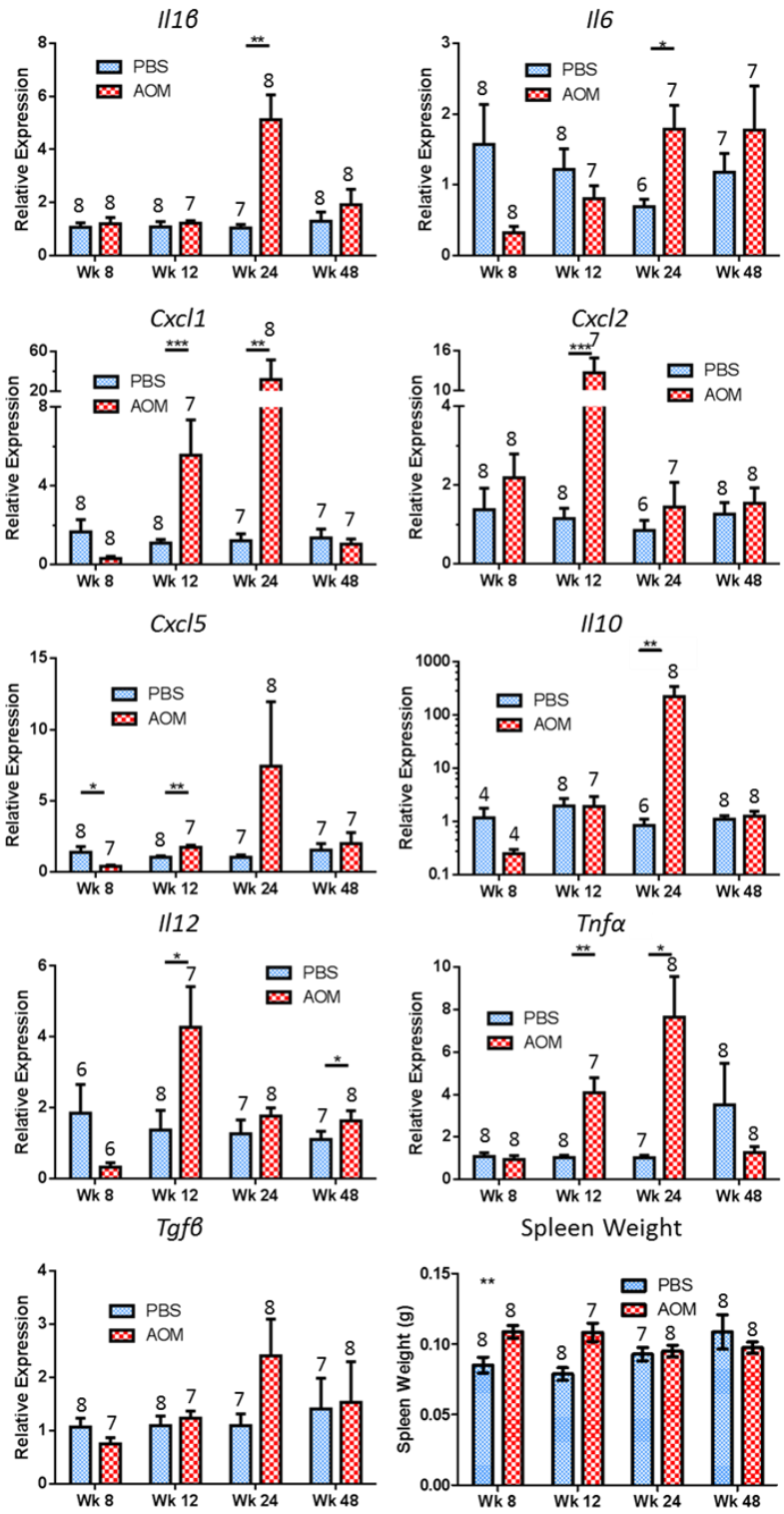

Figure 3.4: Cytokine response is altered in mice administered AOM. The distal 1cm of colon tissue was taken from each mouse at dissection, RNA extracted and converted to cDNA which was analysed by qPCR. A minor down-regulation to cytokine response was observed at Week 8 before pro-inflammatory expression arose at Week 12 and Week 24. This pro-inflammatory profile subsequently subsided by Week 48. Spleens were also removed and weighed at each dissection and a significant increase in mass was observed in mice treated with AOM at Week 8. Graphs present the mean and SEM. *N*-numbers are presented above bars. Note: *Il10* y-axis is presented in the logarithmic scale.

3.2.5 The faecal microbiota is altered in AOM-treated mice

We collected faecal pellets from each mouse on the day prior to cull and performed 16S rRNA gene sequencing to characterise the microbial community and investigate changes that occur in the gut environment before and during tumorigenesis in response to AOM treatment. *N*-numbers are presented in Table 3.1.

We measured the α-diversity by two metrics. These were Shannon diversity, a mathematical measure of the number of species and their relative abundances, and phylogenetic diversity (PD), which measures the total length of the minimum path spanning each node of a cladogram featuring the detected species but does not consider the relative abundance of those species. At Week 8, phylogenetic diversity (PD) was significantly increased in AOM-treated mice (Figure 3.5A; MWU-test $p=0.03$). At Week 12, the Shannon diversity index was significantly decreased in AOM-treated mice relative to PBS controls (Figure 3.5A; MWU-test, $p=0.04$).

When comparing changes within treatments across time, the Shannon α-diversity index rose steadily in PBS-treated mice. AOM-treated mice showed a similar pattern, except for Week 12 in which a decrease in Shannon diversity occurred that was significantly different from each other time-point (Figure 3.5B; Kruskal-Wallis Rank Sum Test followed by pairwise comparisons using the MWU-test, $p<0.05$ after FDR adjustment).

Beta (β)-diversity, on the other hand, is a measure of between-individual diversity in a community. This also differed significantly between treatments. The p-values between AOM- and PBS-treated mice for Weeks 8 to 48 were 0.005, 0.034, 0.012 and 0.004 respectively, corresponding to R^2 values of 0.17, 0.15, 0.19 and 0.24. This suggests a difference due to acute AOM effects at the earliest time-point followed by recovery, before the communities again grow further apart as disease progressed (Figure 3.5C, PERMANOVA of unweighted Unifrac distances, $p<0.05$).

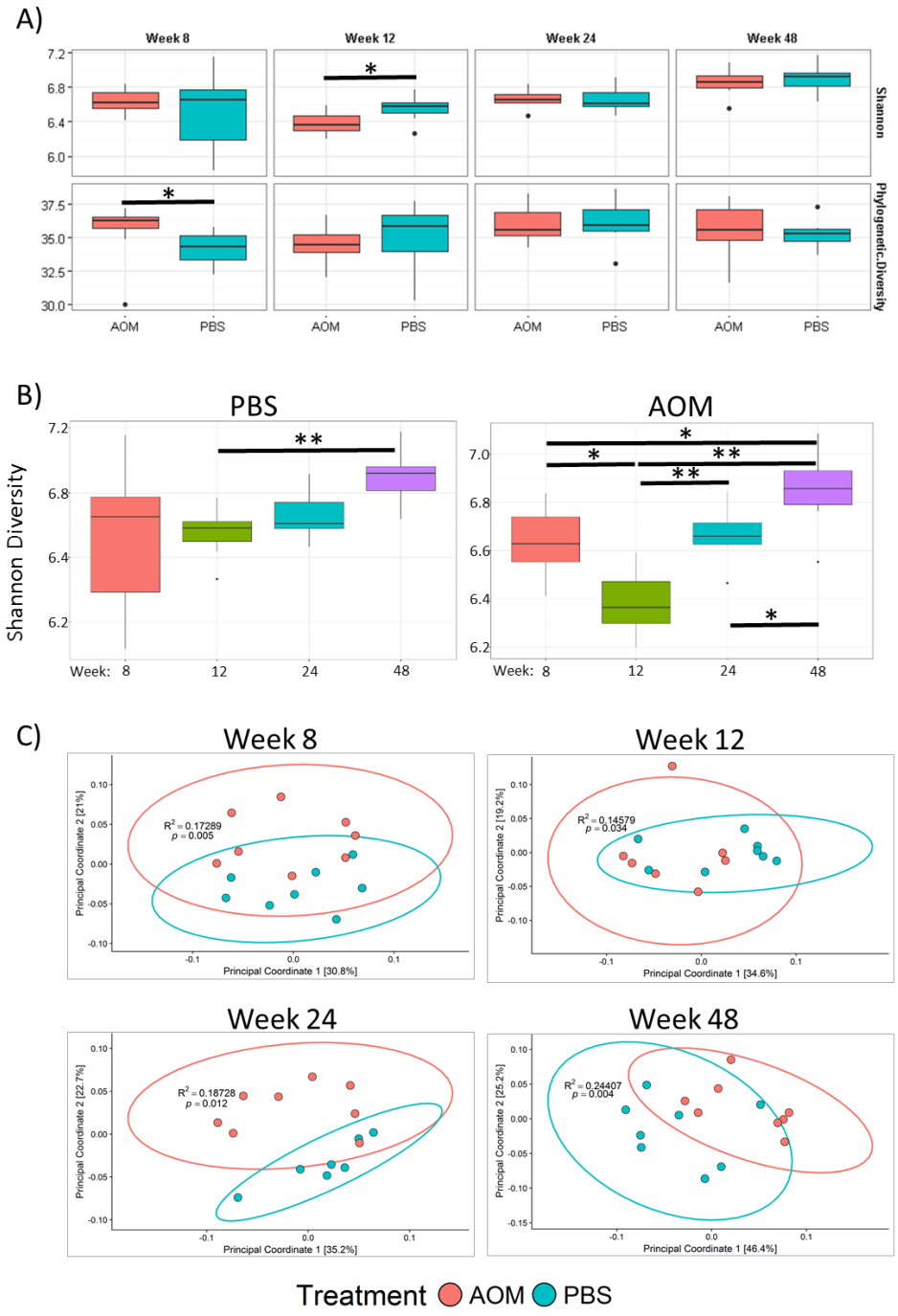

Figure 3.5: Alpha (α)- and beta (β)-diversity are affected in mice administered AOM. Faecal samples were collected throughout the experiment and analysed by 16S rRNA gene sequencing at each dissection to characterise the faecal microbiota. Shannon diversity and phylogenetic diversity were used to interpret the α-diversity while PERMANOVA of unweighted Unifrac distances were used to examine the β-diversity, visualised by principle coordinate analysis. **A)** Phylogenetic diversity was increased in mice administered AOM at Week 8, while Shannon diversity was reduced at Week 12. **B)** Tracking changes in the Shannon diversity across time within each group reveals a significant decrease in the treatment group at Week 12. **C)** We observed a significant difference in the β-diversity between groups at each time-point. *N*=8 per group, except for AOM Week 12 and PBS Week 24 (*N*=7). Figures produced by Calum Walsh at Teagasc, Moorepark.

Next, we considered which individual taxa differed significantly between groups at each time-point. These significantly different taxa are presented in Figure 3.6 (MWU-test with FDR adjustment; $p<0.05$). At Week 8, eleven taxa were significantly decreased in mice treated with AOM and four were significantly increased. The *Turicibacter* genus was noteworthy at this time-point for being decreased 194-fold in mice administered AOM. The communities were more similar at Week 12. *Clostridium sensu stricto 1* and *Ruminococcus 2* were conspicuous for being 27-fold and 47-fold more abundant after AOM treatment at this time-point. *Marvinbryantia* was 40-fold less abundant in mice treated with AOM at Week 24, when twelve species were significantly increased and ten decreased in the cancer model. The microbial gut communities were most dissimilar at Week 48 however, with nine taxa decreased and fourteen increased in mice exposed to AOM. *Prevotellaceae* UCG-001 was 1208-fold more abundant in control mice despite being present in five mice in the treatment group, while *Parasutterella* was 244-fold less abundant in PBS-treated mice. In addition to these, a number of species were present in one treatment group while being absent or virtually absent on the other. In mice treated with AOM, *Prevotellaceae NK3B31 group*, *Clostridium sensu stricto 1, Marvinbryantia, Eubacterium ventriosum group, Citrobacter, Psychrobacter* and *Vibrio* were present in ≤2 mice per group at certain time-points despite being well established in the control group. Moreover, these latter two taxa were significantly increased in PBS-treated mice at each time-point while being virtually absent from the AOM-treatment group. In mice treated with PBS, *Eubacterium ventriosum group*, *Ruminococcus 2, Anaerofilum*, *Prevotellaceae NK3B31 group* and *Citrobacter* were absent or rare. Several species also differ significantly at more than one time-point. As well as *Psychrobacter* and *Vibrio*, *Marvinbryantia* is increased in control mice at Weeks 8, 24 and 48. *Prevotellaceae NK3B31 group* and *Clostridium sensu stricto 1* are increased in control mice at Week 8 but in treatment mice at two later time-points each, while *Eubacterium ventriosum group* is increased in treatment mice at Week 8 and in control mice twice later.

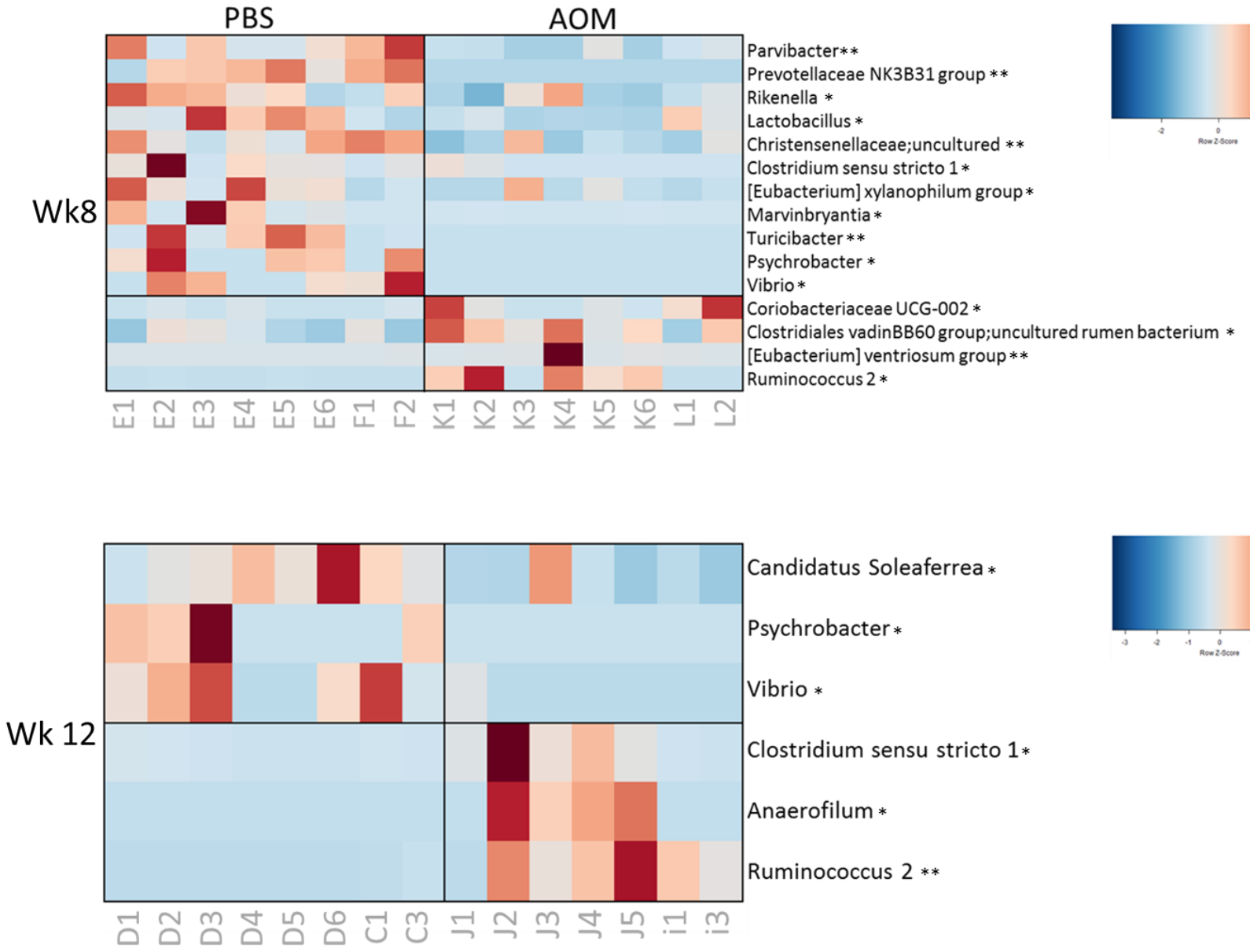
PBS
AOM
Wk8
Parvibacter**
Prevotellaceae NK3B31 group **
Rikenella *
Lactobacillus *
Christensenellaceae;uncultured **
Clostridium sensu stricto 1 *
[Eubacterium] xylanophilum group *
Marvinbryantia *
Turicibacter **
Psychrobacter *
Vibrio *
Coriobacteriaceae UCG-002 *
Clostridiales vadinBB60 group;uncultured rumen bacterium *
[Eubacterium] ventriosum group **
Ruminococcus 2 *
E1 E2 E3 E4 E5 E6 F1 F2 K1 K2 K3 K4 K5 K6 L1 L2
Row Z-Score
Wk 12
Candidatus Soleaferrea *
Psychrobacter *
Vibrio *
Clostridium sensu stricto 1 *
Anaerofilum *
Ruminococcus 2 **
D1 D2 D3 D4 D5 D6 C1 C3 J1 J2 J3 J4 J5 i1 i3
Row Z-Score

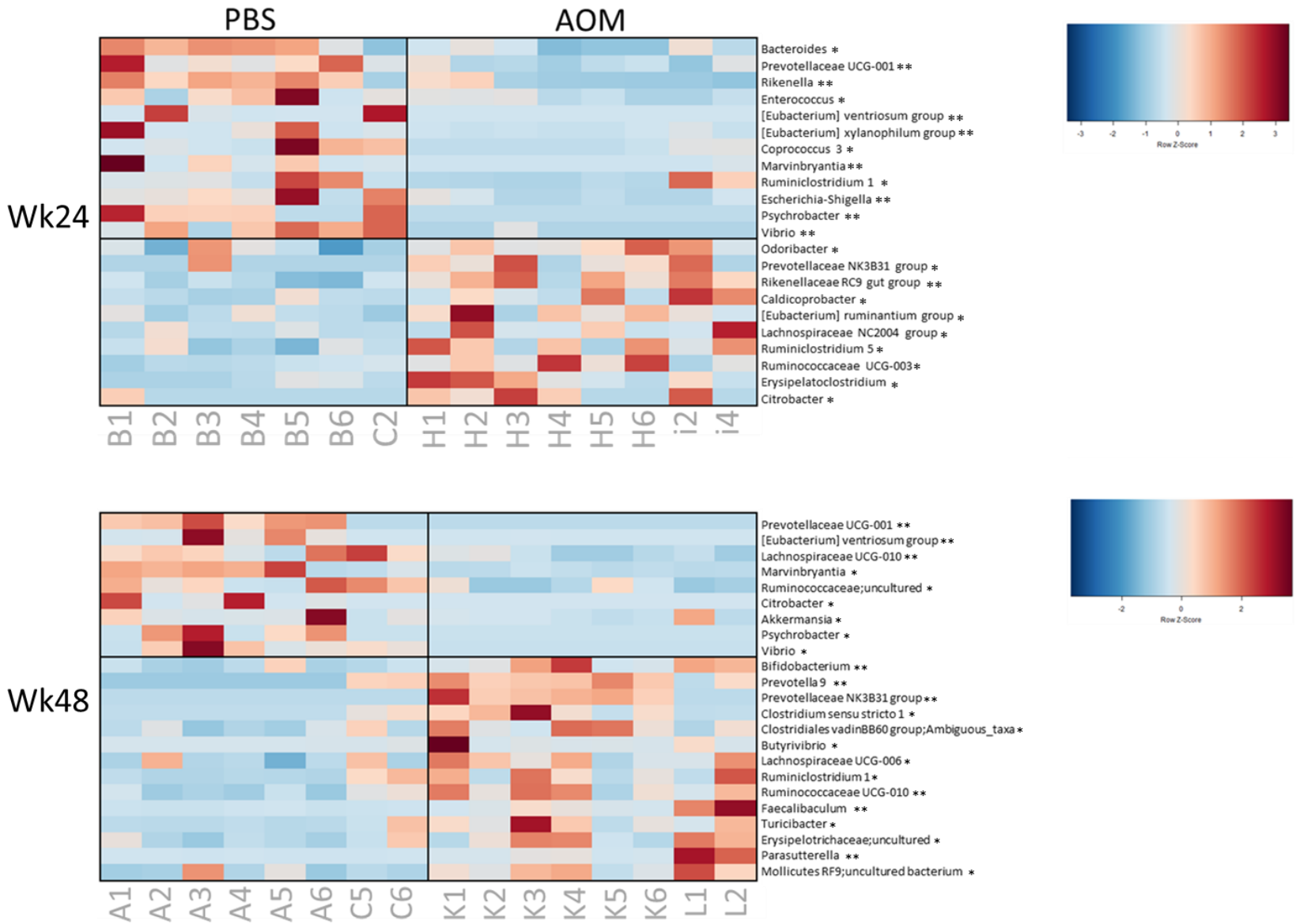
PBS
AOM
Wk24
Bacteroides *
Prevotellaceae UCG-001 **
Rikenella **
Enterococcus *
[Eubacterium] ventriosum group **
[Eubacterium] xylanophilum group **
Coprococcus 3 *
Marvinbryantia **
Ruminiclostridium 1 *
Escherichia-Shigella **
Psychrobacter **
Vibrio **
Odoribacter *
Prevotellaceae NK3B31 group *
Rikenellaceae RC9 gut group **
Caldicoprobacter *
[Eubacterium] ruminantium group *
Lachnospiraceae NC2004 group *
Ruminiclostridium 5 *
Ruminococcaceae UCG-003 *
Erysipelatoclostridium *
Citrobacter *
B1 B2 B3 B4 B5 B6 C2 H1 H2 H3 H4 H5 H6 i2 i4
-3 -2 -1 0 1 2 3
Row Z-Score
Wk48
Prevotellaceae UCG-001 **
[Eubacterium] ventriosum group **
Lachnospiraceae UCG-010 **
Marvinbryantia *
Ruminococcaceae;uncultured *
Citrobacter *
Akkermansia *
Psychrobacter *
Vibrio *
Bifidobacterium **
Prevotella 9 **
Prevotellaceae NK3B31 group **
Clostridium sensu stricto 1 *
Clostridiales vadinBB60 group;Ambiguous_taxa *
Butyrivibrio *
Lachnospiraceae UCG-006 *
Ruminiclostridium 1 *
Ruminococcaceae UCG-010 **
Faecalibaculum **
Turicibacter *
Erysipelotrichaceae;uncultured *
Parasutterella **
Mollicutes RF9;uncultured bacterium *
A1 A2 A3 A4 A5 A6 C5 C6 K1 K2 K3 K4 K5 K6 L1 L2
-2 0 2
Row Z-Score

Figure 3.6: Taxa which differ significantly in their abundance between groups. From the data acquired by 16S rRNA gene sequencing of the faecal microbiota, operational taxonomic units were clustered based on 97% sequence similarity taxonomy was assigned using BLAST against the SILVA SSURef database. Statistically significant differences in abundances of individual taxa between groups were determined using the Mann-Whitney U-test with FDR correction for multiple comparisons. Only significantly different taxa are presented here. Taxa in the top of each section are suppressed in mice administered AOM, while species in the bottom are enriched. Data are presented as the z-scores of the abundances scaled by row. N=8 per group, except for AOM Week 12 and PBS Week 24 (N=7).

Eubacterium xylanophilum group, *Prevotellaceae UCG-001* and *Rikenella* are decreased in control mice at two time-points, while *Ruminococcus 2* is increased in mice administered AOM twice. *Citrobacter, Ruminiclostridium 1* and *Turicibacter* also feature twice, but for a different treatment group each time.

In order to investigate the alterations in the gut bacteria at a higher structural level, we defined a set of bacterial co-abundance groups (CAGs) (Figure 3.7A). PERMANOVA determined that all CAGs were significantly different (Figure 3.7B, $p<0.05$). The taxon composition of each CAG can be found in Table 3.2.

Seven CAGs were identified, labelled CAG1-7. CAG1 was increased in AOM-treated mice at Week 24 (T-test, $p=0.032$). CAG2 was increased in AOM-treated mice at Week 48 (MWU-test, $p<0.001$) while CAG7 was decreased (T-test, $p<0.001$). There were no significant differences between CAGs in PBS- and AOM- treated groups at Weeks 8 or 12. CAG1 is dominated by the *Rikenellaceae* family which comprise >80% of the abundance of this CAG. *Turicibacter* and *Ruminococcus 1* make up over half of CAG2 with *Bifidobacterium* and an uncultured *Erysipelotrichaceae* adding another 22.5%. An uncultured bacterium from the *Ruminococcaceae* family makes up 84% of CAG7.

3.2.6 Bile acids are altered in AOM-treated mice

In order to investigate the potential role of bile acid modification in our mouse model, we analysed the faecal and plasma bile acid profile of the mice by UPLC-MS. PBS-treated mice had a higher total faecal bile acid content than AOM-treated mice at Weeks 8 and 12 (Figure 3.8; T-test, $p<0.01$) and as a result, PBS-treated mice had significantly higher volumes of many bile acids while there were no bile acids increased in AOM-treated mice. We therefore compared the fraction that each bile acid made up of the total bile acid volume. The

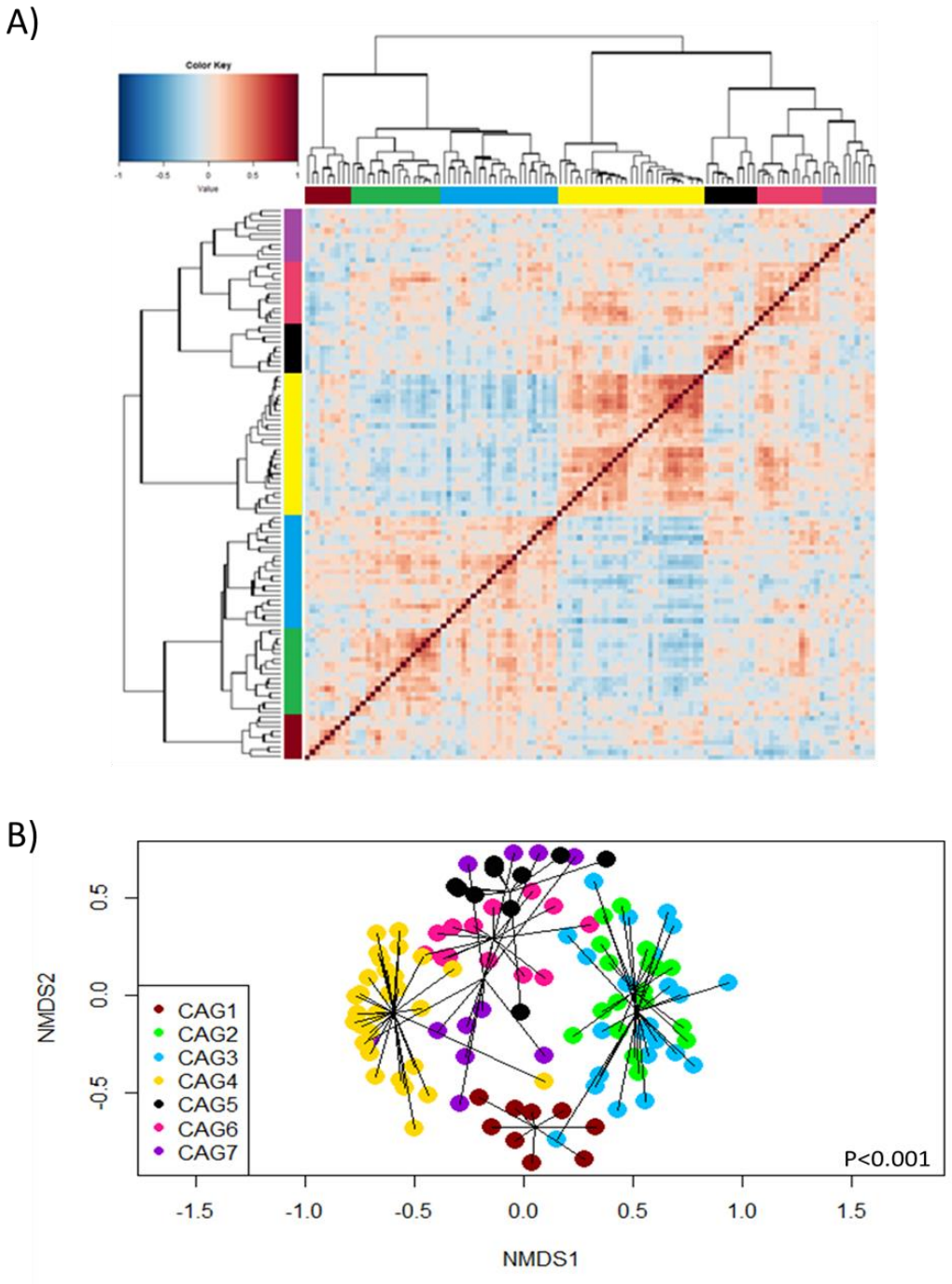

Figure 3.7: Generation of co-abundance groups. The Kendall correlations of OTUs' relative abundances were generated for all 62 mice in the study and clustered by Ward-linkage and Pearson correlation. This defines "co-abundance groups" (CAGs) which describe higher-level structures of the microbiota by highlighting taxa for which changes in abundance correlate. These Kendall correlations were then converted to a distance metric and analysed by PERMANOVA which determined that each CAG was significantly different. Colours represent Pearson's correlation coefficient between pairs of taxa. **A)** A heatplot of Kendall correlation values for each pair of taxa clustered by Ward linkage of their Pearson correlations. Coloured bars along the axes denote the CAGs. The composition if each CAG is presented in Table 3.2. **B)** Non-metric multidimensional scaling (NMDS) of the distance metrics of the CAGs' correlation values.

Table 3.2: The composition of each CAG

CAG1	Prevotella 9
	Alistipes
	Rikenellaceae RC9 gut group
	Ruminococcus 2
	Coprococcus 3
	Papillibacter
	Butyrivibrio
	[Eubacterium] ruminatum group
	Uncultured Firmicutes bacterium
CAG2	Prevotellaceae NK3B31 group
	Lachnospiraceae NC2004 group
	[Eubacterium] coprostanoligenes group
	Clostridium sensu stricto 1
	Turicibacter
	Natranaerovirga
	Streptococcus
	Parasutterella
	Coriobacteriaceae;uncultured
	Clostridiales Family XIII AD3011 group
	Ruminiclostridium 1
	Ruminococcaceae UCG-010
	Coriobacteriaceae UCG-002
	Faecalibaculum
	Bifidobacterium
	Erysipelotrichaceae;uncultured
	Caldicoprobacter
	Ruminococcus 1
CAG3	Anaerobacillus
	Bacteroidales S24-7 group;uncultured bacterium
	Delftia
	Akkermansia
	Christensenellaceae R-7 group
	[Eubacterium] nodatum group
	Chloroplast;uncultured bacterium
	Bacilli;Ambiguous_taxa
	Candidatus Arthromitus
	Bacteroidales S24-7 group;Ambiguous_taxa
	Erysipelatoclostridium
	Mollicutes RF9;uncultured rumen bacterium
	Mollicutes RF9;Ambiguous_taxa
	Ruminococcaceae UCG-014
	Mollicutes RF9;uncultured bacterium
	Anaerofustis
	Ochrobactrum
	Enterococcus
	Lactobacillus
	Candidatus Saccharimonas
	Bacteroides
	Parabacteroides
	Rhodospirillaceae;uncultured

CAG4	Odoribacter
	Ruminiclostridium 6
	Candidatus Soleaferrea
	Mucispirillum
	Lachnospiraceae;uncultured
	Blautia
	Tyzzerella 3
	Anaerovorax
	Ruminiclostridium 5
	Anaerotruncus
	Butyricicoccus
	Clostridiales Family XIII UCG-001
	Peptococcus
	Peptococcaceae;uncultured
	Lachnospiraceae UCG-008
	Faecalibacterium
	Eisenbergiella
	Ruminococcaceae NK4A214 group
	Ruminococcaceae UCG-005
	Lachnospiraceae;uncultured bacterium
	Tyzzerella
	Intestinimonas
	Ruminiclostridium
	Oscillibacter
	Ruminococcaceae UCG-003
	Bilophila
	Ruminococcaceae UCG-009
	Ruminiclostridium 9
	Christensenellaceae;uncultured
CAG5	Rikenella
	Anaeroplasma
	Porphyromonadaceae;uncultured
	Clostridiales vadinBB60 group;uncultured bacterium
	Clostridiales vadinBB60 group;Ambiguous_taxa
	Lachnospiraceae UCG-006
	Gastranaerophilales;uncultured bacterium
	Clostridiales vadinBB60 group;uncultured rumen bacterium
	Hydrogenoanaerobacterium
	Citrobacter
CAG6	Lachnospiraceae UCG-001
	Coprococcus 1
	Lachnospiraceae NK4A136 group
	Roseburia
	[Eubacterium] brachy group
	Lachnoclostridium
	Lachnospiraceae FCS020 group
	Acetitomaculum
	Escherichia-Shigella
	Enterorhabdus
	Parvibacter
	Marvinbryantia
	[Eubacterium] xylanophilum group
CAG7	[Eubacterium] ventriosum group
	Prevotellaceae UCG-001
	Psychrobacter
	Vibrio
	Ruminococcaceae;uncultured
	Ruminococcaceae UCG-013
	Syntrophococcus
	Desulfovibrio
	Bacillus
	Senegalimassilia
	Lachnospiraceae UCG-010

significantly different values are presented in Figures 3.9 to 3.12. The list of bile acids measured are available in Table 3.3.

The proportion of hydrophobic bile acids DCA and LCA were decreased in the faeces of AOM-treated mice at Week 8, with DCA still reduced at Week 12. The proportions of five conjugated faecal bile acids were increased at Week 8 including T-HCA, which was still significantly higher than control at Week 12, along with UDCA and DHCA (Figures 3.9 and 3.10; T-test and MWU-test, $p<0.05$). The concentration of five bile acids are increased in the plasma of mice treated with AOM at Week 12, including the potent FXR antagonist T-α/β/ω-MCA (Figure 3.10; T-test and MWU-test, $p<0.05$). The specific isomer of this bile acid could not be determined by UPLC-MS. The absolute concentrations of twelve faecal bile acid species were increased in AOM-treated mice at Week 24, of which HDCA and β-MCA were the most abundant, while LCA and G-LCA were reduced (Figure 3.11; T-test and MWU-test, $p<0.05$). In the plasma at Week 24, T-α/β/ω-MCA remains increased in AOM-treated mice along with six other bile acids (Figure 3.11; T-test and MWU-test, $p<0.05$). The absolute concentration of only four faecal bile acids differed at Week 48; CA, G-CDCA and G-LCA were decreased in AOM-treated mice, and G-HDCA was increased, while G-LCA was also decreased in the plasma (Figure 3.12; T-test and MWU-test, $p<0.05$).

3.2.7 Correlation analysis reveals relationships between gut bacteria and bile acid composition

A correlation analysis was performed to determine the relationships between the cytokine and chemokine transcription, α-diversity scores and CAG abundances, and each of those variables' relationships with absolute and normalised faecal and plasma bile acid concentrations.

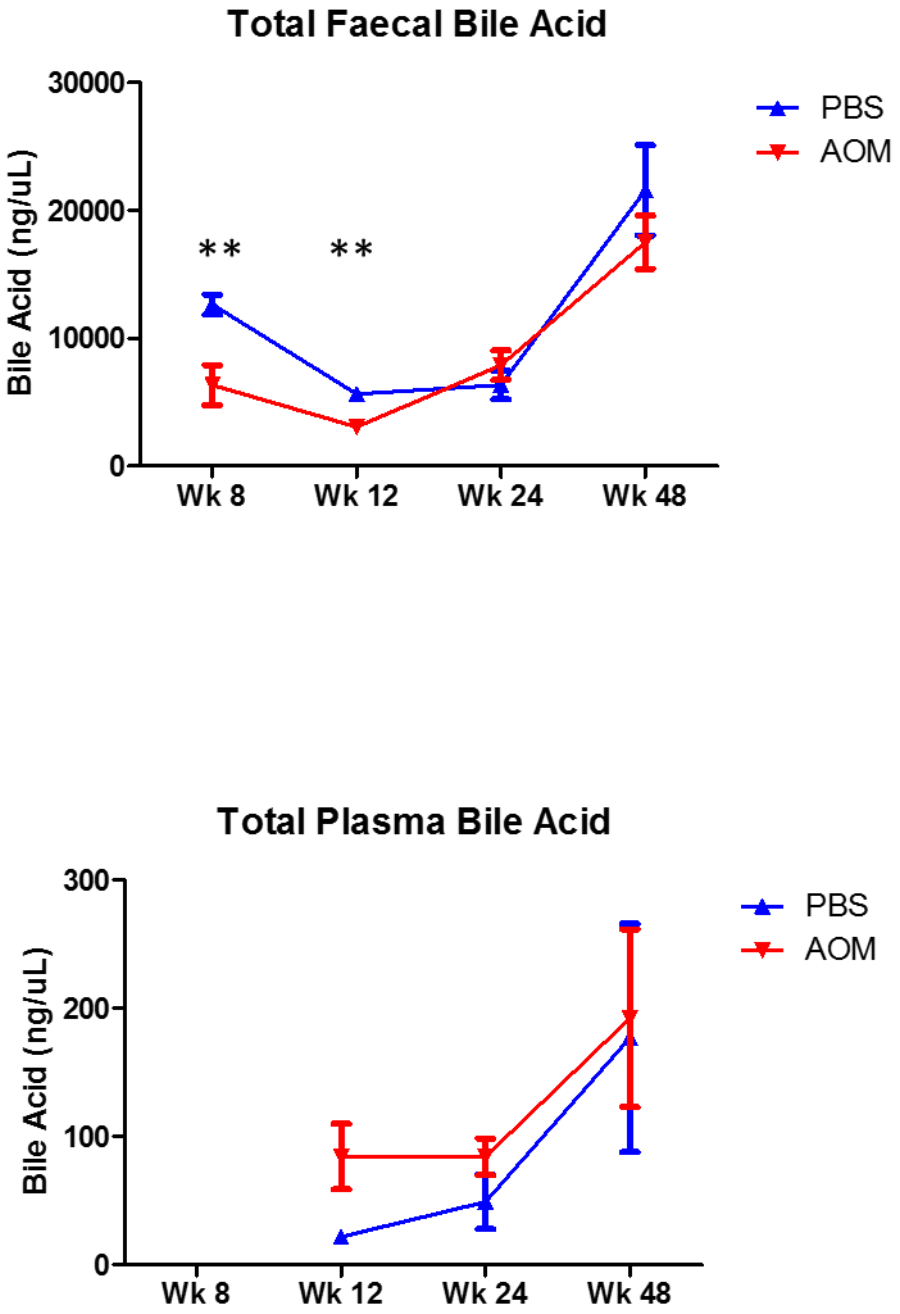

Figure 3.8: Total bile acid concentration is reduced in the faeces of mice administered AOM. Bile acids were determined by UPLC-MS at each dissection. **A)** The total faecal bile acid concentration was significantly reduced at Week 8 and Week 12 in mice administered AOM. **B)** No significant differences in plasma bile acids were detected, although a trend towards lower concentration was observed at Week 12 (P=0.058). Graphs present the mean and SEM. *N*-numbers for PBS and AOM faecal bile acids at Week 8 are 7 and 7; at Week 12 are 7 and 6; at Week 24 are 6 and 6; at Week 48 are 7 and 6. *N*-numbers for PBS and AOM plasma bile acids at Week 12 are 5 and 6; at Week 24 are 5 and 7; at Week 48 are 6 and 7.

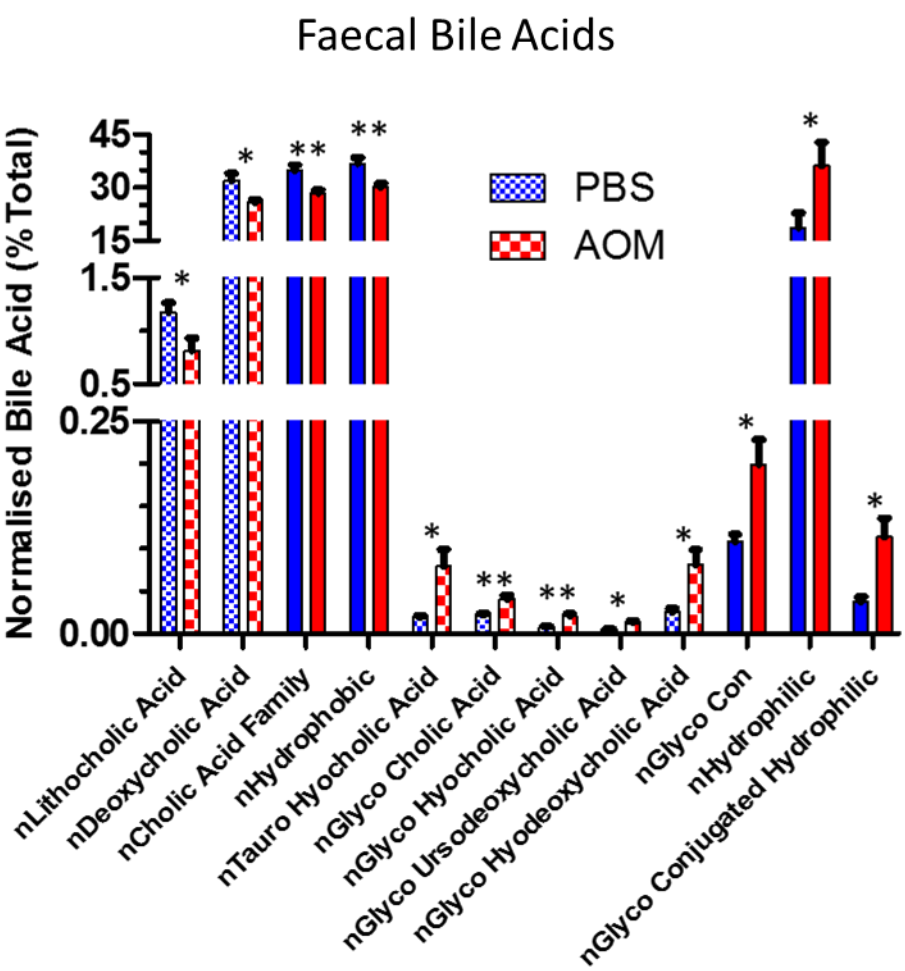

Figure 3.9: Normalised faecal bile acids which differed significantly between groups at Week 8. Faecal bile acids were determined by UPLC-MS at each dissection. Since total faecal bile acid concentration differed significantly between groups at this time-point, we analysed the proportion each bile acid made up of the total faecal bile acid content to unmask treatment effects. Graphs present the mean and SEM. Individual bile acids are represented by chequered bars and families are presented by solid bars. *N*=7 for both groups.

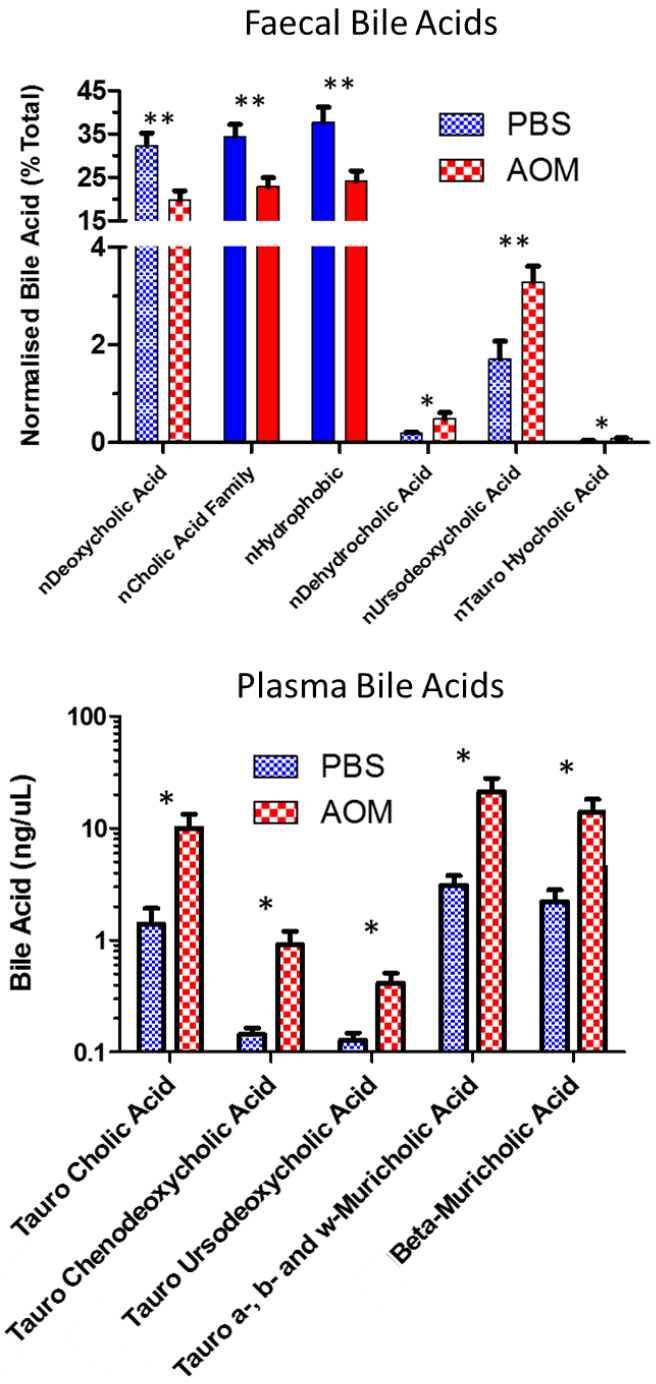

Figure 3.10: Faecal and plasma bile acids which differed significantly between groups at Week 12. Bile acids were determined by UPLC-MS at each dissection. Since total faecal bile acid concentration differed significantly between groups at this time-point, we analysed the proportion each bile acid made up of the total faecal bile acid content to unmask treatment effects. Plasma bile acids are presented as absolute values. Graphs present the mean and SEM. Individual bile acids are represented by chequered bars and families are presented by solid bars. Faecal *n*-numbers for PBS- and AOM-treated mice are 7 and 6, and plasma *n*-numbers are 5 and 6, respectively.

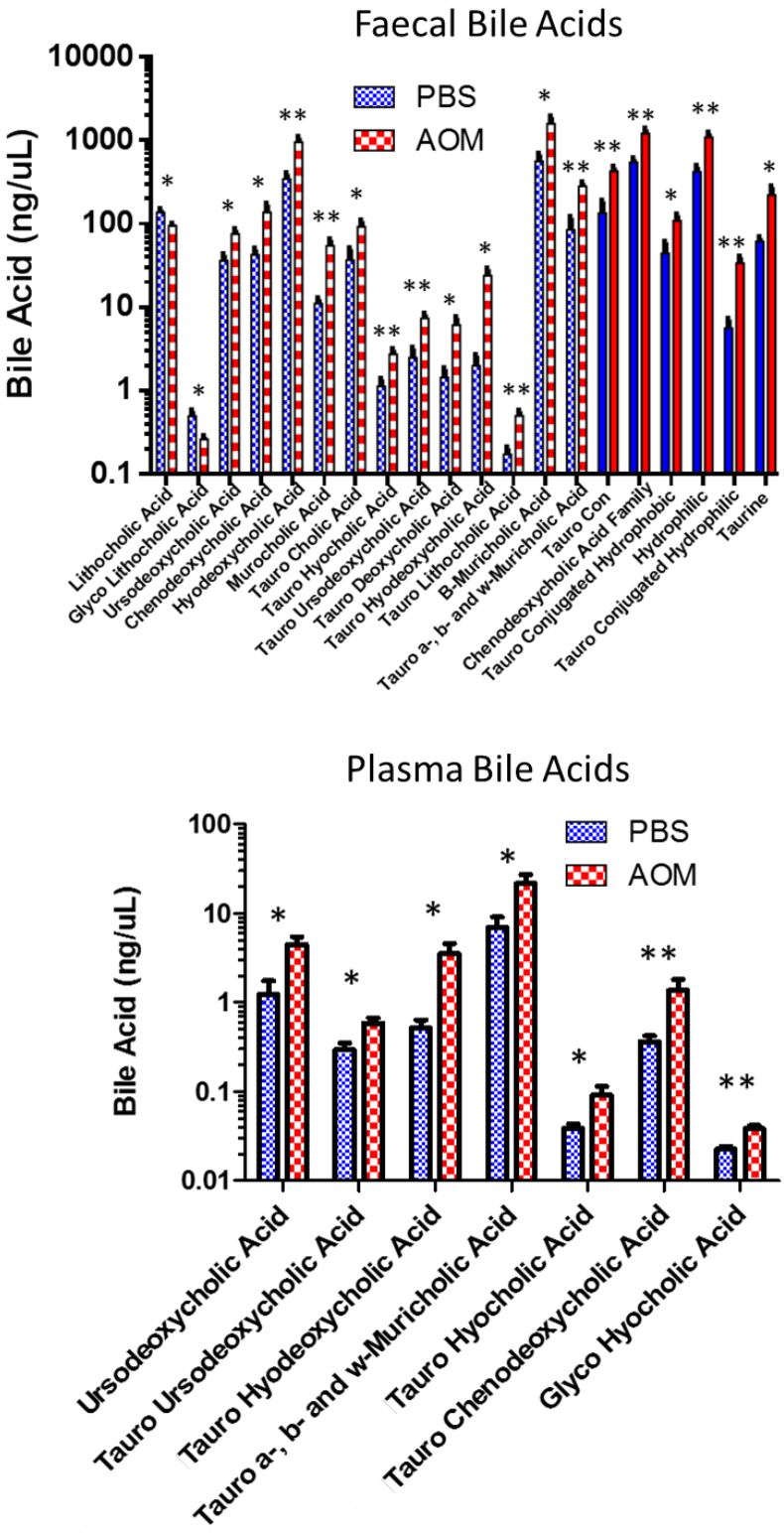

Figure 3.11: Faecal and plasma bile acids which differed significantly between groups at Week 24. Bile acids were determined by UPLC-MS at each dissection. Graphs present the mean and SEM. Individual bile acids are represented by chequered bars and families are presented by solid bars. Faecal *n*-numbers for PBS- and AOM-treated mice are 6 and 6, and plasma *n*-numbers are 5 and 7, respectively.

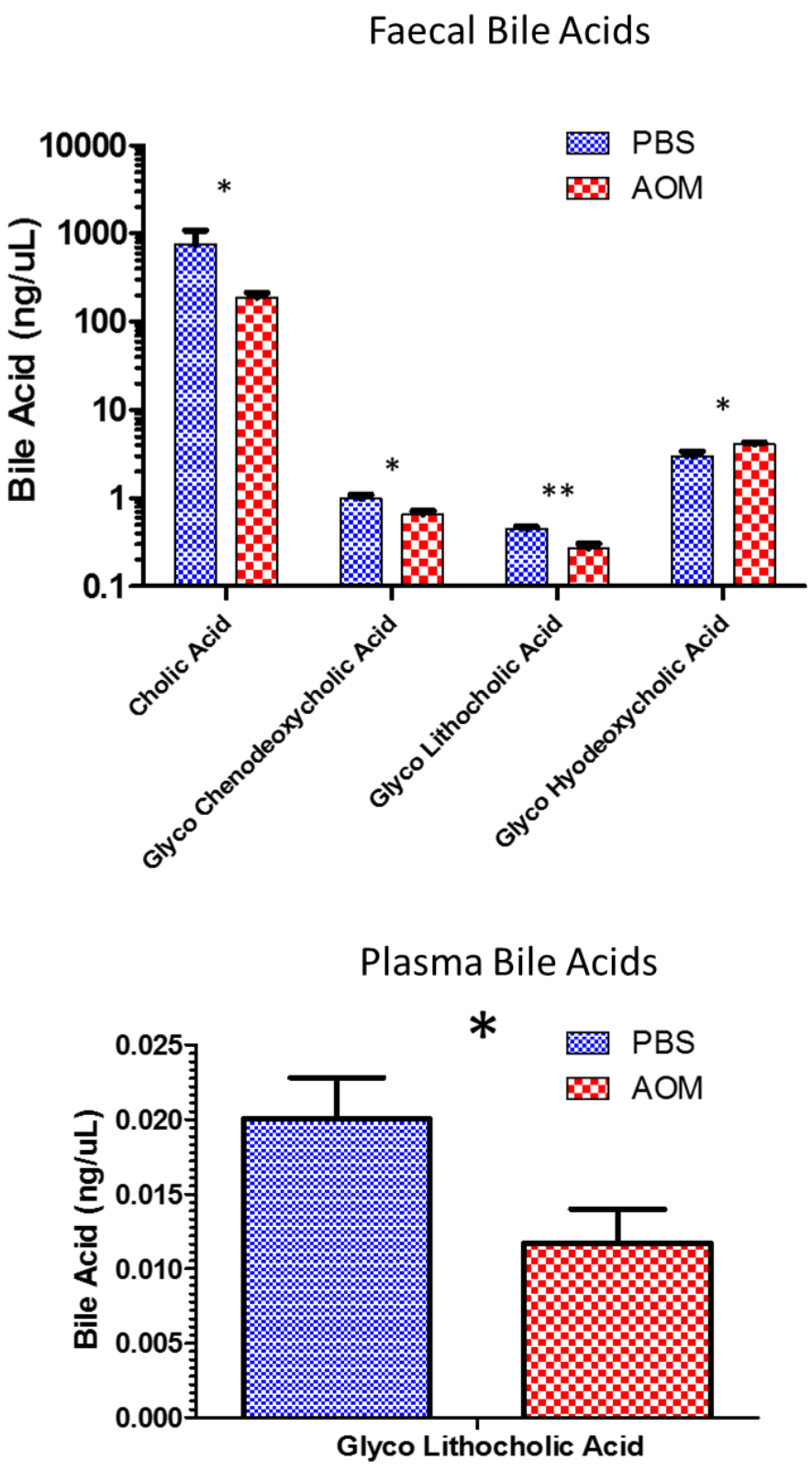

Figure 3.12: Faecal and plasma bile acids which differed significantly between groups at Week 48. Bile acids were determined by UPLC-MS at each dissection. Graphs present the mean and SEM. Faecal *n*-numbers for PBS- and AOM-treated mice are 7 and 6, and plasma *n*-numbers are 6 and 7, respectively.

Table 3.3: Bile acids measured

	Bile Acid	Abbreviation
Individual Bile Acids	Dehydrocholic Acid	DHCA
	Lithocholic Acid	LCA
	Ursodeoxycholic Acid	UDCA
	Chenodeoxycholic Acid	CDCA
	Hyodeoxycholic Acid	HDCA
	Deoxycholic Acid	DCA
	Cholic Acid	CA
	Hyocholic Acid	HCA
	7-Ketolithocholic Acid	7-Keto-LCA
	Tauro-Cholic Acid	T-CA
	Tauro-Hyocholic Acid	T-HCA
	Tauro-Chenodeoxycholic Acid	T-CDCA
	Tauro-Ursodeoxycholic Acid	T-UDCA
	Tauro-Deoxycholic Acid	T-DCA
	Tauro-Hyodeoxycholic Acid	T-HDCA
	Tauro-Lithocholic Acid	T-LCA
	Glyco-Cholic Acid	G-CA
	Glyco-Hyocholic Acid	G-HCA
	Glyco-Chenodeoxycholic Acid	G-CDCA
	Glyco-Ursodeoxycholic Acid	G-UDCA
	Glyco-Deoxycholic Acid	G-DCA
	Glyco-Hyodeoxycholic Acid	G-HDCA
	Glyco-Lithocholic Acid	G-LCA
	Alpha/Gamma (α/ω)-Muricholic Acid	α/ω-MCA
	Beta (β)-Muricholic Acid	β-MCA
	Murocholic Acid	MoCA
	Tauro α-, β-, and ω-Muricholic Acid	T-α/β/ω-MCA
Bile Acid Families	Total Bile Acid Content	Total BAs
	Muricholic Acids	MCAs
	Tauro-Conjugated Bile Acids	T-con BAs
	Glyco-Conjugated Bile Acids	G-con BAs
	Primary Bile Acids	1° BAs
	Secondary Bile Acids	2° BAs
	Free Bile Acids	Free BAs
	Cholic Acid Family	CA family
	Chenodeoxycholic Acid Family	CDCA family
	Hydrophobic Bile Acids	Hydrophobic BAs
	Tauro-Conjugated Hydrophobic	T-Con Hydrophobic
	Glyco-Conjugated Hydrophobic	G-Con Hydrophobic
	Hydrophilic Bile Acids	Hydrophilic BAs
	Tauro-Conjugated Hydrophilic	G-Con Hydrophilic
	Glyco-Conjugated Hydrophilic	G-Con Hydrophilic
	Taurine	
	Deuterated Cholic Acid	CA-d4
	Deuterated Chenodeoxycholic Acid	CDCA-d4

PD correlated positively with *Il6*, *Cxcl1*, *Cxcl5* and *Il12* in AOM-treated mice at Week 8 (Figure 3.13A; Pearson and Spearman correlation, $p<0.05$ after FDR adjustment), suggesting a relationship between pro-inflammatory cytokine transcription and α-diversity. PD also correlated positively with CAGs 2 and 3, and negatively with CAGs 4 and 7, while the correlations with these CAGs were reversed for Shannon diversity (Figure 3.13B; Pearson and Spearman correlation, $p<0.05$ after FDR adjustment). PD also correlated positively with the absolute concentration of nine bile acids and taurine at Week 8 (Figure 3.13C; Pearson and Spearman correlation, $p<0.05$). In contrast, PD correlated negatively with the relative proportions of ten bile acids, but positively with ω/α-MCA at Week 8 (Figure 3.13D; Pearson and Spearman correlation, $p<0.05$).

This pattern of contrasting correlations is reflected in the relationship between absolute and normalised bile acids and CAGs. CAGs 2 and 3 display positive correlations with the absolute concentration of a number of bile acids, while bile acid correlations with CAGs 4 and 7 are exclusively negative (Figure 3.14A; Pearson and Spearman correlation, $p<0.05$). Comparing CAGs to normalised bile acids revealed the opposite pattern, except for the correlation between CAGs and MCAs which match across both analyses (Figure 3.14B; Pearson and Spearman correlation, $p<0.05$).

After Week 8, there were no significant correlations between faecal bile acids and α-diversity after FDR adjustment in mice treated with PBS or AOM. Only one negative correlation between CAG7 and dehydrocholic acid (DHCA) was found in PBS-treated mice at Week 12 (Figure 3.15). DHCA is the lowest abundance free bile acid found in these mice, comprising 0.2% of the total BA content. CAG3 correlates positively with Shannon diversity while CAGs 4 and 6 correlate negatively in PBS-treated mice at Week 8, although there were no conflicting correlations in any CAG between Shannon and PD as we saw in mice treated with AOM at Week 8. CAG4 also correlated positively with PD in PBS-treated mice at Week 24

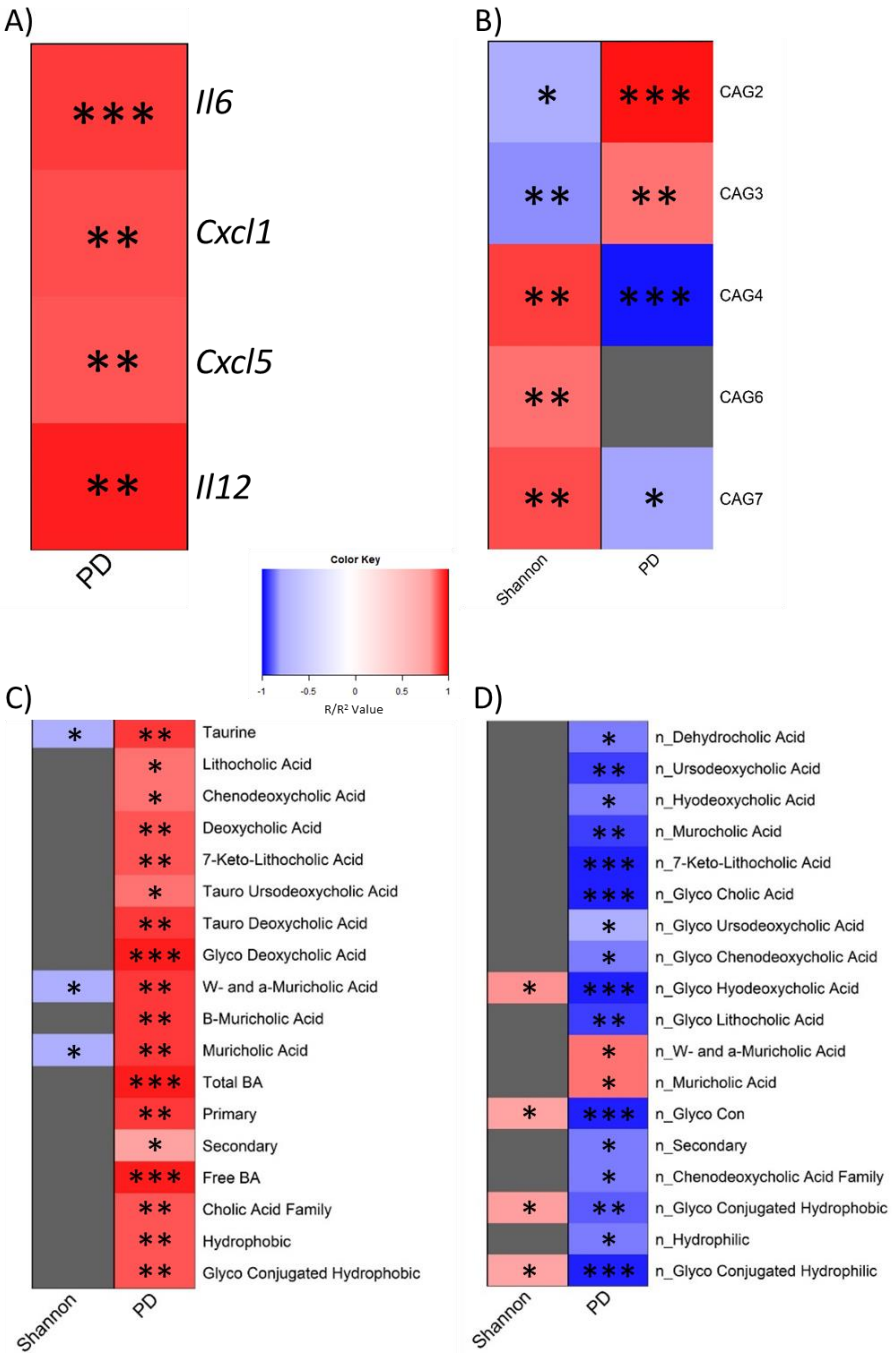

Figure 3.13: Correlations between α-diversity, inflammation, CAGs and bile acids at Week 8. A correlation analysis was performed to examine relationships between α-diversity, inflammation, CAGs and bile acids at Week 8. **A)** Phylogenetic diversity (PD) correlated with a number of pro-inflammatory cytokines. **B)** Shannon diversity and PD showed opposite patterns of correlations with different CAGs 2/3 and 4/7. **C)** A correlation analysis of our α-diversity indices and absolute faecal bile acid values revealed a positive relationship between phylogenetic diversity (PD) and a number of bile acids including the total faecal bile acid concentration. **D)** In order to identify any relationship which exist between PD and faecal bile acids, independent of total bile acid concentration, a correlation analysis was performed between our α-diversity metrics and normalised (n_) faecal bile acids which revealed a negative association with a number of bile acids and a positive relationship between ω/α-Muricholic Acid (MCA) and the MCA family.

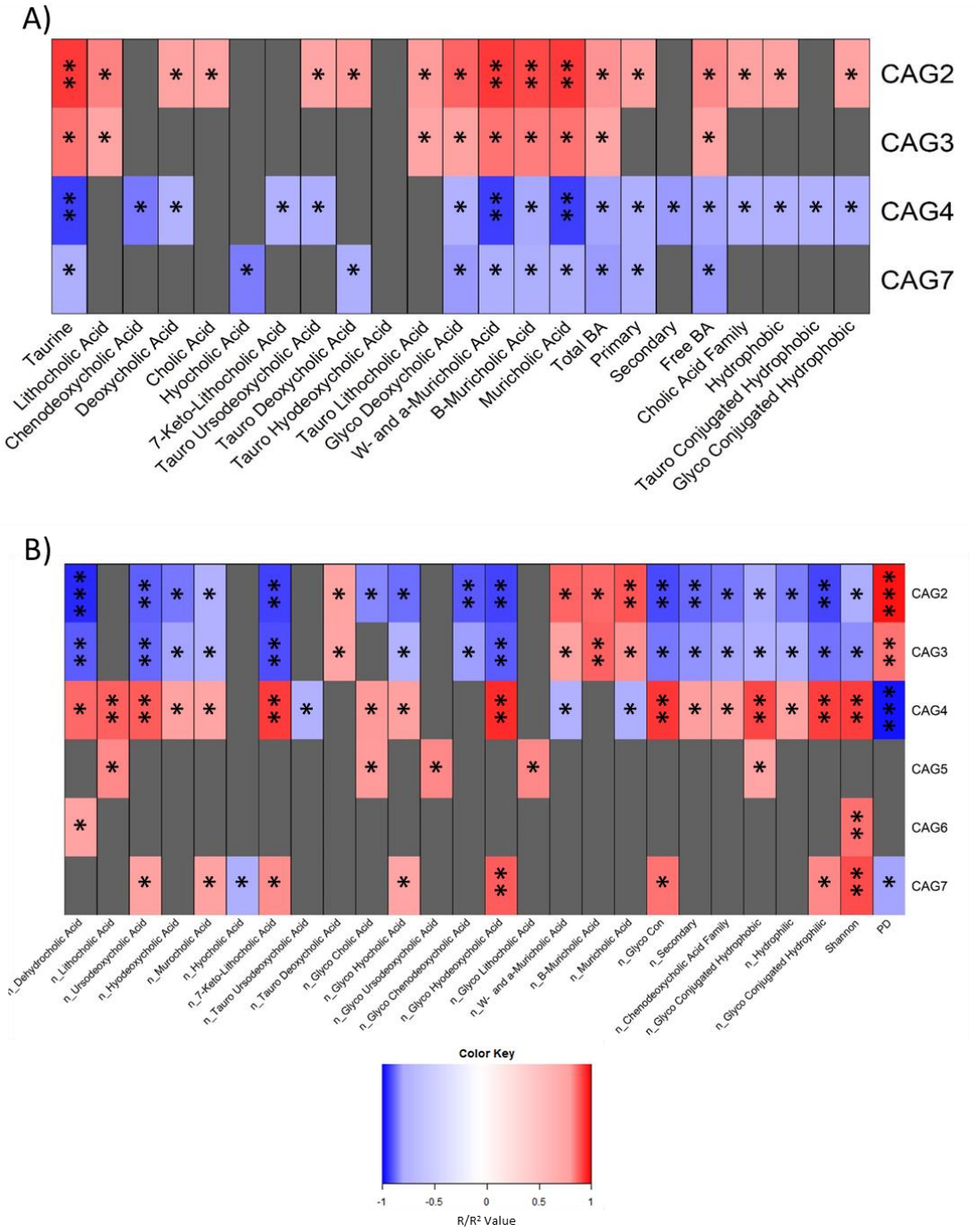

Figure 3.14: Correlations between CAGs and bile acids at Week 8. Bile acids displayed a number of correlations with α-diversity at Week 8. In order to investigate which groups of bacteria may be involved in this effect, a correlation analysis was performed to examine the relationship between absolute and normalised bile acids and CAGs. **A)** CAGs 2 and 3 display positive correlations with a number of bile acids, while bile acid correlations with CAGs 4 and 7 are exclusively negative. **B)** Comparing CAGs to normalised (n_) bile acids revealed the opposite pattern, except for the correlation between CAGs and MCAs.

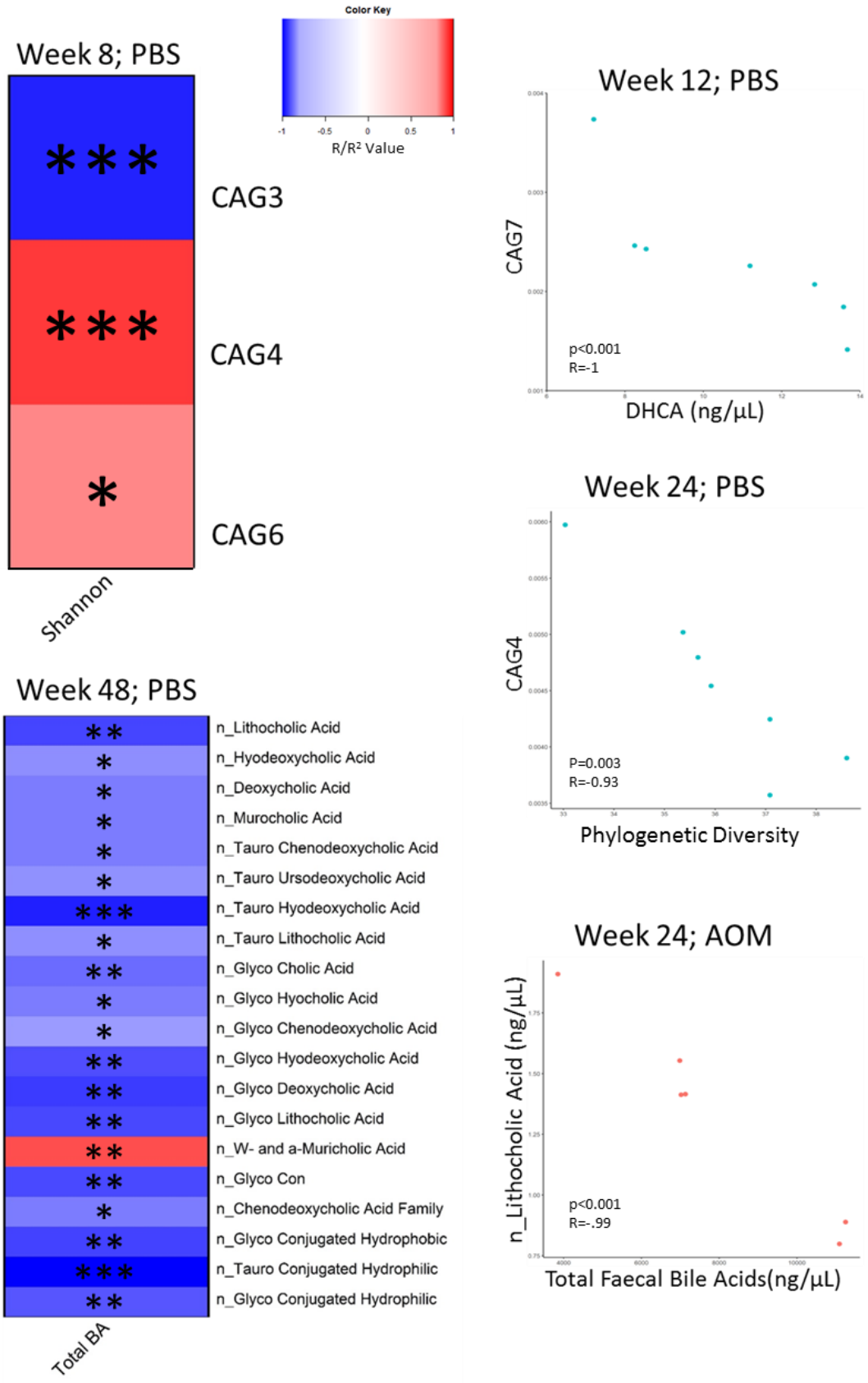

Figure 3.15: Other correlations. Outside of AOM-treated mice at Week 8, the set of significant correlations after correction for multiple comparisons do not present a consistent picture of cancer-associated phenomena (Pearson's R and Spearman's R^2, $p<0.05$ after FDR correction).

(Figure 3.15). At Week 48, a large number of normalised bile acids correlated negatively with total faecal bile acid content, including DCA and HDCA, while normalised ω- and α-MCA correlated positively (Figure 3.15).

3.2.8 Neither the inferred functional diversity nor the bile acid-metabolising capacity of the microbiota predicted by PICRUSt differ between treatments

In order to investigate the metabolic capacity of the microbiota and elucidate its potential contribution to disease, we examined the inferred microbial functional content predicted by PICRUSt. This revealed no significant difference in the α- or β-diversities of the inferred functional content between treatments (Figure 3.16; MWU-test and PERMANOVA, $p>0.05$).

Furthermore, we compared the predicted abundances of microbial gene *bsh* (COG3049) and gene cluster *baiCD* (COG1902), which are involved in the deconjugation and 7α-dehydroxylation of bile acids, respectively. The abundances of these genes did not differ significantly between groups at any time-point (Figure 3.17; MWU-test, $p>0.05$ after FDR adjustment).

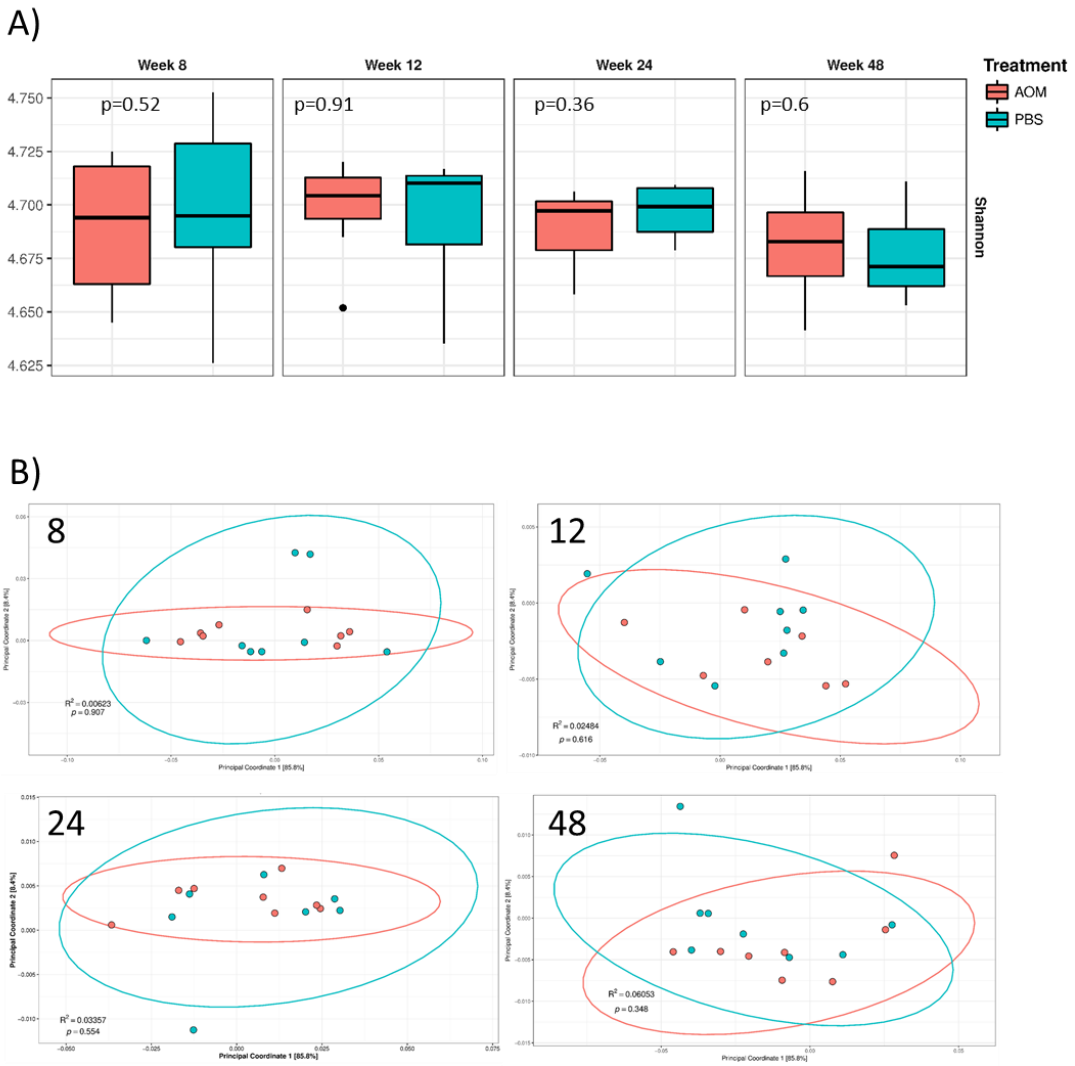

Figure 3.16: PICRUSt α- and β-diversity. A) The Shannon α-diversity of the metagenome predicted by PICRUSt does not differ between treatments at any time-point (MWU-test, p>0.05 after FDR adjustment). **B)** The β-diversity of the metagenome predicted by PICRUSt does not differ between treatments at any time-point (PERMANOVA of unweighted Unifrac distances, p>0.05). *N*=8 per group, except for AOM Week 12 and PBS Week 24 (*N*=7). Figures produced by Calum Walsh at Teagasc, Moorepark.

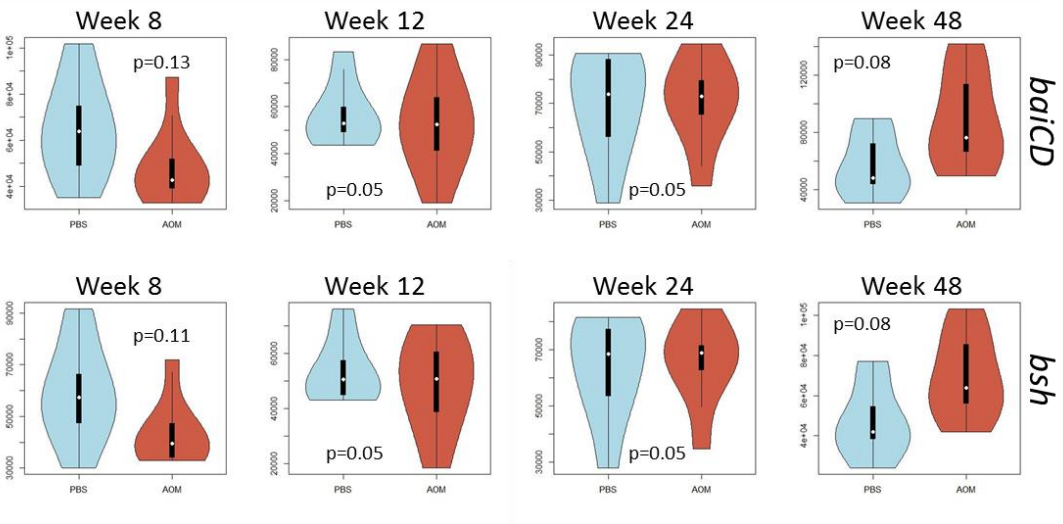

Figure 3.17: Abundance of bile acid-metabolising genes *baiCD* and *bsh* are not significantly different between treatments at any time-point. The microbial genes *baiCD* (COG1902) and *bsh* (COG3049) are involved in the 7α-dehydroxylation and deconjugation of bile acids, respectively. We examined the abundance of these genes predicted by PICRUSt from our 16S rRNA gene sequencing data and found that they did not differ significantly between groups at any time-point (MWU-test, p>0.05 after FDR adjustment). *N*=8 per group, except for AOM Week 12 and PBS Week 24 (*N*=7).

3.3 Discussion

Research shows that the microbiota is altered in human CRC, but the degree to which the host affects the microbiota and the microbiota alters the host is unclear (36). It is possible that alterations in the gut microbiota can promote or inhibit the development of colon cancer, and evidence for this has been provided by animal studies (2, 3). However, it is also possible that tumorigenesis occurs primarily as a result of alterations in the host independent of the microbiota. Similarly, after cancer initiation, components of the microbiota may suppress or promote growth, invasion and metastasis but human evidence for this is lacking (37). Human CRC pathogenesis is a process that takes place over decades. This makes it difficult to track the microbiota in a sufficiently large cohort and impossible to combine those data with the invasive colonoscopies and biopsies necessary to provide comprehensive samples before, during and after tumorigenesis. This provides the rational for using mouse models of CRC to investigate these changes.

The majority of mice in our model did not develop macroscopic adenomas. C57BL/6J mice do display increased resistance to AOM-induced tumorigenesis (38), and while the basis for this differential sensitivity to AOM in inbred mouse strains has not been established, it appears to lie downstream of DNA alkylation, for example in DNA repair (39, 40). Resistance also appears to involve complex polygenic interactions which suggests that several mechanisms may be involved, including cell proliferation and apoptosis (41, 42). The inflammatory phenotype of these mice, however, coupled with disruption to their microbial community mirrors phenomena observed in western societies exposed to cancer risk factors such as alcohol, red meat and processed food which results in an accumulation mutations in the colonic epithelium. While increased doses of AOM in susceptible models can induce tumorigenesis much more rapidly, it is likely these models do not recapitulate the entire

progression of human CRC. As such, our model may reflect the pro-inflammatory, pre-tumorigenic environment observed in western societies more accurately.

The initial immune response appeared to be down-regulation of cytokine transcription in AOM-treated mice. AOM induces methyl adducts in DNA which are repaired by O^6-methylguanine-DNA-methyltransferase (MGMT) and when this repair enzyme is overwhelmed, damaged cells are cleared by apoptosis (43). Apoptotic cells may provide anti-inflammatory stimuli by releasing adenosine which is detected by the adenosine A2A receptor on phagocytes (44, 45). This may contribute to the immune suppression observed at Week 8, although studies suggest that the apoptotic response to AOM is concluded within the first five days after AOM administration (43). The activity of repair enzyme MGMT was shown to increase twelve days after AOM administration, and suppression of this enzyme by promoter methylation is associated with the expression of pro-inflammatory cytokines (46, 47), but its renewed activity may not surpass the baseline level observed in control animals (43). In contrast, spleen weight is significantly increased in AOM-treated mice at this time-point. This may be a due to production of monocyte-derived macrophages (48, 49), as enlarged spleens have been reported in mice treated with AOM which displayed a dramatic increase in splenic macrophages (50, 51).

The increase in pro-inflammatory cytokine transcription in mice following AOM administration becomes apparent at Week 12 and continues through Week 24. Cytokines increased at these times points include *Il1β*, *Il6*, *Il10*, *Il12* and *Tnfα*. Extensive studies to date have demonstrated a pro-tumorigenic role for IL1β in numerous cancer types, including human colon cancer (17). In our study, *Il1β* was significantly increased at Week 24. Other studies have reported increased *Il1β* transcription in outbred Wistar rats at 7 weeks and at 10 months after administration with AOM alone (52, 53). In contrast, no increase was observed in A/J mice between 3 and 48 hours after injection (54), demonstrating that

transcription is not an acute effect of AOM in the colon. In comparison to the models reported in the literature, our mice appear to have a longer incubation period before induction of *Il1β* transcription, and this up-regulation lasts for a shorter period, possibly reflecting the fact that C57BL/6J mice are relatively resistant to AOM-induced carcinogenesis.

Similar to *Il1β*, *Il6* was significantly increased in mice administered AOM compared to PBS in our study. IL6 is also a cytokine which is dysregulated in CRC, and elevated levels are associated with poor prognosis in human patients and in AOM-induced mouse models (18, 55-58). Our IL6 data highlights Week 24 as a key stage in the AOM-induced pro-inflammatory cytokine response.

Il10 was also significantly increased in our model at Week 24, where it displayed a 220-fold induction compared to PBS-treated mice. IL10 has been shown to protect against tumorigenesis both by suppressing the pro-inflammatory milieu that can promote tumour progression and by inducing the cytotoxicity of $CD8^+$ T cells (59). Indeed, in preclinical tumour models, IL10 induces the rejection of tumours through both its pro-immunity and its anti-inflammatory functions (59). IL10 expression may reflect disease stage, as IL10 was reported to be increased in the serum of mice displaying pre-neoplastic changes in their colons, but not in normal or tumour-bearing mice, 28-30 weeks after administration of two doses of AOM (60). Moreover, IL10 may be modulated by the microbiota. Its transcription was induced by dietary supplementation of prebiotics and probiotics in Fischer 344 rats 32 weeks after exposure to two doses of AOM (61). Our *Il10* data suggest that the anti-inflammatory response was functioning normally in our model, reinforced by the observation that pro-inflammatory cytokine transcription was largely suppressed by Week 48.

We observed an increase in *Il12* in mice administered AOM compared to PBS controls at Weeks 12 and 48. IL12 has been shown to suppress cancer by a number of mechanisms (62-

67). Few studies have tracked the effect of AOM administration alone on IL12. However, it is increased in animals treated with AOM/DSS (68-70) and is, at least partly, regulated by the microbiota (26). Its transcription is also noteworthy at Week 48 as it is significantly higher in the mice harbouring colonic adenomas compared to mice administered AOM which were free of adenomas. This could reflect a continued anti-tumour immune response, or IL12 production by innate immune cells in response to antigen stimulation in adenoma-bearing mice.

Tnfα transcription was increased in our AOM-treated mice at Weeks 12 and 24. TNFα is a pro-inflammatory cytokine which can kill tumour cells, but chronic, low-grade expression can contribute to tumorigenesis (19, 71, 72). While *Tnfα* transcription returned to baseline levels by Week 48, our data indicate a window of at least 12 weeks of up-regulation of this cytokine. In a study featuring sensitive 129S6/SvEvTac mice, *Tnfα* correlated with tumour multiplicity (73). In contrast, no significant increase in *Tnfα* was observed in the serum of Wistar rats eighteen weeks after two doses of AOM, despite a significant increase in the number of ACF compared to controls (50), which implies that this cytokine is not required for ACF formation. TNFα expression is also a target of IL10-mediated immune suppression, and the down-regulation of *Tnfα* observed at Week 48 may be in response to the significant induction of *Il10* measured at Week 24 (74).

TGFβ is protective during the early stages of tumorigenesis but advanced cancers often present with a deletion or mutation of TGFβ receptors (75-78). Alterations to the TGFβ signalling pathway may account for some of the differences in sensitivity to AOM in different mouse strains, as sensitive A/J mice showed a greater suppression of TβR-II mRNA levels compared to AKR/J mice (79). Moreover, conditional knockout of the TGFβ Receptor 2 in the colonic epithelium of FVB mice leads to an increased number of ACF, adenomas and adenocarcinomas, two to six months after twelve doses of AOM (80, 81). However, *Tgfβ* did

not differ significantly between treatments at any time-point in our study, although this reflects a differential response in each mouse. At Week 24, two mice in the treatment group transcribe *Tgfβ* at levels less than one tenth of that observed in the control group, while five mice exhibit transcription twice as high as control. Transcription largely returned to normal by Week 48 except in one of the two mice harbouring colonic adenomas which has *Tgfβ* transcription 6.8-fold higher than control. This simultaneous over- and under-expression of *Tgfβ* parallels the differential responses reported in the literature and the complex role of this cytokine in cancer.

Cxcl1, *Cxcl2* and *Cxcl5* were all increased at Week 12 in our model. *Cxcl1* was also up-regulated at Week 24, while *Cxcl5* was suppressed at Week 8 in mice administered AOM, as discussed previously. This is a slightly earlier pattern of transcription than many of the other cytokines we measured, possibly because these chemokines are both produced by, and are chemotactic factors for, neutrophils, which are early response cells in wound healing and cancer (82). There is limited data available on the expression of these chemokines in mice administered AOM alone, but the association between these chemokines and AOM/DSS models of colitis-associated cancer is well established (83-88). There is also evidence that each of these chemokines is regulated by the microbiota, as their expression was reduced by a probiotic cocktail containing four strains of *Lactobacillus*, three strains of *Bifidobacterium* and one strain of *Streptococcus*, which also suppressed tumour formation in the colon of mice treated with AOM/DSS (29). The early pattern of up-regulation in our model also implicates these chemokines in the development of ACF observed at Week 24 and adenomas at Week 48.

Our data reveals a significant up-regulation of pro-inflammatory signalling beginning at Week 12, before detectible neoplastic changes were observed in the colonic epithelium of mice administered AOM. This implies that inflammatory cytokine transcription may have acted as

a tumour-promoter in these mice, and that it is unlikely that neoplastic transformation instigated inflammatory transcription. This is reinforced by the fact that inflammatory transcription had subsided by the time colonic adenomas were observed at Week 48. It also highlights the possible role of chemokines as early response elements in cancer development as each of the chemokines we measured were up-regulated at Week 12, along with *Tnfα* and *Il12*.

Changes to microbial diversity were apparent as early as Week 8 in AOM-treated mice. Human studies on the gut microbiota in cancer often report increased tumour-associated α-diversity as a result of the growth of opportunistic pathogens adapted to the novel tumour microenvironment (89-94). Studies which sample the faecal microbiota tend not to detect a difference between cancer patients and controls however, ostensibly because the faecal microbiota includes bacteria from the entire gastrointestinal tract which dilutes the signal generated by the cancer-associated species (89, 95-100). This is further evidenced by the fact that tissue-associated microbiota has half the diversity of faecal samples (90). Increased α-diversity in the faecal microbiome of CRC patients has been reported, however (2, 101). Studies have also reported a decrease in α-diversity in CRC patients' microbiota in both tissue and faecal samples (102, 103). This decrease in CRC-associated α-diversity was also detected in a retrospective analysis of 156 CRC patients and healthy controls, which further indicated a significant negative correlation between gut microbiota diversity and the stage of CRC (104). Our data suggests different changes associated with disease state. This begins with an increase in diversity following exposure to AOM, followed by microbial suppression, possibly mediated by the immune response (27, 105, 106).

In our data, PD was significantly increased in mice administered AOM at Week 8, while Shannon diversity was significantly decreased at Week 12, which marks the beginning of the cytokine response we observed in these mice. Shannon diversity index considers the

evenness of distribution of species' relative abundances across the population while PD does not. This could explain the increase we observed in PD but not Shannon diversity at Week 8, reflecting an expansion of low-abundance opportunistic pathogens (101). When considering which species might represent these enriched pathogens, we identified six taxa present in AOM-treated mice at Week 8 which were completely absent in PBS-treated controls. These included *Prevotella*, which is often reported as enriched in CRC (36, 107). *Prevotella* is a constituent of the oral microbiome, members of which have previously been associated with CRC (108). These six taxa also include *Chryseobacterium*, which is found in the murine oral microbiome (109). The other taxa are *Subdoligranulum*, and unclassified members of the *Ruminococcaceae*, *Erysipelotrichaceae* and *Bacilli*. A chi-squared test also identified *Ruminococcus 2*, *Faecalibacterium*, and the *Eubacterium ventriosum group* as qualitatively enriched in AOM-treated mice, although correction for multiple comparisons reduces these p-values to insignificance.

Later, an inflammation-induced reduction of these low-abundance opportunistic bacteria could allow their niche to be filled by predominant high-abundance taxa such as *Bacteroidales*, which have been associated with increased CRC risk (110). This would contribute to altered species distribution and suppress Shannon diversity without reducing PD. After Week 12, neither Shannon nor PD display any significant differences between AOM and PBS treatment groups. However, the three mice showing macroscopic signs of disease (ACF or adenomas) were among the four mice with lowest Shannon diversity indices at Week 48.

Beta (β)-diversity demonstrated that the composition of the gut microbiota in AOM-treated mice was significantly different from control at each time-point, with the model explaining between 14.6% and 24.4% of this variation. From Week 24 however, β-diversity becomes more disparate between treatments while α-diversity converges, suggesting that

tumorigenesis affects the specific composition of the gut microbiota more profoundly than the breadth of diversity within the microbiota of individual mice. The gut microbiota is a relatively stable ecosystem, robust against daily exposure to environmental microbes and dietary compounds (111-113). It features a core set of redundant metabolic functions distributed across its component species and recovers quickly from disruptions such as enteric infection and antibiotic exposure (114, 115). We observed a similar process in our α-diversity in response to AOM, but not in our β-diversity, suggesting that α-diversity is a more stable characteristic of the gut microbiota than β-diversity. The α- and β-diversity of the microbial metagenome predicted by PICRUSt also does not differ between treatments at any time-point, highlighting the stability of the metabolic functions provided by the microbiota. The consistent difference in β-diversity between treatments, however, reveals that this stability can be provided by communities of gut bacteria with significantly different compositions, and that the ecological shock of AOM treatment shifted the gut bacteria of these mice into an alternative stable state (116). This has implications for the persistence of disease-associated microbial compositions and treatments intended to restore patients to a "healthy" gut bacteria through treatments such as faecal microbial transfer (117).

In order to investigate if the altered composition of the gut bacteria of mice treated with AOM could contribute to tumorigenesis, we examined the specific species that differed between treatments at each time-point. At Week 8, the trend in taxa suppressed by AOM reflects a reduction in bacteria which produce butyrate, such as *Marvinbryantia* (118-129), and bacteria which are maladapted to inflammatory environments (27, 130-142). Butyrate has anti-inflammatory properties and may protect against CRC (143). Given that there was no increase in inflammation at this time-point, this suggests that changes in inflammation-suppressing microbiota precede induction of a pro-inflammatory immune response. All four species that were enriched in mice administered AOM were associated with cancer risk factors such as processed meat, high-fat diet or high BMI (144-151), while *Clostridiales*

vadinBB60; uncultured rumen bacterium was suppressed by cancer-protective factors such as resistant starch and butyrate (145, 152). However, *Eubacterium ventriosum group* and *Ruminococcus 2,* which are both negatively associated with CRC, were increased in our cancer model (153-157). The totality of the data does suggest that these mice have a cancer- and inflammation-associated microbiota at this time-point however, despite the absence of cytokine response or neoplastic transformation in the colonic mucosa. This would put microbial changes upstream of these effects during tumorigenesis.

By Week 12, the communities become more similar once the cytokine response has begun, which concurs with the idea that α-diversity is increased early in tumorigenesis due to the growth of opportunistic pathogens, but this is reversed later once the immune response begins.

At Week 24, the specific composition of the microbiota becomes more disparate again, even though α-diversities have converged and the cytokine response remains active. Three taxa are reduced at this time-point in AOM-treated mice that were also suppressed at Week 8*, Rikenella, Marvinbryantia* and *E. xylanophilum*, which are associated with factors demonstrated to reduce cancer risk (27, 120-123, 133-137, 158-164). Of note, four species are suppressed that are associated with reduced cancer risk and three of these express *bile salt hydrolase*, implicating bile acid metabolism in CRC (132, 165-167). Bacteria that are increased at Week 24 include two species closely associated with increased cancer risk, *Odoribacter* and *Citrobacter* (168-179). *Lachnospiraceae NC2004*, on the other hand, may be mildly protective by producing butyrate (180, 181). Similar to Week 8, these mice present with a pro-carcinogenic microbial profile, this time alongside a concurrent cytokine response.

At Week 48, when the cytokine response has diminished, the specific microbial changes are no longer conspicuously pro-carcinogenic. Three of the seven taxa reduced in AOM-treated mice at this time-point have negative associations with cancer or colitis (27, 121-123, 149,

150, 153, 160-163, 182), while *Akkermansia*, which is also reduced, has pro- and anti-tumorigenic reports in the literature (143, 183-189). In contrast, *Citrobacter* is closely linked to murine CRC and was increased at Week 24 but is decreased in mice administered AOM here (170-179). Taxa that were increased in AOM-treated mice include protective genera such as *Bifidobacterium, Prevotellaceae NK3B31*, *Butyrivibrio* and *Faecalibaculum* (131, 132, 190-207), and a number of other species with harmful or ambiguous effects in CRC such as *Clostridiales VadinBB60* and *Parasutterella* (208-212). While the microbiota may have contributed the cancer progression earlier in the model, it does not appear to have a significant pro-tumorigenic bias at this time-point.

Research has focussed on the role of individual bacteria in gut health and CRC risk, but this may overlook larger structural trends in the microbiota. In order to investigate these community trends in our model, we defined a set of co-abundance groups (CAG). These describe a set of bacterial taxa which displayed similar shifts in abundance across the experiment, which may be a result of some degree of interaction or inter-dependence, or a reliance on shared metabolic pathways. CAGs showed the opposite pattern of divergence to our α-diversity data. Of the seven CAGs our data produced, none showed any difference between treatments at Week 8 or 12. This suggests that the microbiota at the structural level of CAGs is robust against the forces that affected α-diversity. Differences were detected at Weeks 24 and 48, with CAG1 increased in AOM mice at Week 24, while CAG2 was increased and CAG7 decreased in these mice at Week 48. CAG1 is dominated by the order *Bacteroidales*, especially the *Alistipes* genus, both of which are associated with cancer-inducing inflammation (213, 214). This reinforces the pro-carcinogenic profile we observed in the species composition of mice treated with AOM at Week 24. CAG2 is more diverse, featuring significant proportions of *Erysipelotrichales*, *Clostridiales* and *Bacteroidales*, and several genera with protective associations in CRC including *Bifidobacterium* and *Prevotellaceae NK3B31*. The predominant species in CAG7, meanwhile, are

Ruminococcaceae; uncultured and *Desulfovibrio*, the latter of which is reported as an intestinal pathogen, although there are mixed reports on its role in CRC (215-217). These data also support the observations on species composition of mice treated with AOM at Week 48, in that the communities were significantly different but did not present a conspicuously carcinogenic profile.

One of the primary mechanisms by which the gut microbiota may influence CRC initiation and progression is via modification of host compounds to produce bioactive microbial metabolites, including bile acids. Bile acids have been implicated in the pathogenesis of colon cancer through their potential for cytotoxic effects, and well as by their hormonal signalling via FXR (218, 219). Alterations to bile acid-metabolising species was a characteristic of the microbiota of AOM-treated mice and so we examined the faecal bile acid composition of our mice.

Total faecal bile acid excretion was significantly decreased at Weeks 8 and 12, prior to the development of disease. However, in contrast to studies demonstrating a pro-tumorigenic function for hydrophobic bile acids such as DCA and LCA, these bile acids were reduced in AOM-treated mice before Week 48 (220, 221). These secondary bile acids are the end products of microbial deconjugation by Bsh and dehydroxylation by enzymes in the 7α-dehydroxylation pathway, and a reduction in bacteria expressing these enzymes could explain this effect. We did see a reduction in *Lactobacillus* at Week 8 and these bacteria are major producers of Bsh in the gut, while *Bacteroides* and *Enterococcus* also feature Bsh-producing species and these taxa are decreased at Week 24 (13). The expansion of Bsh-producing *Bifidobacterium* in AOM-treated mice at Week 48 could also contribute to the resolution of this effect. This idea is reinforced by the increase in conjugated bile acids observed in AOM-treated mice at Week 8 and Week 24, although there were no differences in bile acid metabolism genes predicted by PICRUSt.

As regards the reduction in total faecal bile acids up to 12 weeks post treatment, this may be a consequence of reduced microbial bile acid metabolism, as previously described in germ-free mice (222). This increased the levels of T-β-MCA and subsequently up-regulated ileal ASBT, a bile acid transporter, resulting in a decrease in total faecal bile acids, similar to the effects we observe in our model (223). T-β-MCA is an FXR antagonist and may suppress the protective effect of FXR against cancer (224, 225).

Correlation analysis revealed a complex set of interactions at Week 8 post-AOM exposure. It also highlights the relevance of CAGs as distinct, structural units in the microbiota.

PD was increased in our AOM-treated mice at Week 8 and this correlated with the transcription of several pro-inflammatory cytokines. The mice with highest PD values, on which AOM ostensibly had the largest effect on microbial diversity, also had the highest abundance of CAGs 2 and 3 and lowest abundance of CAGs 4 and 7. In fact, these pairs of CAGs tended to have opposite correlations with α-diversity and faecal bile acids. This is especially noteworthy in the correlations between CAG2/3 and CAG4/7 and normalised faecal bile acids. These are primarily negative for CAG2/3 and positive for CAG4/7, but this is reversed for FXR-antagonist MCAs. A similar phenomenon is observed for the correlations between PD and normalised faecal bile acids, which are universally negative except for a subset of MCAs. This hints at a network of interaction between microbial diversity and composition, bile acid regulation and cytokine signalling at this stage of our model which may contribute to CRC progression.

The initial changes we observe in response to AOM occur in the microbiota, which takes on a pro-tumorigenic and pro-inflammatory profile before any inflammatory or tumorigenic changes occur in the host, potentially placing this as an instigating phenomenon. This occurs alongside an increase in microbial richness and alterations to the bile acid pool which suggest a reduction in microbial bile acid metabolism. Our correlation analysis also reveals a

relationship between the microbiota, inflammation and bile acids at this time-point. The cytokine response and bile acid dysregulation are largely ameliorated by Week 48 when macroscopic adenomas appear, while the faecal microbial profile is no longer conspicuously pathogenic. However, we did not sample the tumour-associated microbiota of the two mice which developed adenomas, and bacteria in the tumour microenvironment could still contribute to disease progression locally. Bile acids did not appear to contribute directly to cancer risk as the faecal concentration was reduced in our model, along with the absolute and relative proportions of the major hydrophobic bile acids, but may affect cancer risk indirectly via repression of FXR signalling as a result of alterations in microbial bile acid metabolism. Our data highlights the acquisition of a pro-inflammatory gut microbial composition as the instigating tumorigenic change detected in our model, and suggests that targeting the microbiota with probiotic and/or antibiotic therapy could be an effective prophylactic defence against CRC.

3.4 References

1. Hope ME, Hold GL, Kain R, El-Omar EM. Sporadic colorectal cancer--role of the commensal microbiota. FEMS microbiology letters. 2005;244(1):1-7.
2. Scanlan PD, Shanahan F, Clune Y, Collins JK, O'Sullivan GC, O'Riordan M, et al. Culture-independent analysis of the gut microbiota in colorectal cancer and polyposis. Environmental microbiology. 2008;10(3):789-98.
3. Swidsinski A, Khilkin M, Kerjaschki D, Schreiber S, Ortner M, Weber J, et al. Association between intraepithelial Escherichia coli and colorectal cancer. Gastroenterology. 1998;115(2):281-6.
4. Guo M, Xu E, Ai D. Inferring Bacterial Infiltration in Primary Colorectal Tumors From Host Whole Genome Sequencing Data. Front Genet. 2019;10:213-.
5. Weir TL, Manter DK, Sheflin AM, Barnett BA, Heuberger AL, Ryan EP. Stool microbiome and metabolome differences between colorectal cancer patients and healthy adults. PloS one. 2013;8(8):e70803.
6. Nakanishi M, Chen Y, Qendro V, Miyamoto S, Weinstock E, Weinstock GM, et al. Effects of Walnut Consumption on Colon Carcinogenesis and Microbial Community Structure. Cancer Prevention Research. 2016;9(8):692-703.
7. Moore WE, Moore LH. Intestinal floras of populations that have a high risk of colon cancer. Applied and environmental microbiology. 1995;61(9):3202-7.
8. Ljungh A, Wadstrom T. Lactic acid bacteria as probiotics. Current issues in intestinal microbiology. 2006;7(2):73-89.
9. Wong SH, Zhao L, Zhang X, Nakatsu G, Han J, Xu W, et al. Gavage of Fecal Samples From Patients With Colorectal Cancer Promotes Intestinal Carcinogenesis in Germ-Free and Conventional Mice. Gastroenterology. 2017;153(6):1621-33.e6.
10. Daniel SG, Ball CL, Besselsen DG, Doetschman T, Hurwitz BL. Functional Changes in the Gut Microbiome Contribute to Transforming Growth Factor β-Deficient Colon Cancer. mSystems. 2017;2(5):e00065-17.
11. Gao R, Gao Z, Huang L, Qin H. Gut microbiota and colorectal cancer. Eur J Clin Microbiol Infect Dis. 2017;36(5):757-69.
12. Ferreira-Halder CV, Faria AVS, Andrade SS. Action and function of Faecalibacterium prausnitzii in health and disease. Best practice & research Clinical gastroenterology. 2017;31(6):643-8.
13. Begley M, Hill C, Gahan CGM. Bile salt hydrolase activity in probiotics. Applied and environmental microbiology. 2006;72(3):1729-38.
14. Fitzgerald CB, Shkoporov AN, Sutton TDS, Chaplin AV, Velayudhan V, Ross RP, et al. Comparative analysis of Faecalibacterium prausnitzii genomes shows a high level of genome plasticity and warrants separation into new species-level taxa. BMC Genomics. 2018;19(1):931.
15. Long AG, Lundsmith ET, Hamilton KE. Inflammation and Colorectal Cancer. Current colorectal cancer reports. 2017;13(4):341-51.
16. Voronov E, Apte RN. IL-1 in Colon Inflammation, Colon Carcinogenesis and Invasiveness of Colon Cancer. Cancer Microenviron. 2015;8(3):187-200.
17. Bent R, Moll L, Grabbe S, Bros M. Interleukin-1 Beta-A Friend or Foe in Malignancies? Int J Mol Sci. 2018;19(8):2155.
18. Kumari N, Dwarakanath BS, Das A, Bhatt AN. Role of interleukin-6 in cancer progression and therapeutic resistance. Tumour biology : the journal of the International Society for Oncodevelopmental Biology and Medicine. 2016;37(9):11553-72.
19. Balkwill F. TNF-alpha in promotion and progression of cancer. Cancer metastasis reviews. 2006;25(3):409-16.

20. Chow MT, Luster AD. Chemokines in cancer. Cancer immunology research. 2014;2(12):1125-31.
21. Mantovani A, Allavena P, Sica A, Balkwill F. Cancer-related inflammation. Nature. 2008;454:436.
22. Zuo T, Ng SC. The Gut Microbiota in the Pathogenesis and Therapeutics of Inflammatory Bowel Disease. Front Microbiol. 2018;9:2247-.
23. Klimesova K, Kverka M, Zakostelska Z, Hudcovic T, Hrncir T, Stepankova R, et al. Altered gut microbiota promotes colitis-associated cancer in IL-1 receptor-associated kinase M-deficient mice. Inflamm Bowel Dis. 2013;19(6):1266-77.
24. Lucas C, Barnich N, Nguyen HTT. Microbiota, Inflammation and Colorectal Cancer. Int J Mol Sci. 2017;18(6):1310.
25. Mendes MCS, Paulino DSM, Brambilla SR, Camargo JA, Persinoti GF, Carvalheira JBC. Microbiota modification by probiotic supplementation reduces colitis associated colon cancer in mice. World journal of gastroenterology. 2018;24(18):1995-2008.
26. Xiao Y, Dai X, Li K, Gui G, Liu J, Yang H. Clostridium butyricum partially regulates the development of colitis-associated cancer through miR-200c. Cell Mol Biol. 2017;63(4):59-66.
27. Hu Y, Le Leu RK, Christophersen CT, Somashekar R, Conlon MA, Meng XQ, et al. Manipulation of the gut microbiota using resistant starch is associated with protection against colitis-associated colorectal cancer in rats. Carcinogenesis. 2016;37(4):366-75.
28. Tian Y, Xu Q, Sun LQ, Ye Y, Ji GZ. Short-chain fatty acids administration is protective in colitis-associated colorectal cancer development. J Nutr Biochem. 2018;57:103-9.
29. Song H, Wang W, Shen B, Jia H, Hou Z, Chen P, et al. Pretreatment with probiotic Bifico ameliorates colitis-associated cancer in mice: Transcriptome and gut flora profiling. Cancer Sci. 2018;109(3):666-77.
30. Nguyen TT, Ung TT, Kim NH, Jung YD. Role of bile acids in colon carcinogenesis. World J Clin Cases. 2018;6(13):577-88.
31. Earnest DL, Holubec H, Wali RK, Jolley CS, Bissonette M, Bhattacharyya AK, et al. Chemoprevention of azoxymethane-induced colonic carcinogenesis by supplemental dietary ursodeoxycholic acid. Cancer Res. 1994;54(19):5071-4.
32. Magnuson BA, Carr I, Bird RP. ABILITY OF ABERRANT CRYPT FOCI CHARACTERISTICS TO PREDICT COLONIC TUMOR-INCIDENCE IN RATS FED CHOLIC-ACID. Cancer Res. 1993;53(19):4499-504.
33. Serfaty L, Bissonnette M, Poupon R. Ursodeoxycholic acid and chemoprevention of colorectal cancer. Gastroentérologie Clinique et Biologique. 2010;34(10):516-22.
34. Reddy BS. Diet And Excretion Of Bile Acids. Cancer Res. 1981;41:3766-8.
35. Bernstein H, Bernstein C, Payne CM, Dvorakova K, Garewal H. Bile acids as carcinogens in human gastrointestinal cancers. Mutation Research/Reviews in Mutation Research. 2005;589(1):47-65.
36. Jahani-Sherafat S, Alebouyeh M, Moghim S, Ahmadi Amoli H, Ghasemian-Safaei H. Role of gut microbiota in the pathogenesis of colorectal cancer; a review article. Gastroenterol Hepatol Bed Bench. 2018;11(2):101-9.
37. Zhu GW, Huang Q, Huang YJ, Zheng W, Hua J, Yang SG, et al. Lipopolysaccharide increases the release of VEGF-C that enhances cell motility and promotes lymphangiogenesis and lymphatic metastasis through the TLR4-NF-kappa B/JNK pathways in colorectal cancer. Oncotarget. 2016;7(45):73711-24.
38. Meunier C, Cai J, Fortin A, Kwan T, Marquis JF, Turbide C, et al. Characterization of a major colon cancer susceptibility locus (Ccs3) on mouse chromosome 3. Oncogene. 2010;29(5):647-61.
39. Papanikolaou A, Shank RC, Delker DA, Povey A, Cooper DP, Rosenberg DW. Initial levels of azoxymethane-induced DNA methyl adducts are not predictive of tumor susceptibility in inbred mice. Toxicology and applied pharmacology. 1998;150(1):196-203.

40. Delker DA, Bammler TK, Rosenberg DW. A comparative study of hepatic and colonic metabolic enzymes in inbred mouse lines before and after treatment with the colon carcinogen, 1,2-dimethylhydrazine. Drug metabolism and disposition: the biological fate of chemicals. 1996;24(4):408-13.
41. Bissahoyo A, Pearsall RS, Hanlon K, Amann V, Hicks D, Godfrey VL, et al. Azoxymethane is a genetic background-dependent colorectal tumor initiator and promoter in mice: effects of dose, route, and diet. Toxicological sciences : an official journal of the Society of Toxicology. 2005;88(2):340-5.
42. Guda K, Marino JN, Jung Y, Crary K, Dong M, Rosenberg DW. Strain-specific homeostatic responses during early stages of Azoxymethane-induced colon tumorigenesis in mice. International journal of oncology. 2007;31(4):837-42.
43. Nyskohus LS, Watson AJ, Margison GP, Le Leu RK, Kim SW, Lockett TJ, et al. Repair and removal of azoxymethane-induced O6-methylguanine in rat colon by O6-methylguanine DNA methyltransferase and apoptosis. Mutation research. 2013;758(1-2):80-6.
44. Yamaguchi H, Maruyama T, Urade Y, Nagata S. Immunosuppression via adenosine receptor activation by adenosine monophosphate released from apoptotic cells. Elife. 2014;3:e02172-e.
45. Haanen C, Vermes I. Apoptosis and inflammation. Mediators Inflamm. 1995;4(1):5-15.
46. Sepulveda AR, Yao Y, Yan W, Park DI, Kim JJ, Gooding W, et al. CpG Methylation and Reduced Expression of O⁶-Methylguanine DNA Methyltransferase Is Associated With Helicobacter pylori Infection. Gastroenterology. 2010;138(5):1836-44.e4.
47. Piperi C, Themistocleous MS, Papavassiliou GA, Farmaki E, Levidou G, Korkolopoulou P, et al. High Incidence of MGMT and RARβ Promoter Methylation in Primary Glioblastomas: Association with Histopathological Characteristics, Inflammatory Mediators and Clinical Outcome. Molecular Medicine. 2010;16(1):1-9.
48. Pittet MJ, Nahrendorf M, Swirski FK. The journey from stem cell to macrophage. Annals of the New York Academy of Sciences. 2014;1319(1):1-18.
49. Arandjelovic S, Ravichandran KS. Phagocytosis of apoptotic cells in homeostasis. Nat Immunol. 2015;16(9):907-17.
50. Velázquez KT, Enos RT, Carson MS, Cranford TL, Bader JE, Chatzistamou I, et al. Weight loss following diet-induced obesity does not alter colon tumorigenesis in the AOM mouse model. Am J Physiol Gastrointest Liver Physiol. 2016;311(4):G699-G712.
51. He XQ, Cichello SA, Duan JL, Zhou J. Canola oil influence on azoxymethane-induced colon carcinogenesis, hypertriglyceridemia and hyperglycemia in Kunming mice. Asian Pacific journal of cancer prevention : APJCP. 2014;15(6):2477-83.
52. Bousserouel S, Gosse F, Bouhadjar M, Soler L, Marescaux J, Raul F. Long-term administration of aspirin inhibits tumour formation and triggers anti-neoplastic molecular changes in a pre-clinical model of colon carcinogenesis. Oncol Rep. 2010;23(2):511-7.
53. Bousserouel S, Lamy V, Gossé F, Lobstein A, Marescaux J, Raul F. Early modulation of gene expression used as a biomarker for chemoprevention in a preclinical model of colon carcinogenesis. Pathology International. 2011;61(2):80-7.
54. Tong X, Yin L, Washington R, Rosenberg DW, Giardina C. The p50-p50 NF-kappaB complex as a stimulus-specific repressor of gene activation. Molecular and cellular biochemistry. 2004;265(1-2):171-83.
55. Zeng J, Tang Z-H, Liu S, Guo S-S. Clinicopathological significance of overexpression of interleukin-6 in colorectal cancer. World journal of gastroenterology. 2017;23(10):1780-6.
56. Scheller J, Chalaris A, Schmidt-Arras D, Rose-John S. The pro- and anti-inflammatory properties of the cytokine interleukin-6. Biochimica et Biophysica Acta (BBA) - Molecular Cell Research. 2011;1813(5):878-88.

57. Harpel K, Leung S, Rice PF, Jones M, Barton JK, Bommireddy R. Imaging colon cancer development in mice: IL-6 deficiency prevents adenoma in azoxymethane-treated Smad3 knockouts. Phys Med Biol. 2016;61(3):N60-N9.
58. Grivennikov S, Karin E, Terzic J, Mucida D, Yu GY, Vallabhapurapu S, et al. IL-6 and Stat3 are required for survival of intestinal epithelial cells and development of colitis-associated cancer. Cancer cell. 2009;15(2):103-13.
59. Oft M. IL-10: master switch from tumor-promoting inflammation to antitumor immunity. Cancer immunology research. 2014;2(3):194-9.
60. Mentor-Marcel RA, Bobe G, Barrett KG, Young MR, Albert PS, Bennink MR, et al. Inflammation-associated serum and colon markers as indicators of dietary attenuation of colon carcinogenesis in ob/ob mice. Cancer Prev Res (Phila). 2009;2(1):60-9.
61. Roller M, Femia AP, Caderni G, Rechkemmer G, Watzl B. Intestinal immunity of rats with colon cancer is modulated by oligofructose-enriched inulin combined with Lactobacillus rhamnosus and Bifidobacterium lactis. British Journal of Nutrition. 2007;92(6):931-8.
62. Angiolillo AL, Sgadari C, Tosato G. A role for the interferon-inducible protein 10 in inhibition of angiogenesis by interleukin-12. Annals of the New York Academy of Sciences. 1996;795:158-67.
63. Otani T, Nakamura S, Toki M, Motoda R, Kurimoto M, Orita K. Identification of IFN-gamma-producing cells in IL-12/IL-18-treated mice. Cell Immunol. 1999;198(2):111-9.
64. Trinchieri G, Wysocka M, D'Andrea A, Rengaraju M, Aste-Amezaga M, Kubin M, et al. Natural killer cell stimulatory factor (NKSF) or interleukin-12 is a key regulator of immune response and inflammation. Progress in growth factor research. 1992;4(4):355-68.
65. Zeh HJ, 3rd, Hurd S, Storkus WJ, Lotze MT. Interleukin-12 promotes the proliferation and cytolytic maturation of immune effectors: implications for the immunotherapy of cancer. Journal of immunotherapy with emphasis on tumor immunology : official journal of the Society for Biological Therapy. 1993;14(2):155-61.
66. Parihar R, Dierksheide J, Hu Y, Carson WE. IL-12 enhances the natural killer cell cytokine response to Ab-coated tumor cells. J Clin Invest. 2002;110(7):983-92.
67. Kerkar SP, Leonardi AJ, van Panhuys N, Zhang L, Yu Z, Crompton JG, et al. Collapse of the tumor stroma is triggered by IL-12 induction of Fas. Molecular therapy : the journal of the American Society of Gene Therapy. 2013;21(7):1369-77.
68. Wang Q, Sun P, Li GJ, Zhu K, Wang C, Zhao X. Inhibitory effects of Dendrobium candidum Wall ex Lindl. on azoxymethane- and dextran sulfate sodium-induced colon carcinogenesis in C57BL/ 6 mice. Oncol Lett. 2014;7(2):493-8.
69. Wang W, Li XY, Zheng DW, Zhang DC, Huang S, Zhang XM, et al. Dynamic changes of peritoneal macrophages and subpopulations during ulcerative colitis to metastasis of colorectal carcinoma in a mouse model. Inflamm Res. 2013;62(7):669-80.
70. Shirakami Y, Shimizu M, Tsurumi H, Hara Y, Tanaka T, Moriwaki H. EGCG and Polyphenon E attenuate inflammation-related mouse colon carcinogenesis induced by AOM plus DDS. Mol Med Rep. 2008;1(3):355-61.
71. Wang X, Lin Y. Tumor necrosis factor and cancer, buddies or foes? Acta Pharmacol Sin. 2008;29(11):1275-88.
72. Havell EA, Fiers W, North RJ. The antitumor function of tumor necrosis factor (TNF), I. Therapeutic action of TNF against an established murine sarcoma is indirect, immunologically dependent, and limited by severe toxicity. J Exp Med. 1988;167(3):1067-85.
73. Manna SK, Golla S, Golla JP, Tanaka N, Cai Y, Takahashi S, et al. St. John's Wort Attenuates Colorectal Carcinogenesis in Mice through Suppression of Inflammatory Signaling. Cancer Prev Res (Phila). 2015;8(9):786-95.
74. Murray PJ. The primary mechanism of the IL-10-regulated antiinflammatory response is to selectively inhibit transcription. Proc Natl Acad Sci U S A. 2005;102(24):8686-91.

75. Massague J. TGFbeta in Cancer. Cell. 2008;134(2):215-30.
76. Malliri A, Yeudall WA, Nikolic M, Crouch DH, Parkinson EK, Ozanne B. Sensitivity to transforming growth factor beta 1-induced growth arrest is common in human squamous cell carcinoma cell lines: c-MYC down-regulation and p21waf1 induction are important early events. Cell growth & differentiation : the molecular biology journal of the American Association for Cancer Research. 1996;7(10):1291-304.
77. Levy L, Hill CS. Alterations in components of the TGF-beta superfamily signaling pathways in human cancer. Cytokine & growth factor reviews. 2006;17(1-2):41-58.
78. Landskron G, De la Fuente M, Thuwajit P, Thuwajit C, Hermoso MA. Chronic inflammation and cytokines in the tumor microenvironment. Journal of immunology research. 2014;2014:149185.
79. Guda K, Giardina C, Nambiar P, Cui H, Rosenberg DW. Aberrant transforming growth factor-β signaling in azoxymethane-induced mouse colon tumors. Molecular Carcinogenesis. 2001;31(4):204-13.
80. Biswas S, Chytil A, Washington K, Romero-Gallo J, Gorska AE, Wirth PS, et al. Transforming growth factor beta receptor type II inactivation promotes the establishment and progression of colon cancer. Cancer Res. 2004;64(14):4687-92.
81. Hahm KB, Lee KM, Kim YB, Hong WS, Lee WH, Han SU, et al. Conditional loss of TGF-beta signalling leads to increased susceptibility to gastrointestinal carcinogenesis in mice. Alimentary pharmacology & therapeutics. 2002;16 Suppl 2:115-27.
82. Coussens LM, Werb Z. Inflammation and cancer. Nature. 2002;420(6917):860-7.
83. Hardbower DM, Coburn LA, Asim M, Singh K, Sierra JC, Barry DP, et al. EGFR-mediated macrophage activation promotes colitis-associated tumorigenesis. Oncogene. 2017;36(27):3807-19.
84. Ma X, Aoki T, Tsuruyama T, Narumiya S. Definition of Prostaglandin E2-EP2 Signals in the Colon Tumor Microenvironment That Amplify Inflammation and Tumor Growth. Cancer Res. 2015;75(14):2822-32.
85. Aoki T, Narumiya S. Prostaglandin E(2)-EP2 signaling as a node of chronic inflammation in the colon tumor microenvironment. Inflamm Regen. 2017;37:4-.
86. Coburn LA, Singh K, Asim M, Barry DP, Allaman MM, Al-Greene NT, et al. Loss of solute carrier family 7 member 2 exacerbates inflammation-associated colon tumorigenesis. Oncogene. 2019;38(7):1067-79.
87. Meana C, Garcia-Rostan G, Pena L, Lorden G, Cubero A, Orduna A, et al. The phosphatidic acid phosphatase lipin-1 facilitates inflammation-driven colon carcinogenesis. JCI Insight. 2018;3(18):18.
88. Bugni JM, Rabadi LA, Jubbal K, Karagiannides I, Lawson G, Pothoulakis C. The neurotensin receptor-1 promotes tumor development in a sporadic but not an inflammation-associated mouse model of colon cancer. International journal of cancer. 2012;130(8):1798-805.
89. Hibberd AA, Lyra A, Ouwehand AC, Rolny P, Lindegren H, Cedgård L, et al. Intestinal microbiota is altered in patients with colon cancer and modified by probiotic intervention. BMJ Open Gastroenterol. 2017;4(1):e000145-e.
90. Mira-Pascual L, Cabrera-Rubio R, Ocon S, Costales P, Parra A, Suarez A, et al. Microbial mucosal colonic shifts associated with the development of colorectal cancer reveal the presence of different bacterial and archaeal biomarkers. Journal of Gastroenterology. 2015;50(2):167-79.
91. Lu Y, Chen J, Zheng J, Hu G, Wang J, Huang C, et al. Mucosal adherent bacterial dysbiosis in patients with colorectal adenomas. Scientific reports. 2016;6:26337-.
92. Geng J, Fan H, Tang X, Zhai H, Zhang Z. Diversified pattern of the human colorectal cancer microbiome. Gut Pathog. 2013;5(1):2-.

93. Burns MB, Lynch J, Starr TK, Knights D, Blekhman R. Virulence genes are a signature of the microbiome in the colorectal tumor microenvironment. Genome Med. 2015;7(1):55-.
94. Sanapareddy N, Legge RM, Jovov B, McCoy A, Burcal L, Araujo-Perez F, et al. Increased rectal microbial richness is associated with the presence of colorectal adenomas in humans. Isme j. 2012;6(10):1858-68.
95. Wu N, Yang X, Zhang R, Li J, Xiao X, Hu Y, et al. Dysbiosis Signature of Fecal Microbiota in Colorectal Cancer Patients. Microbial Ecology. 2013;66(2):462-70.
96. Weir TL, Manter DK, Sheflin AM, Barnett BA, Heuberger AL, Ryan EP. Stool microbiome and metabolome differences between colorectal cancer patients and healthy adults. PloS one. 2013;8(8):e70803-e.
97. Zeller G, Tap J, Voigt AY, Sunagawa S, Kultima JR, Costea PI, et al. Potential of fecal microbiota for early-stage detection of colorectal cancer. Mol Syst Biol. 2014;10(11):766-.
98. Vogtmann E, Hua X, Zeller G, Sunagawa S, Voigt AY, Hercog R, et al. Colorectal Cancer and the Human Gut Microbiome: Reproducibility with Whole-Genome Shotgun Sequencing. PloS one. 2016;11(5):e0155362-e.
99. Wang T, Cai G, Qiu Y, Fei N, Zhang M, Pang X, et al. Structural segregation of gut microbiota between colorectal cancer patients and healthy volunteers. Isme j. 2012;6(2):320-9.
100. Chen H-M, Yu Y-N, Wang J-L, Lin Y-W, Kong X, Yang C-Q, et al. Decreased dietary fiber intake and structural alteration of gut microbiota in patients with advanced colorectal adenoma. The American Journal of Clinical Nutrition. 2013;97(5):1044-52.
101. Feng Q, Liang S, Jia H, Stadlmayr A, Tang L, Lan Z, et al. Gut microbiome development along the colorectal adenoma–carcinoma sequence. Nature Communications. 2015;6:6528.
102. Ahn J, Sinha R, Pei Z, Dominianni C, Wu J, Shi J, et al. Human gut microbiome and risk for colorectal cancer. J Natl Cancer Inst. 2013;105(24):1907-11.
103. Shen XJ, Rawls JF, Randall T, Burcal L, Mpande CN, Jenkins N, et al. Molecular characterization of mucosal adherent bacteria and associations with colorectal adenomas. Gut microbes. 2010;1(3):138-47.
104. Ai D, Pan H, Li X, Gao Y, Liu G, Xia LC. Identifying Gut Microbiota Associated With Colorectal Cancer Using a Zero-Inflated Lognormal Model. Front Microbiol. 2019;10(826).
105. Sepehri S, Kotlowski R, Bernstein CN, Krause DO. Microbial diversity of inflamed and noninflamed gut biopsy tissues in inflammatory bowel disease. Inflamm Bowel Dis. 2007;13(6):675-83.
106. Wang X, Ye T, Chen WJ, Lv Y, Hao Z, Chen J, et al. Structural shift of gut microbiota during chemo-preventive effects of epigallocatechin gallate on colorectal carcinogenesis in mice. World journal of gastroenterology. 2017;23(46):8128-39.
107. Flemer B, Lynch DB, Brown JMR, Jeffery IB, Ryan FJ, Claesson MJ, et al. Tumour-associated and non-tumour-associated microbiota in colorectal cancer. Gut. 2017;66(4):633-43.
108. Warren RL, Freeman DJ, Pleasance S, Watson P, Moore RA, Cochrane K, et al. Co-occurrence of anaerobic bacteria in colorectal carcinomas. Microbiome. 2013;1(1):16.
109. Li B, Ge Y, Cheng L, Zeng B, Yu J, Peng X, et al. Oral bacteria colonize and compete with gut microbiota in gnotobiotic mice. Int J Oral Sci. 2019;11(1):10-.
110. Baxter NT, Zackular JP, Chen GY, Schloss PD. Structure of the gut microbiome following colonization with human feces determines colonic tumor burden. Microbiome. 2014;2:20-.
111. Zhang C, Derrien M, Levenez F, Brazeilles R, Ballal SA, Kim J, et al. Ecological robustness of the gut microbiota in response to ingestion of transient food-borne microbes. The Isme Journal. 2016;10:2235.
112. Seksik P, Landman C. Understanding Microbiome Data: A Primer for Clinicians. Digestive diseases (Basel, Switzerland). 2015;33 Suppl 1:11-6.

113. Eng A, Borenstein E. Taxa-function robustness in microbial communities. Microbiome. 2018;6(1):45-.
114. Palleja A, Mikkelsen KH, Forslund SK, Kashani A, Allin KH, Nielsen T, et al. Recovery of gut microbiota of healthy adults following antibiotic exposure. Nature Microbiology. 2018;3(11):1255-65.
115. Singh P, Teal TK, Marsh TL, Tiedje JM, Mosci R, Jernigan K, et al. Intestinal microbial communities associated with acute enteric infections and disease recovery. Microbiome. 2015;3(1):45.
116. Folke C, Carpenter S, Walker B, Scheffer M, Elmqvist T, Gunderson L, et al. Regime Shifts, Resilience, and Biodiversity in Ecosystem Management. Annual Review of Ecology, Evolution, and Systematics. 2004;35(1):557-81.
117. Bakken JS, Borody T, Brandt LJ, Brill JV, Demarco DC, Franzos MA, et al. Treating Clostridium difficile infection with fecal microbiota transplantation. Clin Gastroenterol Hepatol. 2011;9(12):1044-9.
118. Wiegel J, Tanner R, Rainey FA. An Introduction to the Family Clostridiaceae. In: Dworkin M, Falkow S, Rosenberg E, Schleifer K-H, Stackebrandt E, editors. The Prokaryotes: Volume 4: Bacteria: Firmicutes, Cyanobacteria. New York, NY: Springer US; 2006. p. 654-78.
119. Arimochi H, Kinouchi T, Kataoka K, Kuwahara T, Ohnishi Y. Effect of intestinal bacteria on formation of azoxymethane-induced aberrant crypt foci in the rat colon. Biochem Biophys Res Commun. 1997;238(3):753-7.
120. VAN GYLSWYK NO, VAN DER TOORN JJTK. Eubacterium uniforme sp. nov. and Eubacterium xylanophilum sp. nov., Fiber-Digesting Bacteria from the Rumina of Sheep Fed Corn Stover. International Journal of Systematic and Evolutionary Microbiology. 1985;35(3):323-6.
121. Wolin MJ, Miller TL, Lawson PA. Proposal to replace the illegitimate genus name Bryantella Wolin et al. 2004VP with the genus name Marvinbryantia gen. nov. and to replace the illegitimate combination Bryantella formatexigens Wolin et al. 2004VP with Marvinbryantia formatexigens comb. nov. International Journal of Systematic and Evolutionary Microbiology. 2008;58(3):742-4.
122. Jawed K, Mattam AJ, Fatma Z, Wajid S, Abdin MZ, Yazdani SS. Engineered Production of Short Chain Fatty Acid in Escherichia coli Using Fatty Acid Synthesis Pathway. PloS one. 2016;11(7):e0160035.
123. Rey FE, Faith JJ, Bain J, Muehlbauer MJ, Stevens RD, Newgard CB, et al. Dissecting the in Vivo Metabolic Potential of Two Human Gut Acetogens. Journal of Biological Chemistry. 2010;285(29):22082-90.
124. Auchtung TA, Holder ME, Gesell JR, Ajami NJ, Duarte RTD, Itoh K, et al. Complete Genome Sequence of Turicibacter sp. Strain H121, Isolated from the Feces of a Contaminated Germ-Free Mouse. Genome Announc. 2016;4(2):e00114-16.
125. Zhong Y, Nyman M, Fåk F. Modulation of gut microbiota in rats fed high-fat diets by processing whole-grain barley to barley malt. Molecular Nutrition & Food Research. 2015;59(10):2066-76.
126. Nishitsuji K, Xiao J, Nagatomo R, Umemoto H, Morimoto Y, Akatsu H, et al. Analysis of the gut microbiome and plasma short-chain fatty acid profiles in a spontaneous mouse model of metabolic syndrome. Scientific Reports. 2017;7(1):15876.
127. Wu M, Wu Y, Li J, Bao Y, Guo Y, Yang W. The Dynamic Changes of Gut Microbiota in Muc2 Deficient Mice. Int J Mol Sci. 2018;19(9):2809.
128. Rea D, Coppola G, Palma G, Barbieri A, Luciano A, Del Prete P, et al. Microbiota effects on cancer: from risks to therapies. Oncotarget. 2018;9(25):17915-27.
129. Zackular JP, Baxter NT, Iverson KD, Sadler WD, Petrosino JF, Chen GY, et al. The gut microbiome modulates colon tumorigenesis. mBio. 2013;4(6):e00692.

130. Clavel T, Charrier C, Wenning M, Haller D. Parvibacter caecicola gen. nov., sp. nov., a bacterium of the family Coriobacteriaceae isolated from the caecum of a mouse. International Journal of Systematic and Evolutionary Microbiology. 2013;63(7):2642-8.
131. Wei X, Tao J, Xiao S, Jiang S, Shang E, Zhu Z, et al. Xiexin Tang improves the symptom of type 2 diabetic rats by modulation of the gut microbiota. Scientific Reports. 2018;8(1):3685.
132. Jing Y, Li A, Liu Z, Yang P, Wei J, Chen X, et al. Absorption of Codonopsis pilosula Saponins by Coexisting Polysaccharides Alleviates Gut Microbial Dysbiosis with Dextran Sulfate Sodium-Induced Colitis in Model Mice. BioMed research international. 2018;2018:1781036.
133. Bomar L, Maltz M, Colston S, Graf J. Directed Culturing of Microorganisms Using Metatranscriptomics. mBio. 2011;2(2):e00012-11.
134. Couturier-Maillard A, Secher T, Rehman A, Normand S, De Arcangelis A, Haesler R, et al. NOD2-mediated dysbiosis predisposes mice to transmissible colitis and colorectal cancer. J Clin Invest. 2013;123(2):700-11.
135. Liu X, Zeng B, Zhang J, Li W, Mou F, Wang H, et al. Role of the Gut Microbiome in Modulating Arthritis Progression in Mice. Scientific reports. 2016;6:30594-.
136. Sun J, de Vos P. Immunomodulatory Functions of Nutritional Ingredients in Health and Disease: Frontiers in Immunology; 2017.
137. Santoru ML, Piras C, Murgia A, Palmas V, Camboni T, Liggi S, et al. Cross sectional evaluation of the gut-microbiome metabolome axis in an Italian cohort of IBD patients. Scientific Reports. 2017;7(1):9523.
138. Oh NS, Joung JY, Lee JY, Kim Y. Probiotic and anti-inflammatory potential of Lactobacillus rhamnosus 4B15 and Lactobacillus gasseri 4M13 isolated from infant feces. PloS one. 2018;13(2):e0192021.
139. O'Flaherty S, Briner Crawley A, Theriot CM, Barrangou R. The Lactobacillus Bile Salt Hydrolase Repertoire Reveals Niche-Specific Adaptation. mSphere. 2018;3(3):e00140-18.
140. Jones-Hall YL, Kozik A, Nakatsu C. Ablation of tumor necrosis factor is associated with decreased inflammation and alterations of the microbiota in a mouse model of inflammatory bowel disease. PloS one. 2015;10(3):e0119441-e.
141. Rossi G, Pengo G, Caldin M, Palumbo Piccionello A, Steiner JM, Cohen ND, et al. Comparison of microbiological, histological, and immunomodulatory parameters in response to treatment with either combination therapy with prednisone and metronidazole or probiotic VSL#3 strains in dogs with idiopathic inflammatory bowel disease. PloS one. 2014;9(4):e94699-e.
142. Liu W, Crott JW, Lyu L, Pfalzer AC, Li J, Choi SW, et al. Diet- and Genetically-induced Obesity Produces Alterations in the Microbiome, Inflammation and Wnt Pathway in the Intestine of Apc(+/1638N) Mice: Comparisons and Contrasts. Journal of Cancer. 2016;7(13):1780-90.
143. Wu X, Wu Y, He L, Wu L, Wang X, Liu Z. Effects of the intestinal microbial metabolite butyrate on the development of colorectal cancer. Journal of Cancer. 2018;9(14):2510-7.
144. Xie Y, Zhou G, Wang C, Xu X, Li C. Temporal changes in gut microbiota and signaling molecules of the gut–brain axis in mice fed meat protein diets. bioRxiv. 2018:329953.
145. Neyrinck AM, Pachikian B, Taminiau B, Daube G, Frédérick R, Cani PD, et al. Intestinal Sucrase as a Novel Target Contributing to the Regulation of Glycemia by Prebiotics. PloS one. 2016;11(8):e0160488.
146. Etxeberria U, Arias N, Boque N, Macarulla MT, Portillo MP, Milagro FI, et al. Shifts in microbiota species and fermentation products in a dietary model enriched in fat and sucrose. Beneficial microbes. 2015;6(1):97-111.

147. Tims S, Derom C, Jonkers DM, Vlietinck R, Saris WH, Kleerebezem M, et al. Microbiota conservation and BMI signatures in adult monozygotic twins. The ISME journal. 2013;7(4):707-17.
148. Kasai C, Sugimoto K, Moritani I, Tanaka J, Oya Y, Inoue H, et al. Comparison of the gut microbiota composition between obese and non-obese individuals in a Japanese population, as analyzed by terminal restriction fragment length polymorphism and next-generation sequencing. BMC gastroenterology. 2015;15(1):100.
149. Bibiloni R, Simon MA, Albright C, Sartor B, Tannock GW. Analysis of the large bowel microbiota of colitic mice using PCR/DGGE. Letters in Applied Microbiology. 2005;41(1):45-51.
150. Yu J, Feng Q, Wong SH, Zhang D, Liang Qy, Qin Y, et al. Metagenomic analysis of faecal microbiome as a tool towards targeted non-invasive biomarkers for colorectal cancer. Gut. 2017;66(1):70-8.
151. Liu Q, Li F, Zhuang Y, Xu J, Wang J, Mao X, et al. Alteration in gut microbiota associated with hepatitis B and non-hepatitis virus related hepatocellular carcinoma. Gut Pathog. 2019;11(1):1.
152. Zhou Z, Nie K, Huang Q, Li K, Sun Y, Zhou R, et al. Changes of cecal microflora in chickens following Eimeria tenella challenge and regulating effect of coated sodium butyrate. Experimental Parasitology. 2017;177:73-81.
153. Biagi E, Nylund L, Candela M, Ostan R, Bucci L, Pini E, et al. Through ageing, and beyond: gut microbiota and inflammatory status in seniors and centenarians. PloS one. 2010;5(5):e10667-e.
154. David LA, Maurice CF, Carmody RN, Gootenberg DB, Button JE, Wolfe BE, et al. Diet rapidly and reproducibly alters the human gut microbiome. Nature. 2014;505(7484):559-63.
155. Klinder A, Shen Q, Heppel S, Lovegrove JA, Rowland I, Tuohy KM. Impact of increasing fruit and vegetables and flavonoid intake on the human gut microbiota. Food & function. 2016;7(4):1788-96.
156. Ze X, Duncan SH, Louis P, Flint HJ. Ruminococcus bromii is a keystone species for the degradation of resistant starch in the human colon. Isme j. 2012;6(8):1535-43.
157. Le Leu RK, Winter JM, Christophersen CT, Young GP, Humphreys KJ, Hu Y, et al. Butyrylated starch intake can prevent red meat-induced O6-methyl-2-deoxyguanosine adducts in human rectal tissue: a randomised clinical trial. The British journal of nutrition. 2015;114(2):220-30.
158. Duncan SH, Russell WR, Quartieri A, Rossi M, Parkhill J, Walker AW, et al. Wheat bran promotes enrichment within the human colonic microbiota of butyrate-producing bacteria that release ferulic acid. Environmental microbiology. 2016;18(7):2214-25.
159. Rehman A, Heinsen F-A, Koenen ME, Venema K, Knecht H, Hellmig S, et al. Effects of probiotics and antibiotics on the intestinal homeostasis in a computer controlled model of the large intestine. BMC Microbiology. 2012;12(1):47.
160. Desai MS, Seekatz AM, Koropatkin NM, Kamada N, Hickey CA, Wolter M, et al. A Dietary Fiber-Deprived Gut Microbiota Degrades the Colonic Mucus Barrier and Enhances Pathogen Susceptibility. Cell. 2016;167(5):1339-53.e21.
161. Sun Y, Zhou L, Fang L, Su Y, Zhu W. Responses in colonic microbial community and gene expression of pigs to a long-term high resistant starch diet. Front Microbiol. 2015;6:877-.
162. La Rosa SL, Leth ML, Michalak L, Hansen ME, Pudlo NA, Glowacki R, et al. The human gut Firmicute Roseburia intestinalis is a primary degrader of dietary β-mannans. Nature Communications. 2019;10(1):905.
163. Wang J, Qin C, He T, Qiu K, Sun W, Zhang X, et al. Alfalfa-containing diets alter luminal microbiota structure and short chain fatty acid sensing in the caecal mucosa of pigs. J Anim Sci Biotechnol. 2018;9:11-.

164. Smith DL, Keshavan P, Avissar U, Ahmed K, Zucker SD. Sodium taurocholate inhibits intestinal adenoma formation in APCMin/+ mice, potentially through activation of the farnesoid X receptor. Carcinogenesis. 2010;31(6):1100-9.
165. Jones BV, Begley M, Hill C, Gahan CGM, Marchesi JR. Functional and comparative metagenomic analysis of bile salt hydrolase activity in the human gut microbiome. Proceedings of the National Academy of Sciences. 2008;105(36):13580-5.
166. Heinken A, Ravcheev DA, Baldini F, Heirendt L, Fleming RMT, Thiele I. Personalized modeling of the human gut microbiome reveals distinct bile acid deconjugation and biotransformation potential in healthy and IBD individuals. bioRxiv. 2017:229138.
167. Franz CM, Specht I, Haberer P, Holzapfel WH. Bile salt hydrolase activity of Enterococci isolated from food: screening and quantitative determination. Journal of food protection. 2001;64(5):725-9.
168. Zackular JP, Baxter NT, Iverson KD, Sadler WD, Petrosino JF, Chen GY, et al. The Gut Microbiome Modulates Colon Tumorigenesis. mBio. 2013;4(6):e00692-13.
169. Hibberd AA, Lyra A, Ouwehand AC, Rolny P, Lindegren H, Cedgård L, et al. Intestinal microbiota is altered in patients with colon cancer and modified by probiotic intervention. BMJ Open Gastroenterol. 2017;4(1):e000145.
170. Yang L, Pei Z. Bacteria, inflammation, and colon cancer. World journal of gastroenterology. 2006;12(42):6741-6.
171. Zhang J, Jiao Y, Hou S, Tian T, Yuan Q, Hao H, et al. S100A4 contributes to colitis development by increasing the adherence of Citrobacter rodentium in intestinal epithelial cells. Scientific Reports. 2017;7(1):12099.
172. Chandrakesan P, Ahmed I, Anwar T, Wang Y, Sarkar S, Singh P, et al. Novel changes in NF-{kappa}B activity during progression and regression phases of hyperplasia: role of MEK, ERK, and p38. The Journal of biological chemistry. 2010;285(43):33485-98.
173. Umar S. Citrobacter Infection and Wnt signaling. Current colorectal cancer reports. 2012;8(4):10.1007/s11888-012-0143-4.
174. Barthold SW, Jonas AM. Morphogenesis of early 1, 2-dimethylhydrazine-induced lesions and latent period reduction of colon carcinogenesis in mice by a variant of Citrobacter freundii. Cancer Res. 1977;37(12):4352-60.
175. Newman JV, Kosaka T, Sheppard BJ, Fox JG, Schauer DB. Bacterial infection promotes colon tumorigenesis in Apc(Min/+) mice. The Journal of infectious diseases. 2001;184(2):227-30.
176. Kang E, Zhou G, Yousefi M, Cayrol R, Xia J, Gruenheid S. Loss of disease tolerance during Citrobacter rodentium infection is associated with impaired epithelial differentiation and hyperactivation of T cell responses. Scientific Reports. 2018;8(1):847.
177. Borenshtein D, Nambiar PR, Groff EB, Fox JG, Schauer DB. Development of Fatal Colitis in FVB Mice Infected with Citrobacter rodentium. Infection and immunity. 2007;75(7):3271-81.
178. Hoffmann C, Hill DA, Minkah N, Kirn T, Troy A, Artis D, et al. Community-Wide Response of the Gut Microbiota to Enteropathogenic Citrobacter rodentium Infection Revealed by Deep Sequencing. Infection and immunity. 2009;77(10):4668-78.
179. Vong L, Pinnell LJ, Määttänen P, Yeung CW, Lurz E, Sherman PM. Selective enrichment of commensal gut bacteria protects against Citrobacter rodentium-induced colitis. American Journal of Physiology-Gastrointestinal and Liver Physiology. 2015;309(3):G181-G92.
180. Liu S, Li E, Sun Z, Fu D, Duan G, Jiang M, et al. Altered gut microbiota and short chain fatty acids in Chinese children with autism spectrum disorder. Scientific reports. 2019;9(1):287-.

181. Song Y, Malmuthuge N, Steele MA, Guan LL. Shift of hindgut microbiota and microbial short chain fatty acids profiles in dairy calves from birth to pre-weaning. FEMS Microbiology Ecology. 2017;94(3).
182. Barcenilla A, Pryde SE, Martin JC, Duncan SH, Stewart CS, Henderson C, et al. Phylogenetic Relationships of Butyrate-Producing Bacteria from the Human Gut. Applied and environmental microbiology. 2000;66(4):1654-61.
183. Ottman N, Reunanen J, Meijerink M, Pietilä TE, Kainulainen V, Klievink J, et al. Pili-like proteins of Akkermansia muciniphila modulate host immune responses and gut barrier function. PloS one. 2017;12(3):e0173004.
184. Shin NR, Lee JC, Lee HY, Kim MS, Whon TW, Lee MS, et al. An increase in the Akkermansia spp. population induced by metformin treatment improves glucose homeostasis in diet-induced obese mice. Gut. 2014;63(5):727-35.
185. Chia LW, Hornung BVH, Aalvink S, Schaap PJ, de Vos WM, Knol J, et al. Deciphering the trophic interaction between Akkermansia muciniphila and the butyrogenic gut commensal Anaerostipes caccae using a metatranscriptomic approach. Antonie Van Leeuwenhoek. 2018;111(6):859-73.
186. Geerlings SY, Kostopoulos I, de Vos WM, Belzer C. Akkermansia muciniphila in the Human Gastrointestinal Tract: When, Where, and How? Microorganisms. 2018;6(3).
187. Belzer C, Chia LW, Aalvink S, Chamlagain B, Piironen V, Knol J, et al. Microbial Metabolic Networks at the Mucus Layer Lead to Diet-Independent Butyrate and Vitamin B₁₂ Production by Intestinal Symbionts. mBio. 2017;8(5):e00770-17.
188. Bodogai M, O'Connell J, Kim K, Kim Y, Moritoh K, Chen C, et al. Commensal bacteria contribute to insulin resistance in aging by activating innate B1a cells. Science translational medicine. 2018;10(467).
189. Jakobsdottir G, Xu J, Molin G, Ahrné S, Nyman M. High-fat diet reduces the formation of butyrate, but increases succinate, inflammation, liver fat and cholesterol in rats, while dietary fibre counteracts these effects. PloS one. 2013;8(11):e80476-e.
190. Linares DM, Gómez C, Renes E, Fresno JM, Tornadijo ME, Ross RP, et al. Lactic Acid Bacteria and Bifidobacteria with Potential to Design Natural Biofunctional Health-Promoting Dairy Foods. Front Microbiol. 2017;8:846-.
191. Sekine K, Toida T, Saito M, Kuboyama M, Kawashima T, Hashimoto Y. A new morphologically characterized cell wall preparation (whole peptidoglycan) from Bifidobacterium infantis with a higher efficacy on the regression of an established tumor in mice. Cancer Res. 1985;45(3):1300-7.
192. Rowland IR, Rumney CJ, Coutts JT, Lievense LC. Effect of Bifidobacterium longum and inulin on gut bacterial metabolism and carcinogen-induced aberrant crypt foci in rats. Carcinogenesis. 1998;19(2):281-5.
193. Le Leu RK, Hu Y, Brown IL, Woodman RJ, Young GP. Synbiotic intervention of Bifidobacterium lactis and resistant starch protects against colorectal cancer development in rats. Carcinogenesis. 2010;31(2):246-51.
194. Rafter J, Bennett M, Caderni G, Clune Y, Hughes R, Karlsson PC, et al. Dietary synbiotics reduce cancer risk factors in polypectomized and colon cancer patients. The American journal of clinical nutrition. 2007;85(2):488-96.
195. Riviere A, Gagnon M, Weckx S, Roy D, De Vuyst L. Mutual Cross-Feeding Interactions between Bifidobacterium longum subsp. longum NCC2705 and Eubacterium rectale ATCC 33656 Explain the Bifidogenic and Butyrogenic Effects of Arabinoxylan Oligosaccharides. Applied and environmental microbiology. 2015;81(22):7767-81.
196. Fukuda S, Toh H, Hase K, Oshima K, Nakanishi Y, Yoshimura K, et al. Bifidobacteria can protect from enteropathogenic infection through production of acetate. Nature. 2011;469(7331):543-7.

197. Herrmann E, Young W, Reichert-Grimm V, Weis S, Riedel CU, Rosendale D, et al. In Vivo Assessment of Resistant Starch Degradation by the Caecal Microbiota of Mice Using RNA-Based Stable Isotope Probing-A Proof-of-Principle Study. Nutrients. 2018;10(2):179.
198. Higgins JA, Brown IL. Resistant starch: a promising dietary agent for the prevention/treatment of inflammatory bowel disease and bowel cancer. Current opinion in gastroenterology. 2013;29(2):190-4.
199. Ferrario C, Statello R, Carnevali L, Mancabelli L, Milani C, Mangifesta M, et al. How to Feed the Mammalian Gut Microbiota: Bacterial and Metabolic Modulation by Dietary Fibers. Front Microbiol. 2017;8:1749-.
200. Zhao Q, Ou J, Huang C, Qiu R, Wang Y, Liu F, et al. Absorption of 1-Dicysteinethioacetal-5-Hydroxymethylfurfural in Rats and Its Effect on Oxidative Stress and Gut Microbiota. Journal of agricultural and food chemistry. 2018;66(43):11451-8.
201. Ley RE. Prevotella in the gut: choose carefully. Nature Reviews Gastroenterology &Amp; Hepatology. 2016;13:69.
202. Ohkawara S, Furuya H, Nagashima K, Asanuma N, Hino T. Oral Administration of Butyrivibrio fibrisolvens, a Butyrate-Producing Bacterium, Decreases the Formation of Aberrant Crypt Foci in the Colon and Rectum of Mice. The Journal of Nutrition. 2005;135(12):2878-83.
203. Ohkawara S, Furuya H, Nagashima K, Asanuma N, Hino T. Effect of oral administration of Butyrivibrio fibrisolvens MDT-1, a gastrointestinal bacterium, on 3-methylcholanthrene-induced tumor in mice. Nutrition and cancer. 2007;59(1):92-8.
204. Sokol H, Pigneur B, Watterlot L, Lakhdari O, Bermúdez-Humarán LG, Gratadoux J-J, et al. Faecalibacterium prausnitzii is an anti-inflammatory commensal bacterium identified by gut microbiota analysis of Crohn disease patients. Proceedings of the National Academy of Sciences. 2008;105(43):16731-6.
205. Lim S, Chang D-H, Ahn S, Kim B-C. Whole genome sequencing of "Faecalibaculum rodentium" ALO17, isolated from C57BL/6J laboratory mouse feces. Gut Pathog. 2016;8:3-.
206. Wang J, Li Y, Zhao L, Ren F, Guo H. Lactoferrin stimulates the expression of vitamin D receptor in vitamin D deficient mice. Journal of Functional Foods. 2019;55:48-56.
207. Han S, Li T, Ellis E, Strom S, Chiang JY. A novel bile acid-activated vitamin D receptor signaling in human hepatocytes. Molecular endocrinology (Baltimore, Md). 2010;24(6):1151-64.
208. Zhang C, Zhang M, Pang X, Zhao Y, Wang L, Zhao L. Structural resilience of the gut microbiota in adult mice under high-fat dietary perturbations. The ISME journal. 2012;6(10):1848-57.
209. Chiodini RJ, Dowd SE, Chamberlin WM, Galandiuk S, Davis B, Glassing A. Microbial Population Differentials between Mucosal and Submucosal Intestinal Tissues in Advanced Crohn's Disease of the Ileum. PloS one. 2015;10(7):e0134382-e.
210. Wang T, Cai G, Qiu Y, Fei N, Zhang M, Pang X, et al. Structural segregation of gut microbiota between colorectal cancer patients and healthy volunteers. The ISME journal. 2012;6(2):320-9.
211. Zhang Q, Wu Y, Wang J, Wu G, Long W, Xue Z, et al. Accelerated dysbiosis of gut microbiota during aggravation of DSS-induced colitis by a butyrate-producing bacterium. Scientific Reports. 2016;6:27572.
212. Zhu J, Kong Y, Yu J, Shao S, Mao M, Zhao M, et al. Consumption of drinking water N-Nitrosamines mixture alters gut microbiome and increases the obesity risk in young male rats. Environmental Pollution. 2019;248:388-96.
213. Fulbright LE, Ellermann M, Arthur JC. The microbiome and the hallmarks of cancer. PLoS Pathog. 2017;13(9):e1006480-e.

214. Dziarski R, Park SY, Kashyap DR, Dowd SE, Gupta D. Pglyrp-Regulated Gut Microflora Prevotella falsenii, Parabacteroides distasonis and Bacteroides eggerthii Enhance and Alistipes finegoldii Attenuates Colitis in Mice. PloS one. 2016;11(1):e0146162.
215. Scanlan PD, Shanahan F, Marchesi JR. Culture-independent analysis of desulfovibrios in the human distal colon of healthy, colorectal cancer and polypectomized individuals. Fems Microbiology Ecology. 2009;69(2):213-21.
216. Balamurugan R, Rajendiran E, George S, Samuel GV, Ramakrishna BS. Real-time polymerase chain reaction quantification of specific butyrate-producing bacteria, Desulfovibrio and Enterococcus faecalis in the feces of patients with colorectal cancer. Journal of gastroenterology and hepatology. 2008;23(8 Pt 1):1298-303.
217. Chen L, Jiang B, Zhong C, Guo J, Zhang L, Mu T, et al. Chemoprevention of colorectal cancer by black raspberry anthocyanins involved the modulation of gut microbiota and SFRP2 demethylation. Carcinogenesis. 2018;39(3):471-81.
218. Ajouz H, Mukherji D, Shamseddine A. Secondary bile acids: an underrecognized cause of colon cancer. World J Surg Oncol. 2014;12:164-.
219. Degirolamo C, Modica S, Palasciano G, Moschetta A. Bile acids and colon cancer: Solving the puzzle with nuclear receptors. Trends in molecular medicine. 2011;17(10):564-72.
220. Saracut C, Molnar C, Russu C, Todoran N, Vlase L, Turdean S, et al. Secondary bile acids effects in colon pathology. Experimental mice study. Acta cirurgica brasileira. 2015;30(9):624-31.
221. Hori T, Matsumoto K, Sakaitani Y, Sato M, Morotomi M. Effect of dietary deoxycholic acid and cholesterol on fecal steroid concentration and its impact on the colonic crypt cell proliferation in azoxymethane-treated rats. Cancer Lett. 1998;124(1):79-84.
222. Sayin SI, Wahlstrom A, Felin J, Jantti S, Marschall HU, Bamberg K, et al. Gut microbiota regulates bile acid metabolism by reducing the levels of tauro-beta-muricholic acid, a naturally occurring FXR antagonist. Cell metabolism. 2013;17(2):225-35.
223. Neimark E, Chen F, Li X, Shneider BL. Bile acid-induced negative feedback regulation of the human ileal bile acid transporter. Hepatology (Baltimore, Md). 2004;40(1):149-56.
224. Modica S, Murzilli S, Salvatore L, Schmidt DR, Moschetta A. Nuclear bile acid receptor FXR protects against intestinal tumorigenesis. Cancer Res. 2008;68(23):9589-94.
225. Fu T, Coulter S, Yoshihara E, Oh TG, Fang S, Cayabyab F, et al. FXR Regulates Intestinal Cancer Stem Cell Proliferation. Cell. 2019;176(5):1098-112.e18.

Chapter 4

Time course analysis of the gastrointestinal microbiome of APC^{MIN} mice and its association with bile acid signalling

4.0 Abstract

Background: The gut microbiota has been implicated in the initiation and development of colorectal cancer (CRC). Research into the role of the microbiota in CRC has primarily focussed on changes that exist in and around tumour sites at a single point in time. This has made it difficult to differentiate between changes that promote cancer initiation from those that are a result of tumour development. In this study, we tracked changes in the microbiota throughout the course of tumorigenesis in APC^{MIN} mice, a model of familial CRC, to elucidate their potential contribution to disease. In addition, we measured plasma and faecal bile acids and targeted gene expression at the end-point of the study. Our aim was to establish the temporal development of the microbiota in APC^{MIN} mice in order to generate a timeline of alterations and events that may influence tumorigenesis in these animals.

Methods: The faecal microbiome was analysed by 16S rRNA gene sequencing, and faecal and plasma bile acids were determined by UPLC-MS at 14 weeks of age. Host cytokine response, proliferation index, bile acid signalling and polyp multiplicity was measured at Week 14. Correlation analysis was performed to identify any relationships between microbial composition and diversity, transcription of inflammatory cytokines and bile acids.

Results: The gut microbiota of APC^{MIN} mice differs significantly from controls at each time-point analysed. In particular, we identified bacterial taxa that are consistently altered in APC^{MIN} mice throughout the study. These included a reduction of *Akkermansia*, *Bacteroides* and *Lachnospiraceae* species and an increase in *Eubacterium* species in APC^{MIN} mice relative to control animals. Further taxa (including *Allobaculum* and *Lachnoclostridium*) were prone to significant variation throughout the study, a finding which may indicate sensitivity to the changing histopathological landscape associated with tumorigenesis. Only slight differences were observed in the bile acid pool at end-point, with a reduction in plasma lithocholic acid evident in APC^{MIN} mice relative to control animals. Analysis of FXR-regulated gene expression

in the ileum and correlation analysis suggests a suppression of FXR signalling which has previously been linked to tumorigenesis. The metagenome predicted by PICRUSt also identified disruption to bile acid metabolising pathways at 7 weeks of age.

Conclusions: We identified a number of bacterial taxa in APC^{MIN} mice that are changed at key points during tumour onset and progression. We also implicate bile acid signalling in small intestine polyposis in these mice.

Acknowledgements: 16S rRNA gene sequencing of the faecal microbiota was performed by Calum Walsh in Teagasc Moorepark (*Materials and Methods* section 2.5, *Amplicon Sequencing* to end of *Functional Analysis*), who also produced the plots in Figure 4.3 and 4.13. UPLC-MS and extraction from faecal and plasma samples for the detection of bile acids was performed by Peter Cronin (*Materials and Methods* section 2.7, *Ultra-Performance Liquid Chromatography – Mass Spectrometry)*. Some of this work is presented in his submitted MRes thesis (April 2019). The materials and methods sections for these processes are provided by their respective executors. Mice were culled by Cara Hueston.

4.1 Introduction

The onset and development of colorectal cancer (CRC) involves the complex interaction of genetic and environmental factors. Recently, attention has turned to the influence of the gut microbiota on this process (1). Cancer patients display a gut microbial composition that is significantly different to healthy counterparts and certain microbial patterns are associated with increased cancer risk. However, definitive identification of mechanisms and bacterial species involved has proven elusive as taxa associated with human CRC are not consistent across studies (2, 3).

Research into the microbiota in CRC has focussed on patients presenting with active disease, which has left the dynamic interaction of host and microbiota unexplored during the earliest stages of disease onset (4). Animal models provide an inexpensive and predictable tool for the investigation of these stages by allowing timed sampling of large cohorts in controlled conditions. Mice heterozygous for the tumour-suppressor *Apc* gene represent an animal model of familial colorectal cancer (CRC). These mice develop intestinal polyps starting at 7-8 weeks of age, with inflammation becoming apparent at approximately 12 weeks of age (5, 6). Humans with this mutation suffer from Familial Adenomatous Polyposis (FAP) and these patients exhibit dozens of adenomatous polyps in their large intestine with a risk of progressing to malignant CRC approaching 100% in middle age. The microbiota of FAP patients are enriched for pro-tumorigenic bacteria such as *Escherichia coli* expressing colibactin and enterotoxigenic *Bacteroides fragilis* (7), changes which are reflected in APC^{MIN} mice (5). Importantly, APC^{MIN} mice have been utilised to study the role of the microbiota in the progression of CRC and human tumour-associated bacteria have been shown to aggravate tumorigenesis in these mice (8).

One possible mechanism by which the gut microbiota may affect host processes leading to the development of CRC is the production of bacterial metabolites. Aberrant microbial

metabolism of bile salts is associated with cancer risk (9). For example, APC^{MIN} mice fed deoxycholic acid (DCA) had increased tumour multiplicity, and this effect was mediated by the microbiota (10). Bile acids can also modify cancer risk via hormone signalling through the bile acid receptor FXR which suppresses intestinal tumorigenesis *in vivo* (11). High fat diets are also known to increase CRC risk, and also increase bile acid excretion and the faecal concentrations of DCA and lithocholic acid (LCA) (12, 13). This suggests that bile acids and the microorganisms involved in bile acid metabolism may represent potential aetiologic agents of high fat diet-induced colon cancer risk.

Disruption of the normal function of the intestinal immune response may also affect CRC risk (14). Cytokines and chemokines are soluble immune factors which can drive tumorigenesis by production of genotoxic compounds such as reactive oxygen species, by induction of DNA damage and by suppression of apoptosis (15). They are produced by tumour cells, stromal cells and tumour-infiltrating immune cells (16-20). There is also evidence that the microbiota is involved in the regulation of cytokines and chemokines in mouse models of CRC, especially by production of short chain fatty acids such as butyrate (21-27).

To our knowledge, the temporal flux of the community structure of the microbiota has not been previously analysed in APC^{MIN} mice. Such an analysis has the potential to reveal microbial species which distinguish the microbiota of such mice from wild-type counterparts and which may be linked to disease progression. We therefore performed a time-course study of the APC^{MIN} mouse, to examine the progression of microbial changes during disease onset. At the end-point of the experiment, we measured polyp multiplicity, markers of host inflammation and the production of microbial metabolites to identify phenotypic markers of disease progression. Data indicate a distinct microbial profile in APC^{MIN} mice which differs from wild-type animals and coincides with enriched α-diversity and reduced transcription of FXR target genes.

4.2 Results

4.2.1 APC^{MIN} mice develop significantly more polyps in their small intestine

APC^{MIN} mice are a model of familial CRC which develop dozens of polyps in the small intestine and a smaller number in the colon. As expected, we observed significantly more polyps in each segment of the small intestine of APC^{MIN} mice than our wild-type control (Figure 4.1A; T-test and MWU-test, $p<0.001$). All APC^{MIN} mice developed small intestine polyps while none were detected in control. Five APC^{MIN} mice also developed colonic polyps (Figure 4.1A; MWU-test, $p=0.063$).

4.2.2 Faecal microbial diversity is significantly different in APC^{MIN} mice

We collected faecal pellets from each mouse throughout the experiment and performed 16S rRNA gene sequencing at 4, 7, 11 and 14 weeks of age to characterise the microbial community and investigate changes that occur before and during the process of tumorigenesis in APC^{MIN} mice. Alpha (α)-diversity was measured by Shannon diversity and phylogenetic diversity (PD) (Figure 4.2).

At Week 4, both Shannon and PD were increased in APC^{MIN} mice, and Shannon diversity was also increased at Week 14 (Figure 4.2; MWU-test with FDR adjustment, $p<0.05$). No differences were observed at Week 7 or Week 11 (Figure 4.2; MWU-test with FDR adjustment, $p>0.05$).

Beta (β)-diversity is a measure of between-individual diversity in the microbiota which we measured by PERMANOVA of the unweighted Unifrac distances, visualised by PCoA. The

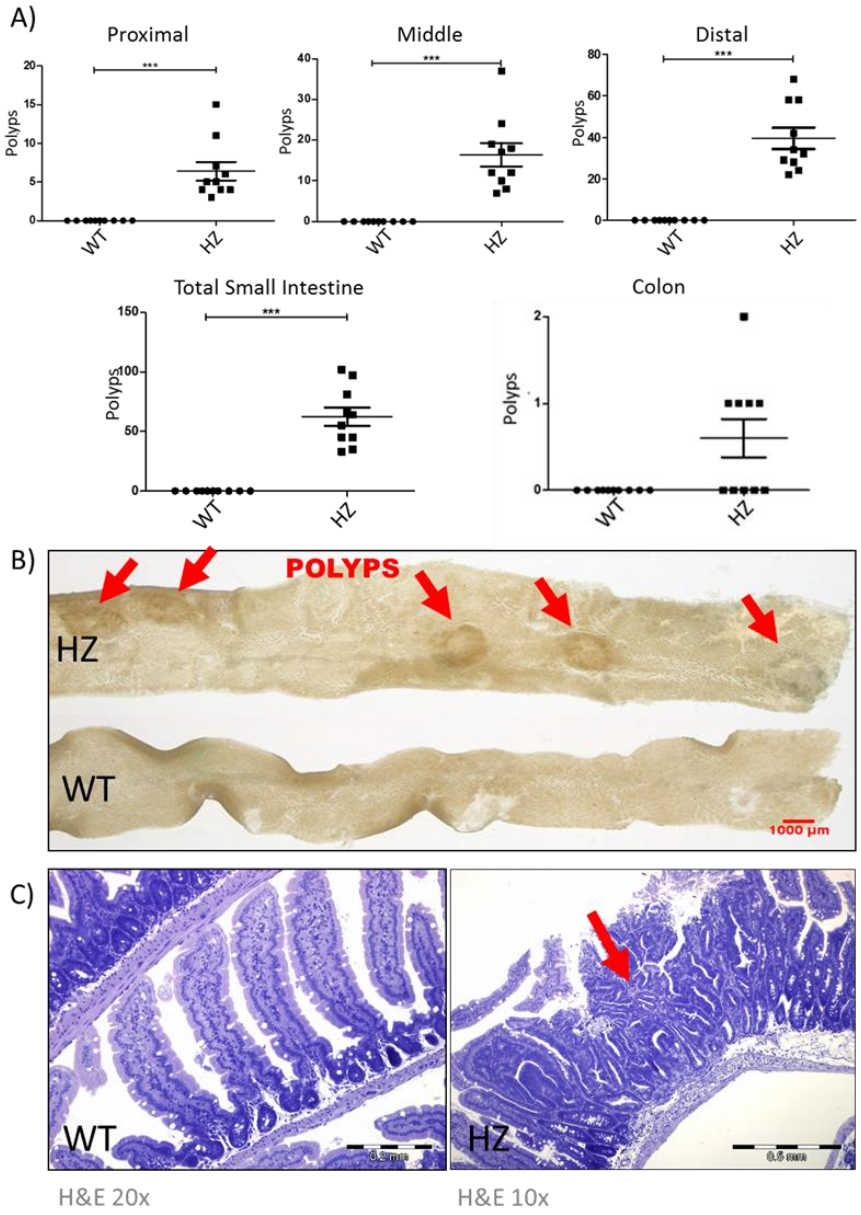

Figure 4.1: APC^{MIN} mice develop significantly more polyps in the small intestine. Mice were culled at 14 weeks of age (*n*=10 per group) and 1cm of their proximal and distal small and large intestine was removed for RNA analysis. The remaining small intestine was divided into three equal portions and the number of polyps in each section was enumerated under a dissecting microscope. The number of polyps in the colon was also determined. ***A)*** APC^{MIN} mice (HZ) had significantly more polyps than controls (WT) in each portion of their small intestine and significantly more total small intestine polyps (T-test, P<0.001). The total number of colonic polyps was not significantly different between groups despite being completely absent in the control group due to the low prevalence of colonic adenomas in APC^{MIN} mice (MWU test, P=0.063). ***B)*** A length of the distal small intestine of an APC^{MIN} mouse and its wild-type equivalent. The APC^{MIN} section displays adenomatous polyps, highlighted by red arrows. ***C)*** After polyps were enumerated, intestinal sections were paraffin-embedded and sectioned for microscopic analysis. Normal wild-type intestinal villi stained with haematoxylin and eosin (H&E) are presented here, as well as an adenomatous polyp from an APC^{MIN} mouse.

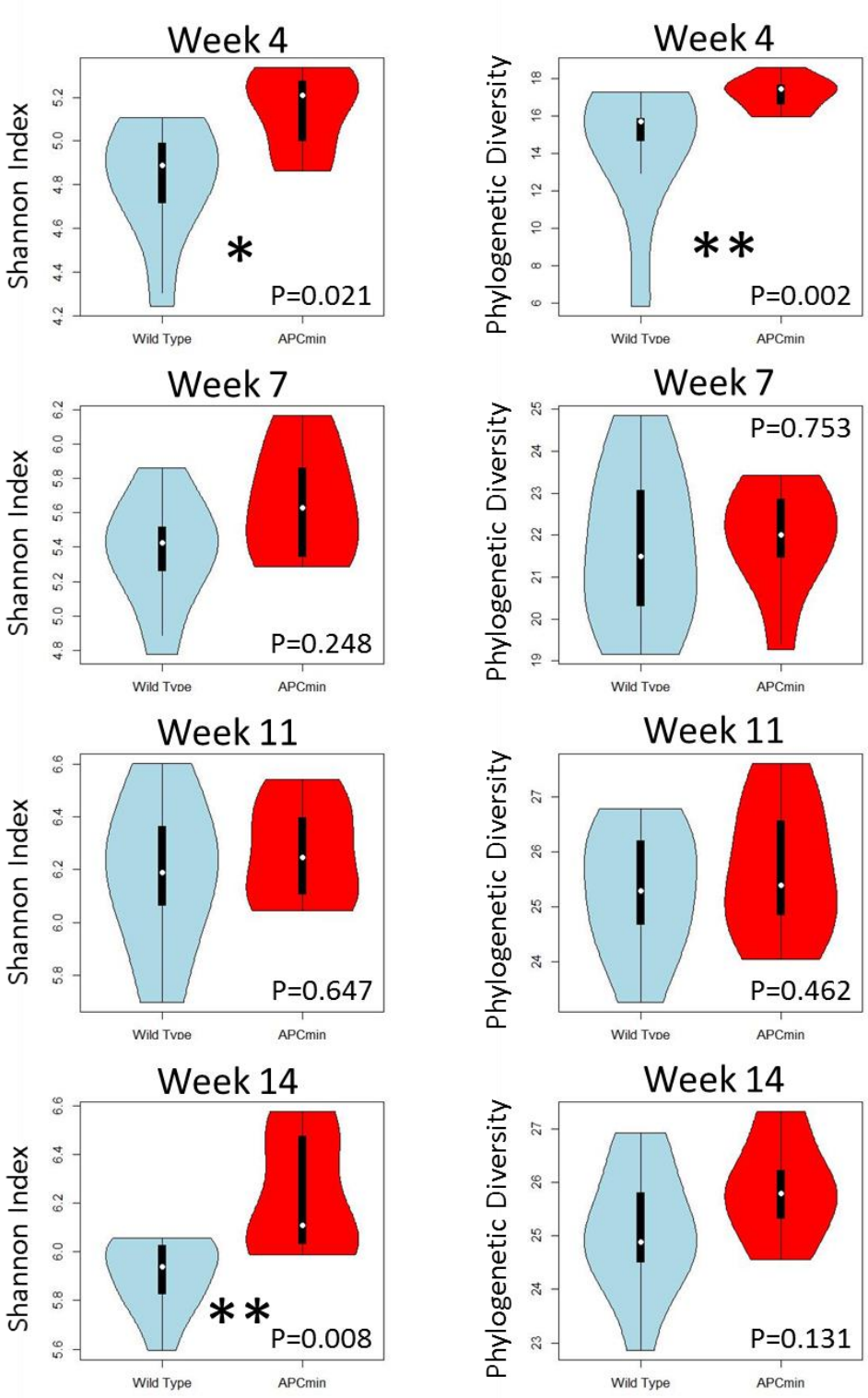

Figure 4.2: Alpha (α)-diversity is significantly altered in APC^{MIN} mice at both Weeks 4 and 14. We performed 16S rRNA gene sequencing for the V3-V4 region of the faecal microbial rRNA and examined the α-diversity by generating the Shannon and Phylogenetic Diversity (PD) metrics. Both of these metrics were significantly different between control and APC^{MIN} animals at Week 4, while only Shannon diversity was different at Week 8. Neither measure of α-diversity was altered between groups at Week 7 or Week 11. *N*=8 per group for Weeks 4-11, *n*=10 per group for Week 14.

communities were significantly different at each time-point, while the genotype explained between 21% and 15% of the difference between groups (Figure 4.3; PERMANOVA, P<0.001).

Finally, we considered individual species differences between groups. The significantly different species are presented in Figure 4.4 (MWU-test with FDR adjustment, p<0.05). At Week 4, eight taxa were decreased in APC^{MIN} mice and twelve were increased. The greatest changes were seen in *Eubacterium ventriosum*, which was 440-fold higher in relative abundance in WT mice, and in *Ruminiclostridium 6* which was 953-fold higher in APC^{MIN}, while *Christensenellaceae; Uncultured*, *Coriobacteriaceae UCG-002* and *Rhodospirillaceae; Uncultured* were present in APC^{MIN} mice but completely absent in WT. At Week 7, nine taxa were decreased and 26 were increased. *Faecalibaculum* was decreased 109-fold in APC^{MIN} mice while *Lachnospiraceae NC2004 Group* was completely absent from APC^{MIN} mice. *Anaeroplasma*, *Anaerovorax*, *Desulfovibrio* and *Eubacterium fissicatena group* were also common in APC^{MIN} mice despite being present in, at most, one member of the control group. At Week 11, eleven taxa were decreased in APC^{MIN} mice and 19 were increased. *Akkermansia* was 120-fold more abundant in WT mice, while *Lachnospiraceae NC2004 Group*, *Lachnospiraceae; Uncultured Bacterium* and *Papillibacter* were present in two or fewer APC^{MIN} mice. *Anaeroplasma* was 278-fold more abundant in APC^{MIN} while ten taxa were common in this group but present in two or fewer WT mice. At Week 14, seven taxa are decreased in APC^{MIN} mice while 17 are increased. *Lachnospiraceae NC2004 Group* is completely absent in APC^{MIN} mice while *Anaerovorax*, *Catenibacterium*, *Eubacterium ruminantium Group*, *Odoribacter* and *Ruminiclostridium 1* are present in, at most, one APC^{MIN} mouse.

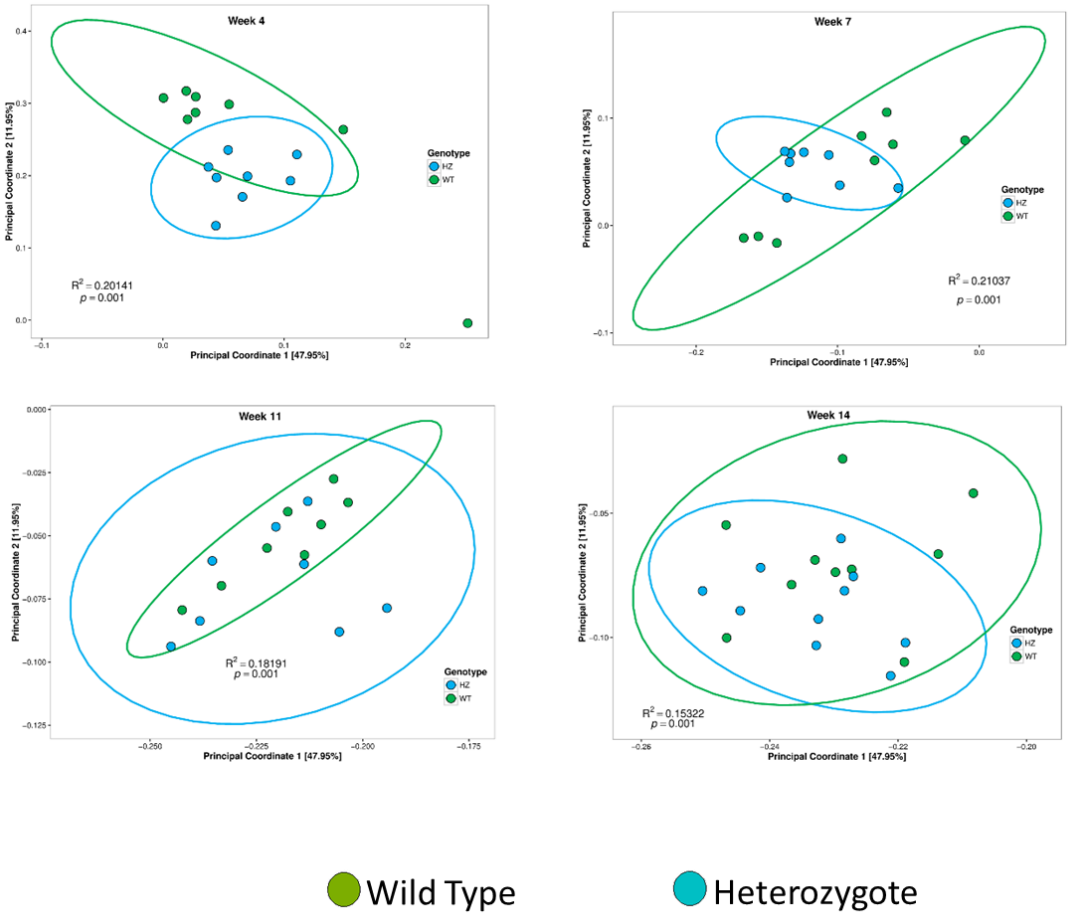

Figure 4.3: Beta (β)-diversity is significantly altered in APC^{MIN} throughout the experiment. We compared the microbial β-diversity between control and APC^{MIN} mice at each time-point by unweighted Unifrac distances, visualised by PCoA. This analysis revealed significant differences between the groups. Figure produced by Calum Walsh at Teagasc, Moorepark.

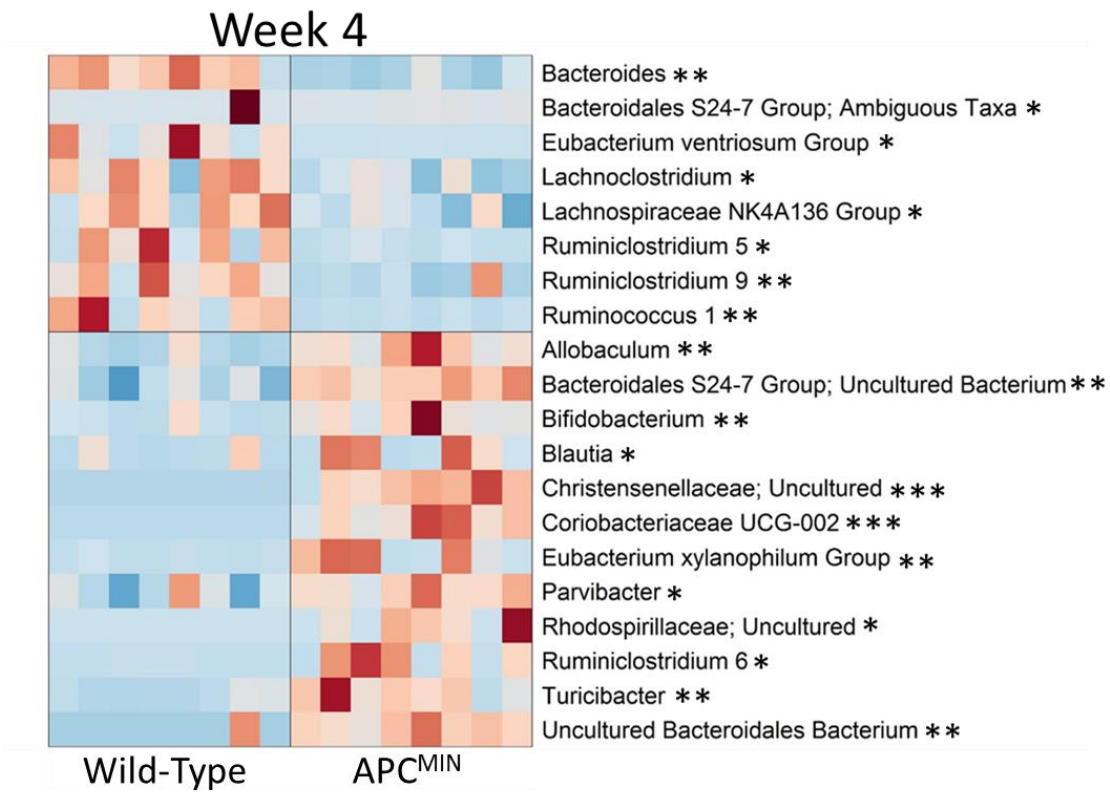
Week 4
Bacteroides **
Bacteroidales S24-7 Group; Ambiguous Taxa *
Eubacterium ventriosum Group *
Lachnoclostridium *
Lachnospiraceae NK4A136 Group *
Ruminiclostridium 5 *
Ruminiclostridium 9 **
Ruminococcus 1 **
Allobaculum **
Bacteroidales S24-7 Group; Uncultured Bacterium **
Bifidobacterium **
Blautia *
Christensenellaceae; Uncultured ***
Coriobacteriaceae UCG-002 ***
Eubacterium xylanophilum Group **
Parvibacter *
Rhodospirillaceae; Uncultured *
Ruminiclostridium 6 *
Turicibacter **
Uncultured Bacteroidales Bacterium **
Wild-Type
APCMIN

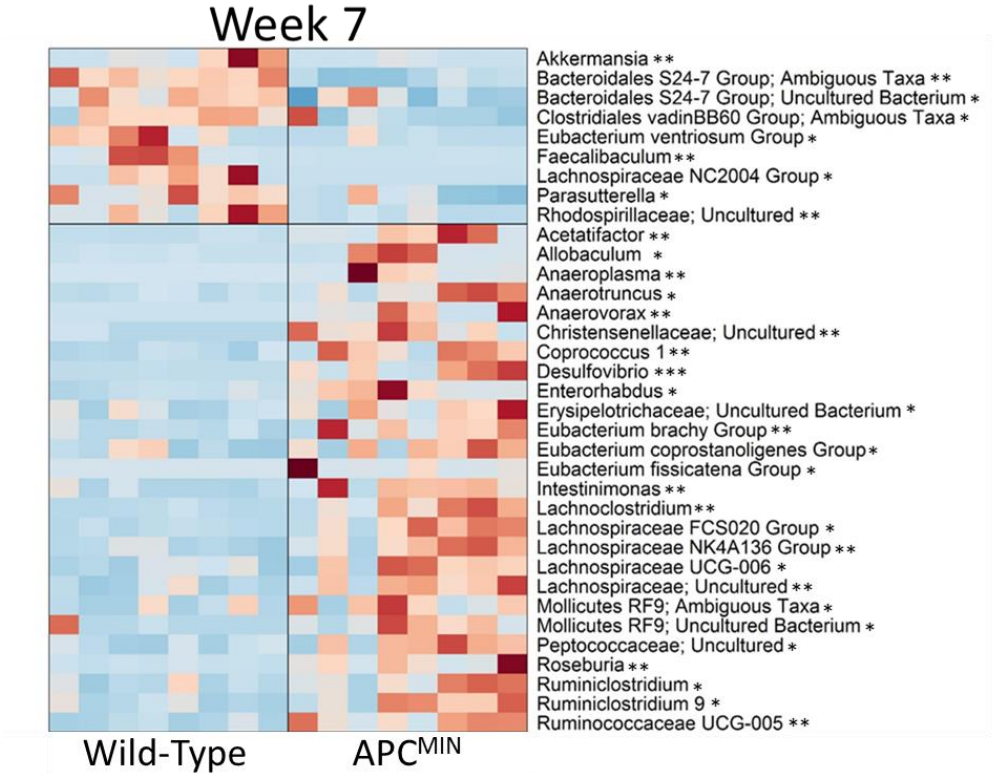
Week 7
Akkermansia **
Bacteroidales S24-7 Group; Ambiguous Taxa **
Bacteroidales S24-7 Group; Uncultured Bacterium *
Clostridiales vadinBB60 Group; Ambiguous Taxa *
Eubacterium ventriosum Group *
Faecalibaculum **
Lachnospiraceae NC2004 Group *
Parasutterella *
Rhodospirillaceae; Uncultured **
Acetatifactor **
Allobaculum *
Anaeroplasma **
Anaerotruncus *
Anaerovorax **
Christensenellaceae; Uncultured **
Coprococcus 1 **
Desulfovibrio ***
Enterorhabdus *
Erysipelotrichaceae; Uncultured Bacterium *
Eubacterium brachy Group **
Eubacterium coprostanoligenes Group *
Eubacterium fissicatena Group *
Intestinimonas **
Lachnoclostridium **
Lachnospiraceae FCS020 Group *
Lachnospiraceae NK4A136 Group **
Lachnospiraceae UCG-006 *
Lachnospiraceae; Uncultured **
Mollicutes RF9; Ambiguous Taxa *
Mollicutes RF9; Uncultured Bacterium *
Peptococcaceae; Uncultured *
Roseburia **
Ruminiclostridium *
Ruminiclostridium 9 *
Ruminococcaceae UCG-005 **
Wild-Type
APCMIN

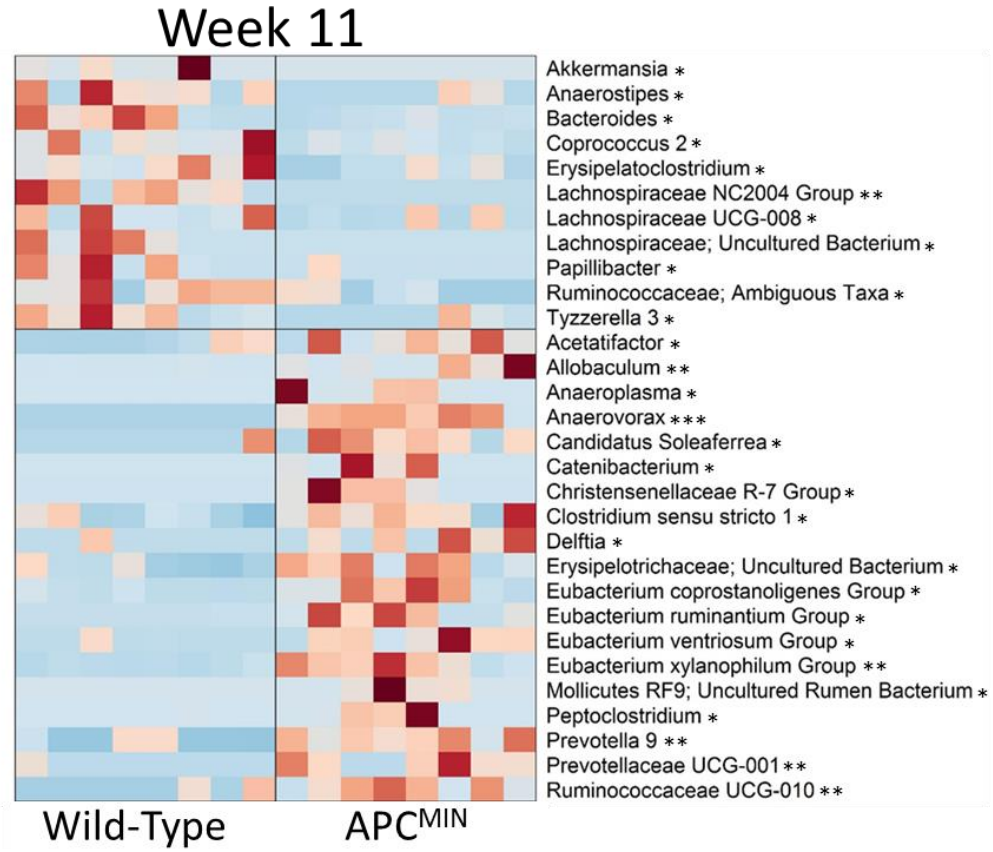
Week 11
Akkermansia *
Anaerostipes *
Bacteroides *
Coprococcus 2 *
Erysipelatoclostridium *
Lachnospiraceae NC2004 Group **
Lachnospiraceae UCG-008 *
Lachnospiraceae; Uncultured Bacterium *
Papillibacter *
Ruminococcaceae; Ambiguous Taxa *
Tyzzerella 3 *
Acetatifactor *
Allobaculum **
Anaeroplasma *
Anaerovorax ***
Candidatus Soleaferrea *
Catenibacterium *
Christensenellaceae R-7 Group *
Clostridium sensu stricto 1 *
Delftia *
Erysipelotrichaceae; Uncultured Bacterium *
Eubacterium coprostanoligenes Group *
Eubacterium ruminantium Group *
Eubacterium ventriosum Group *
Eubacterium xylanophilum Group **
Mollicutes RF9; Uncultured Rumen Bacterium *
Peptoclostridium *
Prevotella 9 **
Prevotellaceae UCG-001 **
Ruminococcaceae UCG-010 **
Wild-Type
APCMIN

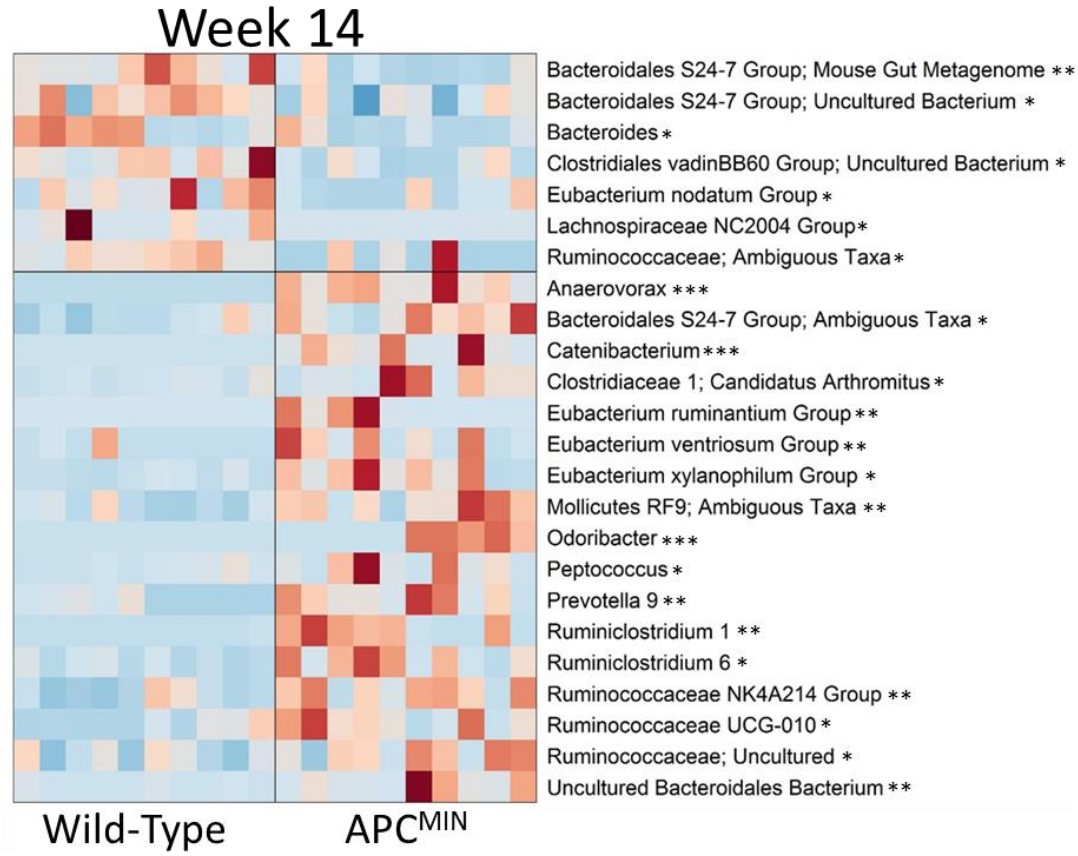
Week 14
Bacteroidales S24-7 Group; Mouse Gut Metagenome **
Bacteroidales S24-7 Group; Uncultured Bacterium *
Bacteroides *
Clostridiales vadinBB60 Group; Uncultured Bacterium *
Eubacterium nodatum Group *
Lachnospiraceae NC2004 Group *
Ruminococcaceae; Ambiguous Taxa *
Anaerovorax ***
Bacteroidales S24-7 Group; Ambiguous Taxa *
Catenibacterium ***
Clostridiaceae 1; Candidatus Arthromitus *
Eubacterium ruminantium Group **
Eubacterium ventriosum Group **
Eubacterium xylanophilum Group *
Mollicutes RF9; Ambiguous Taxa **
Odoribacter ***
Peptococcus *
Prevotella 9 **
Ruminiclostridium 1 **
Ruminiclostridium 6 *
Ruminococcaceae NK4A214 Group **
Ruminococcaceae UCG-010 *
Ruminococcaceae; Uncultured *
Uncultured Bacteroidales Bacterium **
Wild-Type
APCMIN

Figure 4.4: Taxa different significantly between groups. We compared the relative abundance that each taxon comprised in each group. This revealed a number of significantly different bacteria (MWU-test with FDR adjustment, $p<0.05$). Only the significantly different OTUs are presented here. Taxa on the top of each figure are suppressed in APC^{MIN} mice while taxa in the bottom of each figure are enriched in APC^{MIN} mice. Data are presented as Z-scores normalised to the row average. *N*=8 per group for Weeks 4-11, *n*=10 per group for Week 14.

Temporal variations in the microbiota were also considered by highlighting bacteria which differed between APC^{MIN} and WT mice at more than one time-point across the study (MWU-test with FDR adjustment, $p<0.05$). These taxa are presented in Figure 4.5.

In order to investigate the alterations in the gut bacteria at a higher structural level, we defined a set of bacterial co-abundance groups (CAGs) (Figure 4.6A) (28). These correlations were converted to a distance matrix on which PERMANOVA was performed which determined that all CAGs were significantly different (Figure 4.6B, $p<0.05$). The composition of each CAG can be found in Table 4.1.

Eight CAGs were identified, labelled CAG1-8. The relative abundance of CAG1 is increased in APC^{MIN} mice at Week 4 and CAG3 is decreased (T-test, $p<0.01$). CAGs 1 and 7 are decreased in APC^{MIN} mice at Week 7 while CAGs 3, 5, 6 and 8 are increased (T-test and MWU-test, $p<0.05$). At Week 11, only CAG4 is decreased in APC^{MIN} mice (T-test, $p=0.02$), while at Week 14 CAGs 1 and 4 are decreased and CAGs 7 and 8 are increased (T-test, $p<0.05$). Considering CAGs that differ at more than one time-point, CAG1 is increased in APC^{MIN} mice at Week 4, before decreasing in abundance in two later samples. CAG3 is more abundant in WT mice at Week 4 and APC^{MIN} at Week 7, while CAG7 displays the opposite pattern. CAGs 4 and 8 differ at two time-points each but are consistently increased in control group for the former and in the APC^{MIN} group for the latter. CAGs 5 and 6 only differ at Week 7 where they are increased in APC^{MIN}, while CAG2 does not differ at any time-point.

CAG1 is dominated by *Bacteroidales S24-7 group; uncultured bacterium* which makes up more than 90% of this CAG in both groups at each time-point. CAG2 features only five species, with *Eubacterium ventriosum group*, *Clostridiales vadinBB60 group; Ambiguous taxa* and *Marvinbryantia* most prevalent. CAG3 contains 17 species. *Lachnospiraceae NK4A136*

A)

	Week 4	Week 7	Week 11	Week 14
Christensenellaceae; Uncultured	***	**		
Eubacterium xylanophilum Group	**		**	*
Ruminiclostridium 6	*			*
Uncultured Bacteroidales Bacterium	**			**
Acetatifactor		**	*	
Anaeroplasma		**	*	
Erysipelotrichaceae; Uncultured Bacterium		*	*	
Eubacterium coprostanoligenes Group		*	*	
Anaerovorax		**	***	***
Mollicutes RF9; Ambiguous Taxa		*		**
Ruminococcaceae UCG-010			**	*
Catenibacterium			*	***
Eubacterium ruminantium Group			*	**
Prevotella 9			**	**
Bacteroides	**		*	*
Akkermansia		**	*	
Ruminococcaceae; Ambiguous Taxa			*	*
Lachnospiraceae NC2004 Group		*	**	*

B)

	Week 4	Week 7	Week 11	Week 14
Bacteroidales S24-7 Group; Uncultured Bacterium	**	*		*
Rhodospirillaceae; Uncultured	*	**		
Allobaculum	**	*	**	
Lachnoclostridium	*	**		
Lachnospiraceae NK4A136 Group	*	**		
Ruminiclostridium 9	**	*		
Bacteroidales S24-7 Group; Ambiguous Taxa	*	**		*
Eubacterium ventriosum Group	*	*	*	**

Figure 4.5: Taxa which differ at more than one time-point. Understanding the temporal variations of the microbiota over the course of tumorigenesis was a key objective of our study, and identifying taxa which differed at more than one time-point was an important part of this. ***A)*** Taxa that are enriched at more than one time-point in one group. Taxa enriched in APC^{MIN} mice are marked in red and taxa enriched in wild-type controls are marked in blue. ***B)*** Taxa that differ at more than one time-point in different groups. Taxa enriched in APC^{MIN} mice are marked in red and taxa enriched in wild-type controls are marked in blue. *N*=8 per group for Weeks 4-11, *n*=10 per group for Week 14.

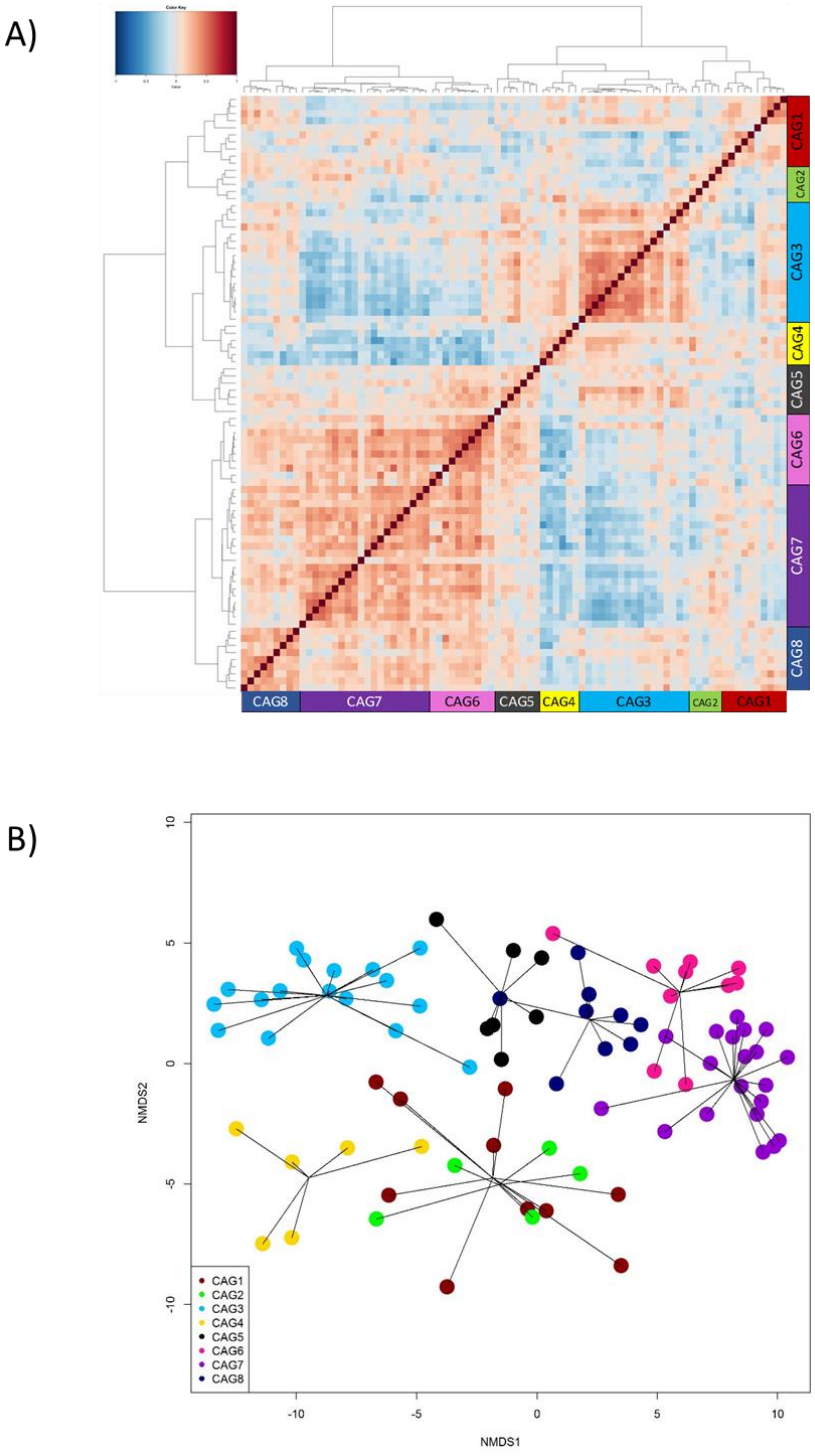

Figure 4.6: Generation of co-abundance groups. The Kendall correlations of OTUs' relative abundance were generated and clustered by Ward-linkage and Pearson correlation. This defines "co-abundance groups" (CAGs) which describe higher-level structures of the microbiota by highlighting taxa for which changes in abundance correlate. These Kendall correlations were then converted to a distance metric and analysed by PERMANOVA which determined that each CAG was significantly different. **A)** A heatplot of Kendall correlation values for each pair of taxa clustered by Ward linkage of their Pearson correlations. Coloured bars along the axes denote the CAGs. The composition if each CAG is presented in Table 4.1. **B)** Non-metric multidimensional scaling (NMDS) of the distance metrics of the CAGs' correlation values.

Table 4.1: CAG Composition

CAG1	Ruminococcaceae UCG-013
	[Eubacterium] nodatum group
	Clostridiales Family XIII; AD3011 group
	Parvibacter
	Escherichia-Shigella
	Bacteroidales S24-7 group; uncultured bacterium
	Coriobacteriaceae UCG-002
	Parasutterella
	Turicibacter
	Bifidobacterium
CAG2	[Eubacterium] ventriosum group
	Staphylococcus
	Clostridiales vadinBB60 group; Ambiguous taxa
	Marvinbryantia
	Lactococcus
CAG3	Ruminococcaceae UCG-005
	Lachnoclostridium
	Ruminiclostridium 5
	Ruminococcus 1
	Peptococcaceae; uncultured
	Acetatifactor
	Ruminococcaceae; uncultured
	Ruminiclostridium 9
	Lachnospiraceae NK4A136 group
	Oscillibacter
	Lachnospiraceae FCS020 group
	Ruminococcaceae UCG-009
	Intestinimonas
	Ruminiclostridium
	Anaerotruncus
	Ruminococcaceae UCG-003
	Lachnospiraceae UCG-006
CAG4	Blautia
	Uncultured Bacteroidales bacterium
	Allobaculum
	Clostridiales vadinBB60 group; uncultured bacterium
	Akkermansia
	Bacteroides
CAG5	Tyzzerella
	Coprococcus 2
	Lachnospiraceae UCG-008
	Lachnospiraceae; uncultured
	[Eubacterium] brachy group
	Butyricicoccus
	Anaerobacillus

CAG6	Ruminococcaceae; Ambiguous taxa
	Coprococcus 1
	Desulfovibrio
	Enterorhabdus
	Roseburia
	Clostridiales Family XIII UCG-001
	Lachnospiraceae UCG-001
	Peptococcus
	Tyzzerella 3
	Gastranaerophilales; uncultured bacterium
CAG7	Prevotella 9
	Coriobacteriaceae; uncultured
	Christensenellaceae; uncultured
	Candidatus Saccharimonas
	Clostridium sensu stricto 1
	Ruminococcaceae UCG-010
	Ruminococcaceae NK4A214 group
	Anaerostipes
	Bacteroidales S24-7 group; mouse gut metagenome
	Erysipelatoclostridium
	Delftia
	Candidatus Arthromitus
	Lactobacillus
	Streptococcus
	Erysipelotrichaceae; uncultured
	Faecalibaculum
	Rhodospirillaceae; uncultured
	Alistipes
	Bacteroidales S24-7 group; Ambiguous taxa
	Ochrobactrum
CAG8	Ruminiclostridium 6
	Anaerovorax
	[Eubacterium] xylanophilum group
	Anaeroplasma
	Mollicutes RF9 uncultured bacterium
	Erysipelotrichaceae; uncultured bacterium
	Ruminococcaceae UCG-014
	[Eubacterium] coprostanoligenes group
	Mollicutes RF9; Ambiguous taxa

group comprises >50% of the abundance of this CAG in both groups at each time-point. CAG4 contains only six species, and *Clostridiales vadinBB60 group; uncultured bacterium*, *Akkermansia* and *Bacteroides* predominate at different time-points. *Lachnospiraceae; uncultured* comprises >80% of CAG5 in each sample. CAG6 is a diverse group, with *Coprococcus 1, Roseburia* and *Lachnospiraceae UCG-001* predominating at different times. Likewise, *Alistipes*, *Bacteroidales S24-7 group; Ambiguous taxa* and *Lactobacillus* are the most common taxon in CAG7 in different samples. *Ruminococcaceae UCG-014* is consistently the highest abundance taxon in CAG8.

4.2.3 Bile acid composition in APC^{MIN} mice

In order to investigate the potential role of microbial bile acid modification in our mouse model, we analysed the faecal and plasma bile acid profile of each group at Week 14 by UPLC-MS. After correction for multiple comparisons, only the plasma concentration of LCA differed between groups (Figure 4.7; T-test, $p<0.001$), and this comprised less than 1% of the total plasma bile acid pool. The list of bile acids measured is presented in Table 4.2. Total bile acid concentration was not significantly different between groups (T-test, $P>0.05$), and there were no differences among the faecal bile acids (T-test and MWU-test, $P>0.05$).

4.2.4 Cell proliferation is not increased in APC^{MIN} mice

Loss of cell cycle control in APC^{MIN} mice has been shown to precede the development of intestinal polyps (5). In order to determine how far this loss of control extends, we measured the degree of proliferation in normal villi in the ileum of APC^{MIN} and control mice at our end-point at Week 14. The expression of proliferation indicator Ki67 did not differ between groups (Figure 4.8; T-test, $p=0.66$).

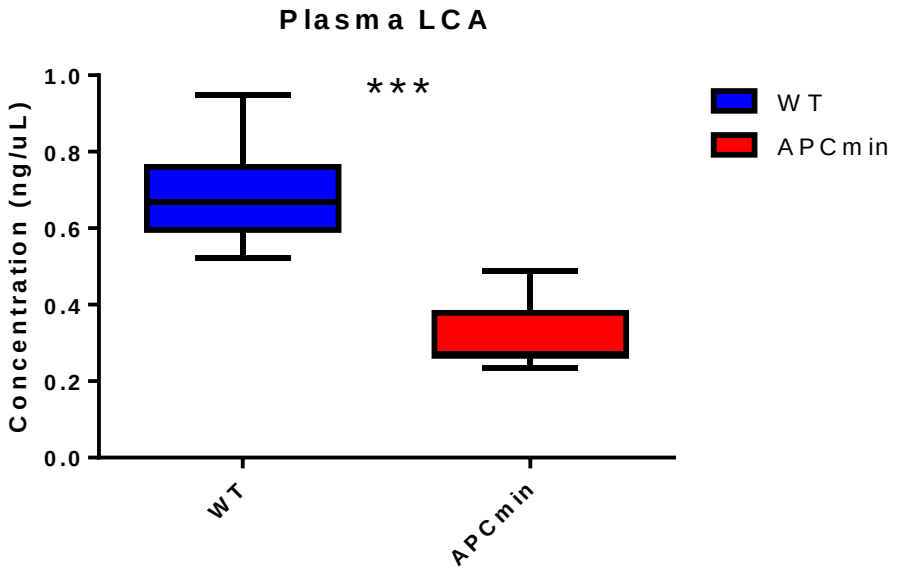

Figure 4.7: Faecal and plasma bile acid composition is largely unchanged in APC^{MIN} mice. Microbial metabolism of bile acids has been implicated in the pathogenesis of colon cancer. To investigate the role bile acids play in our model, we measured the concentration of faecal and plasma bile acids at Week 14 by UPLC-MS. After correction for multiple comparisons, only the concentration of LCA in the plasma was significantly different between groups (T-test and MWU-test with FDR adjustment, $p<0.05$). Each bile acid measured is presented in Table 4.2. *N*=6 for wild-type, *n*=7 for APC^{MIN}.

Table 4.2: Bile acids measured

	Bile Acid	Abbreviation
Bile Acids	Dehydrocholic Acid	DHCA
	Lithocholic Acid	LCA
	Ursodeoxycholic Acid	UDCA
	Chenodeoxycholic Acid	CDCA
	Hyodeoxycholic Acid	HDCA
	Deoxycholic Acid	DCA
	Cholic Acid	CA
	Hyocholic Acid	HCA
	7-Ketolithocholic Acid	7-Keto-LCA
	Tauro-Cholic Acid	T-CA
	Tauro-Hyocholic Acid	T-HCA
	Tauro-Chenodeoxycholic Acid	T-CDCA
	Tauro-Ursodeoxycholic Acid	T-UDCA
	Tauro-Deoxycholic Acid	T-DCA
	Tauro-Hyodeoxycholic Acid	T-HDCA
	Tauro-Lithocholic Acid	T-LCA
	Glyco-Cholic Acid	G-CA
	Glyco-Hyocholic Acid	G-HCA
	Glyco-Chenodeoxycholic Acid	G-CDCA
	Glyco-Ursodeoxycholic Acid	G-UDCA
	Glyco-Deoxycholic Acid	G-DCA
	Glyco-Hyodeoxycholic Acid	G-HDCA
	Glyco-Lithocholic Acid	G-LCA
	Beta (β)-Muricholic Acid	B-MCA
	Alpha/gamma (α/ω)-Muricholic Acid	α/ω-MCA
	Murocholic Acid	MoCA
	Tauro α-, β-, and ω-Muricholic Acid	T-α/β/ω-MCA
	Total Bile Acids	Total BAs

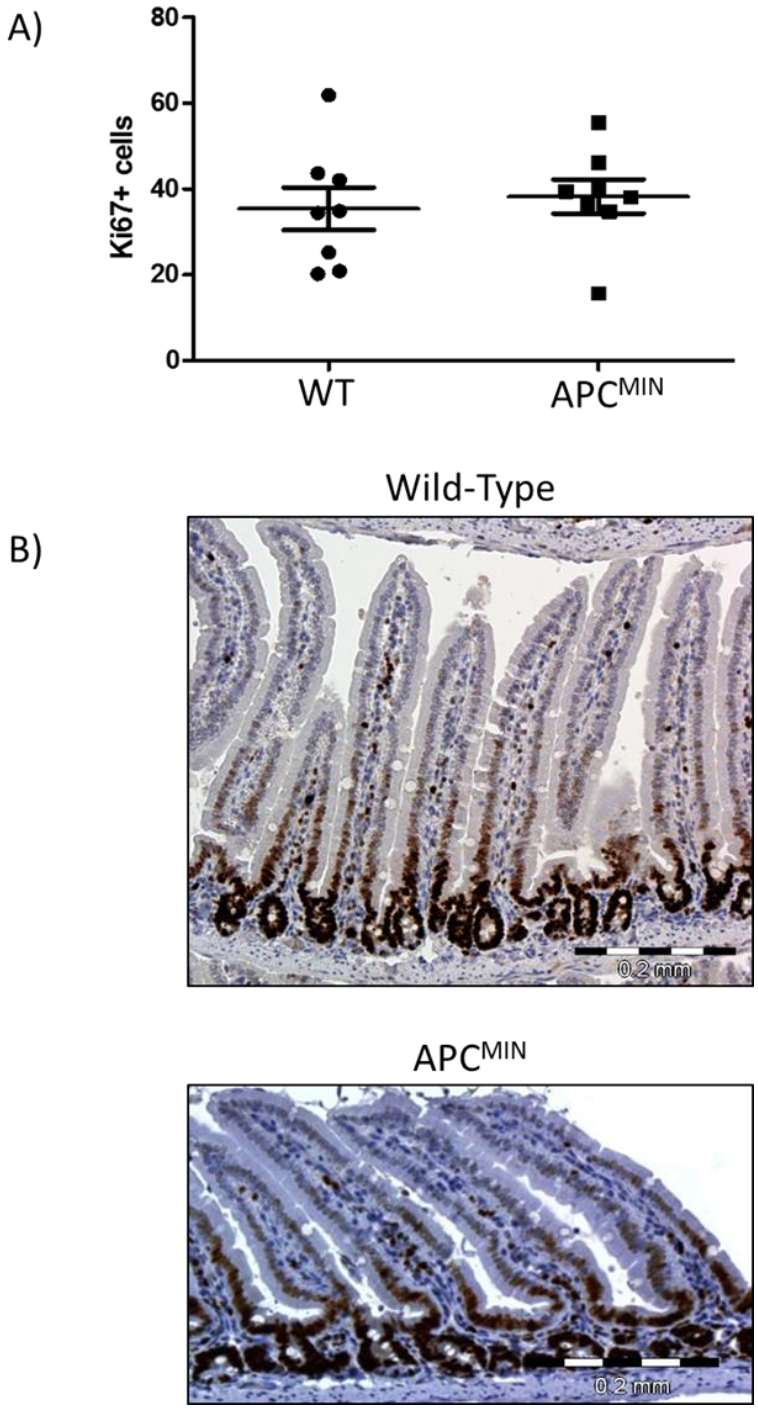

Figure 4.8: Proliferation in normal villi did not differ between groups. Mutation in the tumour suppressor *Apc* gene can lead to constitutive Wnt pathway activation and aberrant cell proliferation. In order to investigate if proliferation is up-regulated in the normal-appearing villi in the small intestine of APC^{MIN} mice prior to the development of polyps, we stained the epithelium for Ki67 and determined the percentage of Ki67+ cells per crypt-villus unit for ten such units per mouse. ***A)*** There was no significant difference in Ki67 expression in the normal villi of APC^{MIN} mice, which suggests that dysregulated proliferation is not ubiquitous in the small intestine of these mice (T-test, P=0.66). ***B)*** Sections of the distal ileum of wild-type and APC^{MIN} stained for Ki67 on a background of haematoxylin. Magnification 200x.

4.2.5 Weight gain was not affected in APC^{MIN} mice

Cancer-associated weight loss, or cachexia, is an indicator of severe disease in human cancer that is also observed in late-stage APC^{MIN} mice. We tracked the body weight of our mice at weekly intervals throughout the study and measured the mass of their mesenteric and epididymal fat after sacrifice at Week 14. There were no differences in body weight or either type of fat over the course of the study (Figure 4.9; 2-way ANOVA and T-tests, P>0.05).

4.2.6 Cytokine and chemokine gene transcription in in APC^{MIN} mice

Inflammation is a risk factor for colon cancer and the tumour microenvironment can modulate inflammatory conditions to promote tumour growth (22, 29). As such, we measured the transcription of several cytokines in the distal small intestine by qPCR, as well as measuring the spleen weight and the length of the small and large intestine, which can be used as indicators in intestinal inflammation (Figure 4.10).

The relative transcription of *Il10* was significantly decreased in APC^{MIN} mice (Figure 4.10; T-test, p=0.045), while their spleen weight was increased (Figure 4.10; T-test, p=0.006). There were no significant differences between relative transcription of *Il1β*, *Cxcl1, Cxcl5, Tgfβ* between groups at Week 14 (Figure 4.10; T-test and MWU-test, p>0.05).

4.2.7 The transcription of FXR target genes is decreased in the ileum of APC^{MIN} mice

Bile acid receptor FXR regulates the transcription of a number of genes in the ileum and has also been implicated in protection from CRC (11, 30). In order to determine if bile acid signalling is affected in our model, we measured the transcription of four FXR target genes (Figure 4.11).

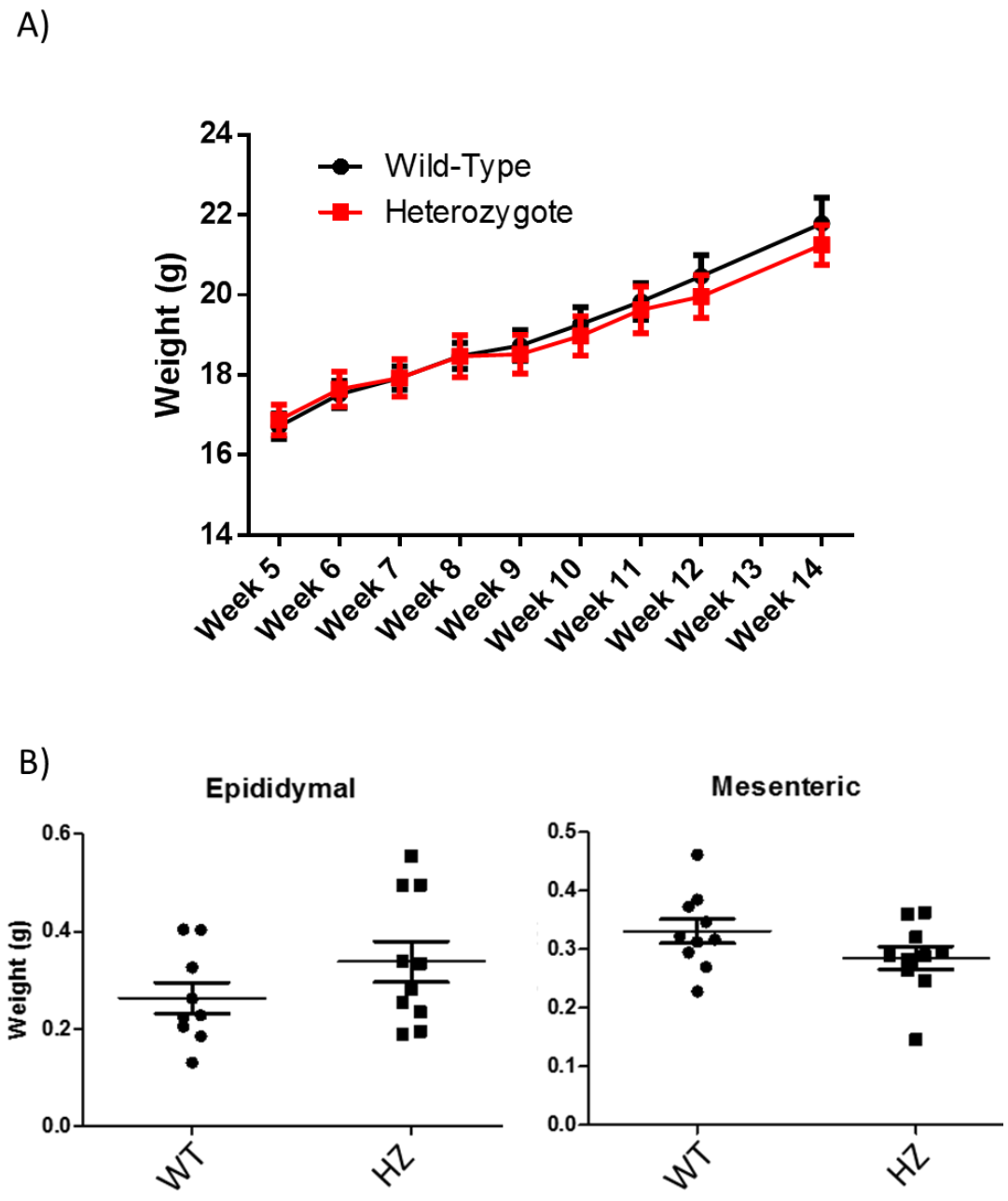

Figure 4.9: Neither body weight nor body fat differed between groups. Weight loss or inhibited weight gain is a sign of severe pathology in human cancer and mouse models of cancer. We tracked the body weight of our mice every week from 5 weeks of age (***A***) and recorded the mass of their mesenteric and epididymal fat after cull (***B***), neither of which differed between groups (Two-way ANOVA and T-tests, P>0.05).

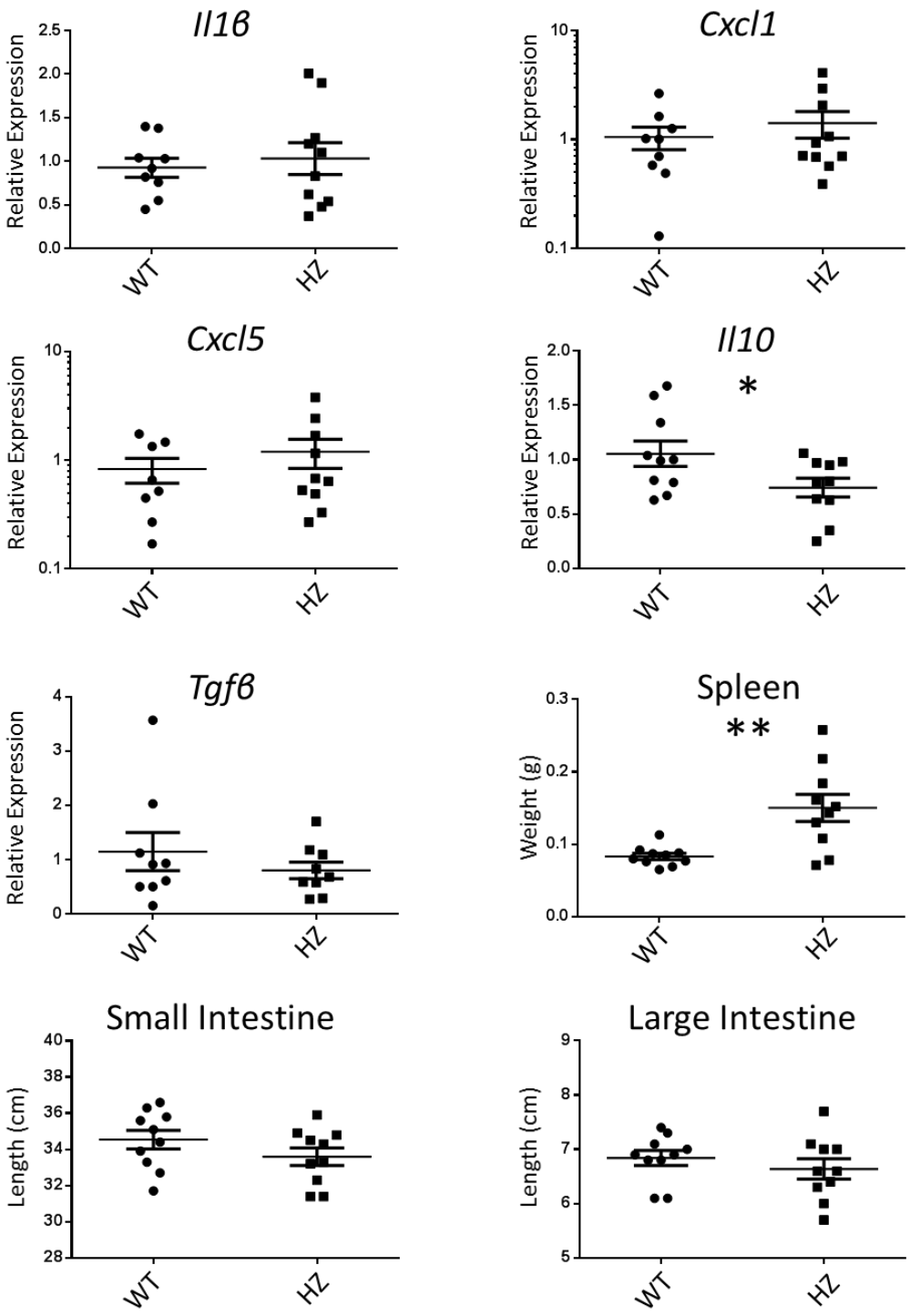

Figure 4.10: Only minor changes in the inflammatory environment are observed in APC^{MIN} mice. Chronic inflammation is a risk factor for colorectal cancer and inflammation in the tumour microenvironment can drive cancer progression. In order to establish if inflammation played a role in the pathogenesis of our model, we extracted RNA from the distal small intestine, the primary site of polyposis in APC^{MIN} mice, and performed qPCR for several cytokines. We also measured spleen weight and the length of the small and large intestine, as inflammation can lead to a shortening of these organs. The expression of IL10 was decreased in APC^{MIN} mice, while their spleen weight was increased. No changes were observed in any other measure.

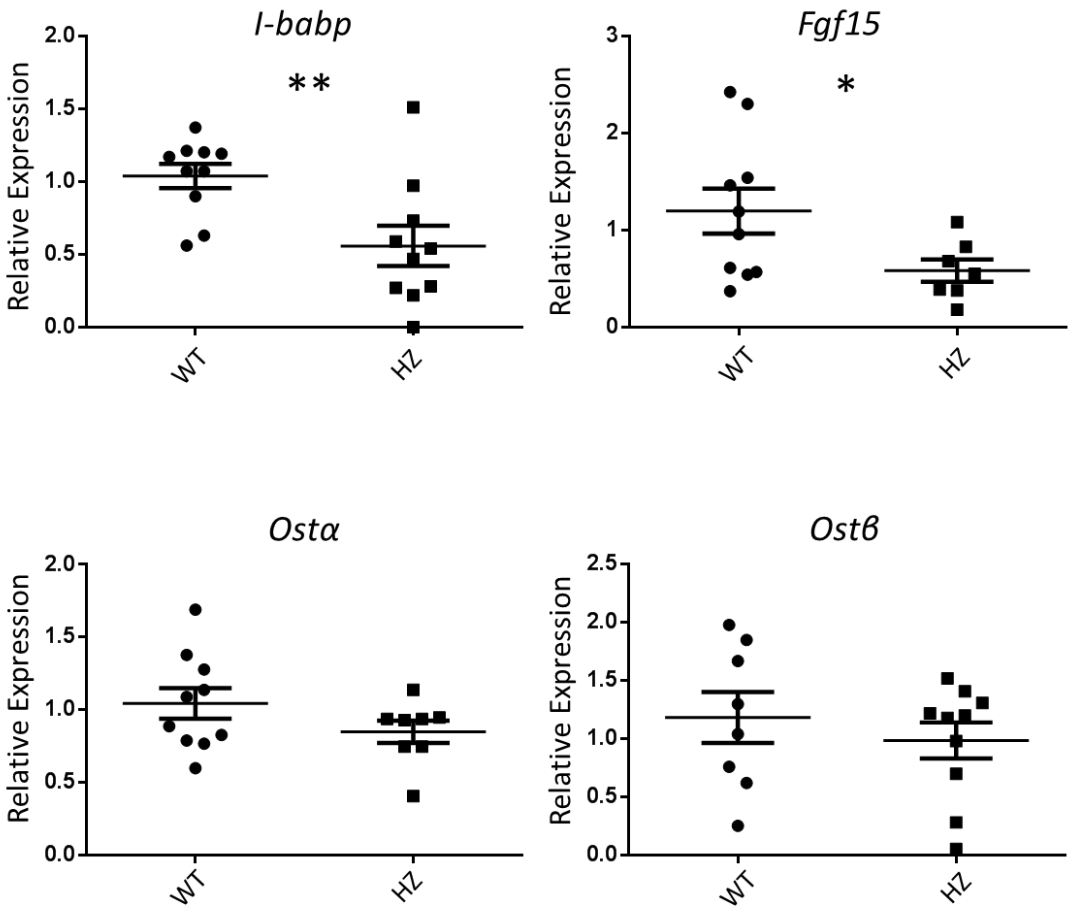

Figure 4.11: Transcription of FXR target genes is decreased in the ileum of APC^{MIN} mice at Week 14. FXR signalling has been shown to be protective against CRC. We measured the expression of four FXR target genes in the distal ileum of control and HZ mice by qPCR. Significantly lower expression of *I-babp* and *Fgf15* was detected in APC^{MIN} mice relative to WT animals, indicating reduced FXR signalling (T-test, $p<0.05$).

The transcription of *I-babp* and *Fgf15* was significantly suppressed in our CRC model (Figure 4.11; T-tests, $p<0.05$), indicative of reduced engagement of FXR. The transcription of the enterocyte basolateral bile acid transporters *Ostα* and *Ostβ* was marginally reduced but not significantly different between groups (Figure 4.11; T-tests, $p>0.05$).

4.2.8 Correlation analysis reveals a possible relationship between APC^{MIN} polyps and both FXR and Wnt signalling

We ran correlation analyses between polyp numbers, α-diversity indices, CAG relative abundances, faecal and plasma bile concentrations, and the relative transcription of our cytokines and FXR target genes within each group, in order to reveal any interactions between these parameters in the context of CRC. The significant correlations, after FDR correction for multiple comparisons, are presented in Figure 4.12.

The number of polyps in the middle and distal portions of the small intestine in our APC^{MIN} mice correlated negatively with FXR target genes *Ostα* (Figure 4.12; Pearson's R^2=-0.8 and -0.79, $p<0.001$) and *Ostβ* (Figure 4.12; Pearson's R^2=-0.9 and -0.91, $p<0.001$). *Il10* also correlated positively with *Ostβ* in APC^{MIN} mice (Figure 4.12; Pearson's R^2=0.88, $p<0.05$), while the plasma concentration of two tauro-conjugated bile acids, tauro-hyodeoxycholic (T-HDCA) acid and T-α/β/ω-MCA, correlated negatively with FXR target gene *Fgf15* (Figure 4.12; Spearman's Rho=-1, $p<0.001$). T-MCAs act as antagonists to FXR but our analysis cannot distinguish between the α-, β- and ω-isomers.

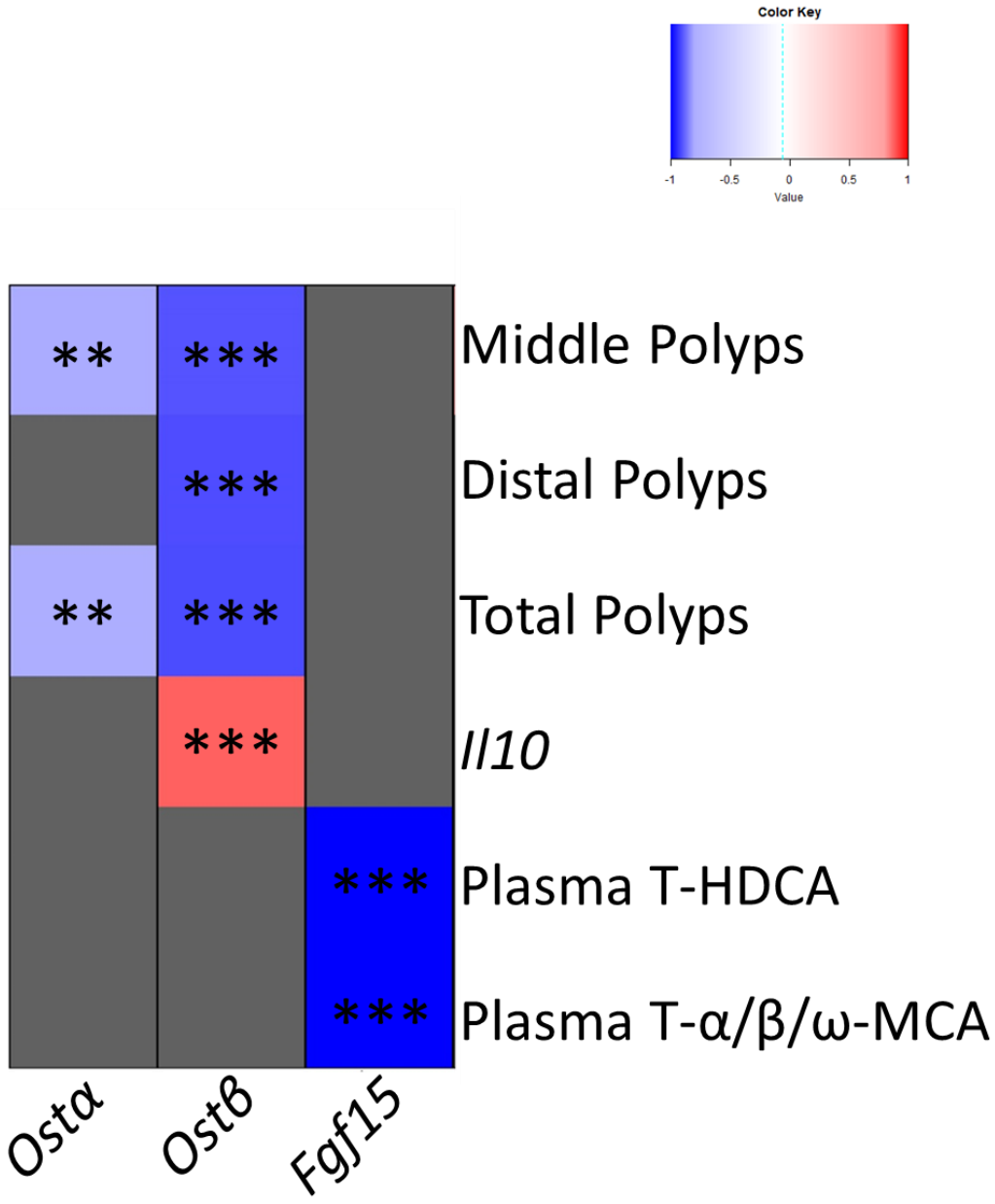

Figure 4.12: Correlation analysis reveals a relationship between polyp multiplicity and FXR target genes. The gut presents a complex milieu of interacting forces. In order to examine possible interactions between different aspects of our data in this environment, we performed a correlation analysis between several datapoints collected in our study. After correction for multiple comparisons, this revealed a strong negative correlation between our FXR target genes and polyp number. *Il10* also correlated positively with FXR target gene *Ostβ*, while *Fgf15* expression correlated negatively with the plasma concentrations of T-HDCA and FXR-antagonist T-MCA (Pearson's R and Spearman's R^2, $p<0.05$ after FDR adjustment).

4.2.9 PICRUSt predicts a significant increase in bile acid-metabolising genes in the faecal microbiota of APC^{MIN} mice at Week 7

We investigated the faecal microbial metagenomic function content of control and APC^{MIN} animals by applying PICRUSt, a software package which predicts whole microbial gene content from 16S rRNA gene sequencing data. This revealed a significant reduction in the α-diversity of the metagenome predicted by PICRUSt in APC^{MIN} mice at Week 7 (Figure 4.13; MWU-test, $p=0.002$). The β-diversities of the predicted metagenomes were also significantly different between genotypes at Weeks 4 and 7 (Figure 4.13; PERMANOVA, $p<0.05$).

In order to assess bile acid metabolism, the relative abundances of *baiCD* (COG1902), a gene cluster involved in the 7α-dehydroxylation of bile acids into secondary bile acids, and *bsh* (COG3049), the enzyme responsible for cleaving the amino acid conjugate from bile acids, were examined. These were significantly increased in their predicted abundance in APC^{MIN} mice at Week 7 (Figure 4.14; MWU-test, $p<0.05$), but not at Week 7, 11 or 14 (Figure 4.14; T-test, $p>0.05$).

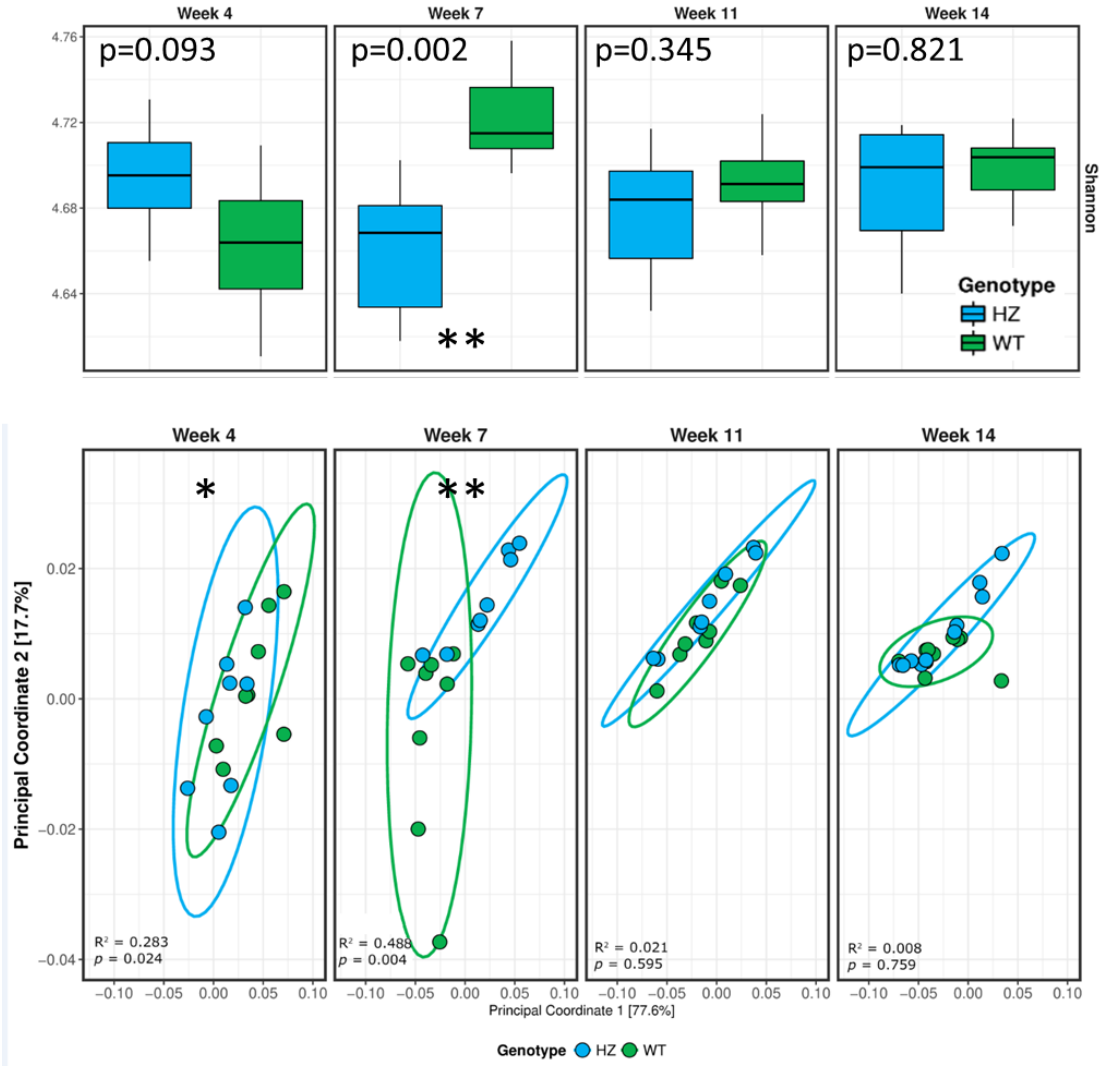

Figure 4.13: A- and β-diversity of the metagenome predicted by PICRUSt is altered in APC^{MIN} mice. We calculated the α- and β-diversity of the metagenomes predicted by PICRUSt and found that these measures are significantly different in APC^{MIN} mice. ***A)*** The Shannon diversity index of the metagenomes predicted by PICRUSt differed significantly between wild-type (WT) and APC^{MIN} (HZ) mice at Week 7 (MWU-test). ***B)*** The β-diversity of the metagenomes predicted by PICRUSt differed significantly between WT and HZ mice at Week 4 and 7 (PERMANOVA). Figure produced by Calum Walsh at Teagasc, Moorepark.

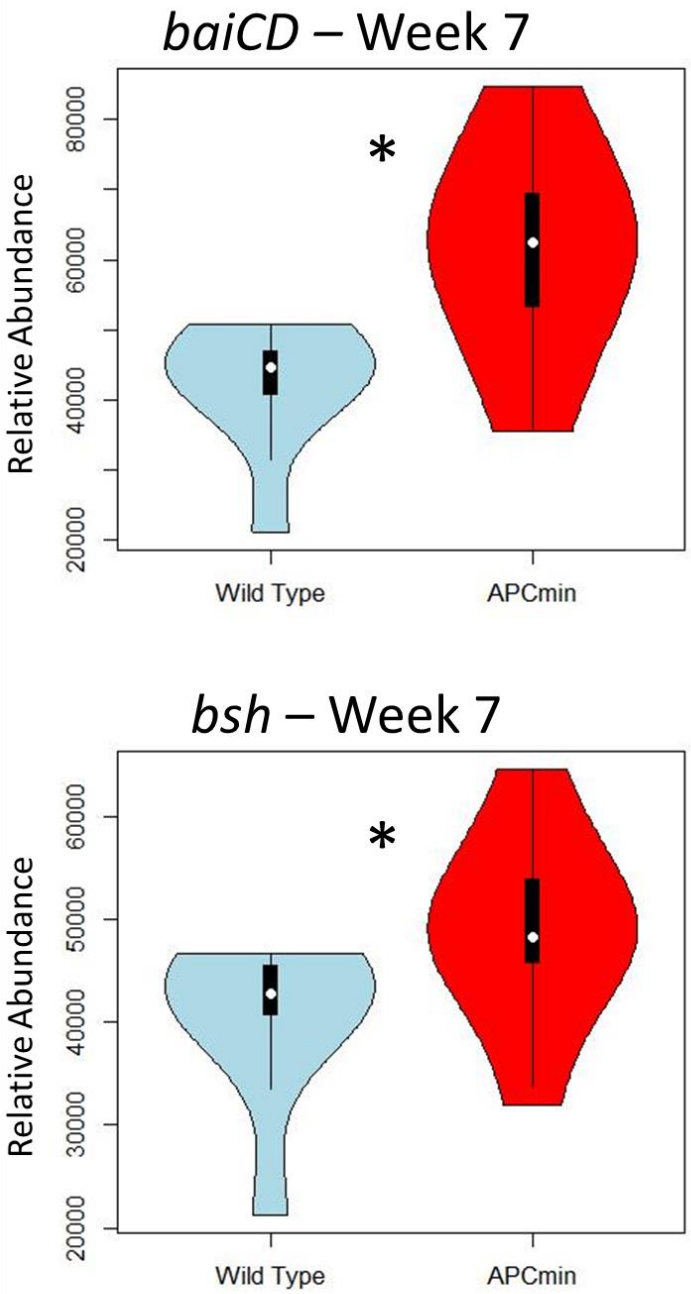

Figure 4.14: Primary and secondary bile acid metabolism gene content predicted by PICRUSt is significantly different between treatments at Week 7 only. We used PICRUSt to predict the gene content of the faecal microbiota in both our groups and compared the abundance of *baiCD* (COG1902), a gene cluster involved in the 7α-dehydroxylation of bile acids into secondary bile acids, and *bsh* (COG3049), the enzyme responsible for cleaving the amino acid conjugate from bile acids. Their predicted abundances were increased in APC^{MIN} mice at Week 7 but not at any other time (MWU-test, $p<0.05$). *N*=8 per group for Weeks 4-11, *n*=10 per group for Week 14.

4.3 Discussion

The microbiota is altered in human CRC, but the degree to which the host affects the microbiota and the microbiota alters the host is unclear (31). It is clear that an intricate dialogue exists between the microbiota and the host which is important in many disease states, particularly in cases of IBD, *C. difficile* and pathogen infections, and the evidence points to altered microbiota in the context of CRC. It is possible that the gut microbiota can both promote or inhibit tumour initiation, and evidence for this has been provided by animal studies (2, 3). However, it is also possible that tumorigenesis occurs entirely as a result of host processes independent of the microbiota. Similarly, after cancer initiation, components of the microbiota may suppress or promote growth, invasion and metastasis (32).

Human CRC pathogenesis is a process that takes place over decades (33). This makes it difficult to track the microbiota in a sufficiently large cohort and impossible to combine those data with the invasive colonoscopies and biopsies necessary to provide comprehensive samples before, during and after tumorigenesis. Some studies have compared the microbiota of human patients presenting with polyps and tumours but these were examined at a single time-point and so did not track the changes that occur across cancer development (28, 34). This provides the rational for using mouse models of CRC to investigate these changes. In this study, an integrated approach was applied through a time-course study of host and microbial changes in a model of familial colon cancer, the APC^{MIN} mouse. Material was collected over 10 weeks which encompassed the period before polyposis to established disease (5, 6). Assessment was made of parameters that are believed to influence the aetiology of CRC including the microbiota, metabolite adjustments by both the host and the microbiota, pro- and anti-apoptotic bile acids and inflammation.

We observed significant polyp development in the genetic CRC model in all areas of the small intestine, as anticipated, at 14 weeks of age. These were accompanied by significant

differences in the diversity and composition of the faecal microbiota in this mouse model. These differences may have initially been driven by pre-neoplastic changes in the intestine of APC^{MIN}, as we observed the first microbial alterations at Week 4, prior to the onset of polyposis reported in the literature (5, 6). These changes could be a caused by mechanisms such as depletion of the intestinal mucus layer reported in antibiotic-treated APC^{MIN} mice (6), however no changes in goblet cell size or number were detected in APC^{MIN} mice in a pilot study (Supplementary Figure S4.1).

Uncertainty surrounds the degree to which the faecal microbiota represent the luminal- and mucosal-associated bacteria of the large intestine, and the composition of the microbiota at the site of polyposis in the small intestine of APC^{MIN} mice. Research in rhesus macaques found high correlations between the composition of the stool microbiota and that of the colonic lumen and mucosa, and a moderate correlation between the stool and distal small intestine (35). In mice, the microbial composition detected in the contents of the large intestine was similar to the stool but distinct from the small intestine, which clustered with the stomach contents instead (36). However, another study by Onishi et al. found that the major genera identified in the small intestine were identical to those in the large intestine (37). In addition, faecal microbial transfer (FMT) from APC^{MIN} mice treated with bile acid DCA to untreated APC^{MIN} mice increased tumour size and number in the small intestine in untreated mice, suggesting that this effect was driven by microbiota present in the faeces (10). The faecal microbiota is also commonly altered in CRC (38), which implies that it reflects some aspect of CRC that may be informative, regardless of how accurately it represents the luminal- and mucosal-associated microbiota. Nonetheless, these limitations should be considered when analysing faecal microbial content in the context of intestinal disease.

Although other studies have reported no change, or a decrease, in the α-diversity in APC^{MIN} mice (5, 39, 40) we detected an increase at 4 and 14 weeks of age, but no change at Weeks

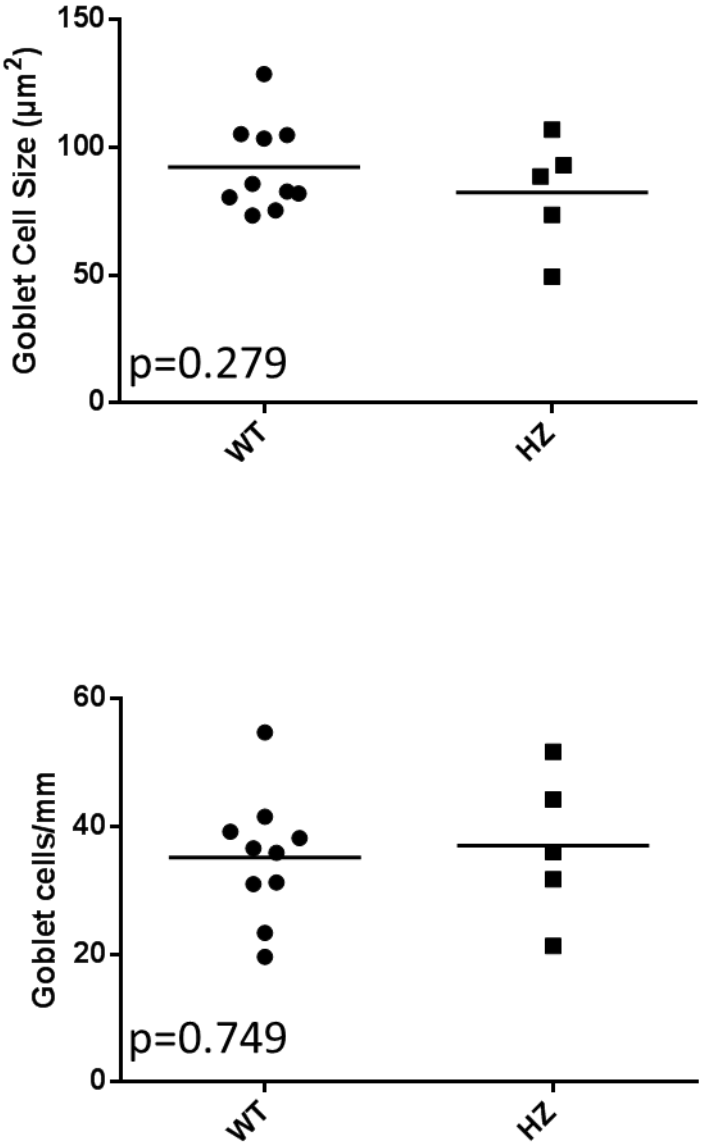

Supplementary Figure S4.1: Goblet cell size and number was not different in APC^{MIN} mice. A pilot study was conducted to estimate appropriate *n*-numbers. During this pilot, the number of goblet cells per millimetre of ileal villus, as well as the average size of goblet cells, was calculated in wild-type (WT) and APC^{MIN} (HZ) mice. No difference was detected in these measures (T-test, $p>0.05$).

7 or 11. These time-points coincide with the stage immediately prior to polyposis, and just before the onset of inflammation and tumour progression as reported by others (5, 6). Increases in α-diversity during cancer onset occur due to an outgrowth of opportunistic pathogens in the disrupted epithelium, often followed by a decrease in α-diversity due to the subsequent immune response (25, 41-43). This could account for the increase in α-diversity we observed, while the instigation of the inflammatory response is expected soon after our final time-point at Week 14. However, the two-stage increase early and late in the experiment is a novel observation. This may be explained by the enrichment of opportunistic pathogens in the disrupted epithelium immediately prior to tumorigenesis, followed by the detection of tumour-associated taxa at Week 14, as has been described previously (43).

Beta (β)-diversity also differs significantly at each time-point we examined, demonstrating that even though α-diversity recovers between Week 7 and Week 11, the composition of the microbiota does not. This implies that there is a consistent baseline α-diversity value to which the faecal microbiota returns after disruption, even though the species comprising the α-diversity do not return to the previous composition. The α-diversity of the microbial metagenome predicted by PICRUSt differs significantly between APC^{MIN} and wild-type mice at Week 7, and the predicted β-diversity differs at Weeks 4 and 7, which is distinct from the changes observed in our microbial α- and β-diversity. The gut microbiota has a consistent set of base metabolic functions that are robust against disruptions to the community (44) and this is demonstrated in our data here, as the predicted metagenome does not exactly parallel the structural changes in microbiota detected in Shannon or β-diversity. The metabolic changes predicted at Week 7, which correlate with the onset of intestinal neoplasia (5, 6), highlight this as a possible key stage in the functional activity of the microbiome during the onset of intestinal neoplasia.

We also considered the individual taxa that were significantly different between groups, where we do not observe a clear pattern of pro-tumorigenic microbial changes in APC^{MIN} mice. Instead, changes include enrichment and suppression of bacteria associated with both pro- and anti-tumorigenic effects at each time-point (45-53). Potentially pro-tumorigenic changes that are observed at Week 4 include enrichment of *Blautia*, reported to be increased in CRC (28), and *Turicibacter*, which is associated with IBD and colitis-associated cancer (54, 55). In contrast, *Ruminiclostridium 5* and *Ruminococcus 1* were suppressed in APC^{MIN} mice at this time-point and are negatively associated with CRC and IBD respectively (56, 57). At Week 7, several genera were increased which are associated with CRC or colitis (58-60), while suppressed species include *Faecalibaculum*, which is protective against inflammation and CRC (61). *Delftia* and *Peptoclostridium* are enriched in APC^{MIN} mice at Week 11, both of which are associated with gastrointestinal inflammation. *Peptoclostridium* genus also includes the pathogen *C. difficile* as well as 7α-dehydroxylating bacteria *C. hiranonis* which may increase the intraluminal concentrations of cytotoxic secondary bile acids (62-64). Taxa suppressed at this time-point include several associated with health and negatively associated with CRC and IBD, such as *Anaerostipes* and *Papillibacter* (52, 65). A similar pattern emerges at Week 14 where *Odoribacter* and the uncultivable *Candidatus Arthromitus* were enriched in APC^{MIN} mice, having previously been associated with inflammation and CRC (54, 66).

Eight taxa enriched in either APC^{MIN} or wild-type mice switched to become more abundant in the opposite experimental group during the study, perhaps reflecting the influence of the changing histopathological environment. These included an uncultured member of the *Rhodospirillaceae* family which was more abundant in APC^{MIN} mice at Week 4 and wild-type mice at Week 7, while *Lachnoclostridium* and the uncultured taxon *Lachnospiraceae NK4A136* displayed the opposite pattern. The former family was reported to be decreased by the chemotherapy drug cyclophosphamide (67), while the latter two taxa were increased by this drug (68, 69), which reflects the changes in abundances in these taxa between Weeks

4 and 7. Cyclophosphamide modulates the immune response to cancer by a number of mechanisms including activation T_h17 cells (69) which are key to intestinal tumorigenesis in APC^{MIN} mice (70, 71) and may be partly regulated by the microbiota (28, 72). Cyclophosphamide also depletes B-cells (73), an effect that is also observed in APC^{MIN} mice (74). These data imply an interaction between the microbiota and immune response in APC^{MIN} mice which reflect those seen in cyclophosphamide chemotherapy, and encompasses a similar pattern of suppression of susceptible bacteria such as *Rhodospirillaceae* and enrichment of resistant species such as *Lachnospiraceae* (75). This could provide another mechanism by which the gut bacteria influence intestinal tumorigenesis and microbial composition early in the experiment.

The *Lachnoclostridium* genus also contains the 7α-dehydroxylating bacteria, *C. scindens* and *C. hylemonae,* which may account for part of the enrichment of the *baiCD* gene predicted by our PICRUSt analysis in APC^{MIN} mice at Week 7. 7α-dehydroxylation is responsible for the formation of secondary bile acids which are cytotoxic and have been implicated in CRC. The enrichment of this taxon at Week 7, after an initial suppression in APC^{MIN} mice, suggests an adaptation to the intestinal environment generated during the onset of polyposis, and that disruption to bile acid signalling by microbial metabolism mediated by *Lachnoclostridia* could play a key role during the disease initiation. This has been previously suggested in human studies where a high fat diet, another risk factor for CRC, has been shown to enrich for bacterial species capable of 7α-dehydroxylation, which may explain the high rate of CRC in western populations (76).

The enrichment of other taxa also alternates between groups across the experiment. These include *Allobaculum*, which is initially more abundant in WT mice but is increased in APC^{MIN} mice at Weeks 7 and 11. This taxon is enriched in models of sporadic and colitis-associated CRC (77-79). *Ruminiclostridium 9* is suppressed in APC^{MIN} mice at Week 4 and enriched at

Week 7. Members of the genus *Ruminiclostridium* are decreased in human CRC patients and APC^{MIN} mice (50, 56) and are associated with high fat diets (50). *E. ventriosum* is suppressed in APC^{MIN} mice at Weeks 4 and 6, and enriched at Weeks 11 and 14. This taxon was also decreased by CRC and increased by high fat diet (80, 81), and was negatively associated with IL6, IL8 and colitis (82, 83). While we did not detect any changes in these cytokines at Week 14, the suppression of this inflammation-intolerant microbe between Weeks 4 and 7 may indicate immune involvement at this stage. The final two taxa that alternate over the course of the experiment are both from the uncultured *Bacteroidales S24-7 group*. However, one subgroup is first enriched in APC^{MIN} before expanding in WT, while the other is increased in WT then APC^{MIN}.

A number of CAGs also differed between groups across the experiment which may describe sets of interacting taxa, as described in section 3.3. The relevance of these groups and interactions to CRC is being investigated.

In summary, our microbiota data provide us with a set of changes associated with different stages of the tumorigenic process in APC^{MIN} mice. Many of these changes have a pro-tumorigenic character but this is not universal. This may be due to limitations in our understanding of the roles of rare or uncultivable taxa *in vivo*, as well as the lack of species-level taxon identification provided by 16S rRNA gene sequencing. It is also possible that APC^{MIN} mice are not solely enriched in pro-tumorigenic species, in which case the contribution of each taxon to tumorigenesis may need to be considered individually. Species associated with CRC are not consistent across studies and the relationship between the microbiota and CRC is likely to be complex (2, 3). In this context, it will require consistent association between taxa and CRC to define key species, which should be combined with a mechanistic understanding of their interaction with the host *in vivo*. Our study does reveal novel temporal variations in the patterns of microbial changes, potentially associating some

taxa with cancer initiation early in the model and others with tumour progression later. This will inform future research and potentially, targeted therapies for specific stages of disease, and could also explain some of the inconsistent associations observed in other studies of the microbiota in CRC which sample the microbial composition at different times.

One of the primary mechanisms by which the gut microbiota may influence CRC initiation and progression is via production of bioactive microbial metabolites. The relative abundance of bile acid-metabolising taxa were altered at different time-points during the study and the predicted abundance of bile acid metabolising genes *baiCD* and *bsh* was also increased in APC^{MIN} mice at Week 7. Bile acids and microbial metabolism of bile acids have been implicated in the pathogenesis of CRC and so we measured faecal and plasma bile acids in our model. Of note, the transcription of target genes of the bile acid receptor FXR, *I-babp* and *Fgf15*, were significantly decreased in the ileum of APC^{MIN} mice which suggests that bile acid signalling was suppressed, which would limit the cancer-protective role of FXR (11, 30). This was supported by the fact that *Fgf15* correlated negatively with tauro-conjugated MCAs, which are FXR antagonists. *Fgf15* also correlated negatively with the conjugated secondary bile acid T-HDCA. HDCA can be formed by 7α-dehydroxylation of ω-MCA, or by 7α-dehydroxylation followed by epimerisation of the 6-carbon hydroxyl group of α- or β-MCA, a capability possessed by the microbiota (84). Another set of FXR target genes, *Ostα* and *Ostβ*, also correlate negatively with the total number of polyps, and polyps in the middle and distal portions of the small intestine, of APC^{MIN} mice. The transcription of anti-inflammatory *Il10* also correlated positively with *Ostα* and this cytokine is also up-regulated by FXR (85, 86) and was significantly reduced in APC^{MIN} mice at this time-point, implicating FXR in this effect. This suggests the possibility that T-MCAs antagonise FXR, a known tumour suppressor, leading to increased polyp multiplicity in the middle and distal small intestine, potentially involving suppression of IL10. While T-MCAs were not significantly different between groups despite their correlation with *Fgf15*, the concentration of potent FXR-agonist bile acids CDCA

and DCA were significantly decreased in APC^{MIN} mice before correction for multiple comparisons. It should be noted, however, that hypermethylation of the *Fxr* promoter has been reported in the tumour-adjacent mucosa of APC^{MIN} mice, and so the relative contribution of bile acid signalling and/or promoter methylation to suppression of FXR signalling is difficult to elucidate (87). Nonetheless, we see alterations in bile acid-metabolising bacteria in APC^{MIN} mice and differences in the predicted abundance of microbial bile acid-metabolising genes, suggesting that the microbiota do play a role in bile acid homeostasis in our model. Additionally, our correlation analysis provides evidence that bile acids are involved in FXR signalling in APC^{MIN} mice.

In conclusion, our data highlight a progression of bacterial changes with the potential to contribute to disease at each time-point. These include distinct changes associated with the periods of cancer onset and progression. This dataset will inform future studies to understand the functional impact of the microbiota on tumorigenesis and to understand the implications of alterations in microbial community structure during this process. Herein we also identify a possible role for bile acid signalling in small intestine polyposis in APC^{MIN} mice mediated by FXR which supports previous studies.

4.4 References

1. Hope ME, Hold GL, Kain R, El-Omar EM. Sporadic colorectal cancer--role of the commensal microbiota. FEMS microbiology letters. 2005;244(1):1-7.
2. Scanlan PD, Shanahan F, Clune Y, Collins JK, O'Sullivan GC, O'Riordan M, et al. Culture-independent analysis of the gut microbiota in colorectal cancer and polyposis. Environmental microbiology. 2008;10(3):789-98.
3. Swidsinski A, Khilkin M, Kerjaschki D, Schreiber S, Ortner M, Weber J, et al. Association between intraepithelial Escherichia coli and colorectal cancer. Gastroenterology. 1998;115(2):281-6.
4. Guo M, Xu E, Ai D. Inferring Bacterial Infiltration in Primary Colorectal Tumors From Host Whole Genome Sequencing Data. Front Genet. 2019;10:213-.
5. Son JS, Khair S, Pettet DW, 3rd, Ouyang N, Tian X, Zhang Y, et al. Altered Interactions between the Gut Microbiome and Colonic Mucosa Precede Polyposis in APCMin/+ Mice. PloS one. 2015;10(6):e0127985-e.
6. Kaur K, Saxena A, Debnath I, O'Brien JL, Ajami NJ, Auchtung TA, et al. Antibiotic-mediated bacteriome depletion in Apc(Min/+) mice is associated with reduction in mucus-producing goblet cells and increased colorectal cancer progression. Cancer medicine. 2018;7(5):2003-12.
7. Dejea CM, Fathi P, Craig JM, Boleij A, Taddese R, Geis AL, et al. Patients with familial adenomatous polyposis harbor colonic biofilms containing tumorigenic bacteria. Science. 2018;359(6375):592-+.
8. Kostic AD, Howitt MR, Garrett WS. Exploring host-microbiota interactions in animal models and humans. Genes Dev. 2013;27(7):701-18.
9. Nguyen TT, Ung TT, Kim NH, Jung YD. Role of bile acids in colon carcinogenesis. World J Clin Cases. 2018;6(13):577-88.
10. Cao H, Xu M, Dong W, Deng B, Wang S, Zhang Y, et al. Secondary bile acid-induced dysbiosis promotes intestinal carcinogenesis. International Journal of Cancer. 2017;140(11):2545-56.
11. Modica S, Murzilli S, Salvatore L, Schmidt DR, Moschetta A. Nuclear bile acid receptor FXR protects against intestinal tumorigenesis. Cancer Res. 2008;68(23):9589-94.
12. Reddy BS. Diet And Excretion Of Bile Acids. Cancer Res. 1981;41:3766-8.
13. Bernstein H, Bernstein C, Payne CM, Dvorakova K, Garewal H. Bile acids as carcinogens in human gastrointestinal cancers. Mutation Research/Reviews in Mutation Research. 2005;589(1):47-65.
14. Long AG, Lundsmith ET, Hamilton KE. Inflammation and Colorectal Cancer. Current colorectal cancer reports. 2017;13(4):341-51.
15. Mantovani A, Allavena P, Sica A, Balkwill F. Cancer-related inflammation. Nature. 2008;454:436.
16. Voronov E, Apte RN. IL-1 in Colon Inflammation, Colon Carcinogenesis and Invasiveness of Colon Cancer. Cancer Microenviron. 2015;8(3):187-200.
17. Bent R, Moll L, Grabbe S, Bros M. Interleukin-1 Beta-A Friend or Foe in Malignancies? Int J Mol Sci. 2018;19(8):2155.
18. Kumari N, Dwarakanath BS, Das A, Bhatt AN. Role of interleukin-6 in cancer progression and therapeutic resistance. Tumour biology : the journal of the International Society for Oncodevelopmental Biology and Medicine. 2016;37(9):11553-72.
19. Balkwill F. TNF-alpha in promotion and progression of cancer. Cancer metastasis reviews. 2006;25(3):409-16.
20. Chow MT, Luster AD. Chemokines in cancer. Cancer immunology research. 2014;2(12):1125-31.

21. Klimesova K, Kverka M, Zakostelska Z, Hudcovic T, Hrncir T, Stepankova R, et al. Altered gut microbiota promotes colitis-associated cancer in IL-1 receptor-associated kinase M-deficient mice. Inflamm Bowel Dis. 2013;19(6):1266-77.
22. Lucas C, Barnich N, Nguyen HTT. Microbiota, Inflammation and Colorectal Cancer. Int J Mol Sci. 2017;18(6):1310.
23. Mendes MCS, Paulino DSM, Brambilla SR, Camargo JA, Persinoti GF, Carvalheira JBC. Microbiota modification by probiotic supplementation reduces colitis associated colon cancer in mice. World journal of gastroenterology. 2018;24(18):1995-2008.
24. Xiao Y, Dai X, Li K, Gui G, Liu J, Yang H. Clostridium butyricum partially regulates the development of colitis-associated cancer through miR-200c. Cell Mol Biol. 2017;63(4):59-66.
25. Hu Y, Le Leu RK, Christophersen CT, Somashekar R, Conlon MA, Meng XQ, et al. Manipulation of the gut microbiota using resistant starch is associated with protection against colitis-associated colorectal cancer in rats. Carcinogenesis. 2016;37(4):366-75.
26. Tian Y, Xu Q, Sun LQ, Ye Y, Ji GZ. Short-chain fatty acids administration is protective in colitis-associated colorectal cancer development. J Nutr Biochem. 2018;57:103-9.
27. Song H, Wang W, Shen B, Jia H, Hou Z, Chen P, et al. Pretreatment with probiotic Bifico ameliorates colitis-associated cancer in mice: Transcriptome and gut flora profiling. Cancer Sci. 2018;109(3):666-77.
28. Flemer B, Lynch DB, Brown JMR, Jeffery IB, Ryan FJ, Claesson MJ, et al. Tumour-associated and non-tumour-associated microbiota in colorectal cancer. Gut. 2017;66(4):633-43.
29. Candela M, Turroni S, Biagi E, Carbonero F, Rampelli S, Fiorentini C, et al. Inflammation and colorectal cancer, when microbiota-host mutualism breaks. World journal of gastroenterology. 2014;20(4):908-22.
30. Fu T, Coulter S, Yoshihara E, Oh TG, Fang S, Cayabyab F, et al. FXR Regulates Intestinal Cancer Stem Cell Proliferation. Cell. 2019;176(5):1098-112.e18.
31. Jahani-Sherafat S, Alebouyeh M, Moghim S, Ahmadi Amoli H, Ghasemian-Safaei H. Role of gut microbiota in the pathogenesis of colorectal cancer; a review article. Gastroenterol Hepatol Bed Bench. 2018;11(2):101-9.
32. Zhu GW, Huang Q, Huang YJ, Zheng W, Hua J, Yang SG, et al. Lipopolysaccharide increases the release of VEGF-C that enhances cell motility and promotes lymphangiogenesis and lymphatic metastasis through the TLR4-NF-kappa B/JNK pathways in colorectal cancer. Oncotarget. 2016;7(45):73711-24.
33. Nguyen M, Weinberg D. The Impact of Colonoscopy on Colorectal Cancer Incidence and Mortality. IntechOpen. 2011.
34. Flemer B, Warren RD, Barrett MP, Cisek K, Das A, Jeffery IB, et al. The oral microbiota in colorectal cancer is distinctive and predictive. Gut. 2018;67(8):1454-63.
35. Yasuda K, Oh K, Ren B, Tickle Timothy L, Franzosa Eric A, Wachtman Lynn M, et al. Biogeography of the Intestinal Mucosal and Lumenal Microbiome in the Rhesus Macaque. Cell Host Microbe. 2015;17(3):385-91.
36. Gu S, Chen D, Zhang J-N, Lv X, Wang K, Duan L-P, et al. Bacterial community mapping of the mouse gastrointestinal tract. PloS one. 2013;8(10):e74957-e.
37. Onishi JC, Campbell S, Moreau M, Patel F, Brooks AI, Zhou YX, et al. Bacterial communities in the small intestine respond differently to those in the caecum and colon in mice fed low- and high-fat diets. Microbiology. 2017;163(8):1189-97.
38. Amitay EL, Krilaviciute A, Brenner H. Systematic review: Gut microbiota in fecal samples and detection of colorectal neoplasms. Gut microbes. 2018;9(4):293-307.
39. Wang H, Guan L, Li J, Lai M, Wen X. The Effects of Berberine on the Gut Microbiota in Apc (min/+) Mice Fed with a High Fat Diet. Molecules. 2018;23(9):2298.

40. Bice BD, Stephens MR, Georges SJ, Venancio AR, Bermant PC, Warncke AV, et al. Environmental Enrichment Induces Pericyte and IgA-Dependent Wound Repair and Lifespan Extension in a Colon Tumor Model. Cell reports. 2017;19(4):760-73.
41. Wang X, Ye T, Chen WJ, Lv Y, Hao Z, Chen J, et al. Structural shift of gut microbiota during chemo-preventive effects of epigallocatechin gallate on colorectal carcinogenesis in mice. World journal of gastroenterology. 2017;23(46):8128-39.
42. Sepehri S, Kotlowski R, Bernstein CN, Krause DO. Microbial diversity of inflamed and noninflamed gut biopsy tissues in inflammatory bowel disease. Inflamm Bowel Dis. 2007;13(6):675-83.
43. Feng Q, Liang S, Jia H, Stadlmayr A, Tang L, Lan Z, et al. Gut microbiome development along the colorectal adenoma–carcinoma sequence. Nature Communications. 2015;6:6528.
44. Eng A, Borenstein E. Taxa-function robustness in microbial communities. Microbiome. 2018;6(1):45-.
45. Saez-Lara MJ, Gomez-Llorente C, Plaza-Diaz J, Gil A. The role of probiotic lactic acid bacteria and bifidobacteria in the prevention and treatment of inflammatory bowel disease and other related diseases: a systematic review of randomized human clinical trials. BioMed research international. 2015;2015:505878-.
46. Duncan SH, Russell WR, Quartieri A, Rossi M, Parkhill J, Walker AW, et al. Wheat bran promotes enrichment within the human colonic microbiota of butyrate-producing bacteria that release ferulic acid. Environmental microbiology. 2016;18(7):2214-25.
47. Tamanai-Shacoori Z, Smida I, Bousarghin L, Loreal O, Meuric V, Fong SB, et al. Roseburia spp.: a marker of health? Future microbiology. 2017;12:157-70.
48. Zhu J, Kong Y, Yu J, Shao S, Mao M, Zhao M, et al. Consumption of drinking water N-Nitrosamines mixture alters gut microbiome and increases the obesity risk in young male rats. Environmental Pollution. 2019;248:388-96.
49. Mancabelli L, Milani C, Lugli GA, Turroni F, Cocconi D, van Sinderen D, et al. Identification of universal gut microbial biomarkers of common human intestinal diseases by meta-analysis. FEMS Microbiology Ecology. 2017;93(12).
50. Zhao L, Chen Y, Xia F, Abudukerimu B, Zhang W, Guo Y, et al. A Glucagon-Like Peptide-1 Receptor Agonist Lowers Weight by Modulating the Structure of Gut Microbiota. Frontiers in Endocrinology. 2018;9(233).
51. Roager HM, Vogt JK, Kristensen M, Hansen LBS, Ibrügger S, Mærkedahl RB, et al. Whole grain-rich diet reduces body weight and systemic low-grade inflammation without inducing major changes of the gut microbiome: a randomised cross-over trial. Gut. 2019;68(1):83-93.
52. Ai D, Pan H, Li X, Gao Y, Liu G, Xia LC. Identifying Gut Microbiota Associated With Colorectal Cancer Using a Zero-Inflated Lognormal Model. Front Microbiol. 2019;10(826).
53. Chen W, Liu F, Ling Z, Tong X, Xiang C. Human intestinal lumen and mucosa-associated microbiota in patients with colorectal cancer. PloS one. 2012;7(6):e39743-e.
54. Zackular JP, Baxter NT, Iverson KD, Sadler WD, Petrosino JF, Chen GY, et al. The Gut Microbiome Modulates Colon Tumorigenesis. mBio. 2013;4(6):e00692-13.
55. Wu M, Wu Y, Li J, Bao Y, Guo Y, Yang W. The Dynamic Changes of Gut Microbiota in Muc2 Deficient Mice. Int J Mol Sci. 2018;19(9):2809.
56. Mangifesta M, Mancabelli L, Milani C, Gaiani F, de'Angelis N, de'Angelis GL, et al. Mucosal microbiota of intestinal polyps reveals putative biomarkers of colorectal cancer. Scientific Reports. 2018;8(1):13974.
57. Nagao-Kitamoto H, Kamada N. Host-microbial Cross-talk in Inflammatory Bowel Disease. Immune Netw. 2017;17(1):1-12.
58. Byerley LO, Samuelson D, Blanchard E, Luo M, Lorenzen BN, Banks S, et al. Changes in the gut microbial communities following addition of walnuts to the diet. The Journal of Nutritional Biochemistry. 2017;48:94-102.

59. Yu Z, Song G, Liu J, Wang J, Zhang P, Chen K. Beneficial effects of extracellular polysaccharide from Rhizopus nigricans on the intestinal immunity of colorectal cancer mice. International Journal of Biological Macromolecules. 2018;115:718-26.
60. Pan P, Lam V, Salzman N, Huang YW, Yu J, Zhang J, et al. Black Raspberries and Their Anthocyanin and Fiber Fractions Alter the Composition and Diversity of Gut Microbiota in F-344 Rats. Nutrition and cancer. 2017;69(6):943-51.
61. Sokol H, Pigneur B, Watterlot L, Lakhdari O, Bermúdez-Humarán LG, Gratadoux J-J, et al. Faecalibacterium prausnitzii is an anti-inflammatory commensal bacterium identified by gut microbiota analysis of Crohn disease patients. Proceedings of the National Academy of Sciences. 2008;105(43):16731-6.
62. Liu W, Zhang Y, Qiu B, Fan S, Ding H, Liu Z. Quinoa whole grain diet compromises the changes of gut microbiota and colonic colitis induced by dextran Sulfate sodium in C57BL/6 mice. Scientific Reports. 2018;8(1):14916.
63. Luo Y, Huang C, Ye J, Fang W, Gu W, Chen Z, et al. Genome Sequence and Analysis of Peptoclostridium difficile Strain ZJCDC-S82. Evol Bioinform Online. 2016;12:41-9.
64. Yutin N, Galperin MY. A genomic update on clostridial phylogeny: Gram-negative spore formers and other misplaced clostridia. Environmental microbiology. 2013;15(10):2631-41.
65. Rehman A, Rausch P, Wang J, Skieceviciene J, Kiudelis G, Bhagalia K, et al. Geographical patterns of the standing and active human gut microbiome in health and IBD. Gut. 2016;65(2):238-48.
66. Santiago A, Sanchez E, Clark A, Pozuelo M, Calvo M, Yañez F, et al. Sequential Changes in the Mesenteric Lymph Node Microbiome and Immune Response during Cirrhosis Induction in Rats. mSystems. 2019;4(1):e00278-18.
67. Xu X, Zhang X. Effects of cyclophosphamide on immune system and gut microbiota in mice. Microbiological Research. 2015;171:97-106.
68. Zhu G, Jiang Y, Yao Y, Wu N, Luo J, Hu M, et al. Ovotransferrin ameliorates the dysbiosis of immunomodulatory function and intestinal microbiota induced by cyclophosphamide. Food & function. 2019;10(2):1109-22.
69. Viaud S, Saccheri F, Mignot G, Yamazaki T, Daillère R, Hannani D, et al. The intestinal microbiota modulates the anticancer immune effects of cyclophosphamide. Science. 2013;342(6161):971-6.
70. Chae W-J, Bothwell ALM. Spontaneous Intestinal Tumorigenesis in Apc (/Min+) Mice Requires Altered T Cell Development with IL-17A. Journal of immunology research. 2015;2015:860106-.
71. Chae W-J, Gibson TF, Zelterman D, Hao L, Henegariu O, Bothwell ALM. Ablation of IL-17A abrogates progression of spontaneous intestinal tumorigenesis. Proc Natl Acad Sci U S A. 2010;107(12):5540-4.
72. Wu S, Rhee KJ, Albesiano E, Rabizadeh S, Wu X, Yen HR, et al. A human colonic commensal promotes colon tumorigenesis via activation of T helper type 17 T cell responses. Nature medicine. 2009;15(9):1016-22.
73. Ahmed AR, Hombal SM. Cyclophosphamide (Cytoxan): A review on relevant pharmacology and clinical uses. Journal of the American Academy of Dermatology. 1984;11(6):1115-26.
74. Coletta PL, Muller AM, Jones EA, Muhl B, Holwell S, Clarke D, et al. Lymphodepletion in the ApcMin/+ mouse model of intestinal tumorigenesis. Blood. 2004;103(3):1050-8.
75. Li M, Wang B, Sun X, Tang Y, Wei X, Ge B, et al. Upregulation of Intestinal Barrier Function in Mice with DSS-Induced Colitis by a Defined Bacterial Consortium Is Associated with Expansion of IL-17A Producing Gamma Delta T Cells. Frontiers in immunology. 2017;8:824-.

76. Ocvirk S, O'Keefe SJ. Influence of Bile Acids on Colorectal Cancer Risk: Potential Mechanisms Mediated by Diet - Gut Microbiota Interactions. Curr Nutr Rep. 2017;6(4):315-22.
77. Zhang Y, Ma C, Zhao J, Xu H, Hou Q, Zhang H. Lactobacillus casei Zhang and vitamin K2 prevent intestinal tumorigenesis in mice via adiponectin-elevated different signaling pathways. Oncotarget. 2017;8(15):24719-27.
78. Wei H, Dong L, Wang T, Zhang M, Hua W, Zhang C, et al. Structural shifts of gut microbiota as surrogate endpoints for monitoring host health changes induced by carcinogen exposure. FEMS Microbiol Ecol. 2010;73(3):577-86.
79. Mendes MCS, Paulino DS, Brambilla SR, Camargo JA, Persinoti GF, Carvalheira JBC. Microbiota modification by probiotic supplementation reduces colitis associated colon cancer in mice. World journal of gastroenterology. 2018;24(18):1995-2008.
80. Etxeberria U, Arias N, Boque N, Macarulla MT, Portillo MP, Milagro FI, et al. Shifts in microbiota species and fermentation products in a dietary model enriched in fat and sucrose. Beneficial microbes. 2015;6(1):97-111.
81. Yu J, Feng Q, Wong SH, Zhang D, Liang Qy, Qin Y, et al. Metagenomic analysis of faecal microbiome as a tool towards targeted non-invasive biomarkers for colorectal cancer. Gut. 2017;66(1):70-8.
82. Biagi E, Nylund L, Candela M, Ostan R, Bucci L, Pini E, et al. Through ageing, and beyond: gut microbiota and inflammatory status in seniors and centenarians. PloS one. 2010;5(5):e10667-e.
83. Bibiloni R, Simon MA, Albright C, Sartor B, Tannock GW. Analysis of the large bowel microbiota of colitic mice using PCR/DGGE. Letters in Applied Microbiology. 2005;41(1):45-51.
84. Eyssen HJ, De Pauw G, Van Eldere J. Formation of hyodeoxycholic acid from muricholic acid and hyocholic acid by an unidentified gram-positive rod termed HDCA-1 isolated from rat intestinal microflora. Applied and environmental microbiology. 1999;65(7):3158-63.
85. Massafra V, Ijssennagger N, Plantinga M, Milona A, Ramos Pittol JM, Boes M, et al. Splenic dendritic cell involvement in FXR-mediated amelioration of DSS colitis. Biochimica et Biophysica Acta (BBA) - Molecular Basis of Disease. 2016;1862(2):166-73.
86. Hucke S, Herold M, Liebmann M, Freise N, Lindner M, Fleck AK, et al. The farnesoid-X-receptor in myeloid cells controls CNS autoimmunity in an IL-10-dependent fashion. Acta neuropathologica. 2016;132(3):413-31.
87. Selmin OI, Fang C, Lyon AM, Doetschman TC, Thompson PA, Martinez JD, et al. Inactivation of Adenomatous Polyposis Coli Reduces Bile Acid/Farnesoid X Receptor Expression through Fxr gene CpG Methylation in Mouse Colon Tumors and Human Colon Cancer Cells. The Journal of nutrition. 2016;146(2):236-42.

Chapter 5

Polyposis in APC^{MIN} mice is suppressed by bacteria expressing *bile salt hydrolase*

5.0 Abstract

Background: Bile salt hydrolase (Bsh) is an enzyme prevalent in probiotic bacteria but concerns exist regarding its ability to increase the concentration of cytotoxic secondary bile acids in the intestines. We investigated the role of Bsh in colorectal cancer (CRC) by treating APC^{MIN} mice, a model for familial colorectal cancer, with *E. coli* engineered to overexpress this enzyme.

Methods: APC^{MIN} mice were treated by gavage with PBS, *E. coli MG1655* or *E. coli MG1655* overexpressing Bsh at 4, 8 and 12 weeks of age before cull at 14 weeks of age. Intestinal polyps were enumerated, the faecal microbial composition was examined by 16S rRNA gene sequencing, faecal and plasma bile acid profiles were determined by UPLC-MS and ileal cytokine expression was measured by qPCR. We also examined FXR and Wnt signalling by qPCR for target genes, and performed a correlation analysis between features of our data.

Results: Gavage with *E. coli* expressing *bsh* significantly reduced small intestine polyposis in APC^{MIN} mice. This occurred alongside an enrichment of hydrophilic bile acid tauro-ursodeoxycholic acid and alterations in the composition of the microbiota. Our correlation analysis revealed a negative association between FXR target gene *I-babp* and the number of small intestinal polyps.

Conclusions: Surprisingly, *Bsh* reduced small intestine polyposis in APC^{MIN} mice by a mechanism which may involve bile acid signalling and a reduction in the hydrophobicity of the bile acid pool, as well as an induction of protective changes in the microbiota.

Acknowledgements: : 16S rRNA gene sequencing of the faecal microbiota was performed by Calum Walsh in Teagasc Moorepark (*Materials and Methods* section 2.5, *Amplicon Sequencing* to end of *Functional Analysis*), who also produced the plots in Figure 5.6b and

5.13b. UPLC-MS and extraction from faecal and plasma samples for the detection of bile acids was performed by Peter Cronin (*Materials and Methods* section 2.7, *Ultra-Performance Liquid Chromatography – Mass Spectrometry)*. Some of this work is presented in his submitted MRes thesis (April 2019). The materials and methods sections for these processes are provided by their respective executors. Gavage and mouse culling were performed by Cara Hueston.

5.1 Introduction

The aetiology of colorectal cancer (CRC) involves the complex interaction of genetic and environmental factors, and recent evidence also suggests it could be influenced by the gut microbiota (1). The gut microbiota of human CRC patients is significantly altered by disease and certain microbial patterns are associated with increased cancer risk, but definitive identification of mechanisms and specific taxa involved has proven elusive as bacterial species associated with human CRC are not consistent across studies (2, 3).

APC^{MIN} mice are used as a model of familial CRC as they harbour heterozygous mutations in the *Apc* gene, similar to human patients suffering from Familial Adenomatous Polyposis (FAP). These mice develop intestinal polyps starting at 7-8 weeks of age, with inflammation becoming apparent at approximately 12 weeks of age (4, 5). In FAP, the microbiota is enriched for pro-tumorigenic bacteria such as *Escherichia coli* expressing colibactin and enterotoxigenic *Bacteroides fragilis* (6), and a similar phenomenon is observed in APC^{MIN} mice (4). Importantly human tumour-associated bacteria has been shown to aggravate tumorigenesis in APC^{MIN} mice (7).

The gut microbiota can influence the development of CRC by production of pro-carcinogenic bacterial metabolites, for example secondary bile acids (8). This was demonstrated by dietary administration of secondary bile acids to APC^{MIN} mice which increased tumour multiplicity in a microbiota-dependent manner (9). Bile acid receptor FXR has also been shown to suppress intestinal tumorigenesis *in vivo* by mechanisms including promotion of apoptosis and differentiation (10). High fat diets also increase the faecal levels of secondary bile acids and are associated with increased cancer risk (11, 12). This suggests that bile acids and the microorganisms that influence their metabolism may represent potential aetiologic agents of high fat diet-induced colon cancer risk.

In this context, the prevalence of bile salt hydrolase (Bsh) enzymes among probiotic bacteria is surprising (13). Bsh enzymes cleave the amino acid side chain of bile salts to form free bile acids, which is a prerequisite for subsequent 7α-dehydroxylation to secondary bile acids (14). Increasing the prevalence of Bsh in the microbiota therefore has potential to increase the luminal concentration of secondary bile acids with the potential to increase cancer risk, although the 7α-dehydroxylation pathway has not been observed in probiotic species (8, 15). Bsh is also found in pathogenic bacteria such as *Listeria monocytogenes* where it improves its gastrointestinal persistence (16). This raises the question as to the role of Bsh *in vivo*, its interaction with the host and its desirability in probiotic bacterial strains.

We applied an engineered strain of laboratory *E. coli MG1655* to overexpress *bsh* in order to investigate the role of this enzyme in APC^{MIN} mice and determine its effects on polyp multiplicity, microbial diversity and composition, proliferation, Wnt signalling, inflammatory transcription, as well as bile acid composition and signalling. We also performed a correlation analysis to identify any relationships between these factors. This work revealed a significant reduction of small intestine polyp number in mice administered *E. coli MG1655* expressing *bsh* by a mechanism which may involve bile acid signalling and a reduction in the hydrophobicity of the bile acid pool, as well as an induction of protective changes in the microbiota.

5.2 Results

5.2.1 Administration of *E. coli* expressing *bsh* significantly decreased polyposis in APC^{MIN} mice

APC^{MIN} mice develop dozens of polyps in their small intestine, and we used the multiplicity of these polyps to determine the effect of bacterial gavage on tumorigenesis in this model. The total number of polyps in the small intestine of APC^{MIN} mice administered EC-BSH was significantly lower than the groups administered either PBS or EC (Figure 5.1; ANOVA and Tukey's HSD, $p<0.05$). The number of polyps in the distal small intestine of EC-BSH mice is also significantly lower than the PBS group (Figure 5.1; ANOVA and Tukey's HSD, $p=0.015$).

There is no difference in polyp number between groups in the proximal or middle sections of the small intestine (Figure 5.1; ANOVA, $p>0.05$) or the colon (Figure 5.1; KW test, $p=0.4$).

5.2.2 Levels of bacterial colonisation were similar in EC and EC-BSH mice

Successful colonisation was confirmed by analysis of faecal colony forming units (CFUs) of *E. coli* and *E. coli* overexpressing *bsh* on LB agar containing streptomycin. No streptomycin-resistant bacteria were detected in mice treated with PBS. CFUs/mL only differed between EC and EC-BSH at 6 weeks of age, with higher colonisation in EC mice (Figure 5.2; Two-way ANOVA followed by T-test, $p=0.023$).

5.2.3 Epididymal fat is reduced in mice administered *E. coli*

Cancer-associated weight loss, or cachexia, is an indicator of severe disease in human cancer that is also observed in late-stage APC^{MIN} mice. We tracked the body weight of our mice at weekly intervals throughout the study and measured the mass of their mesenteric and

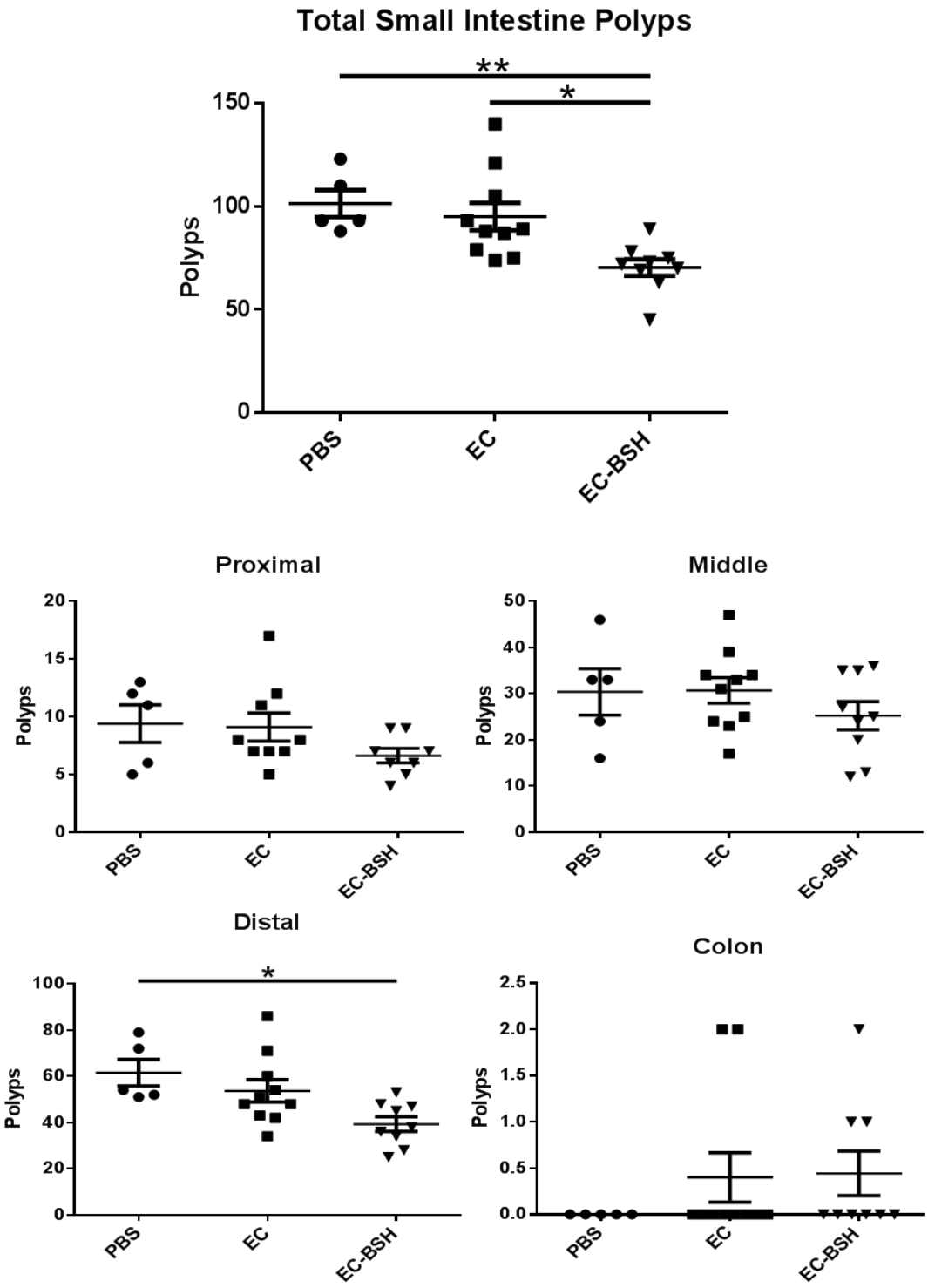

Figure 5.1: EC-BSH mice develop significantly fewer polyps in their small intestine. Mice were culled at 14 weeks of age and 2cm of their proximal and distal small and large intestine was removed for RNA analysis. The remaining small intestine was divided into three equal portions and the number of polyps in each section was enumerated under a dissecting microscope. The number of polyps in the colon was also determined. EC-BSH mice had significantly fewer total polyps in their small intestine than PBS and EC mice (ANOVA and Tukey's HSD, $P<0.05$), and fewer polyps in their distal small intestine than PBS-treated mice (ANOVA and Tukey's HSD, $P=0.015$).

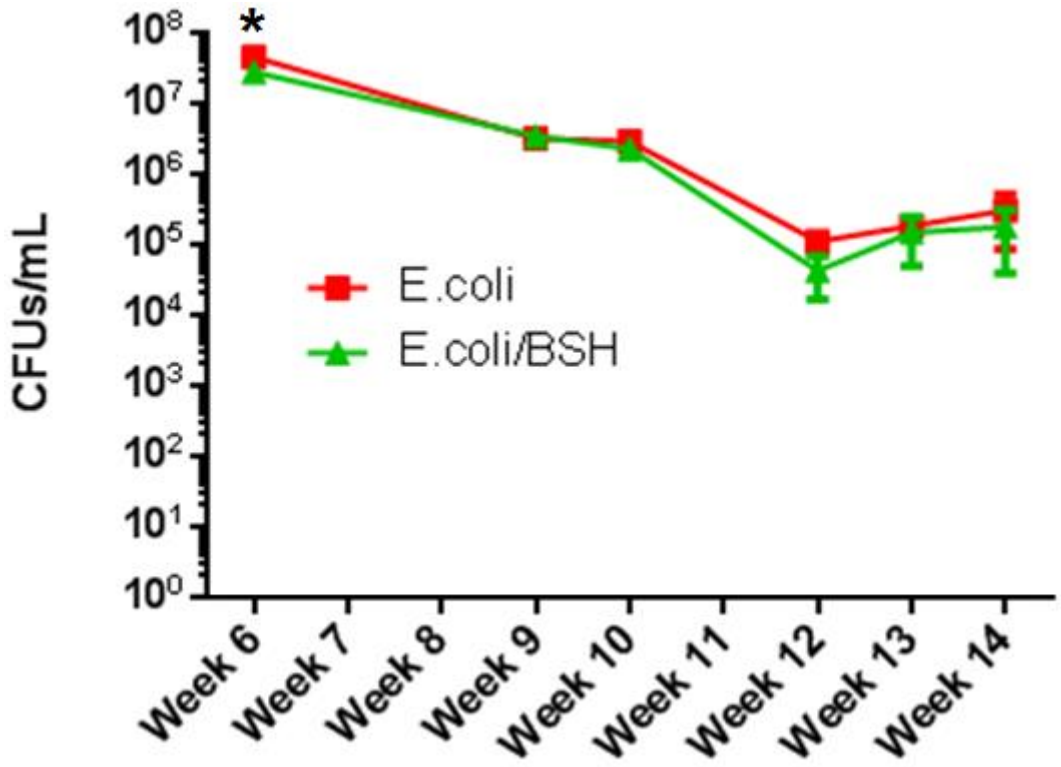

Figure 5.2: Faecal colonisation by *E. coli* and *E. coli* overexpressing *bsh*. Colonisation was determined by plating serial dilutions of faeces suspended in PBS onto LB agar containing streptomycin. CFUs/mL of *E. coli* and *E. coli* overexpressing *bsh* only differed at Week 6 (mixed ANOVA followed by T-test, p=0.023), while no streptomycin-resistant bacteria were detected in the PBS group.

epididymal fat after cull. Body weight did not differ between groups across the study (Figure 5.3; two-way ANOVA, p=0.4212). The mass of epididymal fat was reduced in the EC group (Figure 5.3; ANOVA and Tukey's HSD, p=0.036) and there was no difference in the mass of mesenteric fat between any of the treatments (Figure 5.3; ANOVA, p=0.1).

5.2.4 Ki67 staining is not increased in APC^{MIN} mice

Loss of cell cycle control in APC^{MIN} mice has been shown to precede the development of intestinal polyps (4). In order to determine how far this loss of control extends, we measured the degree of proliferation in normal villi of each group at our end-point. The expression of proliferation indicator Ki67 did not differ between groups (Figure 5.4; ANOVA, p=0.11).

5.2.5 Bacterial gavage affects cytokine and chemokine transcription in APC^{MIN} mice

Inflammation is a risk factor for colon cancer and the tumour microenvironment can modulate inflammatory conditions to promote tumour growth. As such, we measured the transcription of cytokines and chemokines in the distal small intestine by qPCR, as well as measuring the spleen weight and the length of the small and large intestine of our mice, which can be used as indicators of intestinal inflammation (Figure 5.5).

The relative transcription of *Cxcl1* was significantly decreased in both EC and EC-BSH mice compared to PBS (Figure 5.5; ANOVA and Tukey's HSD, $p<0.05$), while *Cxcl5, Tgfβ* and *Jun* are decreased in EC compared to PBS (Figure 5.5; ANOVA and KW tests, followed by Tukey's HSD and MWU tests, $p<0.05$). There were no significant differences between relative transcription of *Il1β*, *Il10*, spleen weight or in the length of small intestine between groups (Figure 5.5; ANOVA, $p>0.05$).

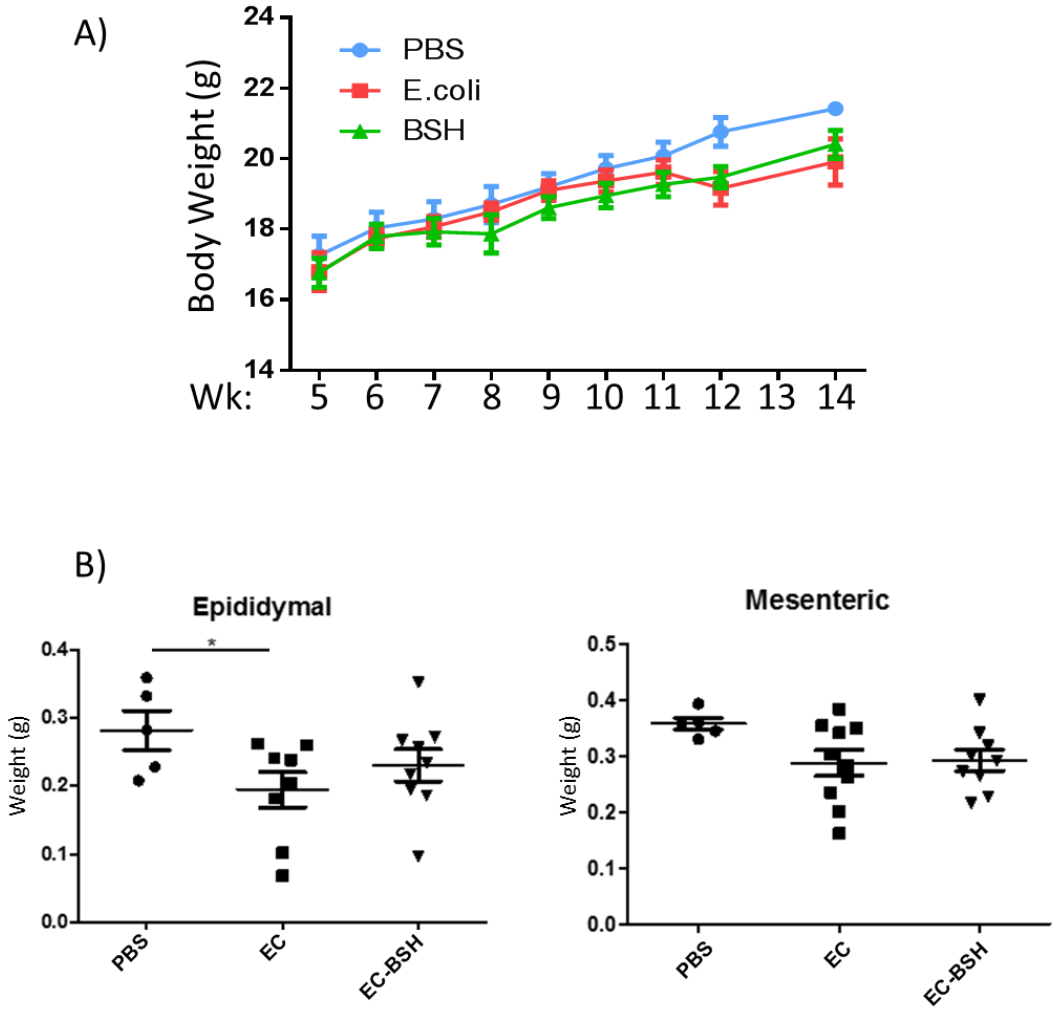

Figure 5.3: Epididymal fat was reduced in EC mice. Weight loss or inhibited weight gain is a sign of severe pathology in human cancer and mouse models of cancer. We tracked the body weight of our mice every week from 5 weeks of age (A) and recorded the mass of their mesenteric and epididymal fat after cull (B). The weight of epididymal fat was reduced in the EC group compared to PBS (ANOVA and Tukey's HSD, p=0.036). Body weight or mesenteric fat did not differ between groups (Two-way ANOVA and ANOVA, P>0.05).

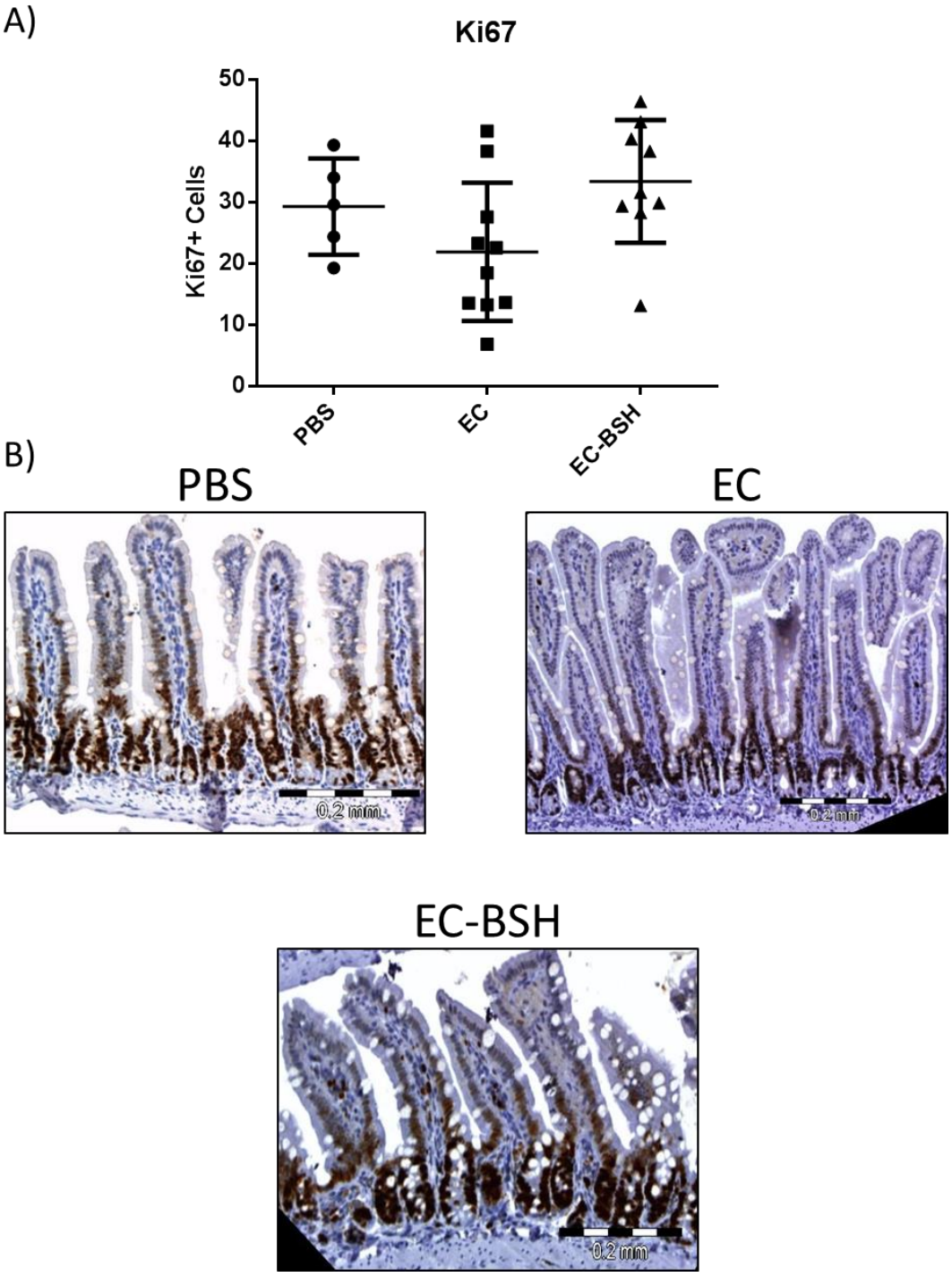

Figure 5.4: Proliferation in normal villi did not differ between groups. Mutation in the tumour suppressor *Apc* gene can lead to constitutive Wnt pathway activation and aberrant cell proliferation. In order to investigate if proliferation is up-regulated in the normal-appearing villi in the small intestine of APC^{MIN} mice prior to the development of polyps, we stained the epithelium for Ki67 and determined the percentage of Ki67-positive cells per crypt-villus unit for ten such units per mouse. ***A)*** There was no significant difference in Ki67 expression in the normal villi of APC^{MIN} mice, which suggests that dysregulated proliferation is not ubiquitous in the small intestine of these mice (ANOVA, P=0.11). ***B)*** Sections of the distal ileum of wild-type and APC^{MIN} stained for Ki67 on a background of haematoxylin. Magnification 200x.

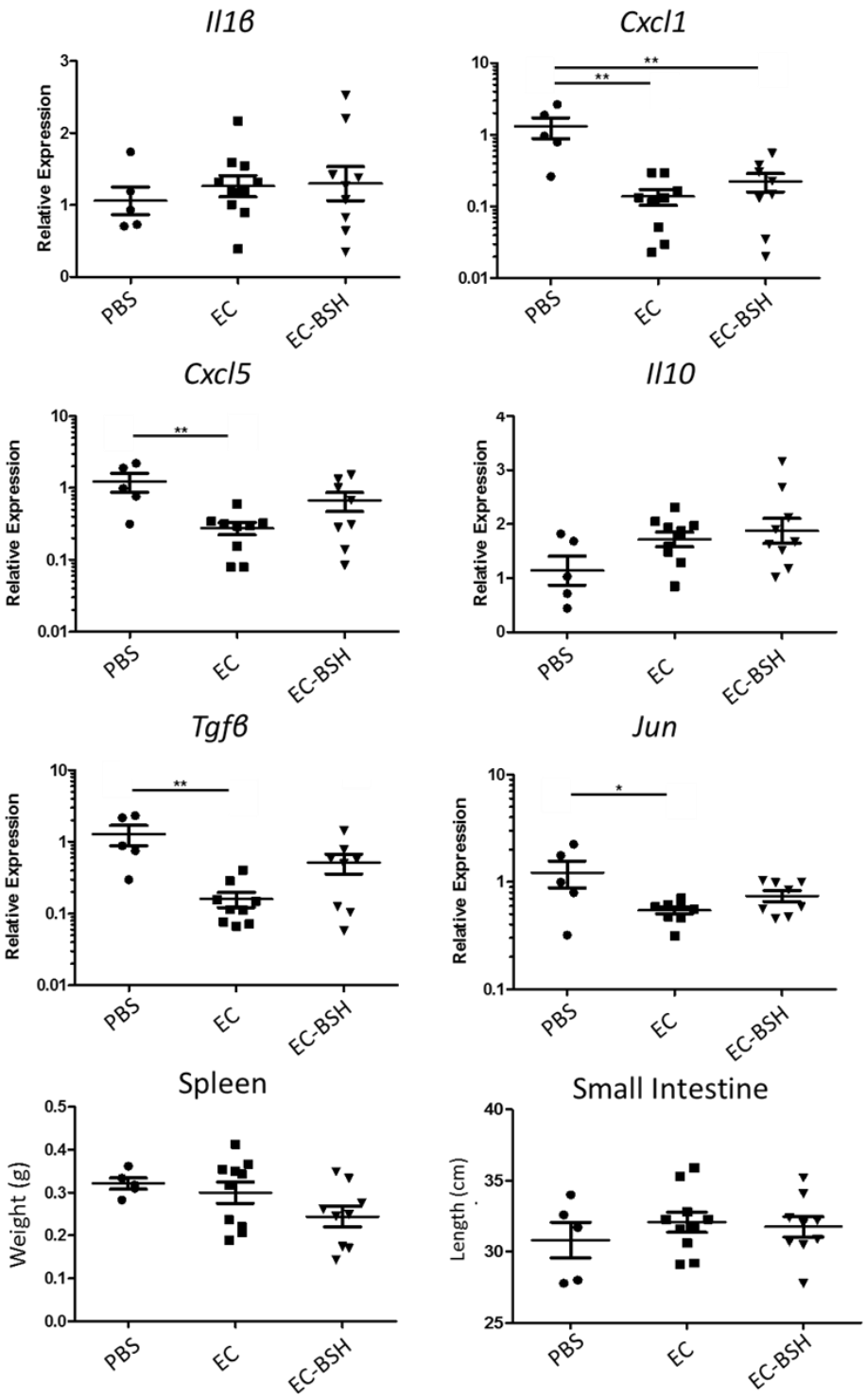

Figure 5.5: Changes in inflammatory transcription are observed in APC^{MIN} mice. Chronic inflammation is a risk factor for colorectal cancer and inflammation in the tumour microenvironment can drive cancer progression. In order to establish if inflammation played a role in the pathogenesis of our model, we extracted RNA from the distal small intestine, the primary site of polyposis in APC^{MIN} mice, and performed qPCR for several cytokines. We also measured spleen weight and the length of the small intestine. *Cxcl1* was increased in PBS mice compared to both other groups, while *Cxcl5*, *Tgfβ* and *Jun* were decreased in EC compared to PBS (ANOVA, $p<0.05$).

5.2.6 The faecal microbiota is significantly different in APC^{MIN} mice

We collected faecal pellets from each mouse at the end-point of the experiment and performed 16S rRNA gene sequencing to characterise the microbial diversity and composition. We measured the α-diversity by two metrics. These were Shannon diversity, a mathematical measure of the number of species and their relative abundances, and phylogenetic diversity (PD), which measures the total length of the minimum path spanning each node of a cladogram featuring the detected species but does not consider the relative abundance of those species (Figure 5.6A).

Shannon diversity is significantly higher in the EC-BSH group compared to EC (Figure 5.6A; KW test and MWU-test, p=0.017). No changes were observed in PD (Figure 5.6A; KW test, p=0.112).

Beta (β)-diversity represents between-individual diversity in the microbiota which we measured by PERMANOVA of the unweighted Unifrac distances, visualised by PCoA. All groups were significantly different from each other, and treatment explained between 13% and 24% of the variation (Figure 5.6B; PERMANOVA, P<0.01).

Finally, we considered individual taxa differences between groups. The significantly different taxa are presented in Figure 5.7 (KW test with FDR adjustment, p<0.05). The largest changes are observed in *Lachnospiraceae UCG-001*, which is 50-fold more abundant in EC than PBS and 19-fold more abundant in EC than EC-BSH. *Ruminococcaceae UCG-010* is 19.3-fold more abundant in PBS than EC and *Faecalibacterium* is 13.9-fold more abundant in PBS than EC. *Clostridiales vadinBB60; uncultured rumen bacterium (URB)* is significantly higher in EC than EC-BSH, where it is completely absent, while this pattern is reversed for *Acetatifactor*. *Anaeroplasma* is also significantly higher in EC and EC-BSH compared to PBS, being absent in the latter group, while *Tyzzerella* is significantly more abundant in EC-BSH than EC or PBS.

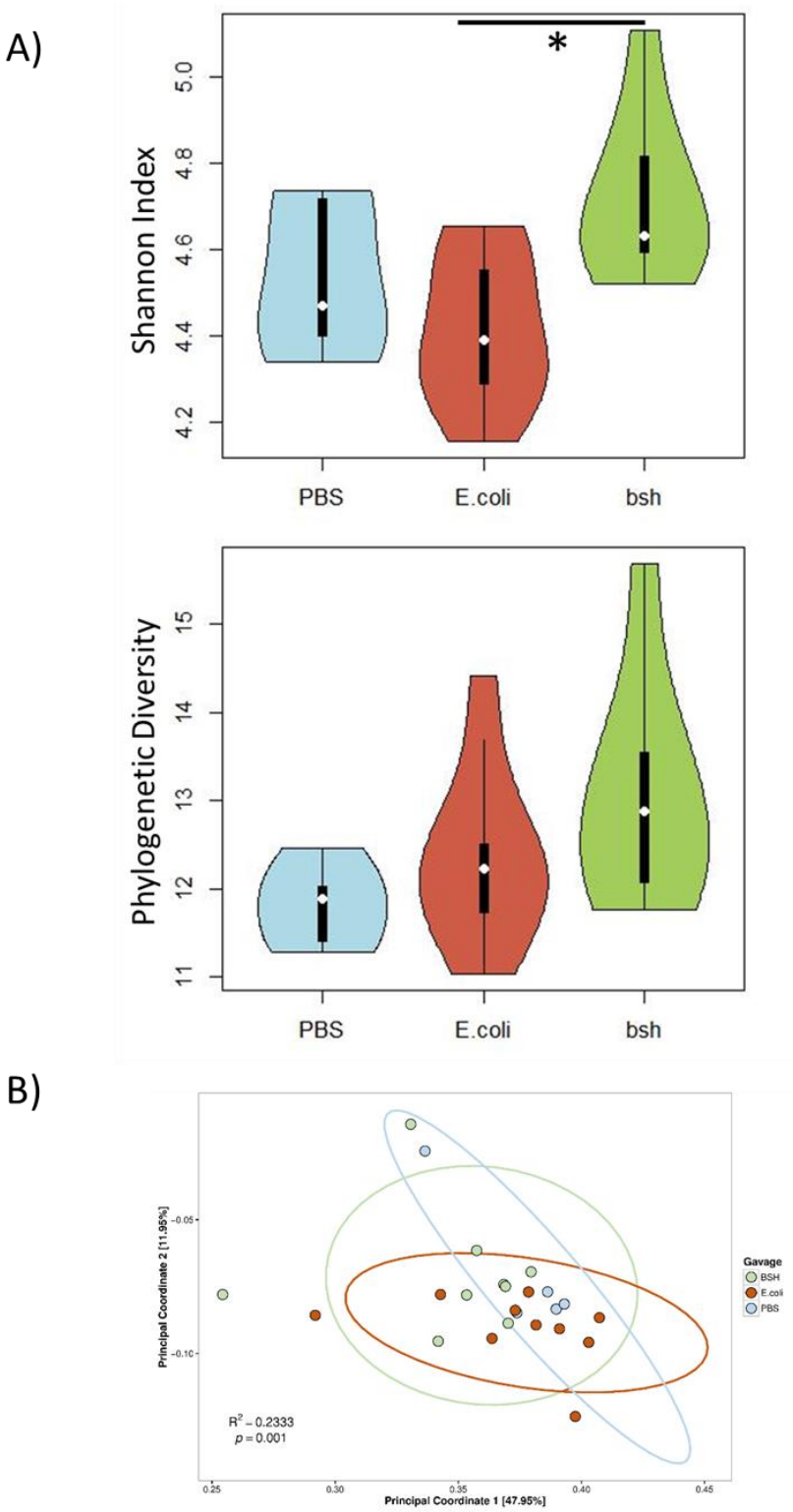

Figure 5.6: A- and β-diversity are significantly different between groups. We performed 16S rRNA gene sequencing for the V3-V4 region and examined the α- and β-diversities by Shannon and Phylogenetic Diversity (PD) metrics and unweighted UniFrac PCoA. ***A)*** This revealed a significant increase in Shannon diversity, but not PD, in the EC-BSH group (KW test and MWU-tests, $p<0.05$). ***B)*** In addition, the β-diversity of each group was significantly different (PERMANOVA, $p<0.01$). *N*=5, 10 and 9 for PBS, EC and EC-BSH. Figure in ***B*** was provided by Calum Walsh at Teagasc, Moorepark.

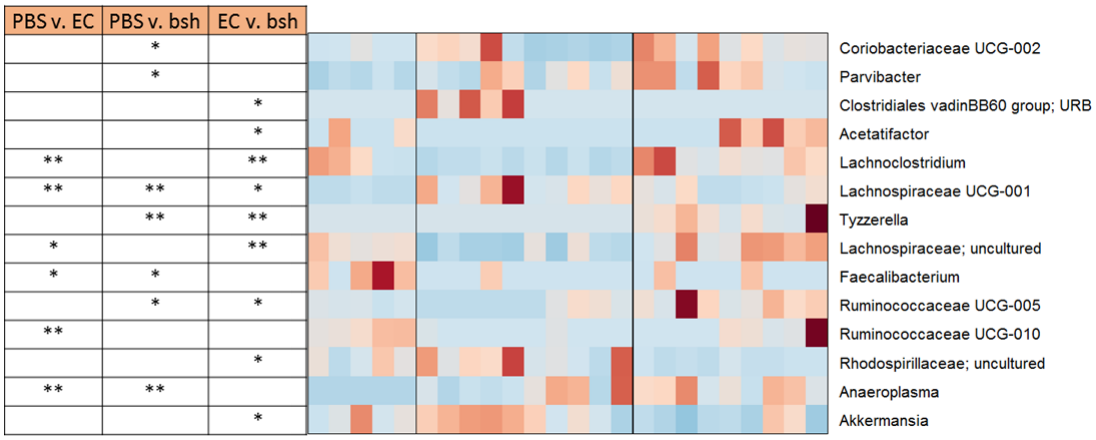

Figure 5.7: Taxa significantly different between groups. We performed 16S rRNA gene sequencing for the V3-V4 region and compared the relative abundance that each taxon comprised in each group. This revealed a number of significantly different bacteria (KW test and MWU-test with FDR adjustment, $p<0.05$). Only the significantly different OTUs are presented here. Data are presented as Z-scores normalised to the row average with asterisks representing the degree of significance as determined by post-hoc analysis ($p<0.05$, <0.01 and <0.001 for *, ** and *** respectively). *N*=5, 10 and 9 for PBS, EC and EC-BSH.

In order to investigate the alterations in the gut bacteria at a higher structural level, we defined a set of bacterial co-abundance groups (CAGs) by finding the Kendall correlation between different bacterial taxa and Ward-clustering these values based on their Pearson correlation coefficients (Figure 5.8A) (17). These correlations were converted to a distance matrix on which PERMANOVA was performed which determined that all CAGs were significantly different (Figure 5.8C, $p<0.01$). The composition of each CAG can be found in Table 5.3.

Seven CAGs were identified, labelled CAG1-7. The relative abundance of CAG1 was higher in EC-BSH mice than EC (Figure 5.8B; KW test and MWU test, $p=0.009$). The relative abundance of CAG3 is increased in EC-BSH mice compared to the PBS and EC groups (Figure 5.8B; KW test and MWU test, $p<0.05$), while CAG4 is increased in PBS compared to EC and EC-BSH (Figure 5.8B; KW test and MWU test, $p<0.05$). The relative abundance of CAG5 in higher in the EC group compared to PBS (Figure 5.9B; ANOVA and Tukey's HSD, $p=0.029$), while the abundance of CAG7 is lower in EC-BSH compared to EC (Figure 5.9B; KW test and MWU test, $p=0.006$).

CAG1 is dominated by an uncultured member of the *Lachnospiraceae* family and *Ruminiclostridium 9*, and comprises an average of 10.6% of the microbiota detected in our mice. CAG3 is more diverse and features large portions of *Blautia*, *Ruminococcaceae UCG-005*, *Eubacterium xylanophilum group* and *Tyzzerella* but makes up less than 1% of the total microbiome of each mouse. *Christensenellaceae; R7 group* and *Eubacterium coprostanoligenes group* predominant in CAG4, but this CAG comprises less than 0.1% of the average total abundance of the microbiome. Taxa in CAG5 constitute 9.6% of the average abundance of the microbiome and the majority of this CAG consists of *Clostridiales vadinBB60 group; uncultured bacterium*, an uncultured *Bacteroidales* bacterium and *Lachnospiraceae UCG-008*. *Akkermansia* and *Clostridiales vadinBB60 group; ambiguous taxa*

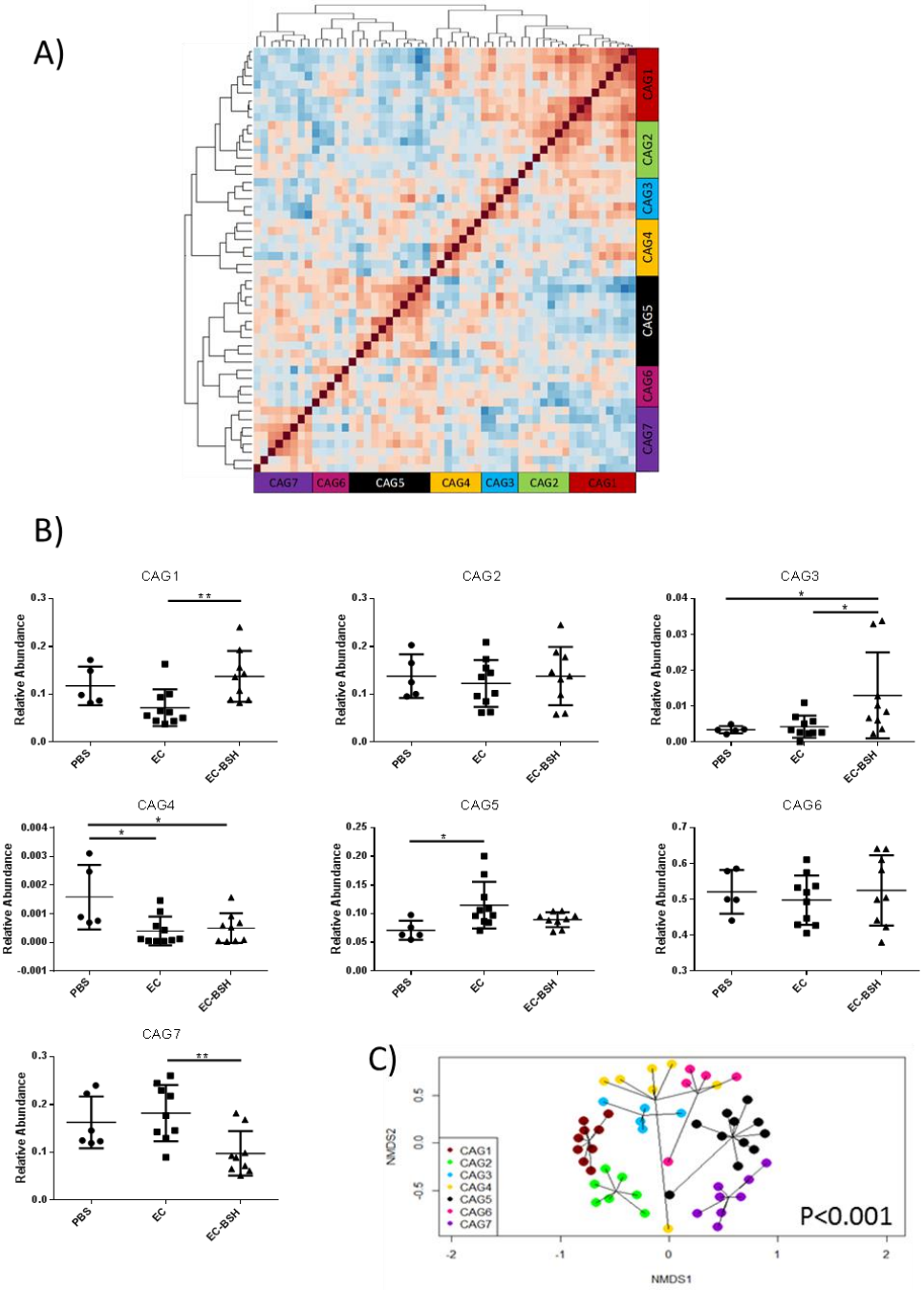

Figure 5.8: Generation of co-abundance groups. The Kendall correlations of OTUs' relative abundances were generated and clustered by Ward-linkage and Pearson correlation. This defined a set of "co-abundance groups" (CAGs) which describe higher-level structures of the microbiota by highlighting taxa for which changes in abundance correlate. These Kendall correlations were then converted to a distance metric and analysed by PERMANOVA which determined that each CAG was significantly different. ***A)*** A heatplot of Kendall correlation values for each pair of taxa clustered by ward linkage of their Pearson correlations. Coloured bars along the axes denote the CAGs. The composition if each CAG is presented in Table 3.1. ***B)*** A number of significantly different CAGs were identified (ANOVA and KW tests, with post-hoc analysis by Tukey's HSD and MWU-tests, $p<0.05$) ***C)*** Non-metric multidimensional scaling (NMDS) of the distance metrics of the CAGs' correlation values. All CAGs were determined to be significantly different (PERMANOVA, $p<0.01$).

Table 5.3: CAG Composition

CAG1	Ruminiclostridium 9 Anaerotruncus Lachnospiraceae Uncultured Intestinimonas Lachnospiraceae UCG-006 Lachnoclostridium Ruminococcus 1 Ruminococcaceae UCG-003 Ruminiclostridium 5
CAG2	Peptococcaceae Uncultured Lachnospiraceae NK4A136 Group Oscillibacter Ruminiclostridium Marvinbryantia Delftia Anaerobacillus
CAG3	[Eubacterium] xylanophilum group Syntrophococcus Blautia Ruminococcaceae UCG-005 Tyzzerella
CAG4	Ruminococcaceae UCG-014 Lactococcus Coriobacteriaceae Uncultured Ruminococcaceae UCG_010 Christensenellaceae R7 Group [Eubacterium] Coprostanoligenes Group Faecalibacterium
CAG5	Escherichia-Shigella Lachnospiraceae UCG-008 Ruminococcaceae UCG-013 Parvibacter Coriobacteriaceae UCG-002 Allobaculum Uncultured Bacteroidales Bacterium Bifidobacterium Anaeroplasma Lachnospiraceae UCG-001 Clostridales VadinBB60 Group; Uncultured Bacterium
CAG6	Candidatus Saccharimonas Ruminococcaceae Uncultured Christensenellaceae Uncultured Bacteroides Bacteroidales S24-7 Group; Uncultured Bacterium
CAG7	Akkermansia Rhodospirillaceae Uncultured Chloroplast; Uncultured Bacterium Bacteroidales S24-7 Group; Ambiguous Taxa [Eubacterium] Nodatum Group Alistipes Ochrobactrum Clostridales VadinBB60 Group; Ambiguous Taxa

compose over 95% of CAG7, which itself forms 14.5% of the average abundance of the microbiota. Of the two CAGs that do not differ between groups, the majority of CAG2 consists of *Lachnospiraceae NK4A136 group* and this CAG encompasses 13.1% of the microbiota on average, while CAG6 is dominated by *Bacteroidales S24-7 group; uncultured bacterium* and *Bacteroides*, and this CAG comprises 51% of the average abundance of the microbiome due to the prevalence of these two taxa.

5.2.7 Tauro-ursodeoxycholic acid is enriched in EC-BSH mice

In order to investigate the potential role of microbial bile acid modification in our model, we analysed the faecal and plasma bile acid profile of each group at the experimental end-point by UPLC-MS. After correction for multiple comparisons, only the faecal concentration of tauro-conjugated ursodeoxycholic acid (T-UDCA) was increased in the EC-BSH group (Figure 5.9; KW test, p=0.001). The list of bile acids measured is presented in Table 5.4. Neither total faecal nor plasma bile acid concentration differed between groups (ANOVA and KW test, P>0.05), and there were no differences among the plasma bile acids (ANOVA and KW-test, P>0.05).

5.2.8 The transcription of FXR target gene *I-babp* is increased by bacterial gavage in APC^{MIN} mice

Bile acid receptor FXR regulates the transcription of a number of genes in the ileum and has also been implicated in protection from CRC (10, 18). In order to determine if bile acid signalling is affected in our model, we measured the transcription of four FXR target genes in the distal ileum (Figure 5.10).

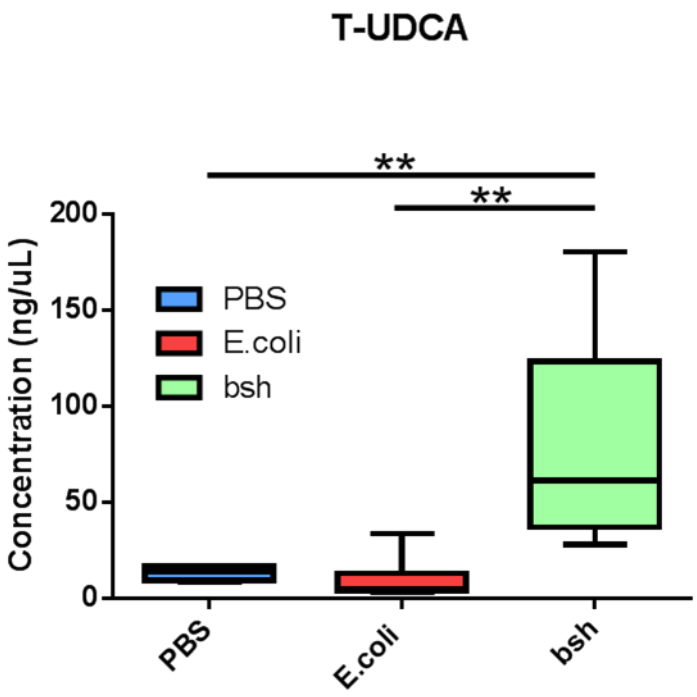

Figure 5.9: T-UDCA is enriched in EC-BSH mice. Microbial metabolism of bile acids has been implicated in the pathogenesis of colon cancer. To investigate the role bile acids play in our model, we measured the concentration of faecal and plasma bile acids by UPLC-MS. After correction for multiple comparisons, only the faecal concentration of T-UDCA was significantly different between groups (KW test and MWU-test with FDR adjustment, p=0.001). Each bile acid measured in presented in Table 5.4. *N*=3, 6 and 7 for plasma bile acids; 4, 8 and 8 for faecal bile acids; for PBS, EC and EC-BSH respectively.

Table 5.4: Bile acids measured

	Bile Acid	Abbreviation
Bile Acids	Dehydrocholic Acid	DHCA
	Lithocholic Acid	LCA
	Ursodeoxycholic Acid	UDCA
	Chenodeoxycholic Acid	CDCA
	Hyodeoxycholic Acid	HDCA
	Deoxycholic Acid	DCA
	Cholic Acid	CA
	Hyocholic Acid	HCA
	7-Keto-Lithocholic Acid	7-Keto-LCA
	Tauro-Cholic Acid	T-CA
	Tauro-Hyocholic Acid	T-HCA
	Tauro-Chenodeoxycholic Acid	T-CDCA
	Tauro-Ursodeoxycholic Acid	T-UDCA
	Tauro-Deoxycholic Acid	T-DCA
	Tauro-Hyodeoxycholic Acid	T-HDCA
	Tauro-Lithocholic Acid	T-LCA
	Glyco-Cholic Acid	G-CA
	Glyco-Hyocholic Acid	G-HCA
	Glyco-Chenodeoxycholic Acid	G-CDCA
	Glyco-Ursodeoxycholic Acid	G-UDCA
	Glyco-Deoxycholic Acid	G-DCA
	Glyco-Hyodeoxycholic Acid	G-HDCA
	Glyco-Lithocholic Acid	G-LCA
	Beta (β)-Muricholic Acid	B-MCA
	Alpha/gamma (α/ω)-Muricholic Acid	α/ω-MCA
	Murocholic Acid	MoCA
	Tauro α-, β-, and ω-Muricholic Acid	T-α/β/ω-MCA
	Total Bile Acids	Total BAs

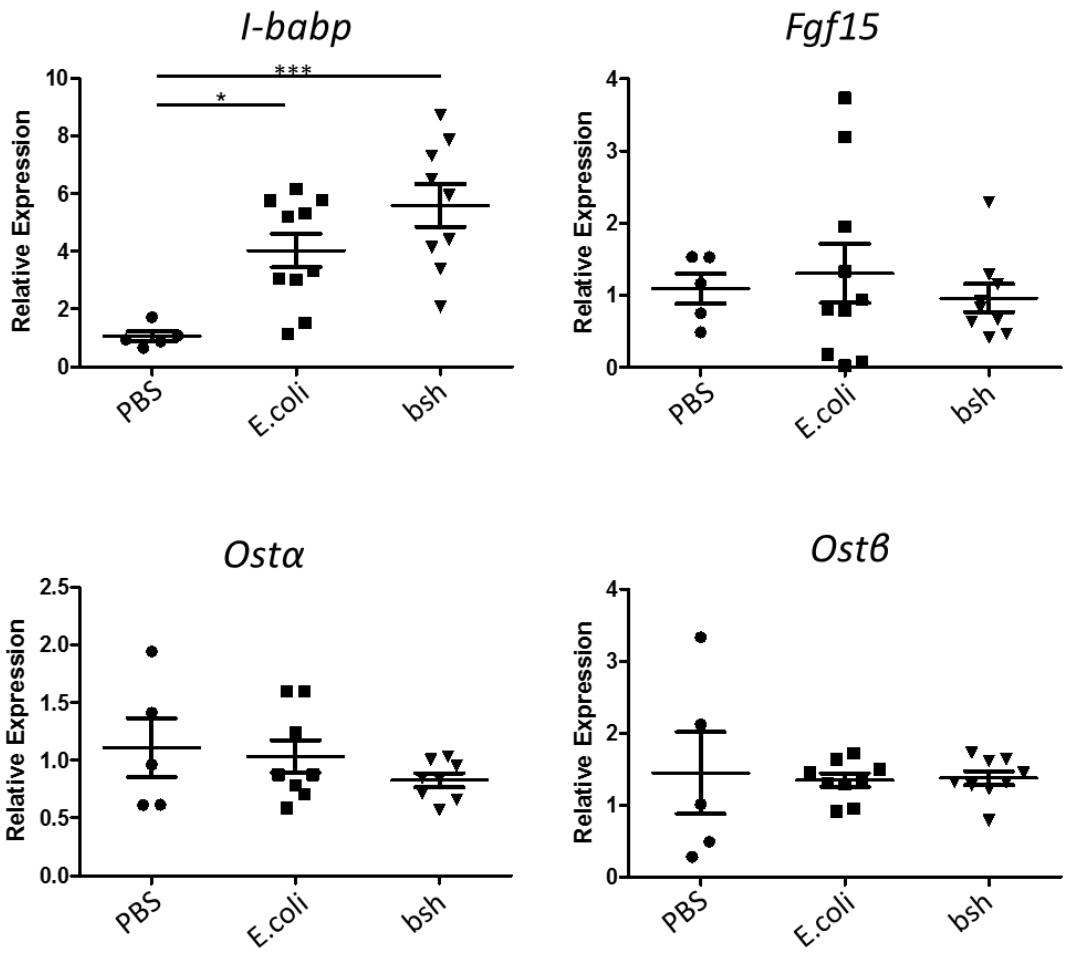

Figure 5.10: Transcription of *I-babp* is increased by bacterial gavage. One mechanism by which bile acids can affect tumour risk is by FXR signalling, which has been shown to be protective against CRC. We measured the expression of four FXR target genes in the distal ileum of our mice by qPCR. This revealed significantly increased expression of *I-babp* and EC and EC-BSH mice, which may indicate activation of FXR signalling (ANOVA and Tukey's HSD, $p<0.05$).

The transcription of *I-babp* was significantly increased in EC and EC-BSH groups compared to PBS (Figure 5.10; ANOVA and Tukey's HSD, $p<0.05$). The transcription of *Fgf15* and enterocyte basolateral bile acid transporters *Ostα* and *Ostβ* were not significantly different between groups (Figure 5.10; ANOVA, $p>0.05$).

5.2.9 The transcription of Wnt target genes is significantly increased by bacterial gavage

In order to determine if the changes in polyposis induced by EC-BSH occur upstream or downstream of activation of Wnt signalling, we measured the transcription of Wnt target genes *Axin2*, *Myc* and *Sox9* in the distal ileum of each mouse (Figure 5.11).

The relative transcription of *Sox9* was increased in EC and EC-BSH groups compared to PBS (Figure 5.11; ANOVA and Tukey's HSD, $p<0.01$), while the levels of *Axin2* was increased in EC-BSH compared to PBS (Figure 5.11; ANOVA and Tukey's HSD, $p<0.05$) and *Myc* was increased in EC compared to PBS (Figure 5.11; ANOVA and Tukey's HSD, $p<0.01$).

5.2.10 Correlation analysis reveals a relationship between polyp multiplicity, *I-babp* and T-UDCA

We ran correlation analyses between polyp numbers, α-diversity indices, CAG relative abundances, faecal and plasma bile concentrations, and the relative transcription of our cytokines, Wnt and FXR target genes. The significant correlations, after FDR correction for multiple comparisons, are presented in Figure 5.12.

Our correlation analysis revealed a negative association between the transcription of *I-babp* and the number of polyps in the distal small intestine, as well as the total number of polyps in the small intestine of each mouse (Figure 5.12A, Pearson's R, $p<0.05$ after FDR adjustment). In contrast, there was a positive relationship between *I-babp* and both *Axin2*

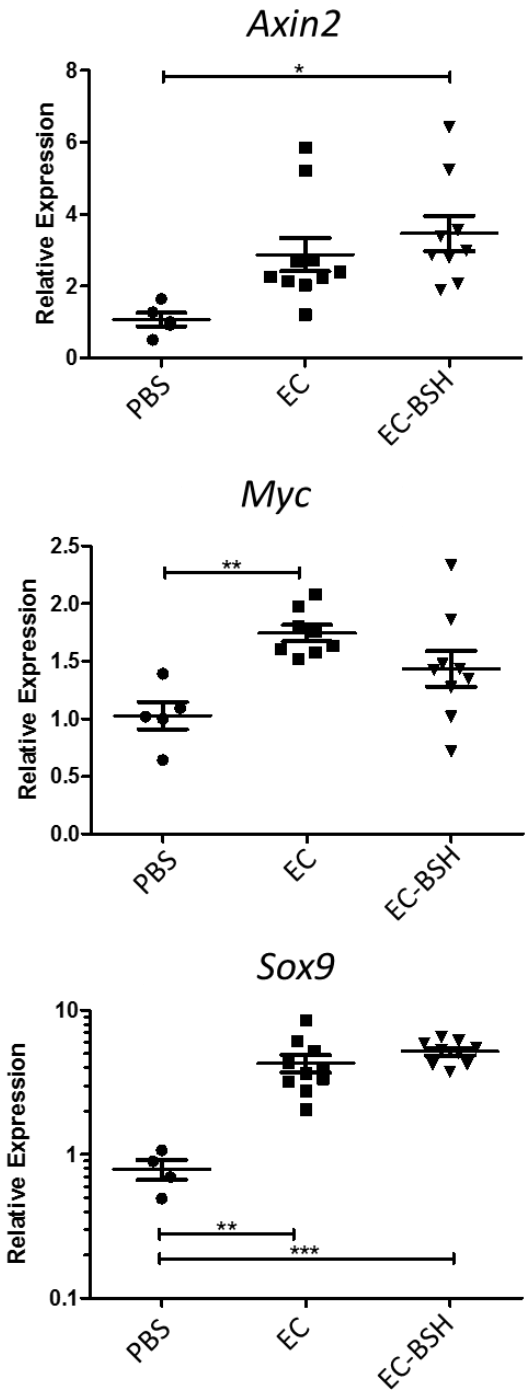

Figure 5.11: Transcription of Wnt target genes is upregulated by bacterial gavage. In order to determine if the changes in polyposis induced by EC-BSH occur upstream or downstream of activation of Wnt signalling, we measured the transcription of Wnt target genes *Axin2*, *Myc* and *Sox9* in the distal ileum of each mouse. mRNA levels of these genes were increased in EC and EC-BSH mice, indicating an activation of Wnt signalling by bacterial gavage (ANOVA and Tukey's HSD, $p<0.05$).

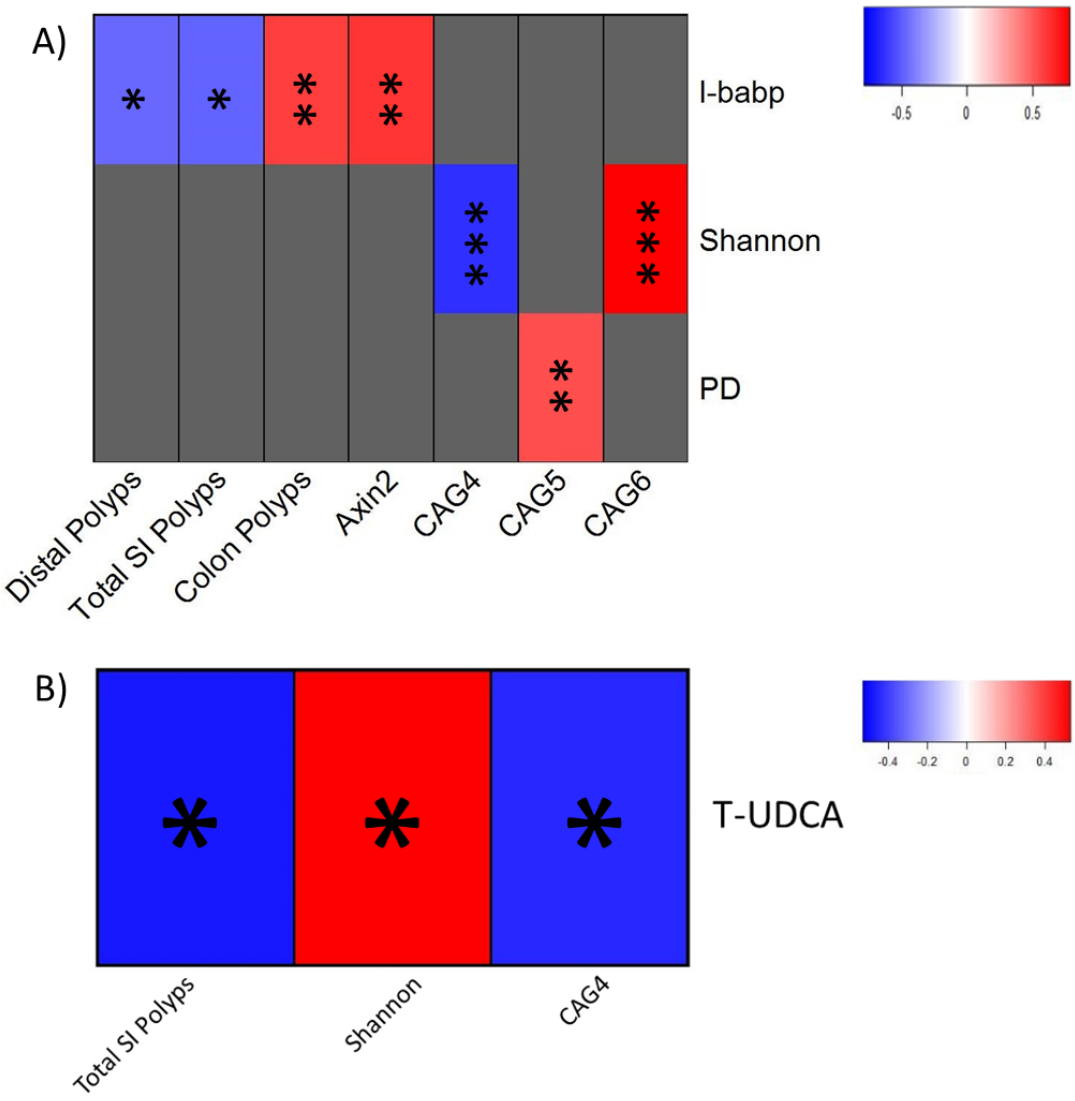

Figure 5.12: Correlation analysis reveals significant relationships between polyp multiplicity, *I-babp* and T-UDCA. The gut presents a complex milieu of interacting forces. In order to examine possible interactions between different aspects of our data in this environment, we performed a correlation analysis between several data-points collected in our study. ***A)*** After correction for multiple comparisons, this revealed a negative correlation between our FXR target gene *I-babp* and polyp number, and a positive correlation between *I-babp* and colonic polyps and transcription of Wnt target gene *Axin2* (Pearson's R and Spearman's R^2, $p<0.05$ after FDR adjustment). ***B)*** Given the enrichment for tauro-ursodeoxycholic acid (T-UDCA) detected by UPLC-MS, we also considered the correlations between this bile acid and other features of our data without correction for multiple comparisons. This revealed a negative correlation between T-UDCA and the total number of small intestine (SI) polyps (Spearman's R=-0.48, p=0.03).

and the number of colonic polyps in each mouse, although the number of colonic polyps was zero-inflated (Figure 5.12A, Pearson's R and Spearman's R^2, $p<0.01$ after FDR adjustment). There were also three correlations between our α-diversity matrices and the relative abundance of CAGs 4, 5 and 6 (Figure 5.12A, Pearson's R, $p<0.01$ after FDR adjustment).

Furthermore, given the enrichment of T-UDCA detected by UPLC-MS, we also considered the correlations between this bile acid and other features of our data without correction for multiple comparisons. This revealed a negative correlation between T-UDCA and the total number of small intestine (SI) polyps (Figure 5.12B; Spearman's R=-0.48, p=0.03).

5.2.11 Diversity of the metagenome predicted by PICRUSt differs between groups

In order to investigate any changes in the capacity of the microbiota to metabolise bile acids after bacterial gavage, we compared the predicted abundance of *baiCD* (COG1902), a gene cluster involved in the 7α-dehydroxylation of bile acids into secondary bile acids, and *bsh* (COG3049), the enzyme responsible for cleaving the amino acid conjugate from bile acids (19). These genes represent the two major pathways of microbial bile acid metabolism. No differences were detected in the abundance of these genes predicted by PICRUSt (Figure 5.13A; ANOVA, $p>0.05$).

We also calculated the α- and β-diversity of the metagenomes predicted by PICRUSt. Alpha (α)-diversity was significantly lower in EC-BSH mice than EC or PBS (Figure 5.13B; KW test followed by MWU-test, $p<0.05$), while β-diversity was significantly different between EC-BSH and EC groups (Figure 5.13B; KW test followed by MWU-test, p=0.032) but not between any other group (Figure 5.13B; KW test followed by MWU-test, $p>0.05$).

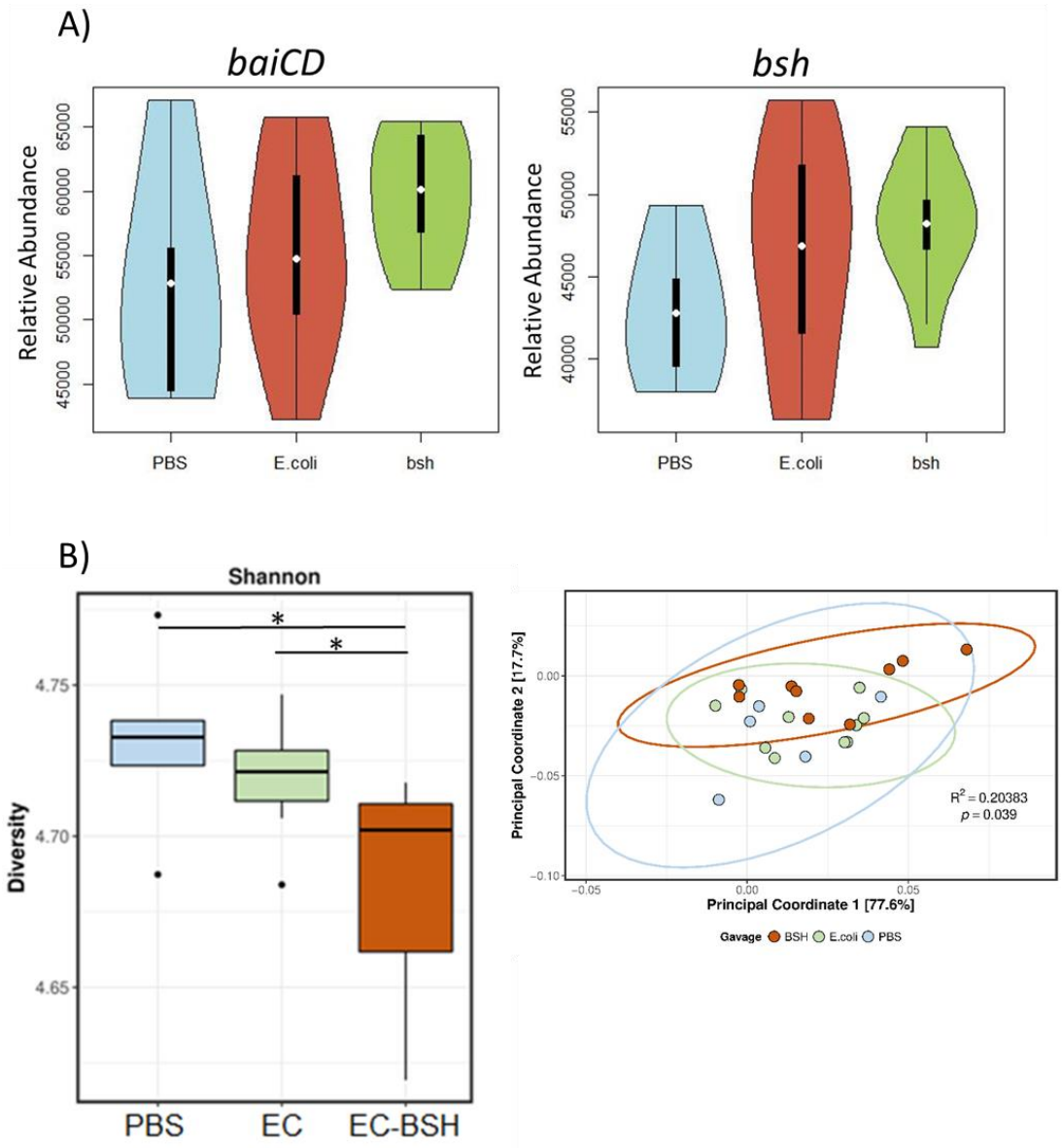

Figure 5.13: Metagenomic α- and β-diversity predicted by PICRUSt differ between groups, but the abundance of bile acid metabolising genes *bsh* and *baiCD* do not. We used PICRUSt to predict the gene content of the faecal microbiota in our groups. We compared their α- and β-diversity, and the abundance of genes *bsh* (COG3049) and *baiCD* (COG1902), a gene involved in the 7α-dehydroxylation of bile acids into secondary bile acids. A- and β-diversity differed significantly between groups, while the predicted abundance of *bsh* and *baiCD* did not (ANOVA, KW test and PERMANOVA, with MWU-test post-hoc analysis). *N*=5, 10 and 9 for PBS, EC and EC-BSH. Figures in ***B*** were provided by Calum Walsh at Teagasc, Moorepark.

5.3 Discussion

Probiotic supplementation is becoming a popular health-promoting regime in modern society and has been linked with a number of positive effects (20). The bile salt-hydrolysing enzyme Bsh is widespread among probiotic bacteria but there is some uncertainty concerning its effects on human health. This is foremost the case for CRC, where the potential for Bsh to increase the colonic luminal content of cytotoxic secondary bile acids could increase cancer risk. We sought to clarify the influence of Bsh by treating a mouse model of CRC with a laboratory strain of *E. coli* overexpressing Bsh. This revealed a significant decrease in polyposis in the small intestine of this model, an effect that was primarily manifested in the ileum.

We also investigated other facets of the host and microbial response in an attempt to identify the mechanism involved in this effect. Modulation of the intestinal immune response may affect carcinogenesis (21). Cytokines and chemokines are soluble immune factors that can increase cancer risk by a number of mechanisms which may also be influenced by the microbiota (22-34). However, cytokine and chemokine transcription in the EC-BSH group did not differ from EC for any of our measures genes. Transcription of *Cxcl1* was decreased in EC-BSH compared to PBS, but this was also the case for EC mice and so does not explain the decrease in polyposis in Bsh-treated mice. It also concurs with the understanding that inflammation occurs late in APC^{MIN} mice and is not required for tumour initiation in the small intestine (4, 35). Chemokines are a class of chemotactic cytokines and their control of immune cell infiltration modulates the composition of the tumour microenvironment (36). Generally, ELR^+ chemokines such as CXCL1 are pro-angiogenic while ELR^- chemokines are angiostatic (37). Chemokines can also drive the expression of growth-promoting genes such as *CCND1*, and suppress apoptosis in tumour cells by up-regulating *MDM2*, inhibiting *BCL-2* expression and suppressing caspase activation (26). Chemokines' ability to induce cell

infiltration has also been co-opted by tumours to promote invasion and migration (38). There is also evidence that each of these chemokines is regulated by the microbiota, as their expression was reduced by a probiotic cocktail containing four strains of *Lactobacillus*, three strains of *Bifidobacterium* and one strain of *Streptococcus*, which also suppressed tumour formation in the colon of a mouse model of colitis-associated CRC (34).

We did observe disruption to the microbial diversity and composition as a result of Bsh treatment, including a significant increase in Shannon diversity compared to the EC group. Studies on α-diversity in CRC have presented conflicting results, reporting both increased and decreased tumour-associated α-diversity (2, 39-54). Further research is necessary to determine if the α-diversity is a useful marker in CRC or whether it simply reflects more informative changes at a compositional level.

The increased Shannon diversity of the microbiota of the EC-BSH group contrasted with the decrease in the diversity of its metagenome predicted by PICRUSt. The microbial and metagenomic β-diversities of this group were also significantly different. The richness of the microbial metagenomic content has previously been associated with positive metabolic effects in obese individuals (55). Our data suggest significant disruption to the composition and function of the microbiome in EC-BSH mice which could have significant effects on host function.

Next, we considered the specific taxa that differed between groups. The abundance of three taxa in the EC-BSH group were significantly altered compared to both other groups. *Ruminococcaceae UCG-005*, an uncultured member of the *Ruminococcaceae* family, was significantly more abundant in EC-BSH than EC or PBS groups. This taxon has been labelled a universal health biomarker and many *Ruminococcaceae* produce butyrate, a short chain fatty acid (SCFA) which is protective against CRC (56, 57). The abundance of *Tyzzerella* was also higher in EC-BSH than EC or PBS. One member of this genus, *T. piliformis* (previously

Clostridium piliformis), was identified as the causative agent of an infectious diarrhoea of laboratory mice (58). It was reduced in Chinese gastric cancer patients (59), and by probiotic treatment of dairy calves (60). *Tyzzerella* is also a member of the *Lachnospiraceae* family which have been associated with butyrate production (57). The abundance of *Lachnospiraceae UCG-001* is increased in EC-BSH compared to PBS but lower than EC. Members of *Lachnospiraceae* family have been associated with butyrate production and some produce Bsh (57, 61). This taxon was decreased in Type II Diabetes Mellitus (TIIDM), where it was negatively associated with TIIDM biomarkers such as cholesterol, triglycerides, IL6 and TNFα (62). It was associated with reduced systemic inflammation and improved intestinal barrier function in a model of liver injury, and with SCFA production and suppression of inflammation in a study of antimicrobial nanocomposites (63, 64). It was also decreased in hepatocellular carcinoma but enriched in obese mice (65, 66), and was suppressed by T-CA injection into the pancreatic duct (67). Of these three taxa, two have strong evidence of positive effects on host health, while the few reports available on *Tyzzerella* are ambivalent. The abundance of *Lachnospiraceae UCG-001* in EC-BSH as an intermediate between both other groups may also hint at two or more interacting effects contributing to the observed differences.

In order to investigate these possible separate effects, we considered the taxa that differed between EC-BSH and one of either PBS or EC. The relative abundances of six taxa were significantly different between EC-BSH and EC groups. *Akkermansia* is a symbiotic mucin degrader of the *Verrucomicrobia* phylum which was decreased in EC-BSH compared to EC (68). It does not produce butyrate but facilitates butyrate production by breaking down complex mucins for fermentation by other species (69). It improves intestinal barrier function and a reduction of *Akkermansia* later in life is associated with inflammation and reduced barrier function which can be rectified by butyrate supplementation (70-72). However, its abundance was increased in CRC patients compared to controls and it was

enriched by a fibre-free and high fat diet with the associated negative metabolic effects (73, 74). *Acetatifactor* is also enriched in EC-BSH compared to EC, where it was completely absent. This *Lachnospiraceae* produces butyrate and was increased in mice by treatment with anti-inflammatory milk (75, 76). However, it was also enriched in mice fed a high fat diet and was suppressed by administration of cancer-protective complex oligosaccharides (77, 78). It was more abundant in arthritic mice and may aggravate colitis (79, 80). It also grew on bile salt-containing media, was induced by FXR agonist fexaramine, and correlated positively with UDCA in mice fed a high-fat diet (75, 77, 81). *Clostridiales vadinBB60; uncultured rumen bacterium (URB)* was also more abundant in EC than EC-BSH, where it was completely absent. This taxon was enriched in mice treated with environmental carcinogen *N*-nitrosamine and by administration of a high fat diet (82, 83). It was increased in mice with an induced allergic response and in protozoan-infected chickens, which could be ameliorated by administration of sodium butyrate (84, 85). It was also suppressed by cancer-protective complex oligosaccharides (86). *Clostridiales vadinBB60; URB* was also completely absent from the PBS group but this was not significantly different from EC, most likely due to the smaller *n*-number in this group, and this suggests its enrichment may be a result of *E. coli* treatment or a cage effect. The uncharacterised taxon *Rhodospirillaceae; uncultured* was decreased in EC-BSH compared to EC. Data are sparse on the role of this *Proteobacterium* in CRC but it was increased in a mouse model of diet-induced obesity, and reduced by vancomycin and the chemotherapeutic drug cyclophosphamide (87, 88). The taxa *Lachnospiraceae; uncultured* and *Lachnoclostridium* were both more abundant in the EC-BSH and PBS groups compared to EC. *Lachnospiraceae* have been discussed previously, while the *Lachnoclostridium* genus has been reported to be decreased in CRC compared to healthy tissue and healthy individuals (89, 90), although the *Lachnoclostridium* species *Clostridium symbiosum* was enriched in CRC patients (91). *Lachnoclostridium* also contains major bile acid 7α-dehydroxylating species *C. scindens* and *C. hylemonae*, responsible for the formation of secondary bile acids.

The relative abundance of four taxa were significantly different between EC-BSH and PBS groups. *Coriobacteriaceae UCG-002* was enriched in EC-BSH compared to PBS. This *Actinobacterium* was associated with propionate and acetate production in dairy calves, but not butyrate, and was increased in mice fed a processed meat diet (92, 93). Other *Coriobacteriaceae* degrade mucin and were associated with cholesterol and triglyceride levels as well as Crohn's disease, while members of the genus *Eggerthella* can oxidise bile acids (94-97). They also correlated positively with reduced IL6 after whole-grain supplementation, and were reduced by butyrate-fortified milk (98, 99). *Coriobacteriaceae* also metabolise isoflavones, including daidzein and genistein (100). Hydrolysing phenylated compounds such as flavonoids has been suggested as a function of Bsh in the microbiota due to their homology to penicillin amidases (13). Consequently, increased luminal expression of Bsh could select for taxa which can utilise this conversion, such as *Coriobacteriaceae*, although Bsh is primarily located intracellularly. Typical isoflavone concentration in the rodent diet provided to our mice was 150 to 250 mg/kg. Consumption of these compounds is associated with reduced CRC risk, possibly mediated by alterations in the composition of the microbiota or by interaction with the oestrogen receptor, which provide additional mechanisms by which Bsh may influence CRC risk (101-104). *Parvibacter* was also increased in EC-BSH compared to PBS. *Parvibacter* is a member of the *Coriobacteriaceae* family which was isolated from a mouse model of IBD (105). It was enriched by cancer-protective green tea supplements, but associated with a reduction in SCFAs in mice fed a high fat diet (82, 106). *Anaeroplasma* is enriched in both EC-BSH and EC compared to PBS, while *Faecalibacterium* shows the opposite pattern. The opportunistic pathogen *Anaeroplasma* is a member of the *Mollicutes* class in the phylum *Tenericutes,* and was enriched in mice treated with genotoxic azoxymethane and fed a high fat diet (107). *Faecalibacterium* is a major butyrate producer associated with anti-inflammatory properties and improved

intestinal barrier function (108-110). It was reported to be reduced in CRC (111, 112), although another study found no change in the stool CRC patients (113).

Finally, one taxon differed between PBS and EC; *Ruminococcaceae UCG-010*. The *Ruminococcaceae* family has been discussed previously while the specific taxon described here was increased in the caecal microbiota of hens by probiotic treatment (114).

A number of CAGs also differed between groups across the experiment which may describe sets of interacting taxa, as described in section 3.3. The relevance of these groups and interactions to CRC is being investigated.

Bsh may modulate the microbiota by a number of mechanisms. The level of *bsh* expression in different bacteria correlates with their sensitivity to bile salts (115). A reduction in luminal bile salt concentrations could reduce this stress on bile salt-sensitive taxa leading to their enrichment. Increased bile salt deconjugation could also provide a nutritional advantage for taxa which can utilise the liberated amino acid as a source of carbon, nitrogen or energy (13). Bsh may also facilitate the incorporation of cholesterol or bile into bacterial membranes to improve membrane integrity and bacterial persistence (13). Bile acid receptor FXR has also been shown to regulate innate immunity in the intestine, and alterations in the bile acid pool precipitated by Bsh may also interfere with intestinal host-microbiota homeostasis (116, 117).

In summary, there is ample evidence of probiotic, anti-tumorigenic changes in the microbiota of mice administered in the EC-BSH group which may account for the reduction in polyps observed in these mice. This is presented most clearly by species whose relative abundance is greater in EC-BSH than both other groups, which was the case for *Ruminococcaceae UCG-005*, a taxon with strong positive associations with health. Taxa which only differed between EC-BSH and one other group only explain part of the discrepancy in polyp multiplicity but may still contribute to our understanding, such as the enrichment of *Lachnoclostridium* and

the suppression of *Clostridiales vadinBB60; URB* in EC-BSH compared to EC; taxa which have conspicuous positive and negative associations with health, respectively. We also observe changes counter to expectation in EC-BSH mice, such as the enrichment of opportunistic pathogen *Anaeroplasma* and suppression of beneficial *Faecalibacterium* compared to PBS. Several taxa have ambivalent or ambiguous effects on health, which may be due to the lack of species-level taxonomic identification provided by 16S rRNA gene sequencing or uncertainty regarding the metabolic capacity of rare and uncultured members of the gut microbiota. In this case, consistent association with health or disease states in studies such as this may highlight key species for deeper investigation.

We also measured the levels of faecal and plasma bile acids in our model at the end of the study. This revealed a significant increase in T-UDCA in the EC-BSH group. This equated to an average of 0.3% of the faecal bile acid content in the EC-BSH group, or 166µM, but this concentration has been shown to have a significant effect *in vitro*, including an inhibition of proliferative response in a murine mixed lymphocyte culture and enhancement of FXR activation by CDCA in Caco-2 cells (118, 119). Additionally, human subjects consuming 900mg of UDCA had average faecal water concentrations of this bile acid of 47µM, and this dose of UDCA has been reported to have biologically relevant effects (120, 121). UDCA protects against cancer and has been reported to be reduced in CRC patients (120, 122-130). UDCA has also been shown to reduce cancer risk factors such as inflammation, oxidative stress and obesity-associated metabolic dysfunction (118, 131-136), and enhance MHC-mediated tumour surveillance (137). T-UDCA may activate FXR (138) and free UDCA can potentiate activation of FXR by other bile acids by increasing their binding affinity for I-BABP (119). The authors suggest this could reduce the levels of free bile acids in colonocytes, which could decrease the risk of unintended pro-tumorigenic effects resulting from an enrichment of free and secondary bile acids by Bsh. This could operate in combination with the inherent reduction in the hydrophobicity of the bile acid pool induced by UDCA (139). FXR has been

shown to be protective against CRC, and suppression of FXR expression by promoter methylation is a feature of APC^{MIN} mice and advanced colorectal carcinomas (10, 18, 140). T-UDCA also correlated negatively with the total number of small intestine polyps in our data before correction for multiple comparisons. We also observed an increase in RNA levels of *I-babp* in our EC-BSH group compared to PBS, and the transcription of this gene correlated negatively with total small intestine polyps, suggesting enhanced activation of tumour-suppressor FXR and adding plausibility to this mechanism (10). However, the increase in transcription of *I-babp* was also observed in the EC group compared to PBS.

The origin of increased T-UDCA in the EC-BSH group in unclear. Low levels of UDCA are found in germ-free mice and higher levels are present in conventionally colonised mice, suggesting that UDCA is a primary bile acid in mice but that levels are increased by microbial bile acid metabolism (141). There have also been reports of a reduction in UDCA in response to treatment with a single antibiotic but a large increase in T-UDCA in response to combined antibiotic treatment, suggesting that the increase is not a product of intestinal bacteria (142). Our mice were exposed to streptomycin but this was the case for all three groups and so would not explain the differences between EC-BSH and the PBS and EC groups, unless there was an interaction between streptomycin and Bsh. Endogenous concentrations of murine CDCA and UDCA are low as these bile acids are converted to α- and β-MCA respectively, by hydroxylation at the 6-carbon position by the *Cyp2c* gene cluster (143). *Cyp2c*-null mice also have high concentrations of UDCA and T-UDCA, and reduced levels of FXR-antagonist MCAs, due to lack of conversion from CDCA and UDCA (143). We did not observe changes in the faecal or plasma concentrations of MCAs, however, which suggests that the increase in T-UDCA is not due to alterations in hepatic bile acid synthesis. The enrichment of T-UDCA in faecal samples, but not plasma, further implies that the changes are as a result of microbial action in the large intestine. UDCA can be formed from CDCA by 7α-hydroxysteroid dehydrogenase enzymes present in the microbiota. These microbial enzymes account for the

greater abundance of β-MCA in mice, despite the greater affinity for the formation of α-MCA in liver extracts, by epimerising the hydroxyl group located in the 7-carbon position of α-MCA. This is the same modification that converts CDCA to UDCA (144). This enzyme is also produced by strains of *E. coli K12* and so epimerisation may be enriched in our model (145, 146). However, levels of endogenous murine CDCA are low, as described previously, and so may not explain the enrichment of UDCA in our data. Other potential routes for UDCA generation include dehydroxylation of the 3-carbon hydroxyl group of CA or ursocholic acid, or the 6-carbon hydroxyl group of MCAs, but enzymes capable of these reactions have not been identified.

Finally, we considered the colonisation levels detected in our gavaged mice. Colony forming units (CFUs)/mL of *E. coli* and *E. coli* overexpressing *bsh* were similar in the EC and EC-BSH groups across the experiment, while no bacteria were detected in the PBS group. This suggests that the effects observed in the EC-BSH group are a consequence of the expression of *bsh* rather than colonisation potential, despite the ability of *bsh* to improve bacterial persistence *in vivo* (147).

In conclusion, we have provided evidence for the protective role of Bsh in polyposis in APC^{MIN} mice. Mechanisms may involve alterations to the composition and function of the microbiota, including in microbial bile acid metabolism resulting in enrichment for T-UDCA. This may reduce polyp multiplicity via FXR signalling, and/or a reduction in bile acid pool hydrophobicity and the intracellular levels of free and secondary bile acids.

5.4 References

1. Hope ME, Hold GL, Kain R, El-Omar EM. Sporadic colorectal cancer--role of the commensal microbiota. FEMS microbiology letters. 2005;244(1):1-7.
2. Scanlan PD, Shanahan F, Clune Y, Collins JK, O'Sullivan GC, O'Riordan M, et al. Culture-independent analysis of the gut microbiota in colorectal cancer and polyposis. Environmental microbiology. 2008;10(3):789-98.
3. Swidsinski A, Khilkin M, Kerjaschki D, Schreiber S, Ortner M, Weber J, et al. Association between intraepithelial Escherichia coli and colorectal cancer. Gastroenterology. 1998;115(2):281-6.
4. Son JS, Khair S, Pettet DW, 3rd, Ouyang N, Tian X, Zhang Y, et al. Altered Interactions between the Gut Microbiome and Colonic Mucosa Precede Polyposis in APCMin/+ Mice. PloS one. 2015;10(6):e0127985-e.
5. Kaur K, Saxena A, Debnath I, O'Brien JL, Ajami NJ, Auchtung TA, et al. Antibiotic-mediated bacteriome depletion in Apc(Min/+) mice is associated with reduction in mucus-producing goblet cells and increased colorectal cancer progression. Cancer medicine. 2018;7(5):2003-12.
6. Dejea CM, Fathi P, Craig JM, Boleij A, Taddese R, Geis AL, et al. Patients with familial adenomatous polyposis harbor colonic biofilms containing tumorigenic bacteria. Science. 2018;359(6375):592-+.
7. Kostic AD, Howitt MR, Garrett WS. Exploring host-microbiota interactions in animal models and humans. Genes Dev. 2013;27(7):701-18.
8. Nguyen TT, Ung TT, Kim NH, Jung YD. Role of bile acids in colon carcinogenesis. World J Clin Cases. 2018;6(13):577-88.
9. Cao H, Xu M, Dong W, Deng B, Wang S, Zhang Y, et al. Secondary bile acid-induced dysbiosis promotes intestinal carcinogenesis. International Journal of Cancer. 2017;140(11):2545-56.
10. Modica S, Murzilli S, Salvatore L, Schmidt DR, Moschetta A. Nuclear bile acid receptor FXR protects against intestinal tumorigenesis. Cancer Res. 2008;68(23):9589-94.
11. Reddy BS. Diet And Excretion Of Bile Acids. Cancer Res. 1981;41:3766-8.
12. Bernstein H, Bernstein C, Payne CM, Dvorakova K, Garewal H. Bile acids as carcinogens in human gastrointestinal cancers. Mutation Research/Reviews in Mutation Research. 2005;589(1):47-65.
13. Begley M, Hill C, Gahan CGM. Bile salt hydrolase activity in probiotics. Applied and environmental microbiology. 2006;72(3):1729-38.
14. Batta AK, Salen G, Arora R, Shefer S, Batta M, Person A. Side chain conjugation prevents bacterial 7-dehydroxylation of bile acids. Journal of Biological Chemistry. 1990;265(19):10925-8.
15. Ahn YT, Kim GB, Lim KS, Baek YJ, Kim HU. Deconjugation of bile salts by Lactobacillus acidophilus isolates. International Dairy Journal. 2003;13(4):303-11.
16. Dussurget O, Cabanes D, Dehoux P, Lecuit M, Buchrieser C, Glaser P, et al. Listeria monocytogenes bile salt hydrolase is a PrfA-regulated virulence factor involved in the intestinal and hepatic phases of listeriosis. Molecular microbiology. 2002;45(4):1095-106.
17. Flemer B, Lynch DB, Brown JMR, Jeffery IB, Ryan FJ, Claesson MJ, et al. Tumour-associated and non-tumour-associated microbiota in colorectal cancer. Gut. 2017;66(4):633-43.
18. Fu T, Coulter S, Yoshihara E, Oh TG, Fang S, Cayabyab F, et al. FXR Regulates Intestinal Cancer Stem Cell Proliferation. Cell. 2019;176(5):1098-112.e18.

19. Tatusov RL, Galperin MY, Natale DA, Koonin EV. The COG database: a tool for genome-scale analysis of protein functions and evolution. Nucleic Acids Res. 2000;28(1):33-6.
20. Guarner F, Malagelada J-R. Gut flora in health and disease. The Lancet. 2003;361(9356):512-9.
21. Long AG, Lundsmith ET, Hamilton KE. Inflammation and Colorectal Cancer. Current colorectal cancer reports. 2017;13(4):341-51.
22. Voronov E, Apte RN. IL-1 in Colon Inflammation, Colon Carcinogenesis and Invasiveness of Colon Cancer. Cancer Microenviron. 2015;8(3):187-200.
23. Bent R, Moll L, Grabbe S, Bros M. Interleukin-1 Beta-A Friend or Foe in Malignancies? Int J Mol Sci. 2018;19(8):2155.
24. Kumari N, Dwarakanath BS, Das A, Bhatt AN. Role of interleukin-6 in cancer progression and therapeutic resistance. Tumour biology : the journal of the International Society for Oncodevelopmental Biology and Medicine. 2016;37(9):11553-72.
25. Balkwill F. TNF-alpha in promotion and progression of cancer. Cancer metastasis reviews. 2006;25(3):409-16.
26. Chow MT, Luster AD. Chemokines in cancer. Cancer immunology research. 2014;2(12):1125-31.
27. Mantovani A, Allavena P, Sica A, Balkwill F. Cancer-related inflammation. Nature. 2008;454:436.
28. Klimesova K, Kverka M, Zakostelska Z, Hudcovic T, Hrncir T, Stepankova R, et al. Altered gut microbiota promotes colitis-associated cancer in IL-1 receptor-associated kinase M-deficient mice. Inflamm Bowel Dis. 2013;19(6):1266-77.
29. Lucas C, Barnich N, Nguyen HTT. Microbiota, Inflammation and Colorectal Cancer. Int J Mol Sci. 2017;18(6):1310.
30. Mendes MCS, Paulino DSM, Brambilla SR, Camargo JA, Persinoti GF, Carvalheira JBC. Microbiota modification by probiotic supplementation reduces colitis associated colon cancer in mice. World journal of gastroenterology. 2018;24(18):1995-2008.
31. Xiao Y, Dai X, Li K, Gui G, Liu J, Yang H. Clostridium butyricum partially regulates the development of colitis-associated cancer through miR-200c. Cell Mol Biol. 2017;63(4):59-66.
32. Hu Y, Le Leu RK, Christophersen CT, Somashekar R, Conlon MA, Meng XQ, et al. Manipulation of the gut microbiota using resistant starch is associated with protection against colitis-associated colorectal cancer in rats. Carcinogenesis. 2016;37(4):366-75.
33. Tian Y, Xu Q, Sun LQ, Ye Y, Ji GZ. Short-chain fatty acids administration is protective in colitis-associated colorectal cancer development. J Nutr Biochem. 2018;57:103-9.
34. Song H, Wang W, Shen B, Jia H, Hou Z, Chen P, et al. Pretreatment with probiotic Bifico ameliorates colitis-associated cancer in mice: Transcriptome and gut flora profiling. Cancer Sci. 2018;109(3):666-77.
35. Tomkovich S, Yang Y, Winglee K, Gauthier J, Mühlbauer M, Sun X, et al. Locoregional Effects of Microbiota in a Preclinical Model of Colon Carcinogenesis. Cancer Res. 2017;77(10):2620-32.
36. Chow MT, Luster AD. Chemokines in cancer. Cancer immunology research. 2014;2(12):1125-31.
37. Strieter RM, Burdick MD, Gomperts BN, Belperio JA, Keane MP. CXC chemokines in angiogenesis. Cytokine & growth factor reviews. 2005;16(6):593-609.
38. Zlotnik A. Chemokines and cancer. Int J Cancer. 2006;119(9):2026-9.
39. Hibberd AA, Lyra A, Ouwehand AC, Rolny P, Lindegren H, Cedgård L, et al. Intestinal microbiota is altered in patients with colon cancer and modified by probiotic intervention. BMJ Open Gastroenterol. 2017;4(1):e000145-e.
40. Mira-Pascual L, Cabrera-Rubio R, Ocon S, Costales P, Parra A, Suarez A, et al. Microbial mucosal colonic shifts associated with the development of colorectal cancer reveal

the presence of different bacterial and archaeal biomarkers. Journal of Gastroenterology. 2015;50(2):167-79.
41. Lu Y, Chen J, Zheng J, Hu G, Wang J, Huang C, et al. Mucosal adherent bacterial dysbiosis in patients with colorectal adenomas. Scientific reports. 2016;6:26337-.
42. Geng J, Fan H, Tang X, Zhai H, Zhang Z. Diversified pattern of the human colorectal cancer microbiome. Gut Pathog. 2013;5(1):2-.
43. Burns MB, Lynch J, Starr TK, Knights D, Blekhman R. Virulence genes are a signature of the microbiome in the colorectal tumor microenvironment. Genome Med. 2015;7(1):55-.
44. Sanapareddy N, Legge RM, Jovov B, McCoy A, Burcal L, Araujo-Perez F, et al. Increased rectal microbial richness is associated with the presence of colorectal adenomas in humans. Isme j. 2012;6(10):1858-68.
45. Wu N, Yang X, Zhang R, Li J, Xiao X, Hu Y, et al. Dysbiosis Signature of Fecal Microbiota in Colorectal Cancer Patients. Microbial Ecology. 2013;66(2):462-70.
46. Weir TL, Manter DK, Sheflin AM, Barnett BA, Heuberger AL, Ryan EP. Stool microbiome and metabolome differences between colorectal cancer patients and healthy adults. PloS one. 2013;8(8):e70803-e.
47. Zeller G, Tap J, Voigt AY, Sunagawa S, Kultima JR, Costea PI, et al. Potential of fecal microbiota for early-stage detection of colorectal cancer. Mol Syst Biol. 2014;10(11):766-.
48. Vogtmann E, Hua X, Zeller G, Sunagawa S, Voigt AY, Hercog R, et al. Colorectal Cancer and the Human Gut Microbiome: Reproducibility with Whole-Genome Shotgun Sequencing. PloS one. 2016;11(5):e0155362-e.
49. Wang T, Cai G, Qiu Y, Fei N, Zhang M, Pang X, et al. Structural segregation of gut microbiota between colorectal cancer patients and healthy volunteers. Isme j. 2012;6(2):320-9.
50. Chen H-M, Yu Y-N, Wang J-L, Lin Y-W, Kong X, Yang C-Q, et al. Decreased dietary fiber intake and structural alteration of gut microbiota in patients with advanced colorectal adenoma. The American Journal of Clinical Nutrition. 2013;97(5):1044-52.
51. Feng Q, Liang S, Jia H, Stadlmayr A, Tang L, Lan Z, et al. Gut microbiome development along the colorectal adenoma–carcinoma sequence. Nature Communications. 2015;6:6528.
52. Ahn J, Sinha R, Pei Z, Dominianni C, Wu J, Shi J, et al. Human gut microbiome and risk for colorectal cancer. J Natl Cancer Inst. 2013;105(24):1907-11.
53. Shen XJ, Rawls JF, Randall T, Burcal L, Mpande CN, Jenkins N, et al. Molecular characterization of mucosal adherent bacteria and associations with colorectal adenomas. Gut microbes. 2010;1(3):138-47.
54. Ai D, Pan H, Li X, Gao Y, Liu G, Xia LC. Identifying Gut Microbiota Associated With Colorectal Cancer Using a Zero-Inflated Lognormal Model. Front Microbiol. 2019;10(826).
55. Le Chatelier E, Nielsen T, Qin J, Prifti E, Hildebrand F, Falony G, et al. Richness of human gut microbiome correlates with metabolic markers. Nature. 2013;500:541.
56. Mancabelli L, Milani C, Lugli GA, Turroni F, Cocconi D, van Sinderen D, et al. Identification of universal gut microbial biomarkers of common human intestinal diseases by meta-analysis. FEMS Microbiology Ecology. 2017;93(12).
57. Vital M, Karch A, Pieper DH. Colonic Butyrate-Producing Communities in Humans: an Overview Using Omics Data. mSystems. 2017;2(6):e00130-17.
58. Yutin N, Galperin MY. A genomic update on clostridial phylogeny: Gram-negative spore formers and other misplaced clostridia. Environmental microbiology. 2013;15(10):2631-41.
59. Qi Y-f, Sun J-n, Ren L-f, Cao X-l, Dong J-h, Tao K, et al. Intestinal Microbiota Is Altered in Patients with Gastric Cancer from Shanxi Province, China. Digestive diseases and sciences. 2019;64(5):1193-203.

60. Fomenky BE, Do DN, Talbot G, Chiquette J, Bissonnette N, Chouinard YP, et al. Direct-fed microbial supplementation influences the bacteria community composition of the gastrointestinal tract of pre- and post-weaned calves. Scientific reports. 2018;8(1):14147-.
61. Labbe A, Ganopolsky JG, Martoni CJ, Prakash S, Jones ML. Bacterial bile metabolising gene abundance in Crohn's, ulcerative colitis and type 2 diabetes metagenomes. PloS one. 2014;9(12):e115175.
62. Wei X, Tao J, Xiao S, Jiang S, Shang E, Zhu Z, et al. Xiexin Tang improves the symptom of type 2 diabetic rats by modulation of the gut microbiota. Scientific Reports. 2018;8(1):3685.
63. Song R, Yao J, Shi Q, Wei R. Nanocomposite of Half-Fin Anchovy Hydrolysates/Zinc Oxide Nanoparticles Exhibits Actual Non-Toxicity and Regulates Intestinal Microbiota, Short-Chain Fatty Acids Production and Oxidative Status in Mice. Mar Drugs. 2018;16(1):23.
64. Wu W, Lv L, Shi D, Ye J, Fang D, Guo F, et al. Protective Effect of Akkermansia muciniphila against Immune-Mediated Liver Injury in a Mouse Model. Front Microbiol. 2017;8:1804-.
65. Song X, Zhong L, Lyu N, Liu F, Li B, Hao Y, et al. Inulin Can Alleviate Metabolism Disorders in ob/ob Mice by Partially Restoring Leptin-related Pathways Mediated by Gut Microbiota. Genomics Proteomics Bioinformatics. 2019;17(1):64-75.
66. Liu Q, Li F, Zhuang Y, Xu J, Wang J, Mao X, et al. Alteration in gut microbiota associated with hepatitis B and non-hepatitis virus related hepatocellular carcinoma. Gut Pathog. 2019;11(1):1.
67. Chen J, Huang C, Wang J, Zhou H, Lu Y, Lou L, et al. Dysbiosis of intestinal microbiota and decrease in paneth cell antimicrobial peptide level during acute necrotizing pancreatitis in rats. PloS one. 2017;12(4):e0176583.
68. Naito Y, Uchiyama K, Takagi T. A next-generation beneficial microbe: Akkermansia muciniphila. J Clin Biochem Nutr. 2018;63(1):33-5.
69. Belzer C, Chia LW, Aalvink S, Chamlagain B, Piironen V, Knol J, et al. Microbial Metabolic Networks at the Mucus Layer Lead to Diet-Independent Butyrate and Vitamin B₁₂ Production by Intestinal Symbionts. mBio. 2017;8(5):e00770-17.
70. Ottman N, Reunanen J, Meijerink M, Pietilä TE, Kainulainen V, Klievink J, et al. Pili-like proteins of Akkermansia muciniphila modulate host immune responses and gut barrier function. PloS one. 2017;12(3):e0173004.
71. Shin NR, Lee JC, Lee HY, Kim MS, Whon TW, Lee MS, et al. An increase in the Akkermansia spp. population induced by metformin treatment improves glucose homeostasis in diet-induced obese mice. Gut. 2014;63(5):727-35.
72. Bodogai M, O'Connell J, Kim K, Kim Y, Moritoh K, Chen C, et al. Commensal bacteria contribute to insulin resistance in aging by activating innate B1a cells. Science translational medicine. 2018;10(467).
73. Jakobsdottir G, Xu J, Molin G, Ahrné S, Nyman M. High-fat diet reduces the formation of butyrate, but increases succinate, inflammation, liver fat and cholesterol in rats, while dietary fibre counteracts these effects. PloS one. 2013;8(11):e80476-e.
74. Wu X, Wu Y, He L, Wu L, Wang X, Liu Z. Effects of the intestinal microbial metabolite butyrate on the development of colorectal cancer. Journal of Cancer. 2018;9(14):2510-7.
75. Pfeiffer N, Desmarchelier C, Blaut M, Daniel H, Haller D, Clavel T. Acetatifactor muris gen. nov., sp. nov., a novel bacterium isolated from the intestine of an obese mouse. Archives of Microbiology. 2012;194(11):901-7.
76. Norris HG, Porter MC, Jiang C, Blesso NC. Dietary Milk Sphingomyelin Reduces Systemic Inflammation in Diet-Induced Obese Mice and Inhibits LPS Activity in Macrophages. Beverages. 2017;3(3).

77. Kübeck R, Bonet-Ripoll C, Hoffmann C, Walker A, Müller VM, Schüppel VL, et al. Dietary fat and gut microbiota interactions determine diet-induced obesity in mice. Molecular Metabolism. 2016;5(12):1162-74.
78. Zhang C, Jiao S, Wang ZA, Du Y. Exploring Effects of Chitosan Oligosaccharides on Mice Gut Microbiota in in vitro Fermentation and Animal Model. Front Microbiol. 2018;9(2388).
79. Liu X, Zeng B, Zhang J, Li W, Mou F, Wang H, et al. Role of the Gut Microbiome in Modulating Arthritis Progression in Mice. Scientific reports. 2016;6:30594-.
80. Lee C, Hong SN, Paik NY, Kim TJ, Kim ER, Chang DK, et al. CD1d Modulates Colonic Inflammation in NOD2−/− Mice by Altering the Intestinal Microbial Composition Comprising Acetatifactor muris. Journal of Crohn's and Colitis. 2019;13(8):1081-91.
81. Pathak P, Xie C, Nichols RG, Ferrell JM, Boehme S, Krausz KW, et al. Intestine farnesoid X receptor agonist and the gut microbiota activate G-protein bile acid receptor-1 signaling to improve metabolism. Hepatology (Baltimore, Md). 2018;68(4):1574-88.
82. Lin H, An Y, Hao F, Wang Y, Tang H. Correlations of Fecal Metabonomic and Microbiomic Changes Induced by High-fat Diet in the Pre-Obesity State. Scientific Reports. 2016;6:21618.
83. Zhu J, Kong Y, Yu J, Shao S, Mao M, Zhao M, et al. Consumption of drinking water N-Nitrosamines mixture alters gut microbiome and increases the obesity risk in young male rats. Environmental Pollution. 2019;248:388-96.
84. Zhou Z, Nie K, Huang Q, Li K, Sun Y, Zhou R, et al. Changes of cecal microflora in chickens following Eimeria tenella challenge and regulating effect of coated sodium butyrate. Experimental Parasitology. 2017;177:73-81.
85. Fu G, Zhao K, Chen H, Wang Y, Nie L, Wei H, et al. Effect of 3 lactobacilli on immunoregulation and intestinal microbiota in a β-lactoglobulin–induced allergic mouse model. Journal of dairy science. 2019;102(3):1943-58.
86. Neyrinck AM, Pachikian B, Taminiau B, Daube G, Frédérick R, Cani PD, et al. Intestinal Sucrase as a Novel Target Contributing to the Regulation of Glycemia by Prebiotics. PloS one. 2016;11(8):e0160488.
87. Clarke SF, Murphy EF, O'Sullivan O, Ross RP, O'Toole PW, Shanahan F, et al. Targeting the microbiota to address diet-induced obesity: a time dependent challenge. PloS one. 2013;8(6):e65790-e.
88. Xu X, Zhang X. Effects of cyclophosphamide on immune system and gut microbiota in mice. Microbiological Research. 2015;171:97-106.
89. Mangifesta M, Mancabelli L, Milani C, Gaiani F, de'Angelis N, de'Angelis GL, et al. Mucosal microbiota of intestinal polyps reveals putative biomarkers of colorectal cancer. Scientific Reports. 2018;8(1):13974.
90. Youssef O, Lahti L, Kokkola A, Karla T, Tikkanen M, Ehsan H, et al. Stool Microbiota Composition Differs in Patients with Stomach, Colon, and Rectal Neoplasms. Digestive diseases and sciences. 2018;63(11):2950-8.
91. Xie Y-H, Gao Q-Y, Cai G-X, Sun X-M, Zou T-H, Chen H-M, et al. Fecal Clostridium symbiosum for Noninvasive Detection of Early and Advanced Colorectal Cancer: Test and Validation Studies. EBioMedicine. 2017;25:32-40.
92. Song Y, Malmuthuge N, Steele MA, Guan LL. Shift of hindgut microbiota and microbial short chain fatty acids profiles in dairy calves from birth to pre-weaning. FEMS Microbiology Ecology. 2017;94(3).
93. Xie Y, Zhou G, Wang C, Xu X, Li C. Temporal changes in gut microbiota and signaling molecules of the gut–brain axis in mice fed meat protein diets. bioRxiv. 2018:329953.
94. Claus SP, Ellero SL, Berger B, Krause L, Bruttin A, Molina J, et al. Colonization-induced host-gut microbial metabolic interaction. mBio. 2011;2(2):e00271.

95. Gérard P. Metabolism of cholesterol and bile acids by the gut microbiota. Pathogens. 2013;3(1):14-24.
96. Looft T, Bayles DO, Alt DP, Stanton TB. Complete Genome Sequence of Coriobacteriaceae Strain 68-1-3, a Novel Mucus-Degrading Isolate from the Swine Intestinal Tract. Genome Announc. 2015;3(5):e01143-15.
97. Willing BP, Dicksved J, Halfvarson J, Andersson AF, Lucio M, Zheng Z, et al. A Pyrosequencing Study in Twins Shows That Gastrointestinal Microbial Profiles Vary With Inflammatory Bowel Disease Phenotypes. Gastroenterology. 2010;139(6):1844-54.e1.
98. Martinez I, Lattimer JM, Hubach KL, Case JA, Yang J, Weber CG, et al. Gut microbiome composition is linked to whole grain-induced immunological improvements. Isme j. 2013;7(2):269-80.
99. O'Hara E, Kelly A, McCabe MS, Kenny DA, Guan LL, Waters SM. Effect of a butyrate-fortified milk replacer on gastrointestinal microbiota and products of fermentation in artificially reared dairy calves at weaning. Scientific reports. 2018;8(1):14901-.
100. Clavel T, Charrier C, Braune A, Wenning M, Blaut M, Haller D. Isolation of bacteria from the ileal mucosa of TNFdeltaARE mice and description of Enterorhabdus mucosicola gen. nov., sp. nov. International Journal of Systematic and Evolutionary Microbiology. 2009;59(7):1805-12.
101. Shin A, Lee J, Lee J, Park MS, Park JW, Park SC, et al. Isoflavone and Soyfood Intake and Colorectal Cancer Risk: A Case-Control Study in Korea. PloS one. 2015;10(11):e0143228-e.
102. Iino C, Shimoyama T, Iino K, Yokoyama Y, Chinda D, Sakuraba H, et al. Daidzein Intake Is Associated with Equol Producing Status through an Increase in the Intestinal Bacteria Responsible for Equol Production. Nutrients. 2019;11(2):433.
103. Williams C, DiLeo A, Niv Y, Gustafsson J-Å. Estrogen receptor beta as target for colorectal cancer prevention. Cancer Lett. 2016;372(1):48-56.
104. Lecomte S, Demay F, Ferrière F, Pakdel F. Phytochemicals Targeting Estrogen Receptors: Beneficial Rather Than Adverse Effects? Int J Mol Sci. 2017;18(7):1381.
105. Clavel T, Charrier C, Wenning M, Haller D. Parvibacter caecicola gen. nov., sp. nov., a bacterium of the family Coriobacteriaceae isolated from the caecum of a mouse. International Journal of Systematic and Evolutionary Microbiology. 2013;63(7):2642-8.
106. Jung ES, Park HM, Hyun SM, Shon JC, Singh D, Liu K-H, et al. The green tea modulates large intestinal microbiome and exo/endogenous metabolome altered through chronic UVB-exposure. PloS one. 2017;12(11):e0187154.
107. Zeng H, Ishaq SL, Liu Z, Bukowski MR. Colonic aberrant crypt formation accompanies an increase of opportunistic pathogenic bacteria in C57BL/6 mice fed a high-fat diet. J Nutr Biochem. 2018;54:18-27.
108. Miquel S, Martín R, Rossi O, Bermúdez-Humarán LG, Chatel JM, Sokol H, et al. Faecalibacterium prausnitzii and human intestinal health. Current Opinion in Microbiology. 2013;16(3):255-61.
109. Lopez-Siles M, Duncan SH, Garcia-Gil LJ, Martinez-Medina M. Faecalibacterium prausnitzii: from microbiology to diagnostics and prognostics. The ISME journal. 2017;11(4):841-52.
110. Sokol H, Pigneur B, Watterlot L, Lakhdari O, Bermúdez-Humarán LG, Gratadoux J-J, et al. Faecalibacterium prausnitzii is an anti-inflammatory commensal bacterium identified by gut microbiota analysis of Crohn disease patients. Proceedings of the National Academy of Sciences. 2008;105(43):16731-6.
111. Balamurugan R, Rajendiran E, George S, Samuel GV, Ramakrishna BS. Real-time polymerase chain reaction quantification of specific butyrate-producing bacteria, Desulfovibrio and Enterococcus faecalis in the feces of patients with colorectal cancer. Journal of gastroenterology and hepatology. 2008;23(8 Pt 1):1298-303.

112. Lopez-Siles M, Martinez-Medina M, Suris-Valls R, Aldeguer X, Sabat-Mir M, Duncan SH, et al. Changes in the Abundance of Faecalibacterium prausnitzii Phylogroups I and II in the Intestinal Mucosa of Inflammatory Bowel Disease and Patients with Colorectal Cancer. Inflamm Bowel Dis. 2016;22(1):28-41.
113. Sobhani I, Tap J, Roudot-Thoraval F, Roperch JP, Letulle S, Langella P, et al. Microbial Dysbiosis in Colorectal Cancer (CRC) Patients. PloS one. 2011;6(1):e16393.
114. Guo JR, Dong XF, Liu S, Tong JM. High-throughput sequencing reveals the effect of Bacillus subtilis CGMCC 1.921 on the cecal microbiota and gene expression in ileum mucosa of laying hens. Poultry Science. 2018;97(7):2543-56.
115. Grill JP, Cayuela C, Antoine JM, Schneider F. Isolation and characterization of a Lactobacillus amylovorus mutant depleted in conjugated bile salt hydrolase activity: relation between activity and bile salt resistance. Journal of applied microbiology. 2000;89(4):553-63.
116. Renga B, Mencarelli A, Cipriani S, D'Amore C, Carino A, Bruno A, et al. The bile acid sensor FXR is required for immune-regulatory activities of TLR-9 in intestinal inflammation. PloS one. 2013;8(1):e54472.
117. Vavassori P, Mencarelli A, Renga B, Distrutti E, Fiorucci S. The bile acid receptor FXR is a modulator of intestinal innate immunity. J Immunol. 2009;183(10):6251-61.
118. Calmus Y, Weill B, Ozier Y, Chereau C, Houssin D, Poupon R. Immunosuppressive properties of chenodeoxycholic and ursodeoxycholic acids in the mouse. Gastroenterology. 1992;103(2):617-21.
119. Fang C, Filipp FV, Smith JW. Unusual binding of ursodeoxycholic acid to ileal bile acid binding protein: role in activation of FXRα. Journal of lipid research. 2012;53(4):664-73.
120. Alberts DS, Martinez ME, Hess LM, Einspahr JG, Green SB, Bhattacharyya AK, et al. Phase III trial of ursodeoxycholic acid to prevent colorectal adenoma recurrence. J Natl Cancer Inst. 2005;97(11):846-53.
121. van Gorkom BA, van der Meer R, Boersma-van Ek W, Termont DS, de Vries EG, Kleibeuker JH. Changes in bile acid composition and effect on cytolytic activity of fecal water by ursodeoxycholic acid administration: a placebo-controlled cross-over intervention trial in healthy volunteers. Scandinavian journal of gastroenterology. 2002;37(8):965-71.
122. Chang E. Ursodeoxycholic acid reduces the risk of developing colorectal cancer in patients with ulcerative colitis and sclerosing cholangitis. Gastroenterology. 2003;124(4):873.
123. Kim YH, Kim JH, Kim BG, Lee KL, Kim JW, Koh SJ. Tauroursodeoxycholic acid attenuates colitis-associated colon cancer by inhibiting nuclear factor kappaB signaling. Journal of gastroenterology and hepatology. 2019;34(3):544-51.
124. Dongfeng D, An C, Shujia P, Jikai Y, Tao Y, Rui D, et al. Explanation of colon cancer pathophysiology through analyzing the disrupted homeostasis of bile acids. Afr Health Sci. 2014;14(4):925-8.
125. Huang W-K, Hsu H-C, Liu J-R, Yang T-S, Chen J-S, Chang JW-C, et al. The Association of Ursodeoxycholic Acid Use With Colorectal Cancer Risk: A Nationwide Cohort Study. Medicine (Baltimore). 2016;95(11):e2980-e.
126. Earnest DL, Holubec H, Wali RK, Jolley CS, Bissonette M, Bhattacharyya AK, et al. Chemoprevention of azoxymethane-induced colonic carcinogenesis by supplemental dietary ursodeoxycholic acid. Cancer Res. 1994;54(19):5071-4.
127. Jacoby RF, Cole CE, Hawk ET, Lubet RA. Ursodeoxycholate/Sulindac combination treatment effectively prevents intestinal adenomas in a mouse model of polyposis. Gastroenterology. 2004;127(3):838-44.
128. Kohno H, Suzuki R, Yasui Y, Miyamoto S, Wakabayashi K, Tanaka T. Ursodeoxycholic acid versus sulfasalazine in colitis-related colon carcinogenesis in mice. Clinical cancer

research : an official journal of the American Association for Cancer Research. 2007;13(8):2519-25.
129. Khare S, Mustafi R, Cerda S, Yuan W, Jagadeeswaran S, Dougherty U, et al. Ursodeoxycholic acid suppresses Cox-2 expression in colon cancer: roles of Ras, p38, and CCAAT/enhancer-binding protein. Nutrition and cancer. 2008;60(3):389-400.
130. Brasitus TA. Primary chemoprevention strategies for colorectal cancer: Ursodeoxycholic acid and other agents. Gastroenterology. 1995;109(6):2036-8.
131. Okada K, Shoda J, Taguchi K, Maher JM, Ishizaki K, Inoue Y, et al. Ursodeoxycholic acid stimulates Nrf2-mediated hepatocellular transport, detoxification, and antioxidative stress systems in mice. American Journal of Physiology-Gastrointestinal and Liver Physiology. 2008;295(4):G735-G47.
132. Van den Bossche L, Hindryckx P, Devisscher L, Devriese S, Van Welden S, Holvoet T, et al. Ursodeoxycholic Acid and Its Taurine- or Glycine-Conjugated Species Reduce Colitogenic Dysbiosis and Equally Suppress Experimental Colitis in Mice. Applied and environmental microbiology. 2017;83(7):e02766-16.
133. Zhang Y, Zheng X, Huang F, Zhao A, Ge K, Zhao Q, et al. Ursodeoxycholic Acid Alters Bile Acid and Fatty Acid Profiles in a Mouse Model of Diet-Induced Obesity. Frontiers in Pharmacology. 2019;10(842).
134. Oh A-R, Bae J-S, Lee J, Shin E, Oh B-C, Park S-C, et al. Ursodeoxycholic acid decreases age-related adiposity and inflammation in mice. BMB Rep. 2016;49(2):105-10.
135. Kim E-K, Cho JH, Kim E, Kim YJ. Ursodeoxycholic acid inhibits the proliferation of colon cancer cells by regulating oxidative stress and cancer stem-like cell growth. PloS one. 2017;12(7):e0181183-e.
136. Shah SA, Volkov Y, Arfin Q, Abdel-Latif MM, Kelleher D. Ursodeoxycholic acid inhibits interleukin 1 beta [corrected] and deoxycholic acid-induced activation of NF-kappaB and AP-1 in human colon cancer cells. Int J Cancer. 2006;118(3):532-9.
137. Rigas B, Tsioulias GJ, Allan C, Wali RK, Brasitus TA. The effect of bile acids and piroxicam on MHC antigen expression in rat colonocytes during colon cancer development. Immunology. 1994;83(2):319-23.
138. Sun S, Zhao B, Qi M, Yao Y, Xu L, Ji R, et al. Tudca Ameliorates Liver Injury Via Activation of SIRT1-FXR Signaling in a Rat Hemorrhagic Shock Model. Shock (Augusta, Ga). 2019.
139. Paumgartner G, Beuers U. Ursodeoxycholic acid in cholestatic liver disease: mechanisms of action and therapeutic use revisited. Hepatology (Baltimore, Md). 2002;36(3):525-31.
140. Selmin OI, Fang C, Lyon AM, Doetschman TC, Thompson PA, Martinez JD, et al. Inactivation of Adenomatous Polyposis Coli Reduces Bile Acid/Farnesoid X Receptor Expression through Fxr gene CpG Methylation in Mouse Colon Tumors and Human Colon Cancer Cells. The Journal of nutrition. 2016;146(2):236-42.
141. Sayin SI, Wahlstrom A, Felin J, Jantti S, Marschall HU, Bamberg K, et al. Gut microbiota regulates bile acid metabolism by reducing the levels of tauro-beta-muricholic acid, a naturally occurring FXR antagonist. Cell metabolism. 2013;17(2):225-35.
142. Zhang Y, Limaye PB, Renaud HJ, Klaassen CD. Effect of various antibiotics on modulation of intestinal microbiota and bile acid profile in mice. Toxicol Appl Pharmacol. 2014;277(2):138-45.
143. Takahashi S, Fukami T, Masuo Y, Brocker CN, Xie C, Krausz KW, et al. Cyp2c70 is responsible for the species difference in bile acid metabolism between mice and humans. Journal of lipid research. 2016;57(12):2130-7.
144. Rudling M. Understanding mouse bile acid formation: Is it time to unwind why mice and rats make unique bile acids? Journal of lipid research. 2016;57(12):2097-8.

145. Yoshimoto T, Higashi H, Kanatani A, Lin XS, Nagai H, Oyama H, et al. Cloning and sequencing of the 7 alpha-hydroxysteroid dehydrogenase gene from Escherichia coli HB101 and characterization of the expressed enzyme. J Bacteriol. 1991;173(7):2173-9.
146. UniPROT. UniProtKB - P0AET8 (HDHA_ECOLI) [Available from: https://www.uniprot.org/uniprot/P0AET8.
147. Begley M, Sleator RD, Gahan CG, Hill C. Contribution of three bile-associated loci, bsh, pva, and btlB, to gastrointestinal persistence and bile tolerance of Listeria monocytogenes. Infection and immunity. 2005;73(2):894-904.

6.0 Final Discussion

The aim of my thesis was to investigate whether alterations in the gut microbiota are a cause or consequence of intestinal neoplasia. Benign and pre-malignant changes in the host can alter the gut microenvironment in such a way as to impact the microbiota. The interactions which occur during the transition from normal to abnormal tissue are less well understood, however, and may reveal a role for the microbiota in cancer initiation. There is also evidence that taxa in the tumour microenvironment influence tumour progression (1), but questions remain regarding the breadth of taxa involved and the mechanisms by which they influence disease. Therefore, we examined host and microbial alterations before, during, and after cancer onset, and set them to a timeline (**Chapters 3** and **4**) and investigated a microbial intervention in CRC (**Chapter 5**). Our time-course studies identified distinct sets of taxa associated with cancer onset and progression which were differentially associated pro- or anti-tumorigenic properties. We also investigated host bile acid homeostasis and revealed its potential role in CRC development and interaction with the gut bacteria. An overview of the effects we saw in each group is presented in Table 6.1.

In **Chapter 3**, we observed pro-tumorigenic changes in the microbial composition of mice administered AOM prior to detection of host neoplastic transformation, which suggests that the microbiota may act as an instigating factor in the development of sporadic CRC and that prophylactic modulation of the gut microbiota could potentially reduce cancer risk. This longitudinal study also provided us with the opportunity to track changes in the microbiota during cancer progression and this identified a set of taxa distinct from those associated with tumour initiation. The bacterial changes at our earliest time-point in mice administered AOM primarily reflected a suppression of anti-inflammatory bacterial species such as those which produce butyrate, which was followed by pro-inflammatory cytokine transcription in these mice. Later, we observed an enrichment of pathogenic taxa which may contribute to cancer

Table 6.1: Comparison of major study effects

Time-point 1		Time-point 2		Time-point 3		Time-point 4			
AOM	APCmin	AOM	APCmin	AOM	APCmin	AOM	APCmin	APC/bsh	
ns	ns	ns	ns	ns	ns	ns	ns	ns	***Body Weight***
↑	↑	↓	ns	ns	ns	ns	↑↑	↑	***Microbial α-diversity***
**	**	*	**	*	**	**	**	**	***Microbial β-diversity***
↓↓	ns	↓↓	ns	ns	ns	ns	ns	ns	***Total Bile Acids***
ns	ns	ns	↓↓	ns	ns	ns	ns	↓	***PICRUSt α-diversity***
ns	ns	ns	**	ns	ns	ns	ns	*	***PICRUSt β-diversity***
ns	ns	ns	↑	ns	ns	ns	ns	ns	***baiCD/bsh***
↓	-	↑↑	-	↑↑	-	↑	↑	ns	***Inflammation***
ns	-	ns	-	↑	-	↑↑	↑↑↑	↓	***Neoplasia***
ns	-	ns	-	ns	-	ns	ns	ns	***Proliferation***
-	-	-	-	-	-	-	↓	ns	***FXR***

Note that time-points 1-4 correspond to Weeks 8, 12, 24 and 48 in the AOM study and Weeks 4, 7, 11 and 14 in the APC^{MIN} longitudinal study, as defined in the respective chapters. The data from our intervention study is presented from mice treated with *E. coli* overexpressing *bsh* compared to wild-type *E. coli* at time-point 4 (Week 14) only. Direction of arrows signify the direction of change compared to control, with the number of arrows representing significance. Cells marked *ns* were not significantly different. Cells marked with a dash (-) were not measured. Asterisks represent degree of significance for statistics without directionality (<0.05, <0.01 and <0.001 for *, ** and *** respectively).

progression. We also measured the α-diversity of the microbiota in this model. The literature is inconsistent with respect to the effects of CRC on α-diversity, with reports of increased and decreased diversity in the microbiota of CRC patients (2-6). Our results may explain part of this discrepancy as we saw a sequential increase and decrease in α-diversity in our AOM-induced mice over time. The reduction in α-diversity occurred concurrently with the initiation of the inflammatory response, suggesting that the inconsistencies observed in the published literature may be explained, in part, by the inflammatory state in the host and that the relationship between the host and microbiota is dynamic over the course of tumorigenesis.

One thread common to each of our studies was the indication that bile acid alterations accompanied changes in the gut microbiota and host in both the AOM and APC^{MIN} mouse models and informed our microbial intervention strategy in Chapter 5. FXR is a nuclear receptor for bile acids and is particularly noteworthy as it regulates bile acid homeostasis and has recently been reported to play an important role in the suppression of CRC by inducing apoptosis of genetically altered cells and inhibiting proliferation by the Wnt signalling pathway (7). In mice which were administered AOM, the reduction in faecal bile acids and concomitant increase in plasma bile acids prior to CRC development might suggest an increase in ileal bile acid uptake by ASBT which is under negative regulation by FXR. This may have been mediated by enrichment for FXR antagonist bile acids such as tauro-conjugated β-muricholic acid (T-βMCA), which we detected in the plasma. Bile acids also correlated with features of the microbiota in this model such as α-diversity and co-abundance groups (CAGs), suggesting a role for the gut bacteria in bile acid dysregulation. One interesting observation from the longitudinal studies in both mouse models was the emergence of key time-points for changes in the microbiota. In AOM-treated mice, we observed a reduction in α-diversity and a number of significantly difference taxa at Week 12, which occurred concurrently with the onset of inflammatory cytokine transcription. This also

signified a switch from a suppression of anti-inflammatory species to the enrichment of opportunistic pathogens in these mice. Separately, correlation analysis suggested major interactions between the microbiota, bile acids and inflammation at Week 8, possibly feeding into these phenomena at Week 12.

Our APC^{MIN} longitudinal study in **Chapter 4** also presented a view of the temporal microbial landscape during tumour development in a model of familial CRC. This separately identified species associated with cancer initiation and progression, as well as taxa consistently altered throughout the experiment and taxa that remained in flux. This highlights an advantage of research which samples the cancer-associated microbiota at several time-points, as a single snapshot may not fully represent the temporal variation of luminal microbial environment. The microbial composition in APC^{MIN} mice did not have distinct pro-inflammatory associations, as observed in **Chapter 3**, but was enriched for other species associated with CRC. In **Chapter 4,** we observed a significant down-regulation of FXR target gene transcription and a negative correlation between these genes and polyp multiplicity. A key time-point in our APC^{MIN} longitudinal study occurred around Week 7, when there was a significant disruption to the predicted metagenome of these mice, including the abundance of bile acid metabolising genes *bsh* and *baiCD*. This coincided with the onset of polyposis reported in the APC^{MIN} model (8, 9). The timing of these key events suggests their relevance to the role of the microbiota in CRC initiation and invites deeper examination in the future.

This association between the microbial patterns, bile acid signalling and CRC lead us to consider the role of Bsh in CRC development. In our intervention study in **Chapter 5**, mice administered a strain of *E. coli* overexpressing *bsh* developed significantly fewer intestinal polyps compared to *E. coli*-treated or PBS-treated controls. This intervention has previously been shown to have positive effects on lipid metabolism, weight gain and cholesterol levels in the host (10). Our analysis of the bile acid pool in these mice revealed an enrichment of

tauro-conjugated ursodeoxycholic acid (T-UDCA). The enrichment of a conjugated bile acid in mice administered a bile acid-deconjugating enzyme is surprising, and may hint at wider alterations in bile acid regulation than simple deconjugation. This enrichment may account for the decrease in intestinal polyposis we observed, however, as T-UDCA and its unconjugated form UDCA, which has been shown to have similar effects *in vivo*, protect against cancer development and have been reported to be reduced in CRC patients (11-20). T-UDCA also correlated negatively with the total number of small intestinal polyps in our study, before correction for multiple comparisons, reinforcing the possibility that it is responsible for the reduction in polyposis in these mice. Moreover, the FXR target gene *I-babp* was up-regulated in mice exposed to *bile salt hydrolase* (Bsh) compared to PBS-treated, but not *E. coli*-treated mice, and a negative correlation was observed between *I-babp* and small intestinal polyps. Each of these results support the hypothesis that cancer risk is increased by suppression of FXR signalling, possibly mediated by microbial-induced bile acid dysregulation.

6.1 Future Perspectives

The initial changes observed in mice administered AOM was a suppression of species negatively associated with cancer risk, including a number of butyrate producers. Supplementation of these mice with butyrate-producing bacteria before Week 8 may prevent the subsequent inflammatory activation and enrichment for opportunistic pathogens, and would confirm the significance of these changes in CRC initiation. In contrast, the contribution of the microbiota to CRC in APC^{MIN} mice is less obvious. However, our *bsh* intervention study also highlighted a possibly key role of T-UDCA which invites further investigation into the role of this bile acid *in vivo*, and into the effect of *bsh* supplementation on wider bile acid regulation. The effect of microbial metabolism of bile acids such as

conjugated muricholic acids (MCAs) was also highlighted in our research as potentially relevant to CRC pathogenesis. MCAs do not feature in the human bile acid pool but the degree of FXR activation and/or antagonism as a result of microbial action should be considered.

Here, we have established a temporal progression of bacterial changes during the process of tumorigenesis in two mouse models of CRC. We identified patterns in the gut bacteria associated with disease initiation and progression. However, the association of any one species with health or disease is difficult, and considering their effects in isolation, for example in mono-associated animals, is perhaps not reflective of the diverse communities which reside in the gut. In this regard, there are parallels between study of the gut microbiome and genomic research since the turn of the millennium. The microbiome has been described as the second genome and the presence or absence of risk-associated taxa may reflect the role of alleles for complex genetic traits, in that they may contribute to overall disease risk, but the scale of that contribution is influenced by cis- and trans-acting elements. Like research into the human genome, elucidation of these interactions may require large-scale meta-analyses such as the Human Microbiome Project; phase II of which considered microbial configurations observed in irritable bowel disease but not CRC (21). Investment into microbiome research has increased considerably in recent years (22), and this research will continue into the foreseeable future. Our identification of species associated with different stages of the tumorigenic process, as well as the temporal variation apparent in our data, may inform this analysis. We furthermore attempted to address this problem by considering co-abundance groups (CAGs) as structural units of the microbiota. The abundances of these CAGs also appeared to vary during disease progression. The relevance of these variations to CRC, and utility of CAGs as a tool to describe the microbiota, requires further investigation.

We also interrogated our 16S rRNA gene sequencing analysis and produced a significant amount of PICRUSt data to generate a picture of the wider metabolic functioning of the microbiota. PICRUSt predicts the metagenomic content of the microbiome by associating 16S marker gene data with closely related whole genome sequences. We detected a large number of significantly different Kyoto Encyclopaedia of Genes and Genomes (KEGG) pathways in each of our models, such as *linoleic acid metabolism* and *bacterial toxins*, which are presented in the appendix. Picking apart these pathways to identify the specific bacterial genes and functions involved may identify novel metabolic processes which influence the role of the microbiota in CRC.

In conclusion, our research has provided a timeline of host and microbial interactions during the onset and progression of intestinal neoplasia, and has provided new evidence that pro-tumorigenic alterations in the microbiota are an instigating factor in sporadic CRC and a contributing factor in familial CRC. It also highlights a number of mechanisms by which this might occur and suggests possible therapeutic interventions, one of which we validated in a mouse model of familial CRC.

6.2 References

1. Ma C-T, Luo H-S, Gao F, Tang Q-C, Chen W. Fusobacterium nucleatum promotes the progression of colorectal cancer by interacting with E-cadherin. Oncol Lett. 2018;16(2):2606-12.
2. Feng Q, Liang S, Jia H, Stadlmayr A, Tang L, Lan Z, et al. Gut microbiome development along the colorectal adenoma–carcinoma sequence. Nature Communications. 2015;6:6528.
3. Scanlan PD, Shanahan F, Clune Y, Collins JK, O'Sullivan GC, O'Riordan M, et al. Culture-independent analysis of the gut microbiota in colorectal cancer and polyposis. Environmental microbiology. 2008;10(3):789-98.
4. Ahn J, Sinha R, Pei Z, Dominianni C, Wu J, Shi J, et al. Human gut microbiome and risk for colorectal cancer. J Natl Cancer Inst. 2013;105(24):1907-11.
5. Shen XJ, Rawls JF, Randall T, Burcal L, Mpande CN, Jenkins N, et al. Molecular characterization of mucosal adherent bacteria and associations with colorectal adenomas. Gut microbes. 2010;1(3):138-47.
6. Ai D, Pan H, Li X, Gao Y, Liu G, Xia LC. Identifying Gut Microbiota Associated With Colorectal Cancer Using a Zero-Inflated Lognormal Model. Front Microbiol. 2019;10(826).
7. Modica S, Murzilli S, Salvatore L, Schmidt DR, Moschetta A. Nuclear bile acid receptor FXR protects against intestinal tumorigenesis. Cancer Res. 2008;68(23):9589-94.
8. Son JS, Khair S, Pettet DW, 3rd, Ouyang N, Tian X, Zhang Y, et al. Altered Interactions between the Gut Microbiome and Colonic Mucosa Precede Polyposis in APCMin/+ Mice. PloS one. 2015;10(6):e0127985-e.
9. Kaur K, Saxena A, Debnath I, O'Brien JL, Ajami NJ, Auchtung TA, et al. Antibiotic-mediated bacteriome depletion in Apc(Min/+) mice is associated with reduction in mucus-producing goblet cells and increased colorectal cancer progression. Cancer medicine. 2018;7(5):2003-12.
10. Joyce SA, MacSharry J, Casey PG, Kinsella M, Murphy EF, Shanahan F, et al. Regulation of host weight gain and lipid metabolism by bacterial bile acid modification in the gut. Proceedings of the National Academy of Sciences. 2014;111(20):7421-6.
11. Chang E. Ursodeoxycholic acid reduces the risk of developing colorectal cancer in patients with ulcerative colitis and sclerosing cholangitis. Gastroenterology. 2003;124(4):873.
12. Kim YH, Kim JH, Kim BG, Lee KL, Kim JW, Koh SJ. Tauroursodeoxycholic acid attenuates colitis-associated colon cancer by inhibiting nuclear factor kappaB signaling. Journal of gastroenterology and hepatology. 2019;34(3):544-51.
13. Dongfeng D, An C, Shujia P, Jikai Y, Tao Y, Rui D, et al. Explanation of colon cancer pathophysiology through analyzing the disrupted homeostasis of bile acids. Afr Health Sci. 2014;14(4):925-8.
14. Alberts DS, Martinez ME, Hess LM, Einspahr JG, Green SB, Bhattacharyya AK, et al. Phase III trial of ursodeoxycholic acid to prevent colorectal adenoma recurrence. J Natl Cancer Inst. 2005;97(11):846-53.
15. Huang W-K, Hsu H-C, Liu J-R, Yang T-S, Chen J-S, Chang JW-C, et al. The Association of Ursodeoxycholic Acid Use With Colorectal Cancer Risk: A Nationwide Cohort Study. Medicine (Baltimore). 2016;95(11):e2980-e.
16. Earnest DL, Holubec H, Wali RK, Jolley CS, Bissonette M, Bhattacharyya AK, et al. Chemoprevention of azoxymethane-induced colonic carcinogenesis by supplemental dietary ursodeoxycholic acid. Cancer Res. 1994;54(19):5071-4.
17. Jacoby RF, Cole CE, Hawk ET, Lubet RA. Ursodeoxycholate/Sulindac combination treatment effectively prevents intestinal adenomas in a mouse model of polyposis. Gastroenterology. 2004;127(3):838-44.

18. Kohno H, Suzuki R, Yasui Y, Miyamoto S, Wakabayashi K, Tanaka T. Ursodeoxycholic acid versus sulfasalazine in colitis-related colon carcinogenesis in mice. Clinical cancer research : an official journal of the American Association for Cancer Research. 2007;13(8):2519-25.
19. Khare S, Mustafi R, Cerda S, Yuan W, Jagadeeswaran S, Dougherty U, et al. Ursodeoxycholic acid suppresses Cox-2 expression in colon cancer: roles of Ras, p38, and CCAAT/enhancer-binding protein. Nutrition and cancer. 2008;60(3):389-400.
20. Brasitus TA. Primary chemoprevention strategies for colorectal cancer: Ursodeoxycholic acid and other agents. Gastroenterology. 1995;109(6):2036-8.
21. Proctor LM, Creasy HH, Fettweis JM, Lloyd-Price J, Mahurkar A, Zhou W, et al. The Integrative Human Microbiome Project. Nature. 2019;569(7758):641-8.
22. Proctor L, LoTempio J, Marquitz A, Daschner P, Xi D, Flores R, et al. A review of 10 years of human microbiome research activities at the US National Institutes of Health, Fiscal Years 2007-2016. Microbiome. 2019;7(1):31.

7.0 Appendix

Table A1: Significantly different pathways predicted by PICRUSt in mice administered AOM

Time	Function	p
Week 8	G protein-coupled receptors	0.001
Week 8	C5-Branched dibasic acid metabolism	0.016
Week 8	Betalain biosynthesis	0.027
Week 8	Indole alkaloid biosynthesis	0.027
Week 12	Vibrio cholerae infection	0.015
Week 12	Ethylbenzene degradation	0.049
Week 12	Ion channels	0.049
Week 12	Linoleic acid metabolism	0.049
Week 24	Amino sugar and nucleotide sugar metabolism	0.008
Week 24	Bacterial toxins	0.011
Week 24	alpha-Linolenic acid metabolism	0.015
Week 24	Bacterial invasion of epithelial cells	0.015
Week 24	Cyanoamino acid metabolism	0.015
Week 24	Phenylpropanoid biosynthesis	0.015
Week 24	Calcium signaling pathway	0.017
Week 24	Lysine degradation	0.021
Week 24	Starch and sucrose metabolism	0.021
Week 24	Carbohydrate digestion and absorption	0.028
Week 24	Glycosphingolipid biosynthesis - lacto and neolacto series	0.028
Week 24	Inorganic ion transport and metabolism	0.028
Week 24	RIG-I-like receptor signaling pathway	0.028
Week 24	D-Alanine metabolism	0.037
Week 24	Insulin signaling pathway	0.049
Week 24	Sphingolipid metabolism	0.049
Week 24	Stilbenoid, diarylheptanoid and gingerol biosynthesis	0.049
Week 24	Transcription machinery	0.049
Week 48	1,1,1-Trichloro-2,2-bis(4-chlorophenyl)ethane (DDT) degradation	0.003
Week 48	Pyruvate metabolism	0.006
Week 48	C5-Branched dibasic acid metabolism	0.009
Week 48	G protein-coupled receptors	0.009
Week 48	Selenocompound metabolism	0.012
Week 48	Valine, leucine and isoleucine biosynthesis	0.012
Week 48	General function prediction only	0.021
Week 48	RIG-I-like receptor signaling pathway	0.021
Week 48	Sphingolipid metabolism	0.021
Week 48	Function unknown	0.036
Week 48	Stilbenoid, diarylheptanoid and gingerol biosynthesis	0.036
Week 48	Apoptosis	0.046

Week 48	Caffeine metabolism	0.046
Week 48	Circadian rhythm (plant)	0.046
Week 48	Fatty acid elongation in mitochondria	0.046
Week 48	Fluorobenzoate degradation	0.046
Week 48	Steroid biosynthesis	0.046
Week 48	Systemic lupus erythematosus	0.046
Week 48	Transcription machinery	0.046

Note: Significance determined by Mann-Whitney U-test. No correction for multiple comparisons. 252 comparisons made.

Table A2: Significantly different pathways predicted by PICRUSt in APC^{MIN} mice at Week 4

Time	Function	p
Week 4	Bisphenol degradation	1.55E-41
Week 4	Carbohydrate digestion and absorption	1.55E-41
Week 4	Other transporters	1.55E-41
Week 4	Insulin signaling pathway	3.11E-41
Week 4	Amino acid metabolism	6.22E-41
Week 4	Ether lipid metabolism	6.22E-41
Week 4	G protein coupled receptors	6.22E-41
Week 4	Pentose phosphate pathway	6.22E-41
Week 4	Aminoacyl tRNA biosynthesis	0.001
Week 4	Fructose and mannose metabolism	0.001
Week 4	Glycosphingolipid biosynthesis lacto and neolacto series	0.001
Week 4	Ascorbate and aldarate metabolism	0.002
Week 4	Carbohydrate metabolism	0.002
Week 4	Pentose and glucuronate interconversions	0.002
Week 4	RIG I like receptor signaling pathway	0.002
Week 4	Colorectal cancer	0.003
Week 4	Huntingtons disease	0.003
Week 4	Influenza A	0.003
Week 4	Small cell lung cancer	0.003
Week 4	Toxoplasmosis	0.003
Week 4	Tryptophan metabolism	0.003
Week 4	Viral myocarditis	0.003
Week 4	p53 signaling pathway	0.003
Week 4	Antigen processing and presentation	0.005
Week 4	Apoptosis	0.005
Week 4	Cell division	0.005
Week 4	Glycine serine and threonine metabolism	0.005
Week 4	Linoleic acid metabolism	0.005
Week 4	NOD like receptor signaling pathway	0.005
Week 4	Others	0.005
Week 4	Progesterone mediated oocyte maturation	0.005
Week 4	Proteasome	0.005
Week 4	Taurine and hypotaurine metabolism	0.005
Week 4	Valine leucine and isoleucine biosynthesis	0.005
Week 4	beta Alanine metabolism	0.005
Week 4	Nucleotide excision repair	0.007
Week 4	Nucleotide metabolism	0.007
Week 4	Other ion coupled transporters	0.007
Week 4	Parkinsons disease	0.007
Week 4	Starch and sucrose metabolism	0.007
Week 4	Amino acid related enzymes	0.010

Week 4	Biosynthesis of ansamycins	0.010
Week 4	Cardiac muscle contraction	0.010
Week 4	Cell cycle Caulobacter	0.010
Week 4	Cellular antigens	0.010
Week 4	DNA repair and recombination proteins	0.010
Week 4	DNA replication	0.010
Week 4	Homologous recombination	0.010
Week 4	N Glycan biosynthesis	0.010
Week 4	Pantothenate and CoA biosynthesis	0.010
Week 4	Ribosome	0.010
Week 4	Translation proteins	0.010
Week 4	Folate biosynthesis	0.015
Week 4	One carbon pool by folate	0.015
Week 4	Propanoate metabolism	0.015
Week 4	Protein export	0.015
Week 4	Purine metabolism	0.015
Week 4	Ribosome Biogenesis	0.015
Week 4	Ribosome biogenesis in eukaryotes	0.015
Week 4	Translation factors	0.015
Week 4	Alzheimers disease	0.021
Week 4	D Glutamine and D glutamate metabolism	0.021
Week 4	Glycan biosynthesis and metabolism	0.021
Week 4	MAPK signaling pathway yeast	0.021
Week 4	Mismatch repair	0.021
Week 4	Pathways in cancer	0.021
Week 4	Peroxisome	0.021
Week 4	Phosphotransferase system	0.021
Week 4	Photosynthesis proteins	0.021
Week 4	Transcription factors	0.021
Week 4	Type I diabetes mellitus	0.021
Week 4	Amino sugar and nucleotide sugar metabolism	0.028
Week 4	Bacterial secretion system	0.028
Week 4	Base excision repair	0.028
Week 4	Biosynthesis of siderophore group nonribosomal peptides	0.028
Week 4	Biosynthesis of vancomycin group antibiotics	0.028
Week 4	DNA replication proteins	0.028
Week 4	Energy metabolism	0.028
Week 4	Epithelial cell signaling in Helicobacter pylori infection	0.028
Week 4	Galactose metabolism	0.028
Week 4	Lipoic acid metabolism	0.028
Week 4	Lipopolysaccharide biosynthesis	0.028
Week 4	Lipopolysaccharide biosynthesis proteins	0.028
Week 4	Penicillin and cephalosporin biosynthesis	0.028
Week 4	Phosphatidylinositol signaling system	0.028
Week 4	Photosynthesis	0.028

Week 4	Benzoate degradation	0.038
Week 4	Biotin metabolism	0.038
Week 4	Glycerophospholipid metabolism	0.038
Week 4	Histidine metabolism	0.038
Week 4	Oxidative phosphorylation	0.038
Week 4	Prenyltransferases	0.038
Week 4	Protein processing in endoplasmic reticulum	0.038
Week 4	RNA degradation	0.038
Week 4	RNA polymerase	0.038
Week 4	Riboflavin metabolism	0.038
Week 4	Sporulation	0.038
Week 4	Terpenoid backbone biosynthesis	0.038
Week 4	Thiamine metabolism	0.038
Week 4	Ubiquinone and other terpenoid quinone biosynthesis	0.038

Note: Significance determined by Mann-Whitney U-test. No correction for multiple comparisons. 252 comparisons made.

Table A3: Significantly different pathways predicted by PICRUSt in APC^{MIN} mice at Week 7

Time	Function	p
Week 7	Arachidonic acid metabolism	1.55E-41
Week 7	Glycerophospholipid metabolism	1.55E-41
Week 7	Parkinsons disease	1.55E-41
Week 7	Phenylalanine metabolism	1.55E-41
Week 7	Protein processing in endoplasmic reticulum	1.55E-41
Week 7	Tryptophan metabolism	1.55E-41
Week 7	Type II diabetes mellitus	1.55E-41
Week 7	Ubiquinone and other terpenoid quinone biosynthesis	1.55E-41
Week 7	Ubiquitin system	1.55E-41
Week 7	PPAR signaling pathway	3.11E-41
Week 7	Transporters	3.11E-41
Week 7	Amyotrophic lateral sclerosis	6.22E-41
Week 7	Biosynthesis of vancomycin group antibiotics	6.22E-41
Week 7	Cell division	6.22E-41
Week 7	Circadian rhythm plant	6.22E-41
Week 7	N Glycan biosynthesis	6.22E-41
Week 7	Phosphonate and phosphinate metabolism	6.22E-41
Week 7	Prenyltransferases	6.22E-41
Week 7	Prion diseases	6.22E-41
Week 7	Ribosome biogenesis in eukaryotes	6.22E-41
Week 7	Thiamine metabolism	6.22E-41
Week 7	Tropane piperidine and pyridine alkaloid biosynthesis	6.22E-41
Week 7	Valine leucine and isoleucine biosynthesis	6.22E-41
Week 7	Carbon fixation in photosynthetic organisms	0.0011
Week 7	DNA replication proteins	0.0011
Week 7	Lipoic acid metabolism	0.0011
Week 7	Meiosis yeast	0.0011
Week 7	Mismatch repair	0.0011
Week 7	Non homologous end joining	0.0011
Week 7	Prostate cancer	0.0011
Week 7	RNA polymerase	0.0011
Week 7	Retinol metabolism	0.0011
Week 7	alpha Linolenic acid metabolism	0.0011
Week 7	Alanine aspartate and glutamate metabolism	0.0021
Week 7	Bacterial motility proteins	0.0021
Week 7	Biosynthesis of unsaturated fatty acids	0.0021
Week 7	D Alanine metabolism	0.0021
Week 7	Drug metabolism other enzymes	0.0021
Week 7	Fatty acid metabolism	0.0021
Week 7	Flagellar assembly	0.0021
Week 7	Fluorobenzoate degradation	0.0021
Week 7	Homologous recombination	0.0021

Week 7	Lipopolysaccharide biosynthesis	0.0021
Week 7	Others	0.0021
Week 7	Pentose and glucuronate interconversions	0.0021
Week 7	Photosynthesis proteins	0.0021
Week 7	Primary immunodeficiency	0.0021
Week 7	Protein kinases	0.0021
Week 7	Translation proteins	0.0021
Week 7	Tyrosine metabolism	0.0021
Week 7	Vitamin B6 metabolism	0.0021
Week 7	Zeatin biosynthesis	0.0021
Week 7	Atrazine degradation	0.0031
Week 7	Bacterial invasion of epithelial cells	0.0031
Week 7	Butanoate metabolism	0.0031
Week 7	Carbon fixation pathways in prokaryotes	0.0031
Week 7	Cell cycle Caulobacter	0.0031
Week 7	Citrate cycle TCA cycle	0.0031
Week 7	Cyanoamino acid metabolism	0.0031
Week 7	Cysteine and methionine metabolism	0.0031
Week 7	Cytoskeleton proteins	0.0031
Week 7	General function prediction only	0.0031
Week 7	Glycolysis Gluconeogenesis	0.0031
Week 7	Huntingtons disease	0.0031
Week 7	Lysine degradation	0.0031
Week 7	Other ion coupled transporters	0.0031
Week 7	Pantothenate and CoA biosynthesis	0.0031
Week 7	Pertussis	0.0031
Week 7	Plant pathogen interaction	0.0031
Week 7	Porphyrin and chlorophyll metabolism	0.0031
Week 7	Signal transduction mechanisms	0.0031
Week 7	Sphingolipid metabolism	0.0031
Week 7	Taurine and hypotaurine metabolism	0.0031
Week 7	Toluene degradation	0.0031
Week 7	Vibrio cholerae pathogenic cycle	0.0031
Week 7	beta Lactam resistance	0.0031
Week 7	African trypanosomiasis	0.0051
Week 7	Basal transcription factors	0.0051
Week 7	Base excision repair	0.0051
Week 7	Biosynthesis and biodegradation of secondary metabolites	0.0051
Week 7	Biotin metabolism	0.0051
Week 7	Chagas disease American trypanosomiasis	0.0051
Week 7	Glycan biosynthesis and metabolism	0.0051
Week 7	Lipid metabolism	0.0051
Week 7	Lipopolysaccharide biosynthesis proteins	0.0051
Week 7	RIG I like receptor signaling pathway	0.0051
Week 7	Toxoplasmosis	0.0051

Week 7	DDT degradation	0.0071
Week 7	C5 Branched dibasic acid metabolism	0.0071
Week 7	Carbohydrate digestion and absorption	0.0071
Week 7	Chromosome	0.0071
Week 7	D Arginine and D ornithine metabolism	0.0071
Week 7	Fatty acid biosynthesis	0.0071
Week 7	Flavonoid biosynthesis	0.0071
Week 7	Geraniol degradation	0.0071
Week 7	Germination	0.0071
Week 7	Glycosaminoglycan degradation	0.0071
Week 7	Glyoxylate and dicarboxylate metabolism	0.0071
Week 7	Ion channels	0.0071
Week 7	Isoquinoline alkaloid biosynthesis	0.0071
Week 7	Novobiocin biosynthesis	0.0071
Week 7	Starch and sucrose metabolism	0.0071
Week 7	Synthesis and degradation of ketone bodies	0.0071
Week 7	Viral myocarditis	0.0071
Week 7	Cell motility and secretion	0.0101
Week 7	Folate biosynthesis	0.0101
Week 7	Lysosome	0.0101
Week 7	Oxidative phosphorylation	0.0101
Week 7	Peptidoglycan biosynthesis	0.0101
Week 7	Phenylpropanoid biosynthesis	0.0101
Week 7	Polyketide sugar unit biosynthesis	0.0101
Week 7	Pores ion channels	0.0101
Week 7	Sulfur relay system	0.0101
Week 7	Two component system	0.0101
Week 7	Vibrio cholerae infection	0.0101
Week 7	Glutathione metabolism	0.0151
Week 7	Glycosphingolipid biosynthesis ganglio series	0.0151
Week 7	Glycosphingolipid biosynthesis lacto and neolacto series	0.0151
Week 7	Linoleic acid metabolism	0.0151
Week 7	MAPK signaling pathway yeast	0.0151
Week 7	Nucleotide metabolism	0.0151
Week 7	Other transporters	0.0151
Week 7	Peroxisome	0.0151
Week 7	Proteasome	0.0151
Week 7	Protein digestion and absorption	0.0151
Week 7	ABC transporters	0.0211
Week 7	Amino acid metabolism	0.0211
Week 7	Bladder cancer	0.0211
Week 7	Carotenoid biosynthesis	0.0211
Week 7	Cellular antigens	0.0211
Week 7	D Glutamine and D glutamate metabolism	0.0211
Week 7	Electron transfer carriers	0.0211

Week 7	Glutamatergic synapse	0.0211
Week 7	Glycerolipid metabolism	0.0211
Week 7	Methane metabolism	0.0211
Week 7	Nitrogen metabolism	0.0211
Week 7	Pyruvate metabolism	0.0211
Week 7	RNA degradation	0.0211
Week 7	Ribosome	0.0211
Week 7	Ribosome Biogenesis	0.0211
Week 7	Staphylococcus aureus infection	0.0211
Week 7	Tetracycline biosynthesis	0.0211
Week 7	Transcription related proteins	0.0211
Week 7	Translation factors	0.0211
Week 7	Xylene degradation	0.0211
Week 7	Amino sugar and nucleotide sugar metabolism	0.0281
Week 7	Energy metabolism	0.0281
Week 7	Lipid biosynthesis proteins	0.0281
Week 7	Nicotinate and nicotinamide metabolism	0.0281
Week 7	One carbon pool by folate	0.0281
Week 7	Pentose phosphate pathway	0.0281
Week 7	Proximal tubule bicarbonate reclamation	0.0281
Week 7	Pyrimidine metabolism	0.0281
Week 7	Riboflavin metabolism	0.0281
Week 7	Stilbenoid diarylheptanoid and gingerol biosynthesis	0.0281
Week 7	Systemic lupus erythematosus	0.0281
Week 7	Tuberculosis	0.0281
Week 7	beta Alanine metabolism	0.0281
Week 7	DNA repair and recombination proteins	0.0381
Week 7	Limonene and pinene degradation	0.0381
Week 7	Pathways in cancer	0.0381
Week 7	Penicillin and cephalosporin biosynthesis	0.0381
Week 7	Polycyclic aromatic hydrocarbon degradation	0.0381
Week 7	Protein folding and associated processing	0.0381

Note: Significance determined by Mann-Whitney U-test. No correction for multiple comparisons. 252 comparisons made.

Table A4: Significantly different pathways predicted by PICRUSt in APC^{MIN} mice at Week 11

Time	Function	p
Week 11	Cytoskeleton proteins	0.0021
Week 11	Small cell lung cancer	0.0101
Week 11	Chromosome	0.0151
Week 11	Fatty acid elongation in mitochondria	0.0211
Week 11	Lysine degradation	0.0211
Week 11	Starch and sucrose metabolism	0.0211
Week 11	C5 Branched dibasic acid metabolism	0.0281
Week 11	Fatty acid biosynthesis	0.0281
Week 11	Influenza A	0.0281
Week 11	One carbon pool by folate	0.0281
Week 11	Synthesis and degradation of ketone bodies	0.0281
Week 11	G protein coupled receptors	0.0381
Week 11	Vibrio cholerae infection	0.0381

Note: Significance determined by Mann-Whitney U-test. No correction for multiple comparisons. 252 comparisons made.

Table A4: Significantly different pathways predicted by PICRUSt in APC^{MIN} mice at Week 14

Time	Function	p
Week 14	Inorganic ion transport and metabolism	0.0071
Week 14	Meiosis - yeast	0.0091
Week 14	Bacterial toxins	0.0231
Week 14	D Alanine metabolism	0.0231
Week 14	Sphingolipid metabolism	0.0291
Week 14	Vibrio cholerae pathogenic cycle	0.0291
Week 14	alpha Linolenic acid metabolism	0.0291
Week 14	Transcription machinery	0.0351

Note: Significance determined by Mann-Whitney U-test. No correction for multiple comparisons. 252 comparisons made.

Table A5: Significantly different pathways predicted by PICRUSt between APC^{MIN} mice administered PBS, *E. coli MG1655* or *E. coli MG1655* expressing *bsh*

Time	Function	p
Week 14	Pathways in cancer	0.001
Week 14	RIG I like receptor signaling pathway	0.001
Week 14	Pentose and glucuronate interconversions	0.002
Week 14	Mineral absorption	0.003
Week 14	Alzheimers disease	0.004
Week 14	Primary immunodeficiency	0.004
Week 14	Transcription machinery	0.004
Week 14	Fatty acid biosynthesis	0.005
Week 14	Lipid biosynthesis proteins	0.005
Week 14	Other ion coupled transporters	0.005
Week 14	Renal cell carcinoma	0.006
Week 14	Tuberculosis	0.006
Week 14	Arachidonic acid metabolism	0.007
Week 14	Fructose and mannose metabolism	0.007
Week 14	Methane metabolism	0.007
Week 14	Starch and sucrose metabolism	0.007
Week 14	Amyotrophic lateral sclerosis	0.008
Week 14	Ether lipid metabolism	0.008
Week 14	Linoleic acid metabolism	0.008
Week 14	Phenylalanine metabolism	0.008
Week 14	Valine leucine and isoleucine degradation	0.008
Week 14	Drug metabolism other enzymes	0.009
Week 14	Huntingtons disease	0.009
Week 14	Selenocompound metabolism	0.009
Week 14	RNA transport	0.01
Week 14	Lysine degradation	0.011
Week 14	Vibrio cholerae pathogenic cycle	0.011
Week 14	African trypanosomiasis	0.012
Week 14	Biosynthesis of ansamycins	0.012
Week 14	Chagas disease American trypanosomiasis	0.012
Week 14	Cyanoamino acid metabolism	0.012
Week 14	Galactose metabolism	0.012
Week 14	Steroid hormone biosynthesis	0.012
Week 14	Sulfur metabolism	0.012
Week 14	Sulfur relay system	0.012
Week 14	Apoptosis	0.013
Week 14	Cardiac muscle contraction	0.013
Week 14	Colorectal cancer	0.013
Week 14	Fatty acid metabolism	0.013
Week 14	Influenza A	0.013
Week 14	Parkinsons disease	0.013

Week 14	Phosphatidylinositol signaling system	0.013
Week 14	Pyruvate metabolism	0.013
Week 14	Small cell lung cancer	0.013
Week 14	Toxoplasmosis	0.013
Week 14	Viral myocarditis	0.013
Week 14	p53 signaling pathway	0.013
Week 14	Cell motility and secretion	0.014
Week 14	Metabolism of cofactors and vitamins	0.014
Week 14	Ubiquitin system	0.014
Week 14	Bacterial secretion system	0.015
Week 14	Drug metabolism cytochrome P450	0.015
Week 14	Caffeine metabolism	0.017
Week 14	Carotenoid biosynthesis	0.017
Week 14	Circadian rhythm plant	0.017
Week 14	Fatty acid elongation in mitochondria	0.017
Week 14	Fluorobenzoate degradation	0.017
Week 14	Glycosyltransferases	0.017
Week 14	Ion channels	0.017
Week 14	Meiosis yeast	0.017
Week 14	Non homologous end joining	0.017
Week 14	Phenylpropanoid biosynthesis	0.017
Week 14	Steroid biosynthesis	0.017
Week 14	Systemic lupus erythematosus	0.017
Week 14	Prion diseases	0.018
Week 14	Tryptophan metabolism	0.018
Week 14	Tyrosine metabolism	0.018
Week 14	Toluene degradation	0.019
Week 14	Bacterial invasion of epithelial cells	0.02
Week 14	Geraniol degradation	0.02
Week 14	Proximal tubule bicarbonate reclamation	0.02
Week 14	Secretion system	0.02
Week 14	Glutathione metabolism	0.021
Week 14	Prenyltransferases	0.021
Week 14	Isoquinoline alkaloid biosynthesis	0.022
Week 14	Biosynthesis of unsaturated fatty acids	0.023
Week 14	Riboflavin metabolism	0.023
Week 14	Lipopolysaccharide biosynthesis	0.024
Week 14	Glycerophospholipid metabolism	0.025
Week 14	Replication recombination and repair proteins	0.027
Week 14	Base excision repair	0.028
Week 14	Caprolactam degradation	0.028
Week 14	N Glycan biosynthesis	0.028
Week 14	Propanoate metabolism	0.029
Week 14	Ubiquinone and other terpenoid quinone biosynthesis	0.029
Week 14	Valine leucine and isoleucine biosynthesis	0.029

Week 14	Penicillin and cephalosporin biosynthesis	0.03
Week 14	Lipopolysaccharide biosynthesis proteins	0.031
Week 14	alpha Linolenic acid metabolism	0.032
Week 14	Citrate cycle TCA cycle	0.037
Week 14	Metabolism of xenobiotics by cytochrome P450	0.038
Week 14	Inorganic ion transport and metabolism	0.04
Week 14	Amoebiasis	0.041
Week 14	Electron transfer carriers	0.042
Week 14	Protein processing in endoplasmic reticulum	0.042
Week 14	Limonene and pinene degradation	0.043
Week 14	Bladder cancer	0.044
Week 14	Primary bile acid biosynthesis	0.044
Week 14	Secondary bile acid biosynthesis	0.044
Week 14	Phosphotransferase system	0.045
Week 14	Amino acid metabolism	0.046

Note: Significance determined by Kruskall-Wallis test. No correction for multiple comparisons. 252 comparisons made.